

**VULNERABILITY ASSESSMENT OF EARTHQUAKE
AND LANDSLIDE HAZARDS IN KOHIMA TOWN
USING REMOTE SENSING AND GIS**

**Thesis submitted to
NAGALAND UNIVERSITY**

In fulfillment of the Degree of
**DOCTOR OF PHILOSOPHY
IN
GEOGRAPHY**

By
Mr. KEDOVIKHO YHOSHÜ
Reg. No. 685/2015, Dated: 27:05:2015

Under the Supervision of
Dr. Y. V. KRISHNAIAH



**DEPARTMENT OF GEOGRAPHY
(School of Sciences)
NAGALAND UNIVERSITY
HQRS: LUMAMI - 798 627**

2017



नागालैण्ड

विश्वविद्यालय

NAGALAND UNIVERSITY

(A Central University estd. by an Act of Parliament No. 35 of 1989)

(संसद द्वारा पारित अधिनियम 1989, क्रमांक 35 के अंतर्गत स्थापित केंद्रीय विश्वविद्यालय)

मुख्यालय : लुमामी, जुन्हेबोटो (नागालैण्ड), पिन कोड - 798627

Hqrs: Lumami, Dist: Zunheboto, Nagaland, Pin Code-798 627

Dr. Y. V. Krishnaiah, M. Sc., Ph. D (Geog), M. Ed., M. Phil (Education),

Assistant Professor,

Department of Geography,

Mobile No. 91-9436608205

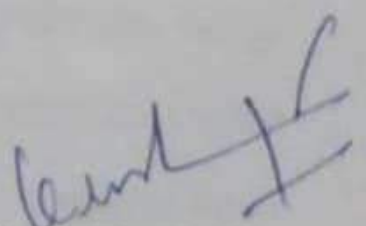
Email: yvkrishna09@gmail.com

CERTIFICATE

I, hereby certify that the thesis entitled “Vulnerability assessment of Earthquake and Landslide Hazards in Kohima Town using Remote Sensing and GIS” submitted to Nagaland University for the partial fulfillment for the award of degree of Doctor of Philosophy by **Mr. Kedovikho Yhoshü**, (Regd. No. 685/2015, dated: 27.05.2015), is the original and independent work carried out under my supervision and that the thesis has not been formed partially or in full for the award of any other degree, diploma or similar titles at the time of submission.

Place: Lumami,

Date :


(Dr. Y. V. Krishnaiah)
Supervisor

1

1.1 Introduction

Hazard has become one of the most pressing and challenging issues in the present times. The erratic climatic change particularly in the hilly terrains has triggered hazard in the form of cloud burst, flash floods etc., leading to landslides and floods where the very existence of man has been threatened. The movement of tectonic plates causing seismic activities has uplifted and deformed landforms. The demographic pressure on the land has further stressed the already fragile ecosystem balance particularly the carrying capacity of the land. With this background, anthropogenic activities particularly urbanisation has been a major driving force of landscape change. Urbanisation has drastically changed the socio-natural landscape, where land has been cut and filled, roads and buildings constructed, vegetation cleared etc. Urbanisation has become a vicious cycle where more and more land

are been engaged in landscape change particularly construction. Unplanned construction has devastated the environment causing catastrophic hazards.

According to World Bank estimation, India losses around 2 percent of National GDP due to natural disaster (Kumar, 2012). Varnes (1984) stated hazard as ‘the probability of occurrence within a specific period of time and within a given area of a potentially damaging phenomenon.’ Ciurean *et al.*, (2013) defined vulnerability as ‘the potential for loss to the elements caused by the occurrence of a hazard, and depends on multiple aspects arising from physical, social, economic and environmental factors, which are interacting in space and time. Vulnerability in short refers to the inability to withstand hostile environment-hazard. Hazard map without vulnerability analysis are not meaningful for effective decision making where each habited area holds significant condition based on population (Rautela and Thakur, 1999).

Rocks are made of elastic material, and so elastic strain energy is stored in them during the deformations that occur due to the gigantic tectonic plate actions that occur in the Earth. However, the materials contained in rocks are also brittle. The rocks along weak region in the Earth’s Crust reach their peak strength when a sudden movement takes place creating seismic waves which reach the surface creating surface undulations. Richter scale was the first earthquake-magnitude scale devised by Charles F. Richter, a Seismologist at the California Institute of Technology. Richter scale is based on amplitude of seismic waves that is stronger the earthquake, the stronger the seismic vibrations it causes. Richter magnitude is that of a logarithmic scale, meaning an increase of one in magnitude corresponds to a factor of ten increases in the amplitude of ground motion. For example- a earthquake of magnitude 6.7 cause shaking of 10 times greater amplitude than a magnitude of 5.7 and 100 times greater than an earthquake magnitude of 4.7.

The vulnerability assessment method for building is divided into two methods- detailed method for individual building and the other for larger areas by efficient analysis method (Mueller *et al.*, 2006). Recently, high resolution satellite imagery has been used extensively for building vulnerability assessment due to its high spatial resolution. High resolution images for vulnerability assessment using object-based image analysis method where buildings were detected based on their elements of interpretation (Hao *et al.*, 2014). The application of remote sensing in social vulnerability was mapped using object based image analysis method where high resolution imagery combined with digital datasets was used to extract semantic information such as position of building in relation to hazard zone to locate its natural and man-made landscape (Ebert and Kerle, 2008). The high resolution satellite imagery can be used to detect the building damage in a period of short time to build a casualty estimation method (Feng *et al.*, 2014). The subsoil involving geological instability of the stratigraphy (Huber *et al.*, 2015) where pluri-gaussain simulation approach was used for generating damage estimation of rigid building. The consequences of subsoil uncertainty was calculated by the fragility curve which quantify the reliability of a structure due to the range of loading conditions to which that structure might be exposed (Schultz *et al.*, 2010).

1.1.1 Study on tectonic plates in Northeast region

The tectonic domain of Northeast India consist of four tectonic units- i) East-West Himalayan arc marking the convergence between Indian and Eurasian plates, ii) North-South oriented Indo-Burmese arc where Indian and Sunda plates interact, iii) the NW-SE oriented Eastern Himalayan syntaxial zone that lies between the two arcs and iv) the Shillong plateau region which is considered as an intra-plate region (Gahalaut *et al.*, 2016). The entire Northeast India region is located in the most intense seismic zone V

(Bhattacharya *et al.*, 2005) and is considered to be one of the most tectonically seismic zones in India jawed between two arcs- Himalayan arc and Indo-Burmese arc (Kayal *et al.*, 2006). Some of the past earthquake along with its focal depth and focal mechanism, the most recent devastating earthquake occurred on 4th January, 2016 in Manipur. The black arrow shows the India Sunda plate motion, yellow arrow shows direction of stress in the Indo-Burmese Wedge (IBW) and Sangaing fault region (Figure 1.1).

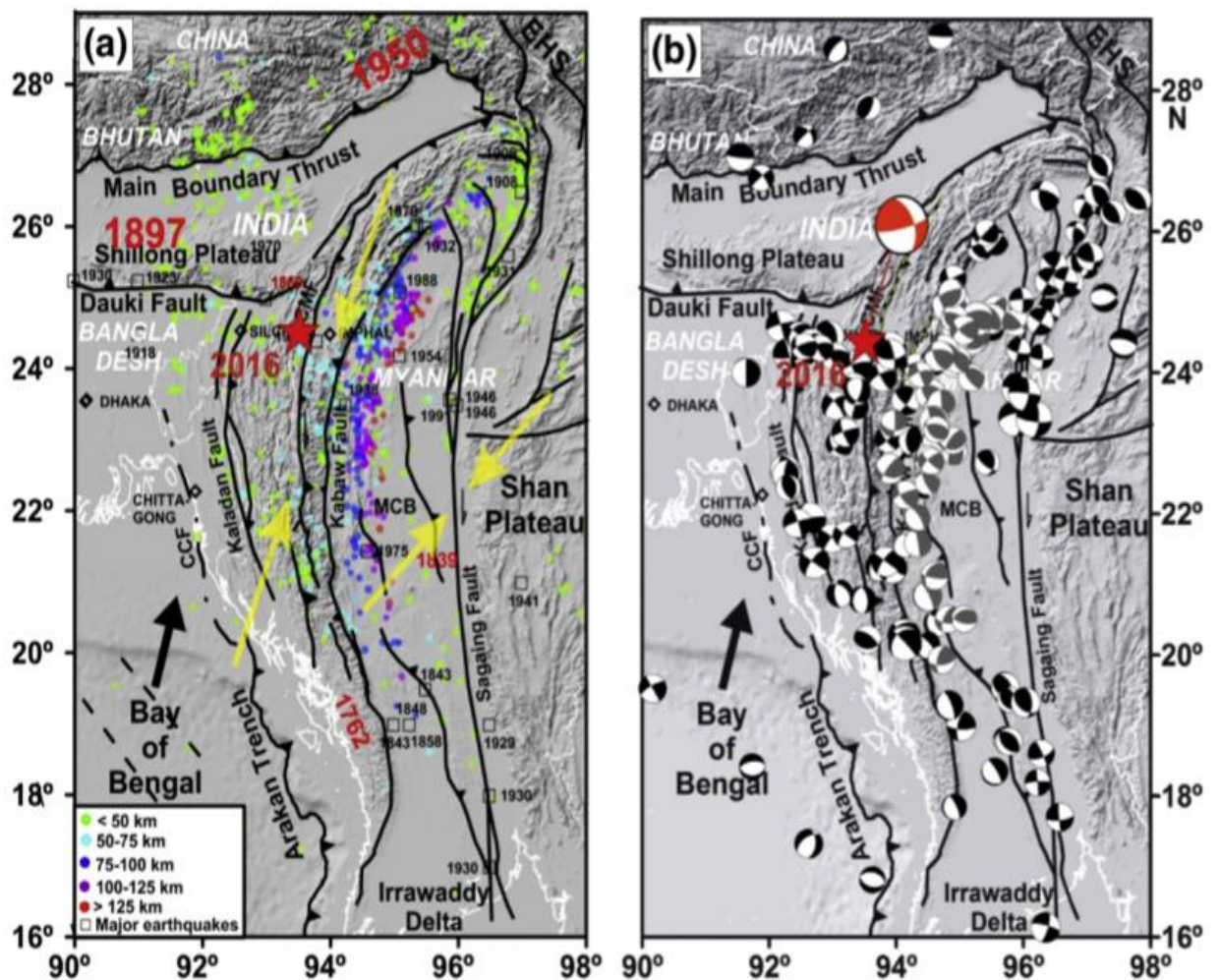


Figure 1.1. Past Earthquake with the various faults and direction of movement around the study area (Gahalaut *et al.*, 2016).

1.1.2 Earthquake Capacity of building

Earthquake capacity defines the deformation capacity of the building structure to withstand seismic shake. Earthquake capacity of a building should be able to withstand

deformation with damage with small intensity shaking and with no collapse under high seismic intensity shaking. A building should be inelastic and should have the strength to withstand the deformation caused by seismic shaking. Earthquake capacity of a building is classified into two- elastic and inelastic property of a building.

1.1.2.1 Elastic behaviour

Elastic behaviour is controlled by the configuration, stiffness, strength and ductility of the building. Geometry, structural system and load paths are the main aspects of configuration. Buildings with simple plan geometries are preferred as they demonstrate stronger seismic performance than the concave and complex plan geometry (Murty *et al.*, 2012).

Structural system should not be used without structures like structural walls and braces in a building. The most common form of structural features for lateral load resisting structural systems is moment frames. Structural wall, frame wall system and braced wall system.

Inertia forces mobilized in buildings during earthquake shaking travel through to the building foundation. The forces travel through structural members, thus choice and structural member location play a major role as it affect the seismic performance of building. A smooth path which will offer less resistance for the force to be transferred to the foundation is hence desirable.

1.1.2.2 Inelastic behaviour

In inelastic behaviour, the load does not retrace after unloaded. In short, it does not follow the loading path. Inelasticity of building is controlled by strength and ductility. The lateral strength of building depends on structural configuration, material strength, relative size of structural members, ductility's, amount of reinforcement and strength and stiffness of joints.

Soft storeys when constructed at the basement of building, it weakens the building. The presence of asymmetrical plan in the columns causes instability to the building. This results in stiffness asymmetry when the columns reach their strengths limit. Ductility of a building is its capacity to accommodate lateral deformations along the building height (Murty *et al.*, 2012). Ductility therefore, exhibits large inelastic deformation capacity without significant loss of strength capacity. Buildings on hill slopes with unequal height columns cause are ill effects like twisting and damage of shorter columns (Murty, 2005).

1.1.3 Landslide

Landslide a natural hazard is the problem seen in many countries resulting in loss of lives and extensive property damages (Khodadad and Jang, 2015). Landslide hold much importance for future planning as from the concept of Uniformitarianism “**the present is the key to the past**” the occurrences of landslide can be understood from the old scar of landslides which may trigger future landslide.

Landslide on mountainous unstable terrain usually occurs after heavy rainfall due to saturation cause loss to human lives and built up environment, identification of such vulnerable area is hence, required to avoid casualties (Dai and Lee, 2002). The potential threat of landslide increased (Wang *et al.*, 2015) owing to its unpredicted and uncertainty predisposing factors. The predisposing factors are not uniform and cannot be universally applied to all slides. Therefore, factors are site specific where it depends on the availability of data and the nature of the study (Che *et al.*, 2012). The pre-requisite and significance of the landslide hazard assessment for environmental protection and rational exploitation in regard to the quick development of urbanization and developmental processes (Wu *et al.*, 2014) (**Table 1.1**).

Table 1.1. Landslide controlling factors

Category	Controlling factors	Availability
Geology	Lithological makeup, rock units (mudstone, sandstone, limestone and greenstuffs), tectonics and bedrock structure	Local
Geomorphology	Elevation, slope, slope shape, aspect, curvature, concavity	Global
Soil	Soil types (Clay, silt, foam, sand...) soil texture, soil depth	Global
Land cover	Vegetated, barren, built-up, developed, grass, shrub..	Global
Hydrology	Rainfall, Soil moisture, snowmelt, drainage density or flow accumulation, flow direction (sliding path), infiltration	Global
Human Impact	Urban built-up, road construction, deforestation (burning), irrigation, mining, artificial vibration...	Regional

Source: Wu *et al.*, 2014.

1.1.3.1 Classification and types of Landslides

Landslides are classified according to the types of material involve and their movement mechanism. Numerous classifications have been done basing on those parameters, of which Varnes (1978) and Hutchison (1988) are commonly used.

Varnes (1978) is more appropriated on the basis of (1) the type of material that existed prior to the landslide and (2) the type of movement that dominates during the landslide (**Table 1.2**). The types of material that might exist prior to a landslide are rock, soil, earth, mud, and debris. Classification of landslide by Hutchison (1988) has been based on movement and their formation (**Table 1.3**).

Table 1.2. Type of movement

Type of movement		Type of Material		
		Bedrock	Engineering soil	
			Predominantly coarse	Predominantly fine
Fall		Rock fall	Debris fall	Earth fall
Topple		Rock topple	Debris topple	Earth topple
Slides	Rotational	Rock slide	Debris slide	Earth slide
	Translational			
Lateral spread		Rock spread	Debris spread	Earth spread
Flow		Rock flow (Deep creep)	Debris flow (Soil creep)	Earth flow
Complex		Combination of two or more principal types of movement		

Source: Varnes, 1978

Table 1.3. Type of Landslide

Rebound	when ground is unloaded either artificially by evacuation or naturally by erosion, the unloaded area responds, initially elastically and subsequently by slow swelling
Creep	Any extremely slow movements which are imperceptible except through long-period measurement
Sagging of mountain slopes	A general term for these deep-seated deformations of mountain slopes, which in their preset state of development, do not justify classification of landslides
Landslide	Relatively rapid downslope movements of soil and rock, which take place characteristically on one or more discrete bounding slip surfaces which divide the moving mass
Debris movement of flow like form	Term covering five types of movement of flow-like form, which differ markedly in mechanism: non-periglacial mudslides, periglacial mudslides, flow slides, debris flow and sturzstroms
Topple	A movement that occurs when the vector of resultant applied forces falls through, or outside a pivot point in the base of the affected block
Fall	The more or less free and extremely rapid descent of masses of soil or rock of any size from steep slopes or cliffs
Complex slope movement	The combination of two or more of the types of movements described above

Source: Hutchison, 1988.

Slope instability hazard assessment is based on the assumption that conditions which led to slope failure in the past will result in potential unstable condition in the present (Van Westen, 2000). Lithology and structure play an important role in delineating slopes which are unstable. Landslide hazard zonation map categorise division of the land surface into various zones where there is finite probability of being affected by slope instability.

Landslide comprises almost all the varieties of mass movements on slopes, rock falls, topples and debris flow that involve little or no sliding. Identification of landslide prone areas through susceptibility assessment is essential to understand landslide phenomena and its relationship with various causative factors. By susceptibility, it refers to

the spatial future likelihood or probability for landslides to occur (Harvas and Bobrowsky, 2009). The recognition and identification of landslide prone area is becoming more crucial for environmental management and is vital for regional and local planning (Vijith, *et al.*, 2013).

Bhandari (2013a) stated that “we understand landslides only by elucidation of landslide boundary-shears, concurrent monitoring of time-dependent piezometric pressures, surface and sub-slope displacements and mapping of ground deformations and shear zones, plus behavioural studies of associated human settlements form an integral part of the landslide investigation”.

Outward and downward movement of mass consisting of rocks, slope instability and soils due to natural or manmade causes are sometimes associated with pre and post earthquake events, soil erosion, rainfall and anthropogenic activities (Abdul *et al.*, 2014). Mass movements, especially landslides, are one of the most damages hazard that have had the increasing momentum manipulating human habitat in natural systems in recent decades (Yazdadiand, 2016).

The overlapping of landslide distribution with the causative factors can delineate the zones which are susceptible to landslide but not the probability of occurrence of the instability processes (Aste, 1991). The spatial information related to the causative factor for landslide can be derived from Remote Sensing and Geographical Information System (RS & GIS) techniques. GIS a powerful tool for integrating different data type has made some significant development especially in spatial data analysis (Rawat *et al.*, 2015). Landslide hazard map divides the landslide prone hilly terrain into different zones according to the relative degree of susceptibility to landslide (Marrapu and Jakka, 2014). Landslide hazard zonation provides information on the susceptibility of the terrain to slope failures and can be used for the estimation of the loss of soil due to slope failures, new

construction sites and road alignment, for prevention, evacuation and mitigation processes (Talib and Napiyah, 2000). Landslide susceptibility mapping provides valuable information concerning the stability conditions of the territory and serve as the first step in a hazard assessment towards the mitigation of natural landslide disaster (Ladas *et al.*, 2007).

1.2 Study area

Kohima, the capital of Nagaland is located in the North-eastern part of India. Its geographical coordinates between 94°05'04'' E and 94°07'23'' E latitude and 25°38'28'' N and 25°39'24''N longitude (**Figure 1.2**). The geographical spatial extent of the study area is 14.03 km². Kohima is located at an elevation between 800 to 1500 m above mean sea level. Annual temperature is moderate ranging from 5°C in winter to 30°C in the summer. Kohima experiences an annual rainfall about 1521.3 mm with 149 numbers of rainy days (2015), precipitation is maximum in the month of June to August month, a maximum rainfall was observed in the month of August (374.1 mm) in Kohima (2015 data). Tectonically, it is unstable as it forms part of the Eastern Himalayas and lies in the seismic zone V which is liable to seismic intensity IX (Khatsü and Van Westen, 2005).

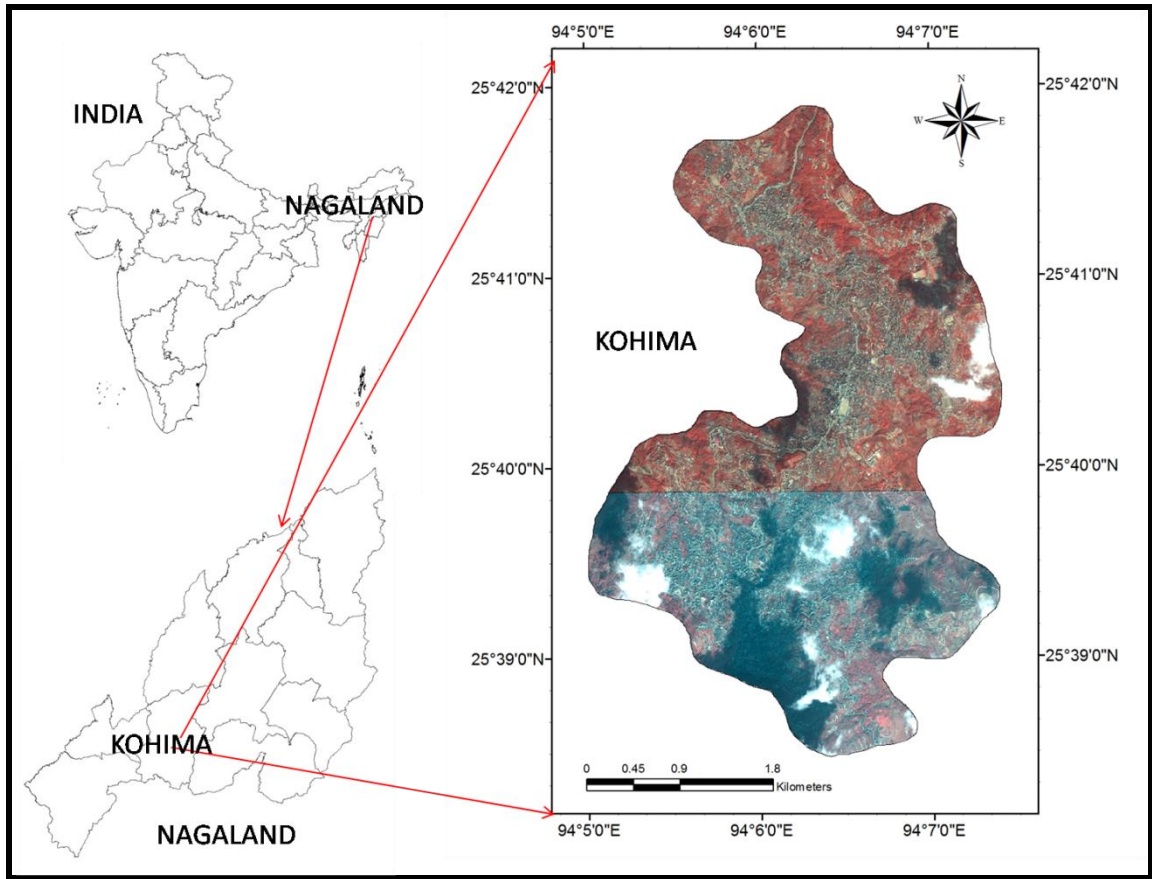


Figure 1.2. Location map of the study area

The number of Municipal ward in the study area is 19, from 2011 the municipal ward increase from 15 to 19 wards. Kohima was also selected as one of the smart cities of India in 2016. The process of urbanisation is progressing rapidly where population has increased from 77,030 in 2001 to 99,039 in 2011 according to Census report 2011. The population density of the study area is 7059 persons per km² displaying a highly dense populated area, it is higher than India population density which is 382 persons per km². The growth of Kohima has increased vertically as well as horizontally. The urban land is very limited but construction and population growth shows more impact on land and another reality that Kohima Town is situated on unstable land as per geology is concerned.

1.3 Objectives of the study area

The main objectives of the present study are

1. To study morphological epitome of Kohima Town.
2. To evaluate the vulnerability of built-up environment and footprint of Kohima Town.
3. To estimate vulnerability of earthquake hazard of Kohima Town.
4. To estimate vulnerability of landslides and generate landslide hazard zonation map of Kohima Town.

1.4 Research question

1. How to generate the geo-database for landslide and earthquake?
2. What parameters are required to assess seismic risk?
3. What will be the distribution of structural buildings which will be affected by seismic waves in the study area?
4. Which geo-statistical method will be used for the landslide zonation map? What will be the spatial extent for each hazard zone?

1.5 Research Methodology

The research methodology is based on vulnerability estimation of two hazards- earthquake/seismic and landslide hazards. Both are quantitatively assess using different methodology; for earthquake, the vulnerability assessment was based on HAZUS and for landslide it was based on bivariate statistical method (Information Value Method). Collection of primary and secondary data was carried out through field survey, visitation of libraries and offices, collection of satellite images etc. Generation of various thematic maps and building footprint was based on Survey of India topographic maps and high resolution satellite imageries, Google Earth platform, supported by field observation.

Primary data include the high resolution satellite imagery which has been pre-processed for correction of distortions in the imageries. Secondary sources include the various digital Ward map and other maps which were collected from various departments and agencies. The pre processing includes the various rectification processes- image to image registration, image to map registration.

Major parameters used in the study are briefly discussed, they are

The satellite imageries used for the study are

1.5.1 Quick bird 2

Quick Bird 2, a US based commercial remote sensing satellite with a three day revisit interval in the range 0.45 μm to 0.90 μm has four band for multi-spectral and one panchromatic band (Unsalan and Boyer, 2011) . It provides 16 bit multispectral data at a spatial resolution of 2.4 m and 11 bit panchromatic spatial resolution at 0.6 m (Xiao, 2008). The acquired date of the satellite data was on 6th November, 2009.

1.5.2 World view 2

It provides 0.46 m panchromatic and 1.8 m multispectral image respectively, there are eight band in multispectral in the spectral range of 0.400 to 1.040 μm and one band in panchromatic band in spectral range 0.450 to 0.800 μm (Nouri *et al.*, 2014, and Unsalan and Boyer, 2011). The date of acquisition of the Worldview 2 imagery was on 15th May, 2013.

1.5.3 Survey of India topographic sheet

The Survey of India (SOI) topographic map (No. 83 K/2) was used to generate the maps. The topographic map showing parts of Manipur, Nagaland with RF. 1:50,000,

contour interval was 20 metre published under the direction of Dr. Hari Narain, Surveyor General of India in 1975. The topographic map was geo-referenced and projection assigned accordingly, it was geo-rectified with the high resolution image through Quick bird 2 data.

1.5.4 Software & Hardware

Processing software like ERDAS Imagine 9.3 and GIS software like Arc GIS 10 has been used. Hardware such as GPS, Geological hammer, Brunton compass, Camera and measuring tape has been used for identifying and locating buildings and for measuring the geological features.

1.5.5 Flow chart

The flow chart was made according to the research methodology steps on which the research has been carried out (Figure 1.3) as follows;

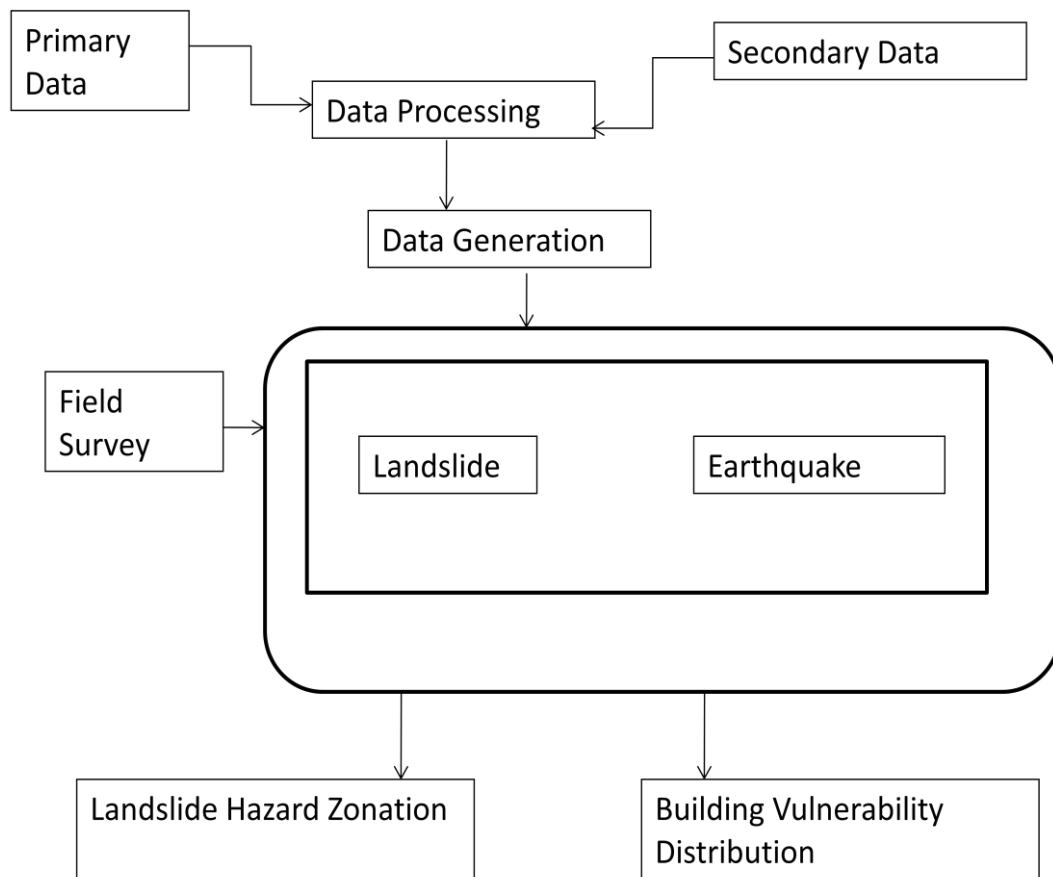


Figure 1.3. Flow chart of the Research methodology.

Pre-processing of the data basing on both primary and secondary data source was generated. The data pre-processing had to be done over the imageries since the ward maps and the Quick bird data were not referenced at the same scale hence, keeping Quick bird as the reference base, the ward had to be geo-rectified. The locations of the pixels in the provided Town Ward map have been realigned to remove distortion. Image to image registration has been carried out using various ground control points. Generally, image registration is the process of superimposing an image over a map or another already registered set of data (the high resolution Quick bird image). Geometric registration process involves identifying the image coordinates of certain points, known as Ground Control Points (GCP), in the distorted image, and matching them to their true positions in ground coordinates (e.g. latitude, longitude). The true ground coordinates are measured

from a map in hard copy of digital format or collected with GPS in the field. This is called image to map registration, which was used for registration of the topographic sheet and the ward maps. The topographic sheets were geo-rectified with the Quick bird data and extracting the region of interest.

Data generation includes the made of various thematic layers for assessing the seismic and landslide hazard. The data generated along with the help of field observation has been incorporated to decipher the vulnerability assessment of the hazards. The working mechanism of the respective models for seismic and landslide hazard has been discussed in the following fourth and fifth chapters respectively. The final hazard maps for earthquake and landslide maps was generated after processing the thematic layers in the GIS models (HAZUS and Bivariate statistical models).

1.6 Review of related literature

Khatsü, (2004) monitored landslide and earthquake hazards in three wards of Kohima town. The susceptibility of landslide was studied based on Information Value Method, it was observed that high landslide hazard zone was observe in geologically weak area which aggravated after the onset of monsoon. For earthquake study, the parameters were based on building material, floor, purpose etc. The susceptible seismic hazard zone was compared with national standard and it fell short of the norms to be considered as an ideal town.

Aier *et al.*, (2012) studied a part of Kohima town – Merhülietsa slide using geotechnical analysis. In the study it was observed that the affected area lies in the Disang sediments and the factor of safety value was 0.60 for slide mass. The rock mass rating of the shales indicate poor rock condition directing towards a progressive sliding area.

Mohan *et al.*, (2008) studied the complex geology of NE India for seismic hazard assessment based on semi empirical modelling technique by Midorikawa (1993). The study covers estimation and comparison of seismic hazard based on peak ground acceleration. It was observed that Kohima experienced a peak ground acceleration of more than 250 cm/sec² which makes it prone to high seismic hazard.

A study based on the scenario of 1987 Shillong earthquake and its impact on the entire Northeastern region of India was conducted by Council of Scientific and Industrial Research- North East Institute of Science and Technology (CSIR-NEIST, 2013) where the vulnerability assessment was done based on the structural buildings response mapped through rapid visual screening.

The earliest works in seismic activity for Northeast India were shown in the works of Oldham (1882) and Oldham (1899) where reports on the damage incurred in the earthquakes of 1869, Cachard 1897 Assam earthquakes were studied. Northeast India is prone to seismic activity due to the collision between Indian plate and Eurasian plate which are mostly located between the Main Boundary Thrust (MBT) and Main Central Thrust (MCT) suggested by Dewey and Bird (1970) and Tandon and Srivastava (1975).

Das *et al.*, (2006) prepared a seismic hazard based on uniform hazard response spectra. The entire area was divided into 0.1° grid size, and the hazard level has assessed for each node within 300 km radius around the node. The study indicated that the Naga thrust fault as one of the potential sources of seismicity where the counters are parallel to the Naga thrust fault and the Pseudo-Spectral Acceleration (PSA) value decrease as it moves away from the fault.

Shape, geometry, size etc., plays an important role in the vulnerable characteristic of a building during a seismic event. Building damages are initiated at storeys which has

lesser column or greater mass or weight than adjacent buildings. Two methods are applied for analysis of building vulnerability; qualitative and quantitative method. Qualitative method is based on statistical evaluation of past earthquake damage and it is suitable for non-engineering buildings that have same type of building character. Quantitative method is based on numerical analysis of the building structure highlighted by Rahman and Salik (2016) and Singh (2005). Building vulnerability gives us a detail assessment of building damage in a seismic event. HAZUS method use spectral displacement of structural and non-structural elements of a building to ground motion for building vulnerability assessment by Gulati, (2006). Yamazaki *et al.*, (2000) classified individual buildings based on 3D data acquisition, colour analysis, texture and coverage area of each building. The number of storeys is based on building height evaluated by stereo matching.

The vulnerability of an urban place is measured by its geologic parameters, building structure such as foundation, column, supporting wall, beam and floor slab. Structural vulnerability is hence, the susceptibility of building parts that are required for physical support when subjected to an earthquake or other hazard commented by Ahmed *et al.*, (2014). Urban vulnerability to hazards is described as degree to which the socio-economic system and physical assets are either susceptible or resilient to the impact of natural hazards emphasized by Rashed and Weeks (2003). Fatalities due to seismic hazard are associated with vulnerability of local buildings, population density and the intensity of ground shaking studied by Nath *et al.* (2015).

Earth observation satellites provide synoptic and temporal coverage of area in near real time. The continuous and repetitive monitoring of Earth surface facilitates the detection and early warning of disasters remarked by Sreekesh (2012). Remotely sensed data potentially provide seismic related information in terms of assessing the potential of risk and defining the state of vulnerability emphasized by Rezaeian and Gruen (2011).

Ebert and Kerle (2008) explored the use of high resolution remote sensing and GIS data in segmentation based analysis to delineate variables for social vulnerability assessment such as socio-economic status, commercial and industrial development, abundance of infrastructure and the distance between them. The non-structural components of building was studied by Dixit *et al.*, (2014) where it stated that earthquake shaking has three effect on non-structural elements; shaking on non-structural element themselves, effect on structural component of non-structural components and pounding effect at the interface between the adjacent structures.

According to UNISDR (2004) there are two essential elements in the formulation of risk- a potential event hazard and the degree of susceptibility of the elements exposed to that source viz- vulnerability ($\text{Risk} = \text{Hazard} \times \text{Vulnerability}$).

Bhandari (2013) and Feng *et al.* (2014) mentioned that the prevention of earthquake is virtually impossible; however, its impact can be mitigated or minimized by proactive risk reduction. In order to check risk, ongoing and new development projects involving risk management, project construction and the corrective action for countering the construction-related, visible or anticipated slope failures and environmental damage before, during or after the construction stage, ought to be considered in design as its inseparable parts.

Van Westen *et al.*, (2008) and Roberds (2005) expressed the elements that can be damaged by any hazard event are known as element at risk. In other words, any entity be it social (population, infrastructure) or physical (buildings) elements which are exposed to the danger of hazard are elements at risk. On the spatial and temporal characters, elements at risk are divided into two; static elements at risk and dynamic elements at risk. Those elements which do not change their location with time eg- buildings and the condition of

their vulnerability remains constant are static elements at risk. Those elements which change their position with time eg- population, landuse etc. are dynamic elements at risk.

Hazard is defined as a dangerous phenomenon, substance, human activity or condition that can cause loss of life, injury or other health impacts, property damage, loss of livelihoods and services, social and economic disruption or environmental damage mentioned by UNISDR, (2009). Natural hazard has been defined as “the probability of occurrence of a potentially damaging phenomenon within a specified period of time and within a given area (Van Westen and Heywood, 1994, and IDNDR, 1993). Sitaram *et al.*, (2006) highlighted that in order to evaluate seismic hazard for particular site, all possible sources of seismic activity must be identified and their potential for generating future strong ground motion must be evaluated. The lineaments and faults present in the region helps in the understanding of the regional seismo-tectonic activity of the area.

Vulnerability generally relates to the potential for loss to the elements at risk caused by the occurrence of a hazard, and depends on multiple aspects arising from physical, social, economic, and environmental factors, which are interacting in space and time analysed by Roxana *et al.*, (2013). Cutter *et al.* (1997) reveals that physical vulnerability involves the determination of the occurrence probability of a given hazard event and the delineation of areas likely to be adversely affected and social vulnerability refers to group of people who are differentially vulnerable due to disabilities, income or other constraining characteristics.

Van Westen *et al.* (2006) stated that “each of the elements at risk has its own characteristics which can be spatial (location in relation to hazard), temporal (population which will differ in time at a certain location) and thematic characteristics (material type of buildings or age distribution of population). Buildings are at risk in developing countries

since in developing countries, the buildings are not designed to withstand the seismic standard of earthquakes analyzed by Kenny (2012). Guzzetti (2005) opined that the focus of landslide risk assessment is an individual element at risk- house, group of elements at risk- village, a class of elements at risk- residential buildings. Landslide risk assessment the focus is on the elements at risk anticipated or present and not on the area per se i.e., the territory unless it is an asset.

Erdik (1994) analysed that vulnerability involves physical, social and economic elements, thus, it is depending of a more diverse amount of fields and cannot be supported by generalizations. Devi and Kalita (2014) described that probabilistic seismic hazard analysis offers a framework for risk management by taking account the probability or frequency of exceedance of ground motion against which structure or facility is designed which is the most common used approach to evaluate seismic design load.

An earthquake is a sudden and violent shaking of the earth when large elastic strain of energy is released and it spreads through seismic waves through the surface of the earth remarked by Levi *et al.*, (2010). According to Disaster Management in India (DMI, 2011), India is divided into seismic zones based on its intensity of earthquake, out of these, zone V is the most active comprising whole of Northeast India, North Bihar, Uttarakhand, Himachal Pradesh, Jammu and Kashmir, Gujarat and Andaman and Nicobar island. Despite the data quality, it is believed that there are seven great earthquakes in Himalayan region since 1800. Out of which four earthquakes were with magnitudes greater than 8 since 1897 described by Kayal (2014). Calvi *et al.* (2006) described vulnerability assessment for building stating that vulnerability assessment needs to be made for a particular characterisation of the ground motion, which represent the seismic demand of the earthquake on the building. The various parameters which are selected should be able to correlate the ground motion with the building damages. Traditionally, macro-seismic

intensity and Peak Ground Acceleration (PGA) have been used, whilst more recent proposals have linked the seismic vulnerability of the buildings to response spectra obtained from the ground motions.

Baruah *et al.*, (2011) and Kramer (1996) based on ground motion parameter observed seismic hazard analysis involves quantitative estimation of ground shaking hazards at a particular area. Barani *et al.*, (2007) estimated deterministically when a particular earthquake scenario is assumed and probabilistically when different earthquake sources can affect a particular area to evaluate the exceedance of ground motion parameters. In earthquake the content of vulnerability concept depends strongly on the specific characteristics of building categories, ways of life, demographic conditions and economic factors; all these factors differ strongly country to country.

Northeast India, one of the most active seismological region is sandwiched between the Himalayan arc and Indo-Burmese arc which has witness two earthquake greater than 8 magnitude and more than 20 earthquake experienced with magnitude greater than 7 since 1897 evaluated by Baruah *et al.*, (2013). Ahmed *et al.*, (2014) pointed that structural vulnerability refers to the susceptibility of those parts of a building that require physical support when subjected to an intense earthquake hazard. Seismic vulnerability factors in structural building include soft storey, heavy overhang, short column, pounding between buildings etc. Vicente *et al.*, (2008) described vulnerability based on the intrinsic property of buildings that limits certain level of damage when exposed to a determined seismic event of defined intensity. Seismic vulnerability of buildings can be evaluated in ways more or less complex in function of scale and specificity of the study.

In India for earthquake risk management, three methods are recommended; a) Rapid Visual Screening (RVS) which requires limited engineering analysis requires only

visual evaluation and limited information. b) Simplified Vulnerability Assessment (SVA) based on visual observation and limited engineering analysis, recommended in high concentration of people. c) Detailed Vulnerability Assessment (DVA) requires detailed computer analysis, recommended for all important and lifeline buildings highlighted by Anbazhagan *et al.*, (2014). Rashed and Weeks, (2003) assess the vulnerability of urban earthquake hazard through multi-criteria analysis where a GIS methodology was developed to highlight the deficiencies of current GIS approach. A new method using fuzzy logic and spatial multicriteria analysis was incorporated to bring out the measures of urban vulnerability in Los Angeles County.

Earthquake intensity defines the strength of seismic shaking at a given location. Whereas an earthquake may just have a single magnitude, it will have different intensities at different locations. The earthquake intensities qualitatively describe the effects of ground shaking rather than the energy released. While an earthquake is described by a single magnitude, it produces a range of shaking intensities across an area. The intensity survey in any region after an earthquake provides information about the directivity, fault strike and attenuation characteristics. This has presented an opportunity to validate our current knowledge of earthquake risk in the region. Effects of earthquake are crucial in understanding the nature of hazard, its impact and extent of the risk exposure to the society opined by Prajapati *et al.*, (2013).

Sharifikia, (2010) estimated earthquake vulnerability assessment and risk mapping using fault identification on multispectral imageries and classified the risk area by applying different buffer over the fault location. High correlation between earthquake damages and area distance from epicentre exist where when the distance increase, damage and risk decrease. Prajapati *et al.*, (2013) using available data of September 18th, 2011 Sikkim earthquake obtained Modified Mercalli Intensity (MMI) to prepare earthquake intensity

map. Intensity depicts the effects of ground shaking which gives important information about the directivity, fault strike and attenuation characters. Comparison of attenuation relationship between Sikkim earthquake and other region has been drawn, and it was observed that attenuation in Sikkim earthquake is high and most of the damage was concentrated towards the southeast side of the epicentre.

HAZUS (Hazard US) is a comprehensive software tool developed by Federal Emergency Management Agency (FEMA) of the United States through the National Institute of Building Sciences (NIBS) to estimate potential losses from natural disasters. HAZUS provides a standardized methodology for assessing potential losses from earthquakes, floods and hurricanes. HAZUS is software to estimate damage and losses caused by natural disasters. HAZUS earthquake model is developed to provide a nationally applicable methodology for loss estimate of damages and loss to buildings, essential facilities, transportation and utility lifelines and population based on scenario or probabilistic earthquakes expressed by Ploeger *et al.*, (2010); Neighbors *et al.*, (2013); Erdik *et al.*, (2014) and Vahdani *et al.*, (2015)

HAZUS was originally developed to assist emergency response planners to supply the local, state and regional officials with the tools to stimulate and plan efforts to reduce risk from earthquakes and to prepare for emergency response and recovery from an earthquake. In HAZUS method, liquefaction, ground shaking, and landslides are the earthquake hazard models used. The ground motion in terms of Spectral Acceleration (SA) and Peak horizontal Ground Acceleration (PGA) are estimated based on their location, size and type of earthquake and local geology as described by Kircher (2003) and Guragain (2000).

Karaca and Luco (2008) explained, HAZUS buildings types are of three components are i) structural ii) drift-sensitive non-structural and iii) acceleration-sensitive non-structural components. Where the fragility functions are derived for each of these components for the four damage states considered that is slight, moderate, extensive and complete.

According to FEMA, (2003) building capacity curve known as a push-over curve, is a plot of a building's lateral load resistance as a function of a characteristic lateral displacement (i.e., a force deflection plot). It is derived from a plot of static-equivalent base shear versus building (e.g., roof) displacement. In order to facilitate direct comparison with earthquake demand (i.e. overlaying the capacity curve with a response spectrum), the force (base shear) axis is converted to spectral acceleration and the displacement axis is converted to spectral displacement. The building capacity curves developed for the methodology are based on engineering design parameters and judgment. Three control points that define model building capacity describe each curve; Design, Yield and Ultimate capacity curves respectively.

Structural damage fragility curves are expressed in terms of an equivalent value of PGA (rather than spectral displacement) for evaluation of Special buildings that are components of lifelines. Only structural damage functions are developed based on PGA, since structural damage is considered the most appropriate measure of damage for lifeline facilities. Fragility curves describe the probability of reaching or exceeding different states of damage giving peak building response. Structural damage fragility curves for buildings are described by median values of drift that define the thresholds into Slight, Moderate, Extensive and Complete damage states. HAZUS define the fragility curve for all the four damage states for number of buildings. These curves are developed in the form of lognormal probability distribution suggested by NIBS (2002). Vulnerability functions (or

fragility curves) of an element at risk represent the probability that its response to earthquake excitation exceeds its various performance limit states based on physical and socio-economic considerations opined by Hancilar *et al.*, (2010).

Panahi *et al.*, (2014); Sharifzadegan and Fathi, (2008); Hataminejad *et al.*, (2009) and BHRC, (1988, 1999, 2005) explained that building a structure involves the interaction of different groups, and each of them has the responsibility for different parts of that building. The quality of a structure depends on various factors, such as the level of the employer's education and income, the standards of structural design, the quality of materials used in the manufacture, and the insurance status of the structure. The longer a building's lifetime is greater is its vulnerability. Furthermore, according to Standard 2800, the amount of structural damage shows a step-linear function in an earthquake because the quality and the type of construction materials changed at each period during various editions of the regulations.

Peak building response (either spectral displacement or spectral acceleration) at the point of intersection of the capacity curve and demand spectrum is the parameter used with fragility curves to estimate damage state probabilities. Capacity curves hence, describe the displacement of push-over in each building type and seismic design level as a function of laterally applied earthquake load as characterised by FEMA, (2003).

Landslide, one of the most common hazard and most damaging leading to environmental and human impact are mass movement of rock and debris or earth down a hill slope pointed by Dhakal *et al.*, (2000); Mohamed *et al.*, (2016); Highland *et al.*, (2008) and Farrokhnia *et al.*, (2011). Influencing factor which can trigger instability in a slope can be due to intrinsic factors- geological conditions, morphology, slope and extrinsic variables such as rainfall, seismic, anthropogenic activities etc., (Wang *et al.*, 2005, and Shit *et al.*,

2016). The definition of landslide is diverse and it reflect the complex nature of various disciplines, such as geology, geomorphology and soil engineering discussed by Highland *et al.*, (2008) and Jebur *et al.*, (2014). Pareek *et al.*, (2014) mentioned that landslides occur when the conditions of geology are favourable for slope failures eg-steep slopes and low-strength soil, however it become worsen when unplanned civil construction activities take place in seismically active area. Landslide occurrence depends on complex interaction among large number of factors stated by Hong *et al.*, (2007).

The increasing popularity of GIS has lead to a majority of studies mainly using indirect susceptibility mapping. The database management system acts as the most powerful store house in GIS which is designed to store and manipulate the attribute data. The usage of GIS is very suitable for indirect landslide susceptibility mapping, in which all possible landslide contributing terrain factors are combined with landslide inventory map using data integration techniques estimated by Aleotti and Chowdury (1999); Bonham-Carter, (1994); Chung *et al.*, (1995). Landslide in general term is the down slope movement of soil and rock under the effects of gravity. Landslides are characterized by various continuous movements, sometimes with certain phases of reactivation. A low-intensity movement has annual mean velocity less than 2 cm/ year, medium intensity corresponds to a velocity ranging from 1 to approximately 10 cm/ year and high-intensity class is usually assigned to shear zones or zones with clear differential movements worked out by Cruden, (1991) and Lateltin *et al.*, (2005).

Satellite images offer larger spatial cover and are cheaper than aerial photo, the availability of commercial high resolution satellite imagery like IKONOS, Quickbird and World view has facilitated the study of building attributes for vulnerability assessment by Mueller *et al.*, (2006); Panagiota *et al.*, (2012) and Valero *et al.*, (2008). Wu *et al.*, (2014) with the help of high resolution remote sensing imagery extracted building attributes to

assess building seismic vulnerability through object based image analysis. Montoya, (2002) used high resolution imagery to delineate built-up area on the basis of texture, pattern, tone, size and shadows. Lidar provides rapid acquisition of data over widespread areas, ability to access rugged topography data from the inaccessible area, high-resolution DEMs generated from LiDAR, time, and accuracy with a cheaper production of DEMs in a long term are the advantages compared with traditional photogrammetric techniques.

Buildings extraction using advanced morphological operator in high resolution imagery method was devised, where it was observed that mathematical operators offer processing tools that are used to detect building anomalies. Besides high resolution imageries, Digital Elevation Model (DEM) was also used to extract information regarding building structures using pre-segmentation methods by Mayer, (1990); Kimand and Nevatia, (2004) and Lefevre and Weber, (2007). Age is also a significant factor in determining the strength of a building, Landsat satellite data was used to assess the age of buildings using change detection techniques by Taubenbock *et al.*, (2007).

GIS is an effective tool used commonly in mapping landslide susceptibility areas using different approaches and methodologies. Two main methods used in landslide assessment are qualitative method-which are direct hazard mapping techniques and quantitative method which are indirect method. GIS acts as a tool to model and predict landslide hazard spatially, where handling, interpretation and dissemination of data and their effect on landslide hazard can be cost cutting and efficiently accomplished with the use of GIS revealed by Mezughi *et al.*, (2011) and Lan *et al.*, (2004). Imagery with a spatial resolution of 10m or less, the buildings are detectable only on block level however with a resolution of 1m or better, more accurate information of building level damage is possible was stated by Dong and Shah (2013).

Remote sensing and GIS have revolutionized the domain of natural hazards. Geospatial database consists of different data types that are required to be transferred from one format to another because specific programs accept only specific data formats. GIS is capable of storing, analyzing, and showing geographic information making it possible to collect, organize, explore, model and view the spatial data for solving complex problems expressed by Jebur *et al.*, (2013a, b) and Barreca *et al.*, (2013). Scientists have started to develop new programs in hazard studies because of the vital role of early warning systems in such applications by Osna *et al.*, (2014) and Pradhan *et al.*, (2014). Different types of spatial data analysis range from the simple overlaying, to the more complex use of mathematical equations or combined statistical models for natural hazards prediction. The importance of GIS in catastrophic evaluation was proven through studies related to the GIS tools usage in various data exploration by Steiniger and Hunter (2013).

The use of GIS based techniques in landslide study has changed over time. Van Westen *et al.*, (1997) and Van Westen (2000) have differentiated various methodologies for susceptibility in GIS.

Empirical based approach which are suited for small scale regional survey. It depends on production of hazard map which are investigated and controlled by earth scientist responsible for the analysis outlined by Stevenson (1997) and Kienholz *et al.*, (1983)

- a) Statistical quantitative approach for medium scale survey or inventory based approach. It represents better relation between preparatory factors and landslide and lowers subjectivity level. In statistical approach the factors that lead to landslide occurrence in the past are determined statistically and quantitative predictions can be made for areas free of landslide. Statistical approaches are divided into

Multivariate and bivariate statistics. Multivariate approaches which are data-driven considers all the parameters at unstable sites using multi-regression techniques where the parameters are crossed with landslide and correlation is established between stable and unstable areas. One of the pioneer works in multivariate approach was started by Carrara *et al.*, (1977). Bivariate approaches are experience-driven statistical analysis. The parameters are crossed with landslide using different method- weight of evidence (Bonham Caretr *et al.*, (1988), landslide index method (Van Westen, 1993) and matrix method by De Graf and Romesburg (1980).

- b) Physical or process based approach which consists of slope stability analysis aimed at determining the factor of safety (Okimura and Kawatani, 1986 and Pack *et al.*, 1998).

Landslide study are work out indirectly through multivariate and bivariate statistical methods. In bivariate method for landslide assessment, weights are assigned to various factors based on statistical relationships between past landslide and various other factors. Multivariate method use equation where geo-environmental factors are the independent factors with coefficients maximizing the predictive capability of the model and independent variable is the present/absence of landslides (Ayele *et al.*, 2005 and Singh *et al.*, 2014).

Spatial relationship between landslide distribution and landslide controlling factors are the fundamental concept of bivariate analysis by Guzzetti *et al.*, (1999). Bivariate method assumes factors are independent and the influence of each factor is treated independently and is summed up. The susceptibility map is therefore controlled by the theoretical bases and assumptions made in the model by Carrara *et al.* (1999). In bivariate only the landslide detachment area is used as the factors which are held responsible for the

landslides are assumed to cause landslide in the future too. Nagarajan *et al.*, (2000) reported that bivariate discriminate function for grading and weighting of landslide illustrative variables can be efficiently considered to generate landslide susceptibility map.

Bivariate statistical analysis techniques can be used as a simple geospatial analysis tool to determine the probabilistic correlation among dependent variables (produced by using the inventory map of a hazard incidence) and independent variables (conditioning factors) containing multi-categorized maps by Oh *et al.*, (2011).

Bivariate approaches are considered to be robust and flexible methods, but they have several limitations. Limitations can include a loss of data quality and accuracy with oversimplification of input thematic data, as well as a loss of data sensitivity in forced individual analysis of causative factors analysed by Thiery *et al* (2007). The main concept of bivariate is to determine the relationship between spatial landslide distribution and landslide controlling factors evaluated by Khatsu and Van Westen (2005).

Information value method, a probabilistic approach based on the observed relationship between each factor with the occurrence of past and present landslide in the area described by Yin and Yan (1988). The information values are determined for each subclass of landslide in a given mapping unit (Pardeshi *et al.*, 2013). Information Value Method an indirect statistical method assesses landslide susceptibility in an objective way- it quantifies prediction of susceptibility by means of a score on terrain which are not even affected by slides. Information value method is an important bivariate statistical method used in LHZ mapping. Potentiality of landslide hazard is based on the various causative factors and the relationship between them which triggers the slope instability by Sarkar *et al.*, (2013).

Zeze (2002) stated that in Information Value Method “each instability factor is crossed with landslide distribution and weighted values based on landslide densities are calculated for each parameter class.” This method is also known as landslide index (Wi) method, in which the weighted value for a parameter class is defined as the natural logarithm of the landslide density in the class, divided by the landslide density in the entire map (Van Westen, 1997)

Information value model is a statistical analysis method which was developed from information theory and is now often applied to spatial prediction of geological hazards and disaster risk assessment expressed by Chen *et al.*, (2014); Sharma *et al.*, (2015) and Xu *et al.*, (2013).

Sreekesh, (2012) highlighted that a sound GIS provides the necessary tools to collect, collates, overlay, analyse, display the spatial information and help in taking decisions. GIS based landslide susceptibility mapping can be broadly divided into two categories; direct and indirect hazard mapping. According to Van Westen (2000) degree of hazard determines the experience and knowledge of terrain conditions is known as direct hazard mapping and hazard mapping which implies statistical models or deterministic models to predict landslide prone areas are indirect hazard mapping.

Raman and Punia, (2012) stated that GIS integrated with earth observation systems are useful to create spatial landslide inventories and related attributes for assessment of landslide hazard and susceptibility mapping. Ranjbar *et al.*, (2016) calculated earthquake loss estimation based on GIS approach using 0.5m Geo-Eye 1 imagery where GIS database on landuse, structural material and occupancy was prepared. The model estimated casualties based on two event- activity and inactivity of landuse based on population

residing in each building and according to time of earthquake, structure material and destruction percentage.

. Landslide susceptibility mapping provides valuable information concerning the stability conditions of the territory and serve as the first step in a hazard assessment towards the mitigation of natural landslide disaster outlined by Ladas, *et al.*, (2007). Tarolli and Tarboton (2006) found that landslide susceptibility prediction performance decreases at finer resolutions because too localized topography does not represent the processes governing landslide initiation. Catani *et al.*, (2010) found that the importance of landslide predicting parameters changed with spatial scale, and concluded that for some parameters, scale representing not local values but their trends should be evaluated. However, they did not conduct a concrete study to incorporate the variability of parameter importance at different scales for landslide susceptibility mapping. Landslide Susceptibility (LS) deals with the likelihood of landslide occurrence in an area on the basis of local terrain conditions remarked by Brabb (1984).

Identification of landslide prone areas through susceptibility assessment is essential to understand landslide phenomena and its relationship with various causative factors. By susceptibility it refers to the spatial future likelihood or probability for landslides to occur suggested by Harvas and Bobrowsky, (2009). Landslide susceptibility mapping is defined as the quantitative prediction of the spatial distribution of both landslide deposits and slopes described by Guzzetti *et al.*, (1999).

Landslide susceptibility can be defined as the probability of the occurrence of a landslide based on the relationship between the occurrence distribution and a set of predisposing factors, i.e. geo-environmental thematic variables in the area described by Guzzetti *et al.*, (2005). Landslide susceptibility mapping involves handling, processing and

interpreting a large amount of geographical data. The overlapping of landslide distribution with the causative factors can delineate the zones which are susceptible to landslide but not the probability of occurrence of the instability processes opined by Aste, (1991) and Tseng *et al.*, (2015).

International decade for natural disaster reduction (IDNDR) an initiative by the United Nations saw number of seismic risk assessment carried throughout the World. RADIUS (Risk Assessment tools for Diagnosis of Urban areas against Seismic disasters) a practical tool for preliminary estimation of the possible damage scenarios and for preparation of risk management plans for cities was developed by GHI, (2004). In Europe, RISK-UE lead to the development of assessing earthquake risk scenarios with focus on distinctive features of European cities including buildings and monuments revealed by Risk-UE, (2004). Bayraktarli and Faber, (2009) developed a method using Bayesian probabilistic networks (BPNs) which utilises the probabilistic description of potential future earth shaking intensity, a module on probabilistic assessment of spatial variability of soil liquefaction, a module on damage assessment of buildings and a fourth module on the consequences of an earthquake. Farsi *et al.*, (2015) presented a work to estimate the seismic vulnerability of existing buildings in Algeria. For this purpose, capacity curves were developed for the reinforced concrete buildings using push-over method.

Panikkar and Subramaniyan, (1997) carried out landslide hazard assessment using GIS based weighted overlay method in the area around Dehradun and Messori of Uttar Pradesh, currently Uttarakhand in India. The study revealed that rapid deforestation and urbanization have triggered landslides in the study area. Work based on multi-criteria decision such as Analytical Hierarchy Process (AHP) was used to study seismic urban vulnerability assessment where weights of criteria such as landuse, types of structure and density showed more weights. To improve the assessment other criteria such as geological

fault were added to increase its accuracy was highlighted by Shayannejad and Angerabi, (2014). Chiroiu, (2002) used IKONOS image to assess the damaged area and to rapidly assess the number of casualties in the affected area during the Bhuj (India) earthquake in 2001. Jagadish *et al.*, (2003) studied the behaviour of masonry structure during Bhuj earthquake 2001, it was observed that some of the traditional masonry structures had no earthquake resistant features and suffered considerable damage while some used earthquake resistant features like lintel band and corner reinforcement which had withstand the earthquake. Nagarajan *et al.*, (1996) has estimated landslide assessment in the Western Ghat, India using spatial and temporal remote sensing data and knowledge based GIS for data collection, integration and analysis of spatially-oriented data and finding relation between inherent relations between separate entities. Kohle *et al.*, (2007) studied the buildings and social vulnerability in GIS environment. The study highlighted that the vulnerability is dynamic and it should be assessed by taking its spatial and temporal aspect into consideration. Buildings type, age, height and its use has been taken as the basis to assess the degree of loss. Weight linear combination method as a multi criteria evaluation was applied to assign the weight for each factor by assuming that not all the factors are equally important for overall vulnerability. Human vulnerability was assessed on the basis of density of population and the vulnerability of building.

Singleton *et al.*, (2014) used TerraSAR-X for measuring slow moving landslide in the dense vegetated area of three Gorges, China. In the study, Sub-Pixel Offset Technique (SPOT) was applied to the corner reflectors using frequently acquired SAR images to quantitatively evaluate and compare the landslide monitoring. Van Westen (2006) in his study observed that the vulnerability to landslide is very much dependent on the spatial-temporal location and thematic characteristic of elements at risk. The study points out that determination of temporal vulnerability of element at risk is time consuming and might be

difficult to model. Shahabi and Hashim (2015) generated landslide susceptibility mapping using GIS based models such as Analytical Hierarchy Process(AHP), Weighted Linear Combination (WLC) and Spatial Multi-Criteria Evaluation (SMCE) where it was observed precipitation was most important among the factors. The number of causative factors to be used as input can hence change the output of the landslide susceptibility mapping depending on the conditional circumstances.

1.6 Organisation of Thesis

The thesis is divided into six chapters. The first chapter consists of introduction, statement of the problem, significance of the study area, objectives, research questions, methodology, and organisation of the thesis. The second chapter discuss the physical, administration and social set up of the study area. Physical and social parameters are seismicity, lithology, geology, drainage, climate, landuse, Municipal wards, population etc. The third chapter highlights about the urban classification and its building footprint of Kohima. Further it explains the different classification of the buildings and the building types according to HAZUS. The buildings of Ward no. 4 along with the sampling process of the other wards have been classified in accordance with HAZUS building code for vulnerability assessment. The fourth chapter explains the various steps and methods involved in the generation of parameters for the vulnerability assessment of earthquake hazard. It discuss about the ground motion parameters, building vulnerability and damage probability. It gives the results obtained from the HAZUS damage assessment. The fifth chapter depicts various methods for assessment of landslide hazard. Further this chapter focus on generating landslide hazard models and also computing landslide susceptibilities. The last chapter deals with the summary and conclusion of research work being carried out.

2

2.1 Introduction

Kohima, the capital of Nagaland was established initially as a chief administrative centre by the British government on July 1878 to control and monitor the Angami Naga area and the frontiers of Manipur. In 1881, the district of Kohima was established by the British regime as a subdivision of former Naga Hills districts. Kohima witness one of the greatest battles during the World War II- the Battle of Kohima (Photo plate 1). The Battle of Kohima was referred as the “Stalingrad of the East”, it was a turning point of the Japanese “U Go” offensive into India in 1944. Nagaland became a fully fledged state with Kohima as its Capital on 1st December, 1963. Kohima is one of the oldest township in Nagaland, started its civic body known as Kohima Town Committee (KTC) in 1957. With the enactment of Municipal Act 2001, the erstwhile KTC was upgraded to Kohima Municipal Council (KMC) in 2004. With this historical background, the morphological structure in Kohima has grown from an administrative centre to a Smart City (2016). The

study area covers nineteen municipal wards of Kohima and outer ward of Kohima Town. Its geographical extents are 94°05'04'' E and 94°07'23'' E latitude and 25°38'28'' N and 25°39'24''N longitude with an average elevation of 1444m above MSL. The geographical extent of the study area covers 14.03 km² spatially.

2.2 Geology of North East Region of India

Geologically, it comprises generally of the Disang shales in the north and northeastern part and Barail sandstone series mainly delineate the south and south western part of the study area. According to Bureau of India Standard (BIS) classification Kohima Town tectonically is active and it comes under seismic zone-V.

Table 2.1. Stratigraphy of Nagaland

Age	Group	Litho-formations		
Oligocene	Barail	Renji	Tikak Parbat	Jogi/ Phokphur Formation Tuffaceous shale, sandstone, greywacke, grit and conglomerate. Minor limestone and carbonaceous matter
		Jenam	Baragolai	
		Laisong	Naogaon	
Upper Cretaceous-Eocene	Disang	Upper		Shale/ Slate/ Phyllite with calcareous lenses in basal sections and invertebrate and plant fossils in upper sections with brine springs
		Lower		

Source: Mathur and Evans, (1964), and Ghose *et al.*, (2010).

The stratigraphy of Nagaland explains Barail sandstone (Photo plate 6) and Disang groups of rock make the lithostratigraphy of the study area. Barail sandstone groups occurred under the age of Oligocene series and Disang group of shales are of Upper Cretaceous-Eocene series (**Table 2.1**).

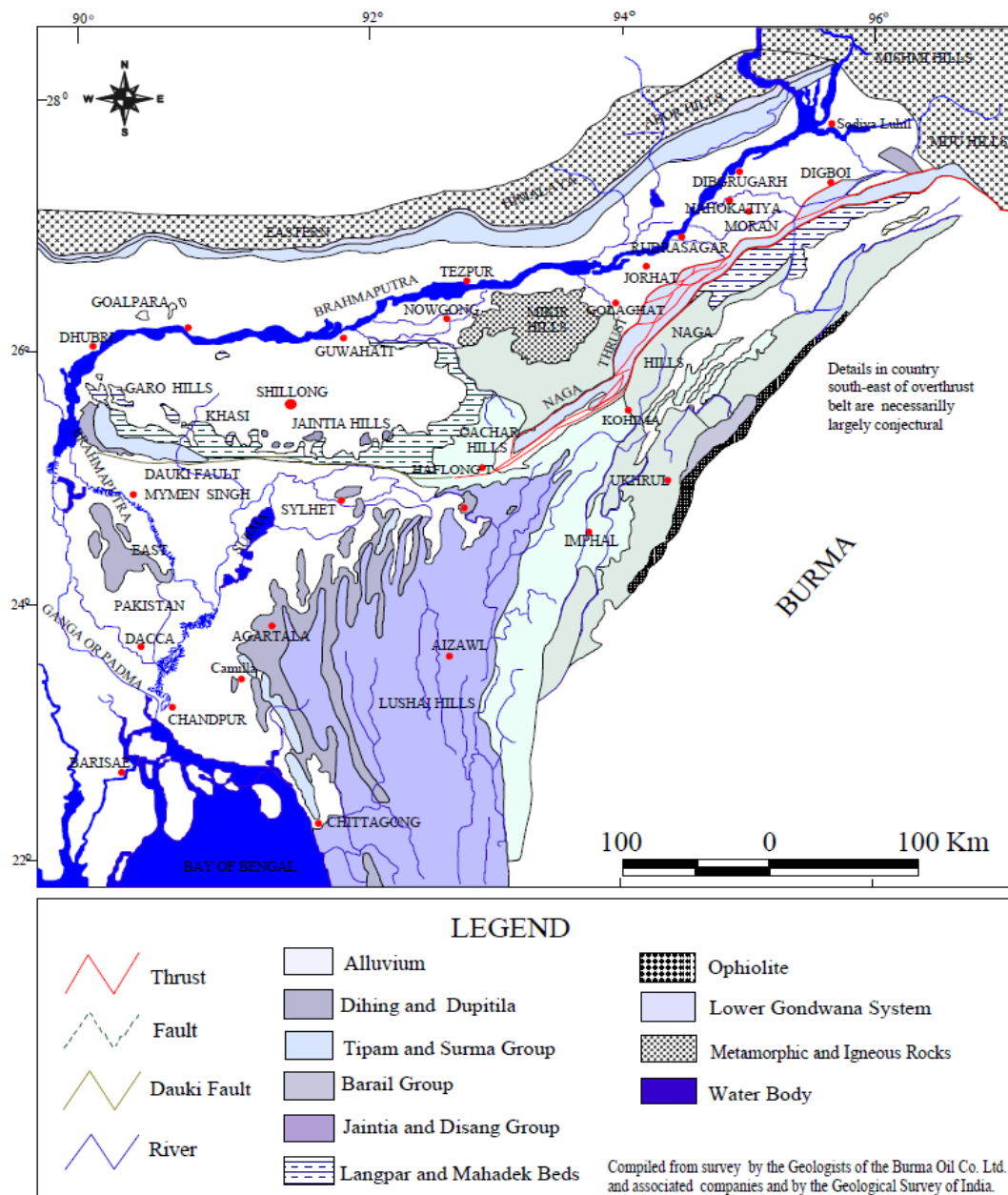


Figure 2.1: Tectonic stratigraphy of Northeast India (Mathur and Evans, 1964)
Source: Geologist of the Burma Oil Co. Ltd and associated companies and by the Geological survey of India

The first stratigraphy and tectonic map of Nagaland was drawn by Mathur and Evans (1964). The geological setting of Nagaland consist of four main tectonic-stratigraphy; Metamorphic complex, Naga Hills Ophiolite, Inner Fold Belt and Belt of Schuppen. Kohima the study area lies in the Inner Fold Belt (IFB) (**Figure 2.1**).

The Inner Fold Belt lies between Disang thrust on the west and Naga Hill Ophiolite on the east. Splintery shale interbedded with sandstone (Photo plate 4) form lithology of the study area. The sequence of sandstone and shale are primarily exposed in Kohima Synclinerium. Disang shales are splintery with thin quartz vein and serpentine intrusion. Due to active tectonic plate movements, high stress was observed in rock outcrops (Photo plate 3 & 5).

2.3 Seismicity of Northeast region of India

The entire study area falls under seismic zone-V which makes it vulnerable to earthquake related hazard. From past records, no major earthquake has occurred in the study area. However, Northeast India is not new to seismic activities as in the past four major earthquakes has occurred (Kaya *et al.*, 2006) (**Figure 2.2**). Recent earthquake occurrences observed near the study area is in Phek and in Manipur, western part. Phek earthquake occurred on 15th July, 2012 at 01:25 Am 24 km South of Phek, its epicentre was located 43 km ESE of Kohima (**Figure 2.3**). The magnitude of the earthquake was 5.6 and epicentre was at a depth of 6.5 km (Vervaeck and Daniell, 2012).

Manipur earthquake occurred on 03rd January, 2016 as a result of strike slip faulting in the complex plate boundary between India and Eurasian plate. The magnitude of the earthquake was 6.7 located 119 km away from Kohima, epicentre was at a depth of 55 km (**Figure 2.4**). The earthquake was felt in Kohima however no casualties or damage was sustained (USGS, 2016).

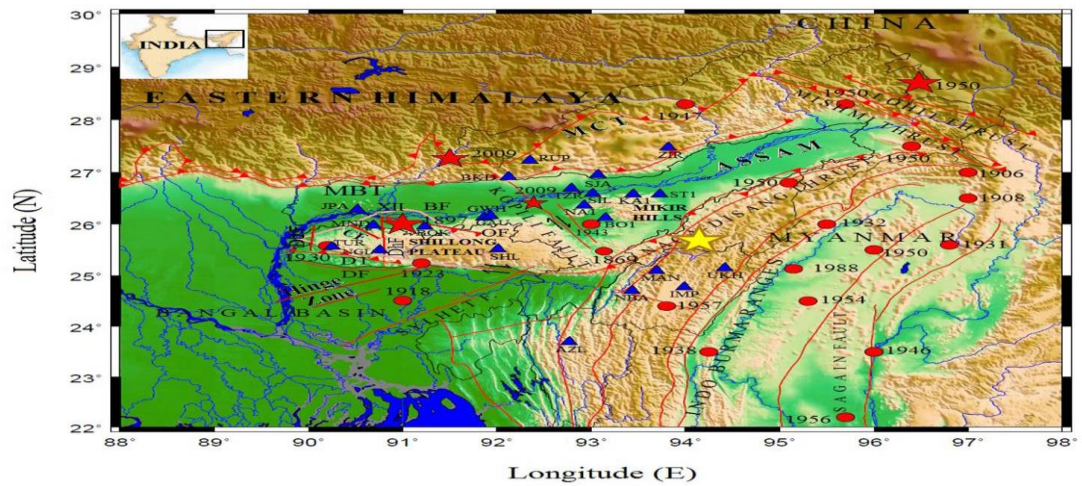


Figure 2.2: Earthquake event in Northeast India
Source: Kayal *et al.*, 2006.

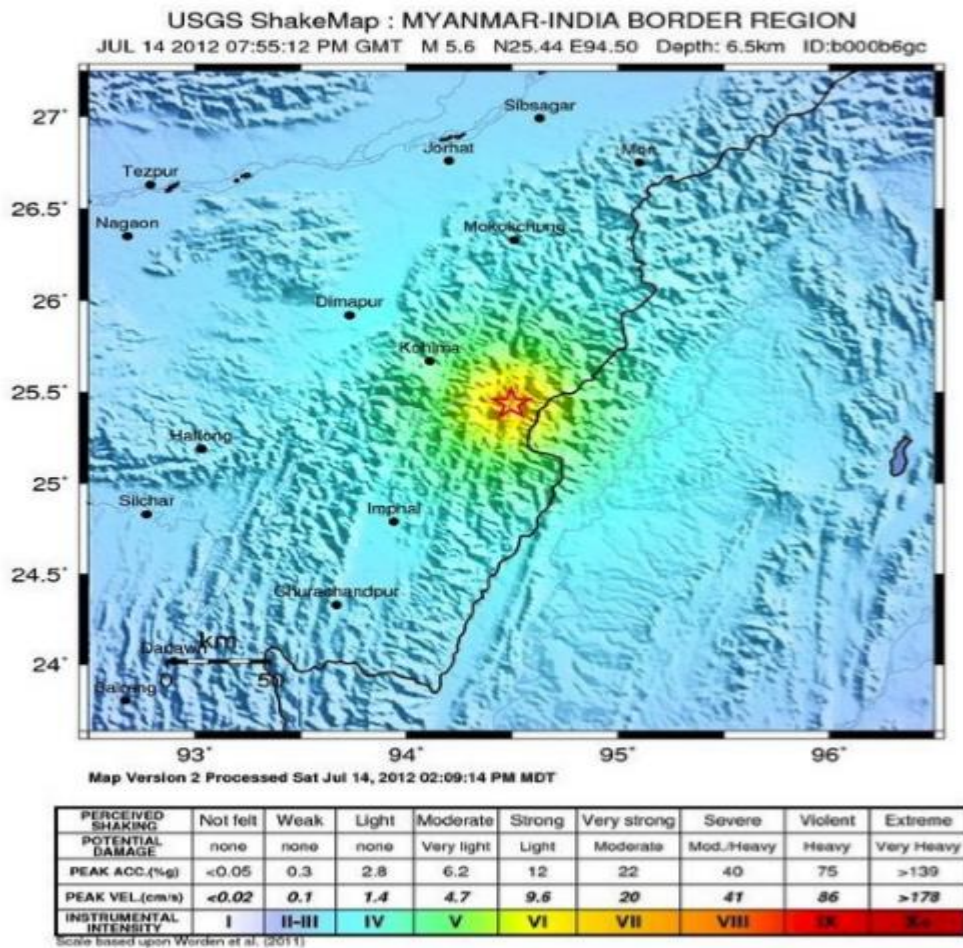


Figure 2.3: Phek earthquake
Source: Vervaeck and Daniell, 2012.

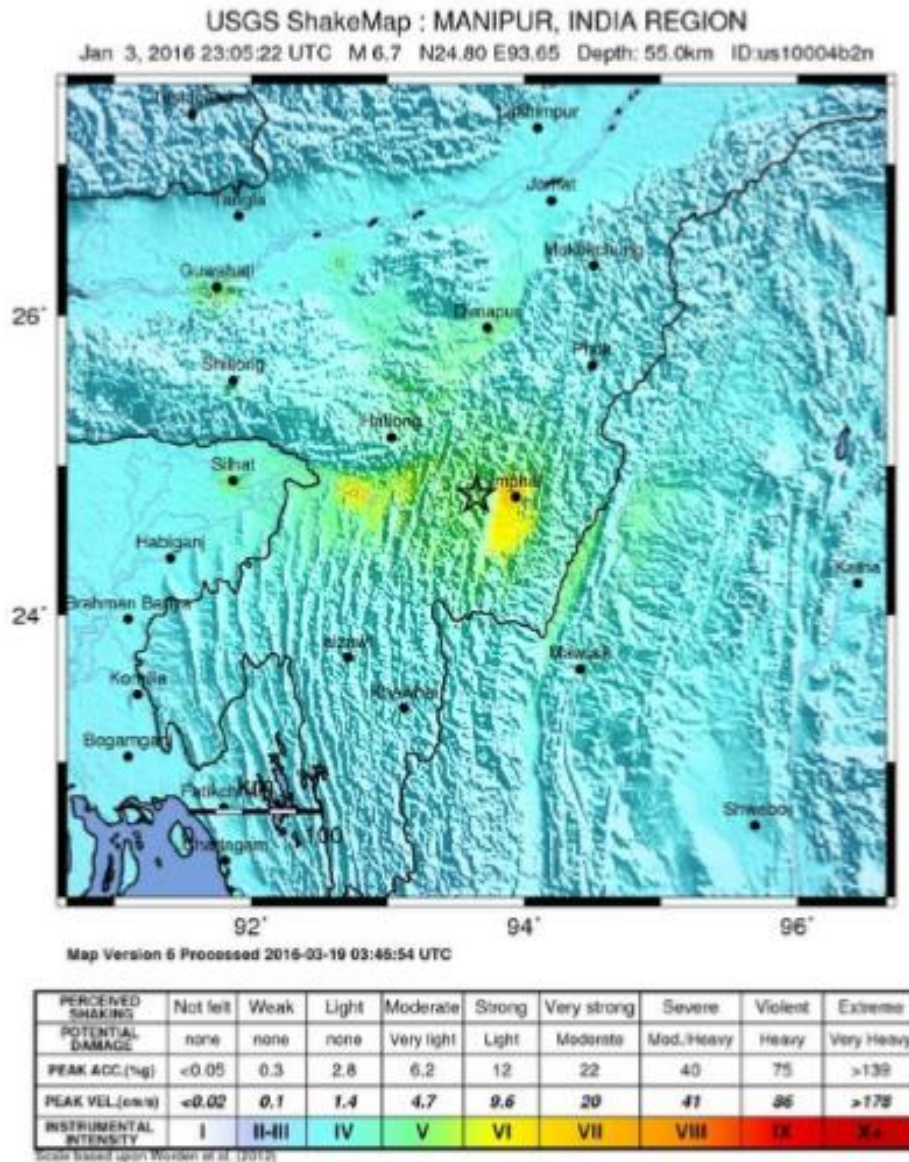


Figure 2.4: Manipur earthquake (USGS, 2016)

2.4 Climate of Kohima Town

Kohima experience a pleasant climate, summer is pleasantly warm and winter cold. Average maximum temperature was 23.49 °C in 2014 and average minimum temperature was 11.43 °C in 2013. Highest dew point was recorded in the year 2015 and lowest was in 2011. In 2013, the annual rainfall recorded was 1749.1 mm in 151 rainy days and an average rainfall was 1552.2 mm from 2011 to 2015. An average of 146 rainy days are observed by comparing 2011 to 2015 (**Table 2.2**).

Table 2.2. Climatic parameter of Kohima town (2011 to 2015).

Parameters	Year				
	2011	2012	2013	2014	2015
Average Maximum temperature (°C)	22.28	22.64	23.73	23.49	23.22
Average Minimum temperature (°C)	11.77	11.69	11.43	13.55	12.74
Average Dew point(°C)	12.36	13.86	13.46	16.01	18.25
Average Relative humidity (%)	65.39	68.58	65.15	73.72	83.13
Annual Rainfall (in mm)	1735.8	1370.7	1749.1	1383.3	1522.1
Number of rainy days	141	146	151	142	149

Source: Compiled by Scholar

2.5. Population distribution of Kohima town

The present study consists of nineteen wards and outward ward including Kohima village. Population was 1,14,773 where 99,039 was distributed by the nineteen wards remaining 15,734 population was contributed from outer ward including Kohima Village (Census, 2011). The population growth of Kohima town from 1901 to 1961 was less than 10,000. However, from 1961 onwards, the population has increase rapidly and number of wards has also increased (**Table 2.3**). One of the reasons for the rapid increase in population is due to the declaration of Statehood and state Capital which made Kohima an attractive hub for others to settle down in Kohima.

2.5.1 Decadal wise growth of population

The population of Kohima town during 1901 was 3,093 (**Table 2.3**). By 1911, the population growth decline that is 2,423 and the decadal growth of population shows in negative growth value about -21.7%. In 1921, the growth was increased to 2,790; the decadal growth was 15.1. In the year 1931 the population growth declined dramatically in negative growth value about -1.1%. During 1941, the population of Kohima town was

3,507; the decadal growth was 27.1. Again in 1951 the population growth decline about 17.6%. In 1961 the population was about 7,246 and the decadal growth 75.7%. During 1971 the population growth was immensely increased about 21,745. The decadal growth was 200%. During 1971 to 2011, population growth gradually increased from 7,246 to 99,039 but in 1981 the decadal wise population variation suddenly fell from 200% (1971) to 57.9%. From 1981 to 2001 the decadal population growth steadily grew, but in 2011 population growth was 28.6% only.

2.5.2 Decadal wise population density

In 1901, the population density of Kohima town was 220 person per sq.km. Population density person per sq. km during 1901 to 1931 slowly declined. From 1941 to 2011, the population density tremendously increased about 250 to 7059 person per sq. Km (Table 2.3).

Table 2.3: Decadal wise growth of population in Kohima Town

Year	Population	Ward	Decadal Variation	% of decadal variation	Density of population (per sq.km)
1901	3,093	NA			220
1911	2,423	NA	-670	-21.7	173
1921	2,790	NA	367	15.1	199
1931	2,759	NA	-31	-1.1	197
1941	3,507	NA	748	27.1	250
1951	4,125	NA	618	17.6	294
1961	7,246	NA	3,121	75.7	516
1971	21,745	8	14,499	200.1	1550
1981	34,340	9	12,595	57.9	2448
1991	51,418	15	17,078	49.7	3665
2001	77,030	15	25,612	49.8	5490
2011	99,039	19	22,009	28.6	7059

Source: Scholar computed according to Census of India, 2011

Municipal ward in Kohima was initiated during the 1970s' with eight wards and decadal variation in population was 200.1%. After a decade, it was increased to nine wards with decadal population variation of 57.9%. Fifteen wards were introduced in the 1990s'

with a variation of 49.7%, ward number remain the same in 2001s' with 49.8% and in the last decade the wards were increased to nineteen with variation of 28.6% (**Table 2.3 & Figure 2.5**).

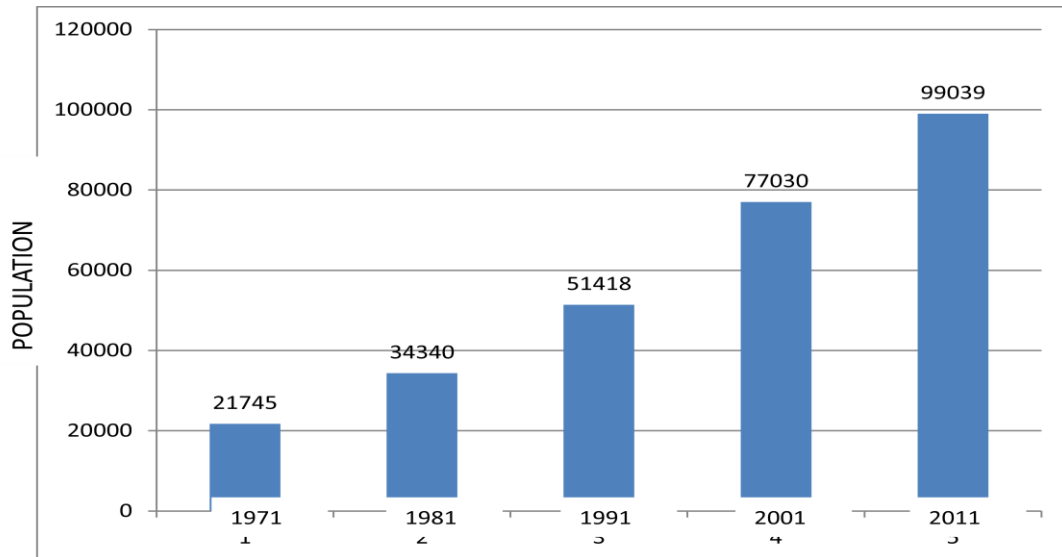


Figure 2.5: Decadal growth of the Study area

Source: Scholar computed according to Census of India, 2011

2.5.3 Ward-wise distribution of population

The study area comprises of nineteen wards and an outer ward. Among the wards in the municipal, the highest population was observed in ward number 16 and the lowest was shown in Ward number 8. The outer ward has a population of 15, 734 with 7,818 males and 7,916 females. The sex ratio between male and female in the study area was 107.44 (**Table 2.4 & Figure 2.6**).

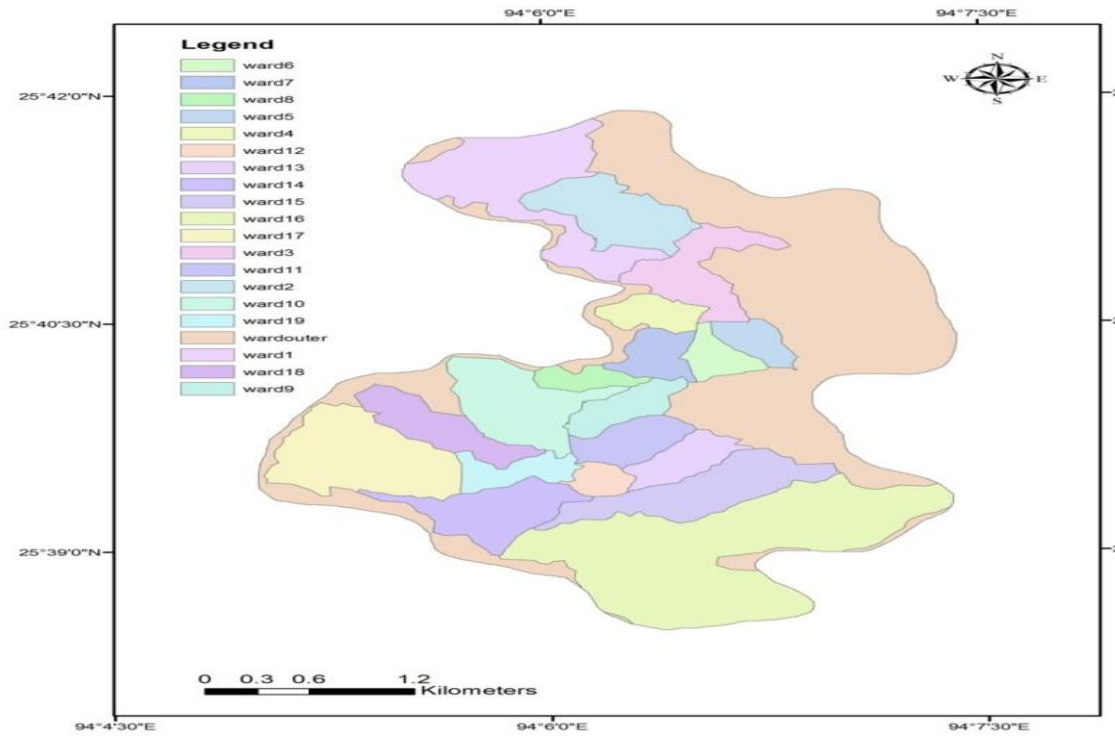


Figure 2.6: Location of municipal wards in the study area.

Table 2.4. Ward-wise distribution of population along with geographical area and density of population

Area	Geographical area	Population	Density of population (per hectare)
Ward 1	7082	7082	3383
Ward 2	5207	5207	2626
Ward 3	5692	5692	2800
Ward 4	3568	3568	1674
Ward 5	3197	3197	1640
Ward 6	5381	5381	1992
Ward 7	2721	2721	1205
Ward 8	2348	2348	1134
Ward 9	4808	4808	2218
Ward 10	4820	4820	2308
Ward 11	5267	5267	2613
Ward 12	3848	3848	1912
Ward 13	3228	3228	1663
Ward 14	6101	6101	2858
Ward15	7970	7970	3845
Ward 16	11603	11603	5776
Ward 17	7775	7775	3792
Ward 18	4809	4809	2308
Ward 19	3614	3614	1666
Periphery	15734	15734	7916

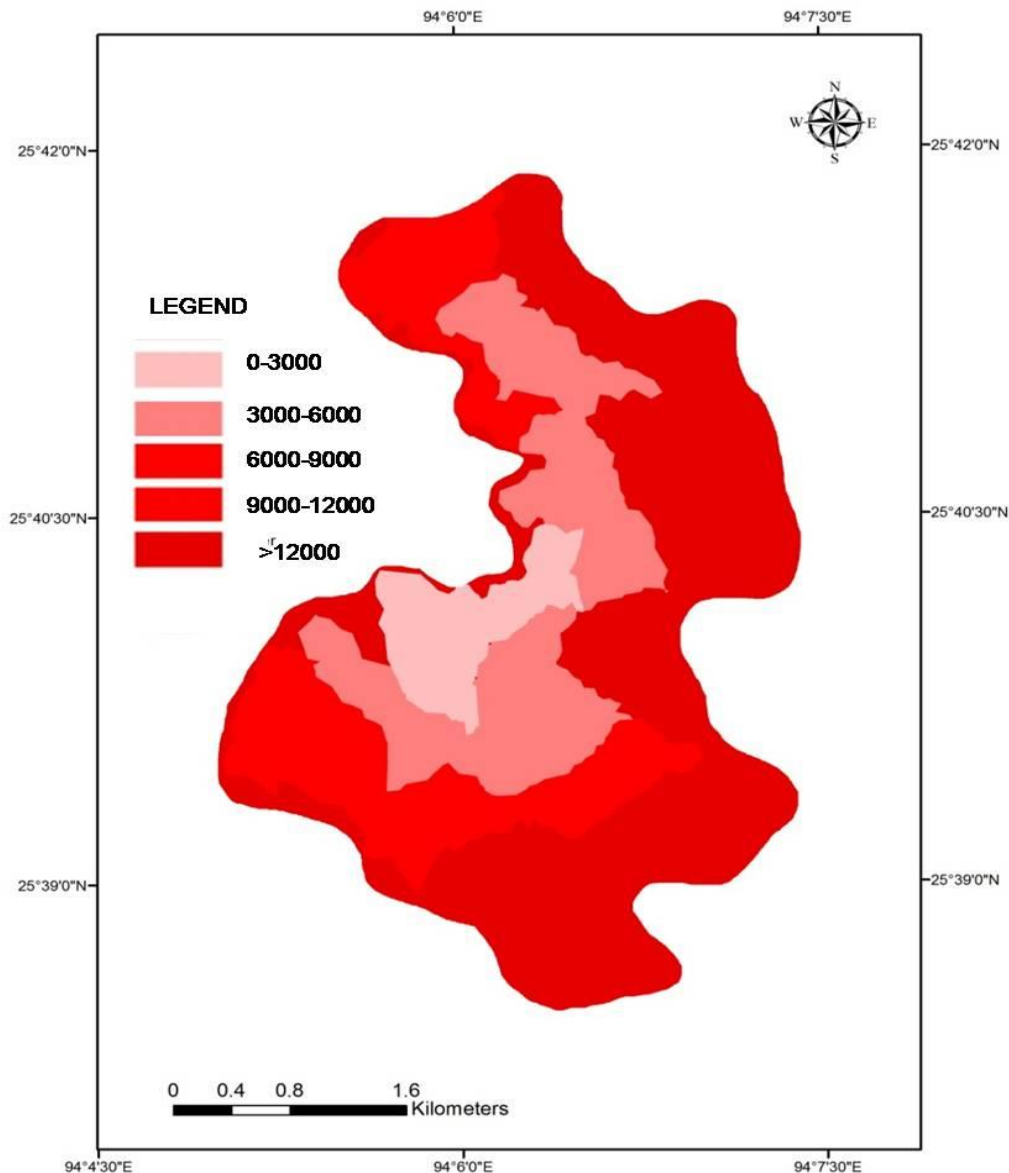


Figure 2.7: Ward wise population distribution map

2.5.4 Ward-wise male, female and gender ratio distribution

The total population of Kohima Town and outer ward including Kohima village was 1, 14,773, out of this, population of male is 59,444 (51.8%) and female is 55,329 (48.2%). The ward wise distribution of population showed that minimum of 2,348 (6.2%) was occupied in ward no. 8 and maximum population of 15,734 (13.7%) was found in outer ward (**Table 2.6 &Figure 2.7**).

The maximum population of male was concentrated in outer ward (7818) and minimum population of female was concentrated in ward no. 8 (1214). The maximum percentage of male and female ward-wise occupied in ward no. 6 (37%) and ward no.13 (52%). The minimum percentage found is in ward no.13 (48%) and ward no.6 (37%) respectively. The gender ratio as female per 1000 male showed ward no. 2, 5, & 13 and outer ward exceeding more than 1000 and much variation in gender distribution is showed in ward no. 6 (588 female per 1000 male) (**Table 2.6**).

Table 2.6. Ward-wise male, female and gender ratio

Ward	Total population	Percentage of total population	Male	Percentage of male	Female	Percentage of female	Gender ratio (female per 1000 male)
Ward 1	7082	6.2	3699	52	3383	48	915
Ward 2	5207	4.5	2581	50	2626	50	1017
Ward 3	5692	5	2892	51	2800	49	968
Ward 4	3568	3.1	1894	53	1674	47	884
Ward 5	3197	2.8	1557	49	1640	51	1053
Ward 6	5381	4.7	3389	63	1992	37	588
Ward 7	2721	2.4	1516	56	1205	44	795
Ward 8	2348	2	1214	52	1134	48	934
Ward 9	4808	4.2	2590	54	2218	46	856
Ward 10	4820	4.2	2512	52	2308	48	919
Ward 11	5267	4.6	2654	50	2613	50	985
Ward 12	3848	3.4	1936	50	1912	50	988
Ward 13	3228	2.8	1565	48	1663	52	1063
Ward 14	6101	5.3	3243	53	2858	47	881
Ward15	7970	6.9	4125	52	3845	48	932
Ward 16	11603	10.1	5827	50	5776	50	991
Ward 17	7775	6.8	3983	51	3792	49	952
Ward 18	4809	4.2	2501	52	2308	48	923
Ward 19	3614	3.1	1948	54	1666	46	855
Outer ward	15734	13.7	7818	49.7	7916	50.3	1013
Total	114773		59444	51.8	55329	48.2	931

Source: Computed by scholar according to Census, 2011.

2.5.5 Ward-wise household population distribution

Ward wise population in 2011, 2001 and 1991 were about 25,686, 18,311 and 12,242 respectively. Number of household population gradually increases from 1991 to 2011. (Table 2.7 & Figure 2.8).

Table 2.7. Ward wise number of Household population

Area	Number of house hold
Ward 1	1524
Ward 2	1127
Ward 3	1262
Ward 4	860
Ward 5	757
Ward 6	1181
Ward 7	691
Ward 8	555
Ward 9	1221
Ward 10	1133
Ward 11	1215
Ward 12	918
Ward 13	666
Ward 14	1359
Ward 15	1718
Ward 16	2437
Ward 17	1716
Ward 18	1127
Ward 19	845
Outer ward	3374

Source: Computed by scholar according to Census, 2011

The recorded number of household population was highest in outer ward (3374) followed by ward no. 16 (2437) and ward no. 15 (1718). The minimum household population was found in ward no. 8 (555) followed by ward no. 13 (666).

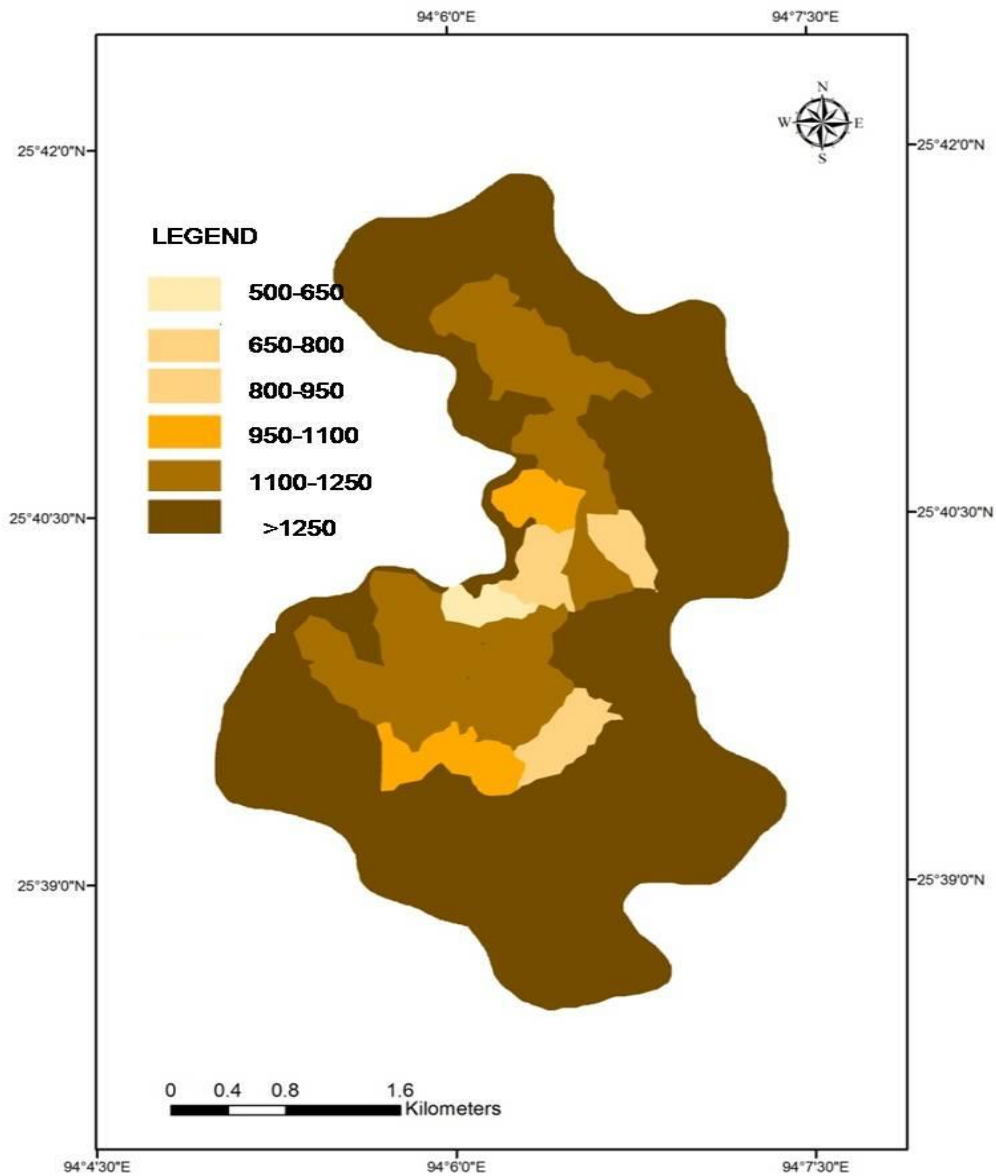


Figure 2.8: Ward wise household population in Kohima

2.6 Topography of Kohima town

Kohima is situated on the foothills of Japfü range (Photo plate 2). The topography of Kohima shows a moderate slope, where the southern part show higher elevation than the northern part. The present study exhibit highest elevation is approximately 1747 m above MSL. The longitudinal profile of the study area trends in north-south direction. Population has expanded towards the north and south eastern parts of the study area. Figure shows the cross profile picture of the section.

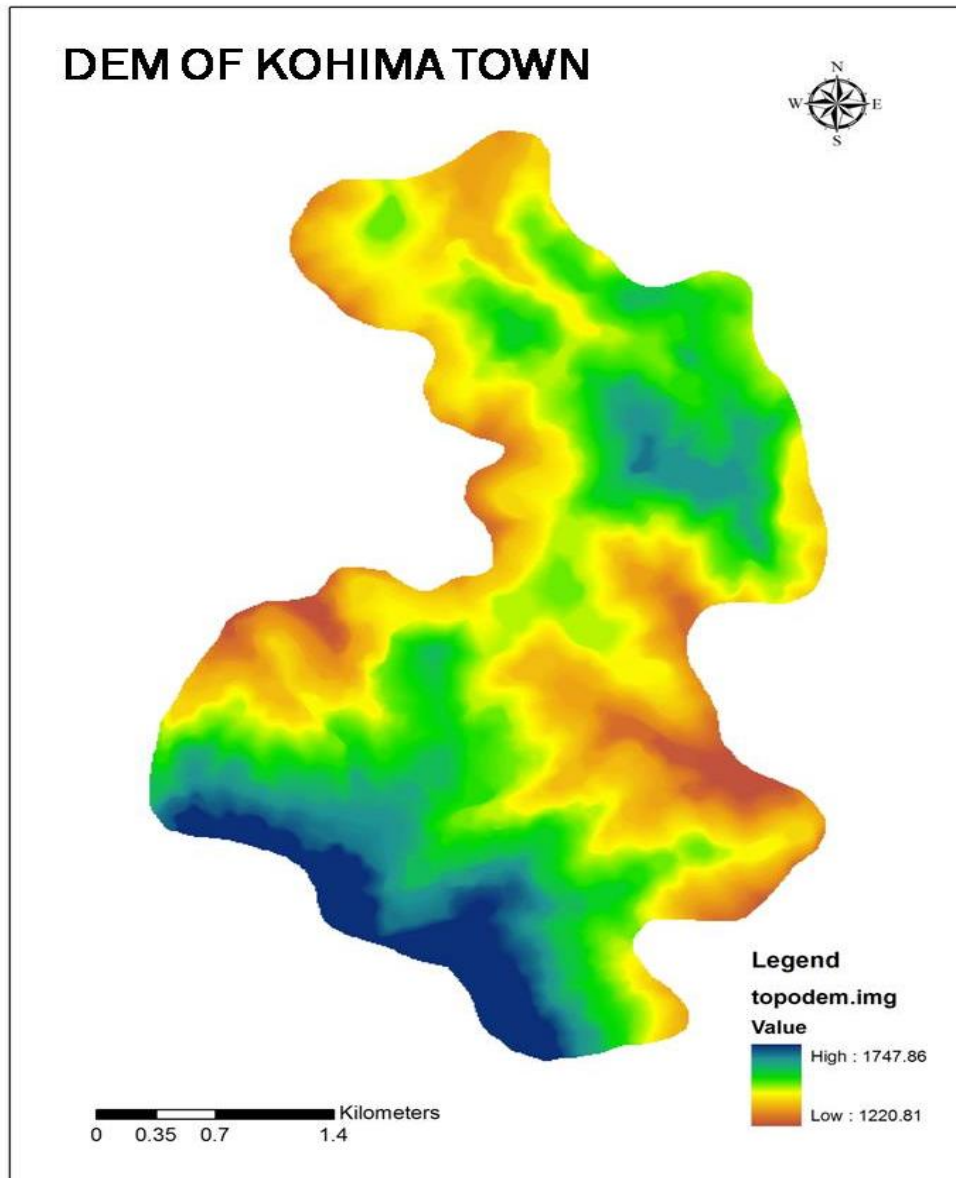


Figure 2.9: Digital Elevation Model of Kohima

The Digital Elevation Model (DEM) of Kohima has highest elevation at the range of 1747 m above msl and lowest elevation is 1220.61 m above msl. The southern part of Kohima is higher in elevation than the northern part (**Figure 2.9**).

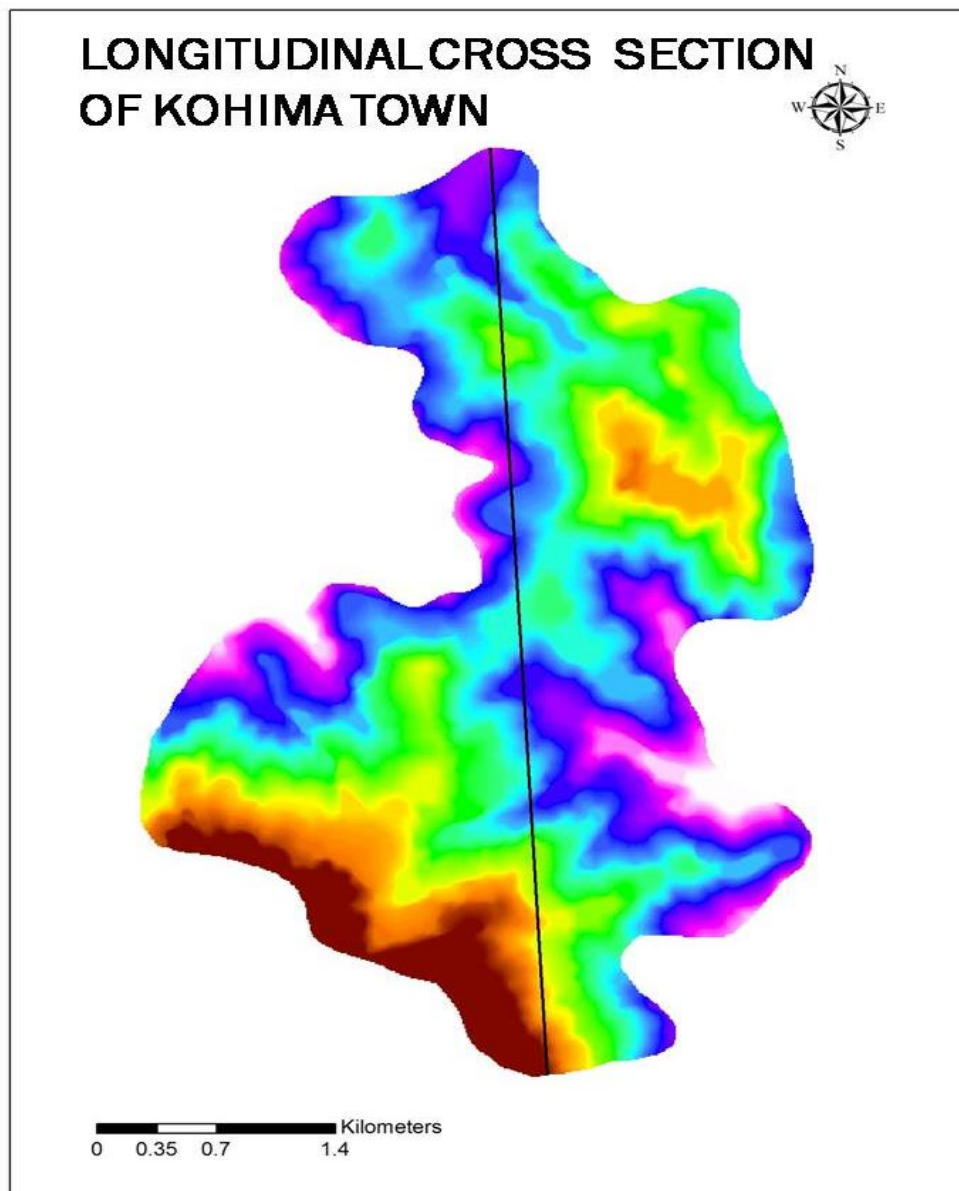


Figure 2.10. Longitudinal profile of Kohima town.

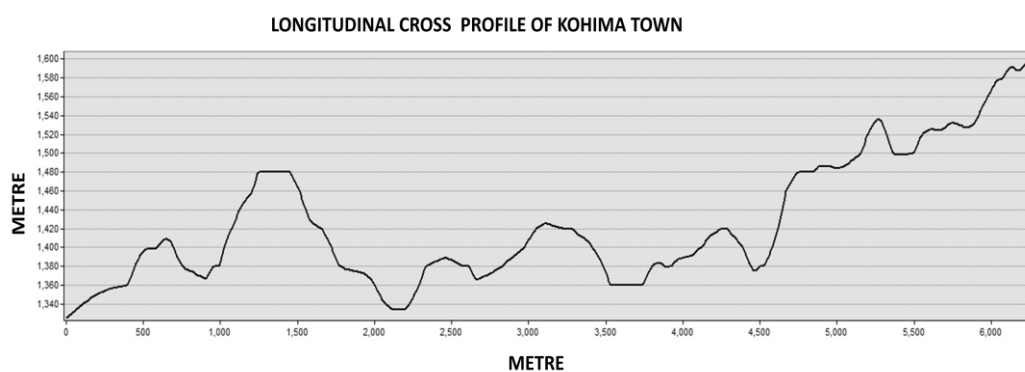


Figure 2.11: Longitudinal cross profile of Kohima town

The cross section of longitudinal profile extends from left to right where the right profile representing the southern part of the digital elevation model increases in height as it progresses. The left cross section profile height reduces towards the left portion of the relief profile (**Figure 2.10 & 2.11**).

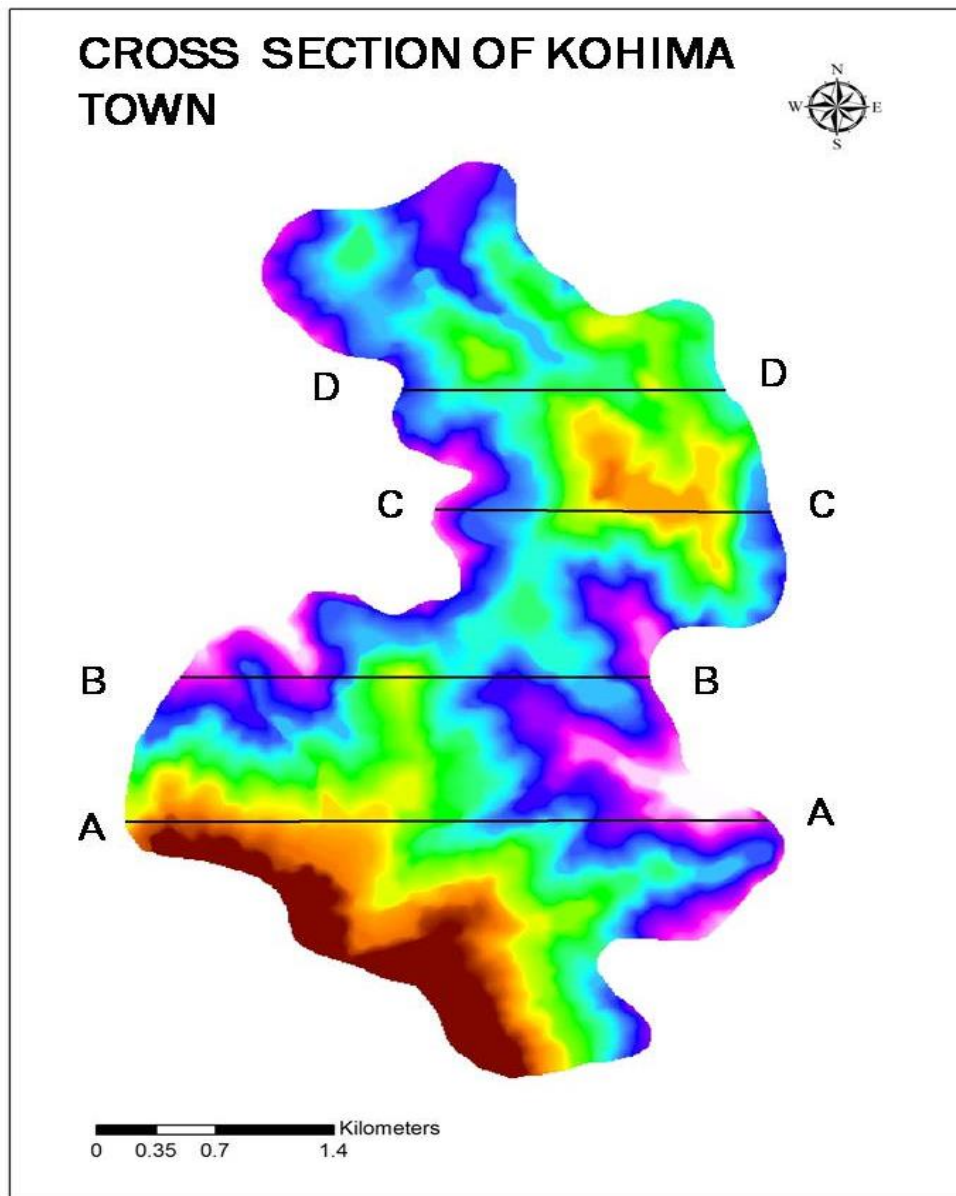


Figure 2.12: Cross sectional profiles of Kohima

The cross section profile of Kohima was studied using four axis (A axis, B axis, C axis and D axis). The cross profile 'A' of Kohima located to the south part show a rolling elevated profile. Cross profile 'B' show elevated and steep topography. Cross section

profile 'C' show an elevated topography. Cross section profile 'D' show an elevated towards the right portion of the profile. The general description of the profiles shows an elevated topography (**Figure 2.12**).

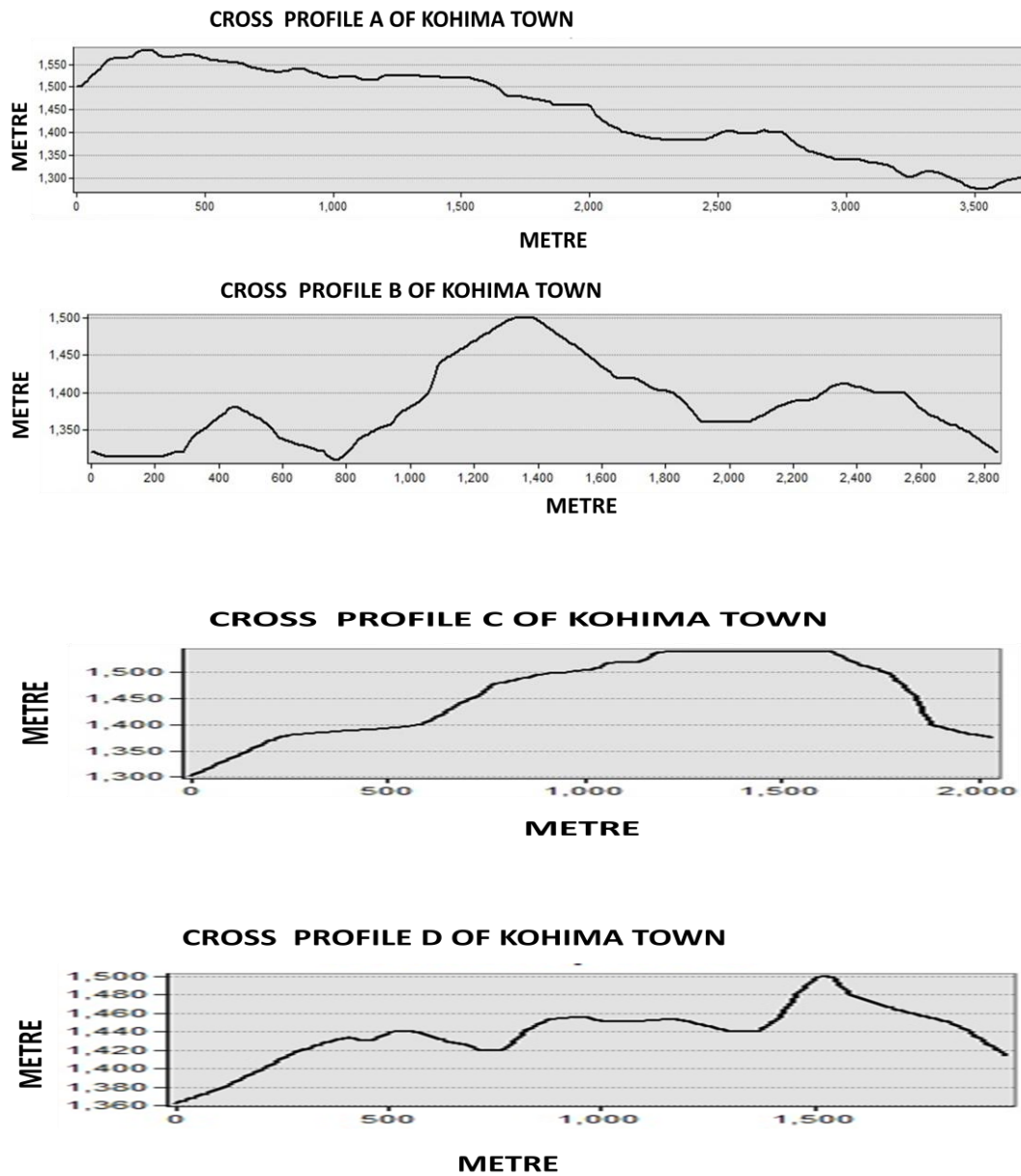


Figure 2.13: Cross Profile of A,B,C and D representing elevation of Kohima.

The topography of cross profile 'A' shows that the western part is higher in elevation compared to the eastern part. The profile showing 'B' represents an elevated middle portion with sloping sides on both sides a gentle rolling ridge. Profile 'C' shows the eastern part is higher in elevation with a raised top. Profile 'D' shows undulations on the cross profile of the area, where the western part shows another mount. Overall, the topography from the cross profile shows a rugged rolling hill with gentle slopes. Therefore, land utilisation for settlement is high except in few places where the slope is steep making it unfavourable. The expansions of buildings on all fronts have made the topography susceptible to slope failure (**Figure 2.12 and 2.13**).

2.7 Landslide distribution of Kohima Town

Landslides are related to geo-environmental factors such as geology, topography and hydrologic factors, which will help to generate landslide susceptibility maps. The important parameters are geology, lithology, drainage, landuse land cover etc., and it depends on data availability of any particular region (Yalcin, 2008). The landslide distribution map has been mapped using field and image interpretation of the study area. About 66 small and large scale landslides were observed in the study area. The Landslides are mostly observed in the geologically weak structural zones towards the central part of the study area. The geographical area under landslide susceptibility is 0.33 km² out of the total geographic area of 14.03 km² (**Figure 2.14**).

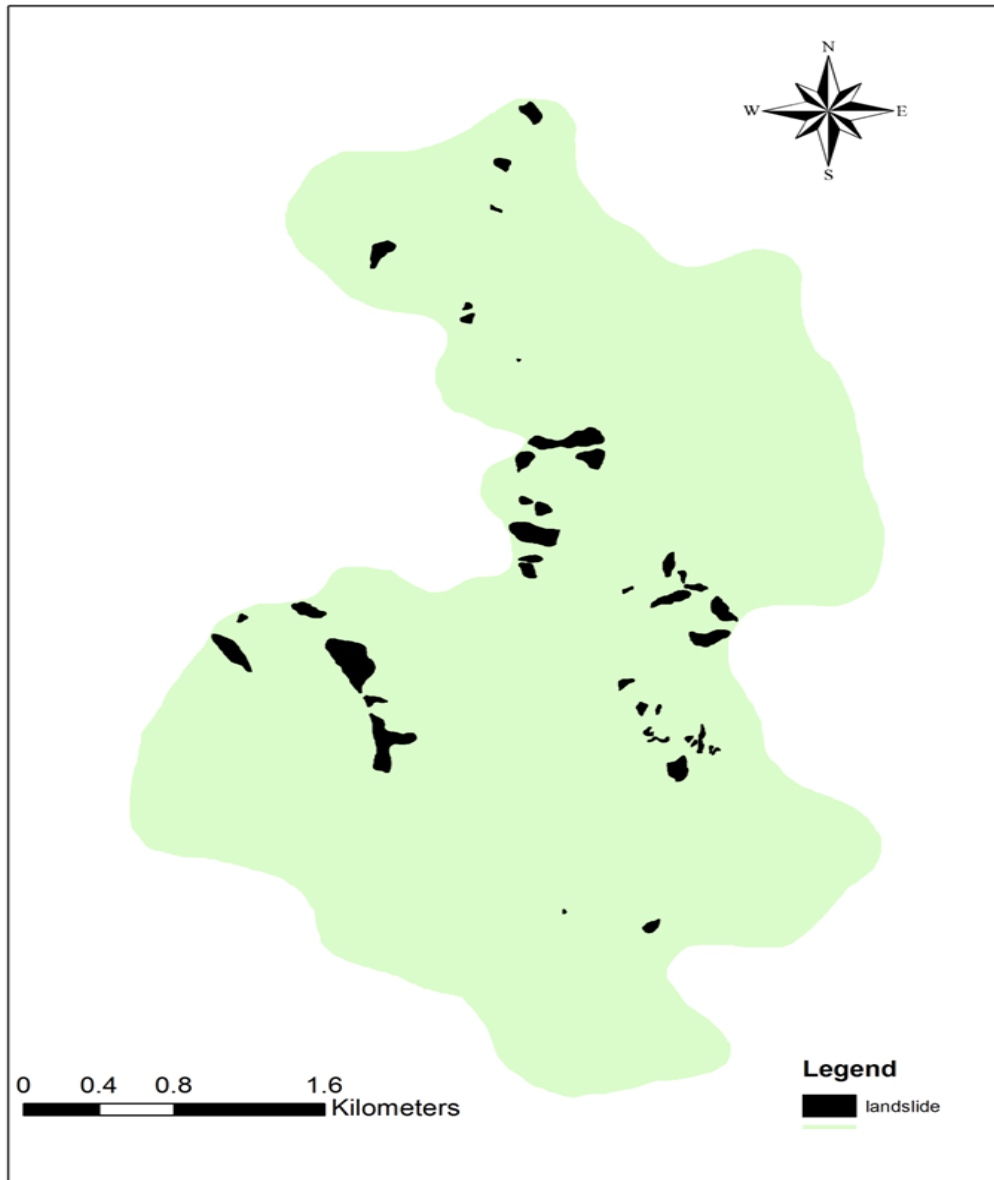


Figure 2.14: Landslide distribution map of Kohima.

2.7.1 Topographic parameter

The topographic parameters deal with the general physical aspect of a region. Topographic parameters for the study have been derived from the digital elevation model generated from 20m contour interval. Slope aspect and slope angle has been derived using Arc GIS software to correlate the phenomena of landslide and the topography of the study area. Topographical factors in landslide studies are commonly considered as major factor controlling landslide occurrences and ground movement processes. Terrain derived from

DEM datasets using GIS application is an effective way to provide the various landform characteristics with available information and is time effective.

2.7.1.1 Aspect

Aspect has an effect on the exposure to sunlight and wind, which affect other factor such as flora distribution, degree of saturation and evapotranspiration of the slopes and soil thickness (Ladas et al. 2007). Aspect determines the direction of maximum slope of the terrain surface and also influences the occurrence of landslides. Aspect can influence the distribution and density of landslides by controlling the concentration of soil moisture (Wieczorek *et al.*, 1997). It is generally considered that larger numbers of landslides occur in the wetter north facing aspect than the drier south facing aspect (Lineback *et al.*, 2001). The frequency of landslide is expected to be higher on north and northwest facing slopes than the east facing and southeast facing slopes due to decreasing wetness. The aspect map in the study area is divided into nine classes ranging from -1 to 337.5°. The aspect classes categorised into nine classes as follows; Flat (-1), North (0 - 22.5°), Northeast (22.5° - 67.5°), East (67.5° - 112.5°), Southeast (112.5° - 157.5°), South (157.5° - 202.5°), Southwest (202.5° - 247.5°), West (247.5° - 292.5°) and Northwest (292.5° - 337.5°) (**Figure 2.15**).

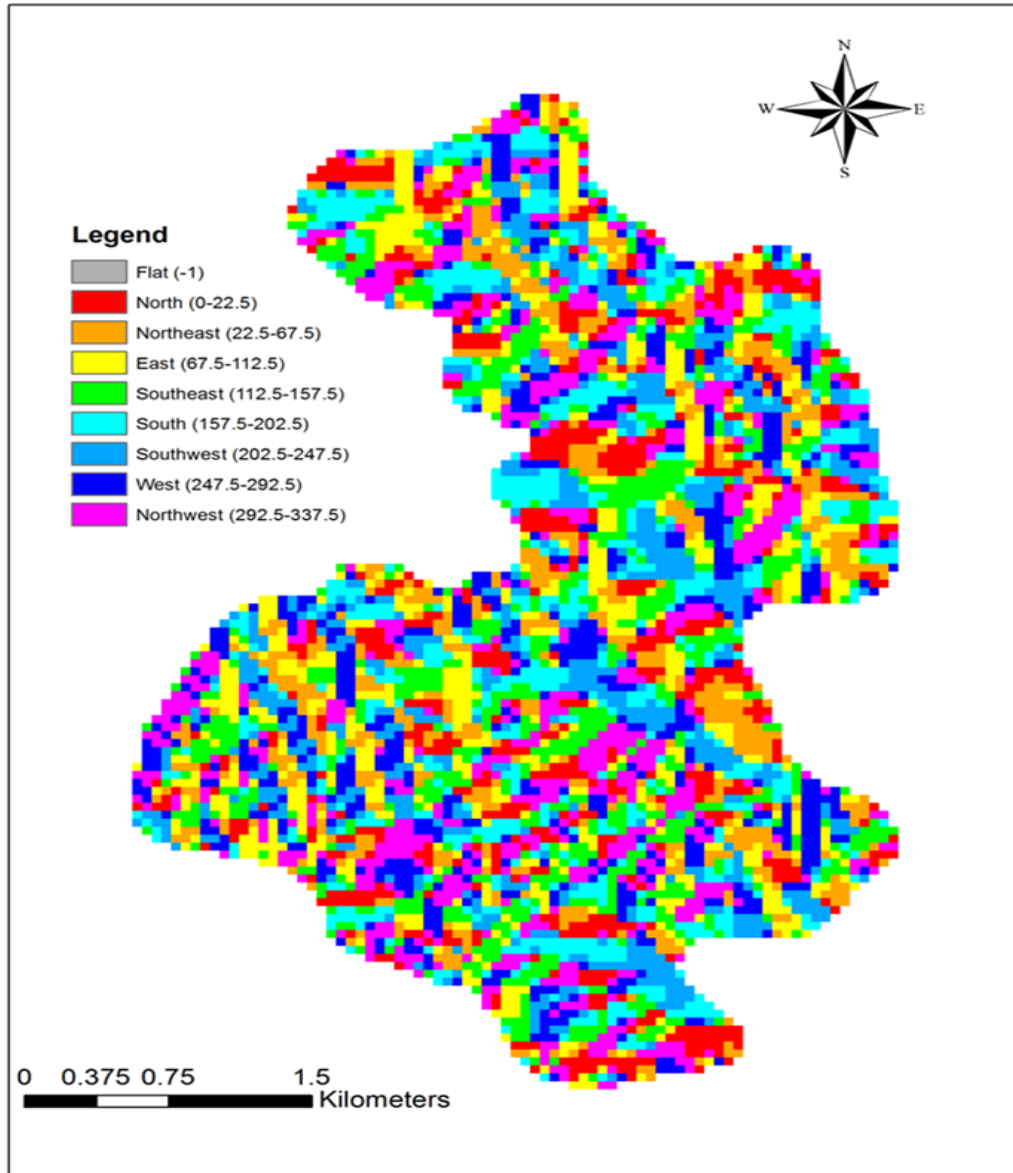


Figure 2.15: Aspect distribution map of Kohima

2.7.1.2 Slope

Slope is an important parameter as it controls the subsurface flow velocity, runoff velocity and soil water content. The slope instability is influenced by the concentration of moisture and level of pore water pressure. Slope plays a great factor in landslide as the greater the slope higher is the influence for landslide occurrence. Kohima is located in a hilly terrain (Photo plate 1 and 2) where the undercutting of drainage especially in the steep slopes are evident of active erosion causing landslides.

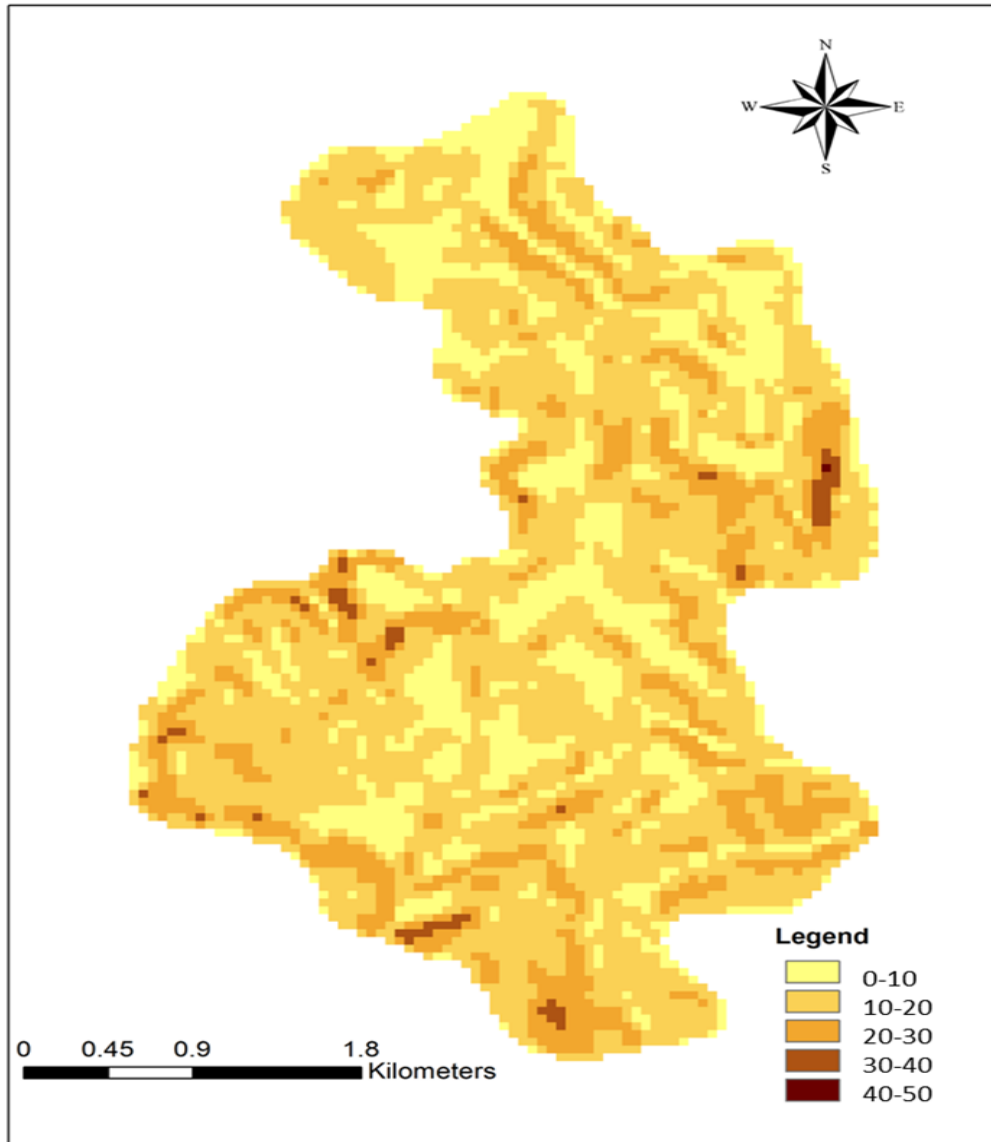


Figure 2.16: Slope distribution map of Kohima.

According to Dai and Lee (2002) landslide frequency will increase with higher slope angle. With the increase in slope angle, the level of gravitational shear stress in the soil colluviums increase hence the slope becomes unstable. Gentle slope are expected to have lower frequency of landslide because of lower shear stress associated with lower gradients (Dai and Lee, 2001). In the study area, the slope degree ranges from 0° - 50° . Five classes has been divided with an interval of 10° ; very gentle slope (0° - 10°), gentle slope (10° - 20°), moderate slope (20° - 30°) steep (30° - 40°) and very steep slope (40° - 50°) as shown in figure. In the study landslides are more generally found in the class range (10° -

20°) reason may be due to weak geology structure- weathered and crumpled shales, sediments and landslide was lesser in the higher slope class especially in south of study area due to the presence of resistant Barail rock in the higher slope range (**Figure 2.16**).

2.7.2 Geologic parameter

Geological parameters are important as they constitute are the underlying structure which determines the strength of the surface to various erosional processes. Geologically the study area comes under Tertiary rocks of Barail and Disang series. The Disang series composed of unfossiliferous shales, sandstone, slates and phyllites. Sandstone is fine grained to flaggy in nature and prone to landslide due to splintery characteristic. The Disang are of Upper Cretaceous-Eocene age and dominantly argillaceous (I aier et al. 2012). The Barail are generally arenaceous in nature that conformably overlay the Disang series. The Barail series are alteration of hard massive sandstone and thin shales. They range in age from Upper Eocene to Oligocene (NESAC and NASTEC, 2008). The broad based lithology stratigraphy of Kohima is divided into two; Barail sandstone and Disang shales. Further division of the lithology is divided into five classes (modified after Walling, 2005) for the study- shale with minor sandstone, weathered shale, shale, crumpled shale and sandstone with minor shale. The structural geology of the study area is marked with faults and lineaments. Fault and lithology thematic layers have been considered for the geological parameters to be implemented for the study.

2.7.2.1 Fault

Faults are structural features which describe a zone of weakness with relative movement along which susceptibility of landslide is high. The proximity of landslide to fault is a consequence of contrast between overlying more permeable rocks and underlying

less permeable or impermeable formation resulting in abundance of springs.

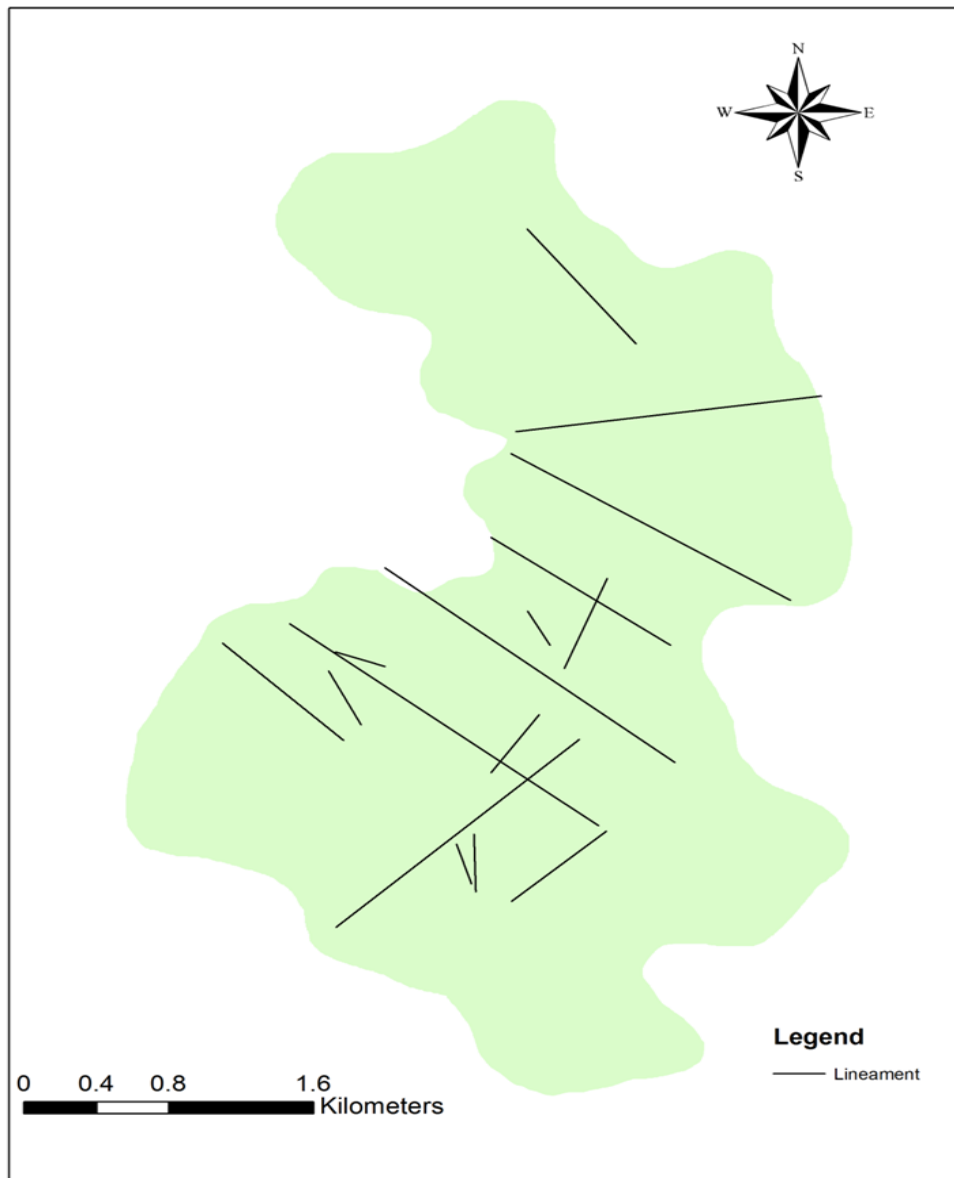


Figure 2.17: Fault distribution map of Kohima

The fault zone increase potentiality of landslide by creating steep slopes and sheared zones of weakened rock and fractured rocks (Ladas *et al.*, 2007). Raman and Punia (2012) stated fault include tectonic structures and geomorphic signature such as topographic breaks, abrupt relief changes, valleys and cliffs with sharp tonal contrast, lithological variations, erosional features and changes in drainage pattern. A buffer of 10 m and greater than 10 m buffer zones were been categorised to study the impact of fault on

the landslide distribution. It is observed that majority of the faults follow NW –SE direction. The presences of fault structures are one of the most important geologic factors contributing to the stability of a slope (**Figure 2.17**).

2.11.2 Lithology

Lithology is one of the major determining factors for landslide classification. Different rock types have varied composition and structure which contribute to the strength of the material. Stronger rock gives more resistance to the driving force compared to weaker rocks (Raman and Punia, 2012). The stratigraphy is basically composed of Barail sandstone and the Disang shales. Different lithology units behave differently with respect to occurrences of slides because of varying strength and resistance to weathering processes (Stein and Hack, 2010). The lithology map unit has been divided into five units modified after Walling. The lithological units are shale, crumpled weathered shale, weathered shale, shale with sandstone and sandstone with shale (**Figure 2.18**). Majority of the occurrences of landslide is observed in weathered shales, which are structurally fragile triggering landslides.

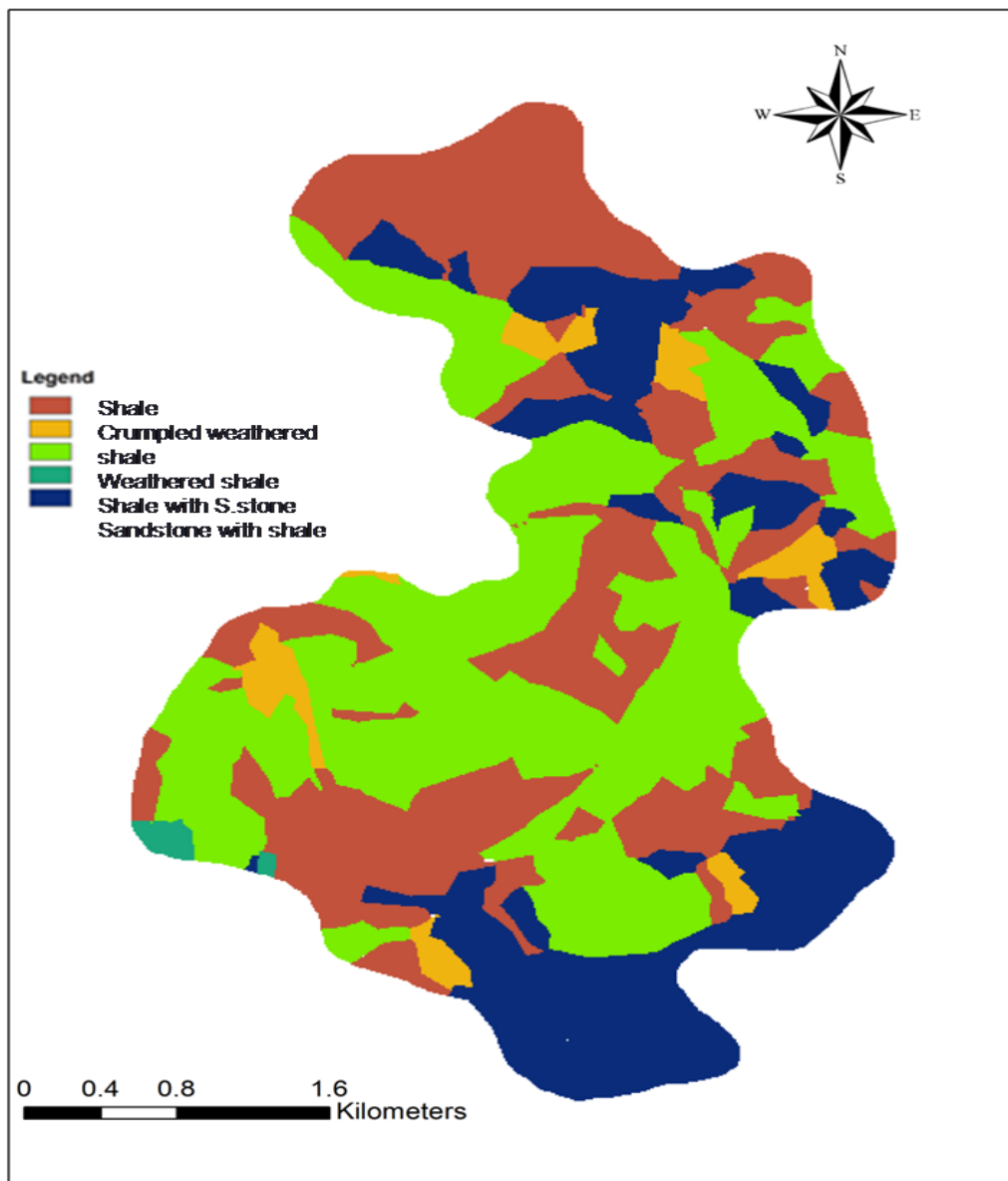


Figure 2.18: Lithology distribution map of Kohima
Source: Compiled by Scholar and modified after Walling, 2005.

2.12 Anthropogenic parameter

Human activities such as building construction and road cutting have influence the land use and land cover (LULC) which directly reflects the susceptibility of an area to landslide. Landslides are confined to certain distances eg. road corridor, therefore, 20 m buffer for landslide study in road corridor was considered. LULC map has been classed into water body, open space, built up, barren ground, agriculture and vegetation to highlight and determine the impact of LULC pattern on landslide events

2.12.1 Road

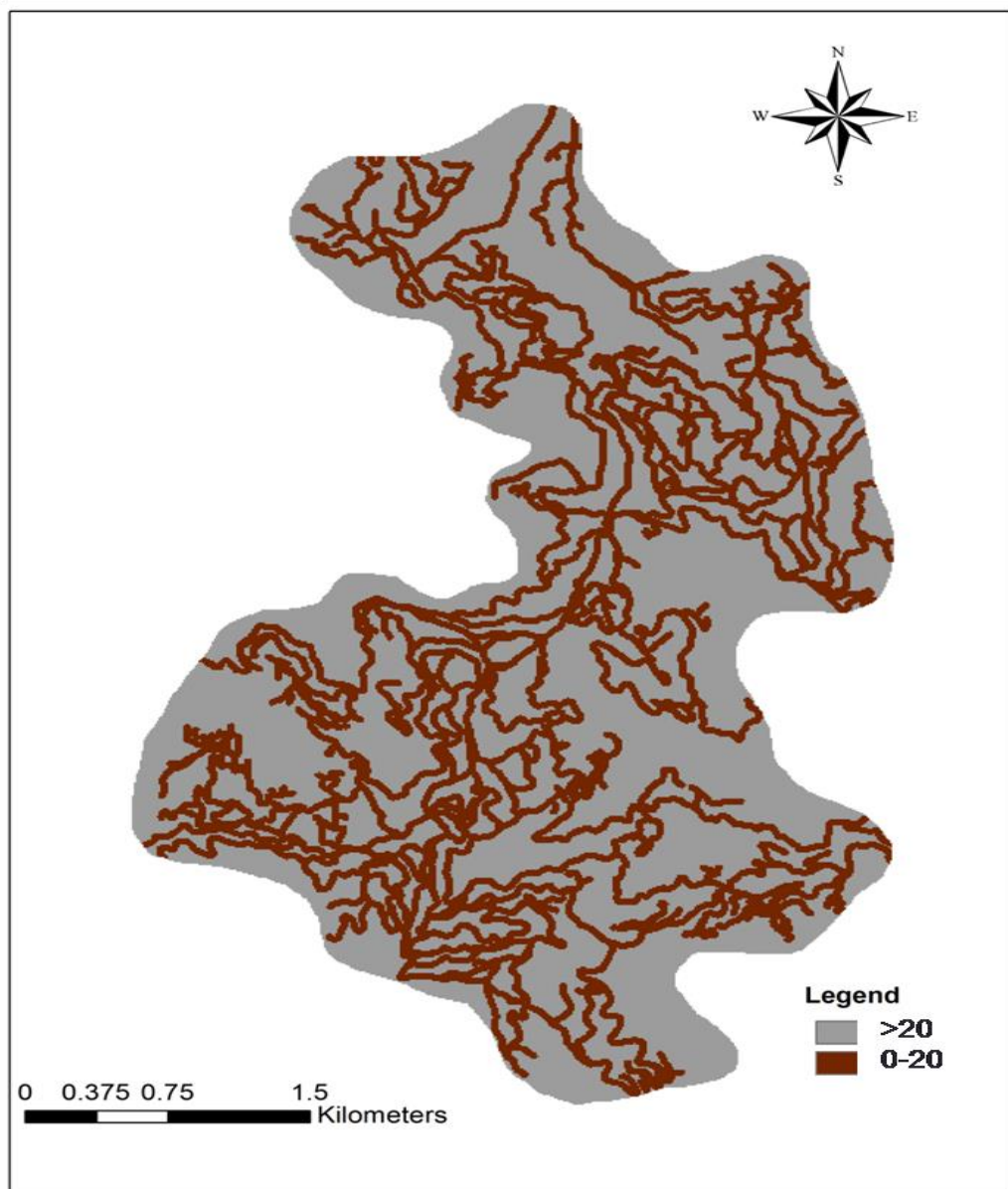


Figure 2.19: Road distribution map of Kohima.

Road plays an important anthropogenic factor for landslide occurrences especially on hilly terrains. Undercutting of roads and widening of roads lead to slope instability triggering landslides. The study of landslide and its relation with road network has been studied in the study area based on the buffering zonation of the road. The roads has been divided into two buffer zone; 0-20 m and >20 m. It is observed that landslides are observed in the peripheries of road. The areal extent of geographical area in the zone 0-20 m has

47,516 pixels and > 20 m buffer zone has 92,822 pixels. The total length of road linkage in the study area is 8.236 km (**Figure 2.19**).

2.12.2 Landuse and land cover

Landuse and land cover is responsible for mass movement. Changes in land use and land cover are mainly contributed by anthropogenic activities such as deforestation, slope cutting, construction and cultivation which can impact the mass movement process (Glade, 2003). Landuse and land cover are indirect indicators of slope stability (Cevik and Topal, 2003). It acts as a cover and reduces soil susceptibility of soil erosion and landslides (Yalcin *et al.*, 2011). The extent of vegetated land can determine the landslide susceptibility of the area. Lesser vegetated area eposes more land to certain agents of erosion and weathering. Agricultural land is located on the outskirts of Kohima (Photo plate 7, 8 and 10). Presence of vegetation cover in Kohima (Photo plate 9) safeguard the soil from been eroded where its canopy and roots hold the soil together. Carrara *et al.*, 1991 observed that between vegetated and un-vegetated land it was observed that non vegetated land were more prone to landslides they exhibit faster rate of erosion and greater instability (**Figure 2.20**).

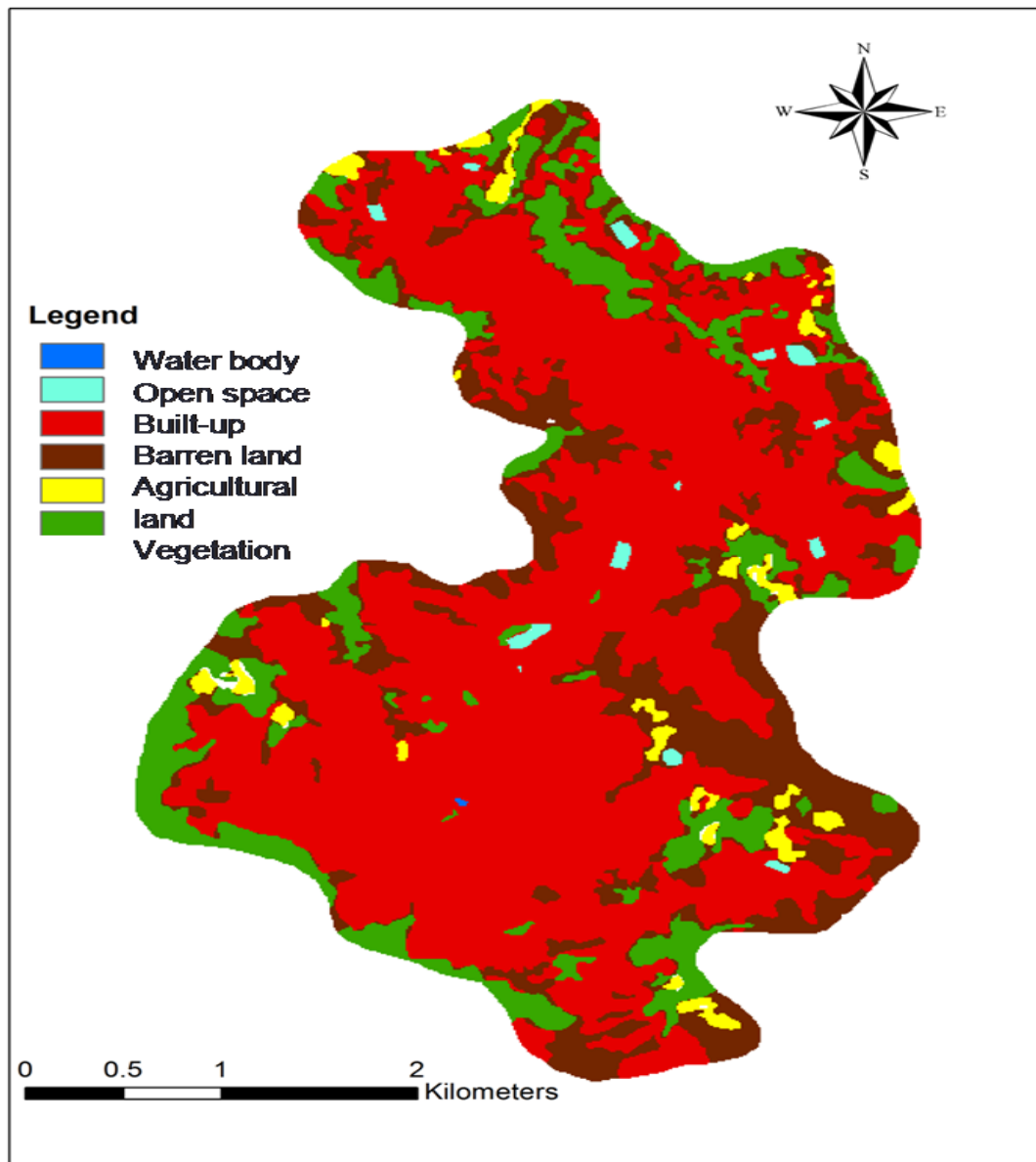


Figure 2.20: LULC distribution map of Kohima.

The occurrences of shallow landslide were more prone in barren slopes than vegetated slopes (Greenway, 1987 and, Styczen and Morgan, 1995). The land use and land cover parameter for the study area has been divided into six classes; water body covering an area of 22 pixels, open space includes the parks and play grounds which covers an area of 1049 pixels, built up area has the highest areal extent with 89070 pixels, barren land constitute 27629 pixels, agricultural land with 3548 pixels include the terrace cultivation and the horticulture practised on the outskirts of the study area and lastly, vegetation cover

extends an area of 18800 pixels which are mainly observed in NNE and SWW part of the study area.

2.13 Hydrological parameter

The proximity of an area drainage sources are important, the drainage can affect the area by eroding the soil. For drainage delineation, only the natural stream was considered and not the drainage line within the settlement area which have a cemented base. In case of cemented drainage canal, erosion is negligible or absent.

2.13.1 Drainage

Drainage of the study area has been divided into two zones; 0-50 m and 50- 100 m basing on the hypothesis that streams affect the stability of slopes by saturating and undercutting them. It is commonly observed that as distance from drainage increases the occurrences of landslide decreases. The higher drainage density cause accelerated soil erosion resulting in mass wasting in areas close to the drainages (Barredo *et al.*, 200). In the study area, the total length of drainage is 42.80 km and the total area of the drainage area in 0-50 m buffer zone was 37,927 pixels and greater than 50 m buffer zone was 32,515 pixels (**Figure 2.21**).



Figure 2.21: Drainage distribution map of Kohima.

3

3.1 Introduction

Kohima the capital of Nagaland has diverse types of houses, colonial houses to recently built houses, traditional houses, Reinforced Cement Concrete (RCC) structures. The principal buildings constructed are basically framed structure made up of concrete RCC materials. Building bye-law for Kohima was introduced in 2012 (The Nagaland Gazette, 2013). However, the bye-laws are not implemented strictly or totally ignored. Of all the regulations, the lack of setting maximum building height restriction was observed. Hill area states like Meghalaya and Sikkim has a maximum height restriction bye-law, Nagaland should also follow suit. In the building bye-law section 2.2 of the Nagaland Gazette (2013), maximum height restriction is quoted as “Maximum height of building should depend on building plans accompanied by relevant structural design and drawing”. That quote itself is vague as no restriction of height is mentioned.

The built up composition of the study area, a sample ward which could represent the whole of Kohima town was selected. Parameter which was conducive to represent Kohima was selected. Parameters like- proximity to National highway, roads, shopping complex, types of building which can be represented in HAZUS, construction material, different purpose of the building, distribution etc., was considered for the sampling purpose. For representation and the validation process, Ward no. 4 (Photo plate 11) was chosen for the build up foot print. For classification of the buildings this parameters are included, they are building plan (regular, irregular), condition of buildings, purpose of building, floor characteristics, material used for construction etc. For the composition setting, the entire building present in Ward no. 4 was digitised and personal geo-database created for the process. Stratified random sampling was used for the entire study area where an average of the sample (Ward no. 4), was applied for the entire study area. For the sampling process, a sample of 50 buildings was selected in each ward.

3.2 Building footprint

To assess the seismic vulnerability of the buildings, it was necessary to segregate the built-up and non-built-up land cover. The built up area was manually digitised basing on the various elements of interpretation especially – shape, tone etc., and field based survey. To get a good built-up representation for the study area, as discussed earlier, a ward which could present the entire study area was selected for the seismic vulnerability assessment.

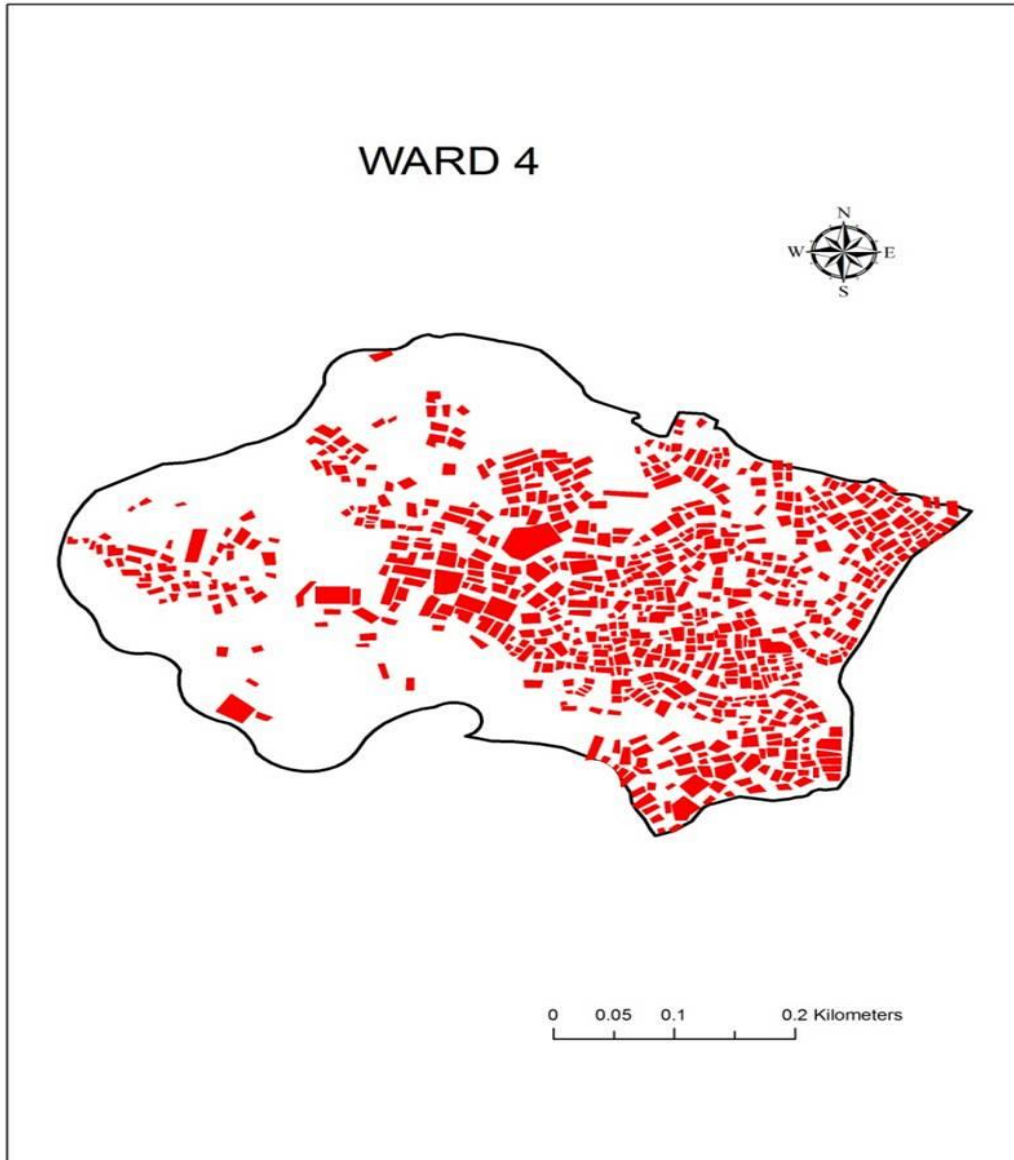


Figure 3.1: Building distribution in Ward no.4.

Ward no.4 was selected for the process; the digital footprint of the ward was extracted where it was applied for the entire study area at a later stage. In the digital footprint of Ward no. 4, a total of 721 buildings were digitised. For estimating the vulnerability of seismic effect on the buildings, the buildings have been categories according to HAZUS building classification (**Table 3.1 & Figure 3.1**). Types of building according to HAZUS footprint input has been classed into W1, C3L, C3M and C3H for seismic assessment.

3.3 Architectural building plan

The shape and structural feature gives the architectural backbone of a building. Height of a building plays an important role in resisting an earthquake disaster. The higher buildings have greater chance to displacement. Natural period is the time taken by a building to undergo one complete oscillation; it is controlled by mass and stiffness. Greater natural period is recorded in higher mass building than smaller mass buildings, as the height increase the mass, its stiffness decrease. The proximity of buildings also plays a role during earthquake, building starts oscillating during earthquake, and if buildings are close to each other, pounding of the buildings especially in case of higher buildings are inevitable as they vibrate in horizontal direction. Building pounding possibilities was observed in the study area (Photo plate 19) due to the close proximity which is a common sight in the study area due to lack of space.

3.3.1 Earthquake resistant design / structure

A building comprises of two components- structural like beam, column and non-structural components like door, windows etc. Earthquake resistant design do not necessarily mean it is earthquake proof i.e., no damages will occur, damages are acceptable until and unless the building collapses. Old and unsafe buildings are not considered as they are liabilities in case of a seismic hazard, old buildings are observed in the study area (Photo plate 18). Murty *et al.*, (2012) stated that in an earthquake resistant structure a normal building should resist;

- i). Minor (and frequent) shaking with no damage to structural and non-structural elements;
- ii). Moderate shaking with minor damage to structural elements, and some

damage to non-structural elements; and

- iii). Severe (and infrequent) shaking with damage to structural elements, but with no collapse (to save life and property inside/adjoining the building).

Designing a structure to possess certain initial stiffness and lateral strength by appropriately proportioning the size and material of the members is simpler. However, ductility of a structure requires extensive and involves preferable methods of detailing.

3.4 General building stock

The general building stock, building height parameters are added to reflect the variation of typical building periods and other parameters with regard to building heights. Buildings are classified both in terms of their use, or occupancy class, and in terms of their structural system, or model building type. Damage was predicted based on model building type, since the structural system is considered as the key factor in assessing overall building performance, loss of function and casualties (FEMA, 2001). In HAZUS building type, twenty-eight occupancy classes are defined to distinguish among residential, commercial, industrial or other buildings; and thirty six building model types are used to classify buildings within the overall categories of wood, steel, concrete, masonry or mobile homes.

3.5 Model building type

The type of building found in the study area according to National Earthquake Hazards Reduction Program (NEHRP) handbook for seismic evaluation of existing buildings (FEMA, 1992 and FEMA, MH2) are as follows;

3.5.1 Wood, Light Frame (W1)

These are typically single-family or small, multiple-family dwellings of not more than 5000 square feet of floor area. The essential structural feature of these buildings is repetitive framing by wood rafters or joists on wood stud walls. Loads are light, and spans are small. These buildings may have relatively heavy masonry chimneys and may be partially or fully covered with masonry veneer (**Table 3.1**).

Table 3.1. Building type

No.	Label	Description	Height			
			Range		Typical	
			Name	Storeys	Storeys	Feet
1	W1	Wood, Light Frame (≤ 5000 sq. Ft)		All All	1 2	14 24
2	C3L	Concrete Frame with Unreinforced Masonry Infill walls	Low-rise	1-3	2	20
3	C3M		Mid-rise	4-7	5	50
4	C3H		High-rise	8+	12	120

Source: Federal Emergency Management Agency (FEMA), 2001.

Most of these buildings, especially the single-family residences, are not engineered but constructed in accordance with “conventional construction” provisions of building codes. Hence, they usually have the components of a lateral-force-resisting system even though it may be incomplete. Lateral loads are transferred by diaphragms to shear walls. The diaphragms are roof panels and floors that may be sheathed with sawn lumber, plywood or fiberboard sheathing. Shear walls are sheathed with boards, plaster, plywood, gypsum board, particle board, or fiberboard, or interior partition walls sheathed with plaster or gypsum board.

3.5.2 Concrete Frame with Unreinforced Masonry Infill walls (C3)

These buildings have bearing walls similar to steel frame buildings with unreinforced masonry infill walls except the frames are of reinforced concrete the shear strength of the columns in the building after cracking of the infill, may limit the semi-ductile behaviour of the system.

3.6 HAZUS building type structural damage

FEMA highlighted the structural damage in the classified building of HAZUS as follows;

3.6.1 Wood, Light Frame (W1)

Slight Structural Damage: Small plaster or gypsum-board cracks at corners of door and window openings and wall-ceiling intersections; small cracks in masonry chimneys and masonry veneer.

Moderate Structural Damage: Large plaster or gypsum-board cracks at corners of door and window openings; small diagonal cracks across shear wall panels exhibited by small cracks in stucco and gypsum wall panels; large cracks in brick chimneys; toppling of tall masonry chimneys.

Extensive Structural Damage: Large diagonal cracks across shear wall panels or large cracks at plywood joints; permanent lateral movement of floors and roof; toppling of most brick chimneys; cracks in foundations; splitting of wood sill plates and/or slippage of structure over foundations; partial collapse of “room-over-garage” or other “soft-story” configurations; small foundations cracks.

Complete Structural Damage: Structure may have large permanent lateral displacement, may collapse, or be in imminent danger of collapse due to cripple wall failure or the failure of the lateral load resisting system; some structures may slip and fall off the foundations; large foundation cracks. Approximately 3% of the total area of W1 buildings with complete damage is expected to be collapsed.

3.6.2 Concrete Frame Buildings with Unreinforced Masonry Infill walls (C3)

Slight Structural Damage: Diagonal hairline cracks on most infill walls, cracks in infill- frame interfaces.

Moderate Structural Damage: Most infill wall surfaces exhibit larger diagonal or horizontal cracks; some walls exhibit crushing of bricks around beam-column connections. Diagonal shear cracks may be observed in concrete beams or columns.

Extensive Structural Damage: infill walls exhibit large cracks; some bricks may dislodge and fall, some may bulge out, few walls may partially or fully, few concrete beam and column may fail in shear resulting in partial collapse. Structure may exhibit permanent lateral deformation.

Complete Structural Damage: Structure has collapsed or is in imminent danger of collapse due to combination of total failure of the infill walls and nonductile failure of concrete columns and beams. Approximately 15% (low-rise), 13% (mid-rise) or 5% (high-rise) of the total area of C3 buildings with complete damage is expected to collapsed.

3.7 Building type

The observed building types in the study area in accordance with the building type from FEMA technical book are W1, C3L, C3M and C3H. The material commonly used in

the study area was mainly concrete beside concrete, building materials such as bamboo, asbestos sheet, mixture of bamboo and cement, wood and brick etc (**Table 3.1**).

3.7.1 W1 building type

W1 describe the wooden, light framed structure buildings. From field study, under W1 building category, houses which were not made/built up of RCC has been considered. Houses made of asbestos sheet (Photo plate 12), wood, cement, bamboo, bamboo and cement, wood and brick etc., has all been categories under W1. From Ward no. 4, a number of 484 was delineated, out of which 6 buildings are made of bamboo, bamboo and cement building comprise of 39 buildings, buildings made of brick was 150. In the study area, combination of different material for building was observed, number of brick and bamboo with cement material was 5 buildings, brick and asbestos sheet was 1, wood and brick was 2, brick with wood material was 4 buildings and asbestos sheet with brick was 4. Building consisting of asbestos sheet was 234, wooden house was 33. Some sample of W1 building types are shown in Photo plate 22 to 26 (**Figure 3.2**).

The number of floors in W1 category range from 1 to 5 storeys. Kohima has a sloping surface, buildings are usually build on the slopes in accordance with the surface, which encourages multi-storey buildings even in W1 type of building (Photo plate 15). Number of building with one storey is 189, two storeys are 251, three storeys are 37, four storeys are 3 and five storey building 3. Besides categorising the material type and floor, the building purpose, building condition and building plans have also been considered while delineating the buildings.

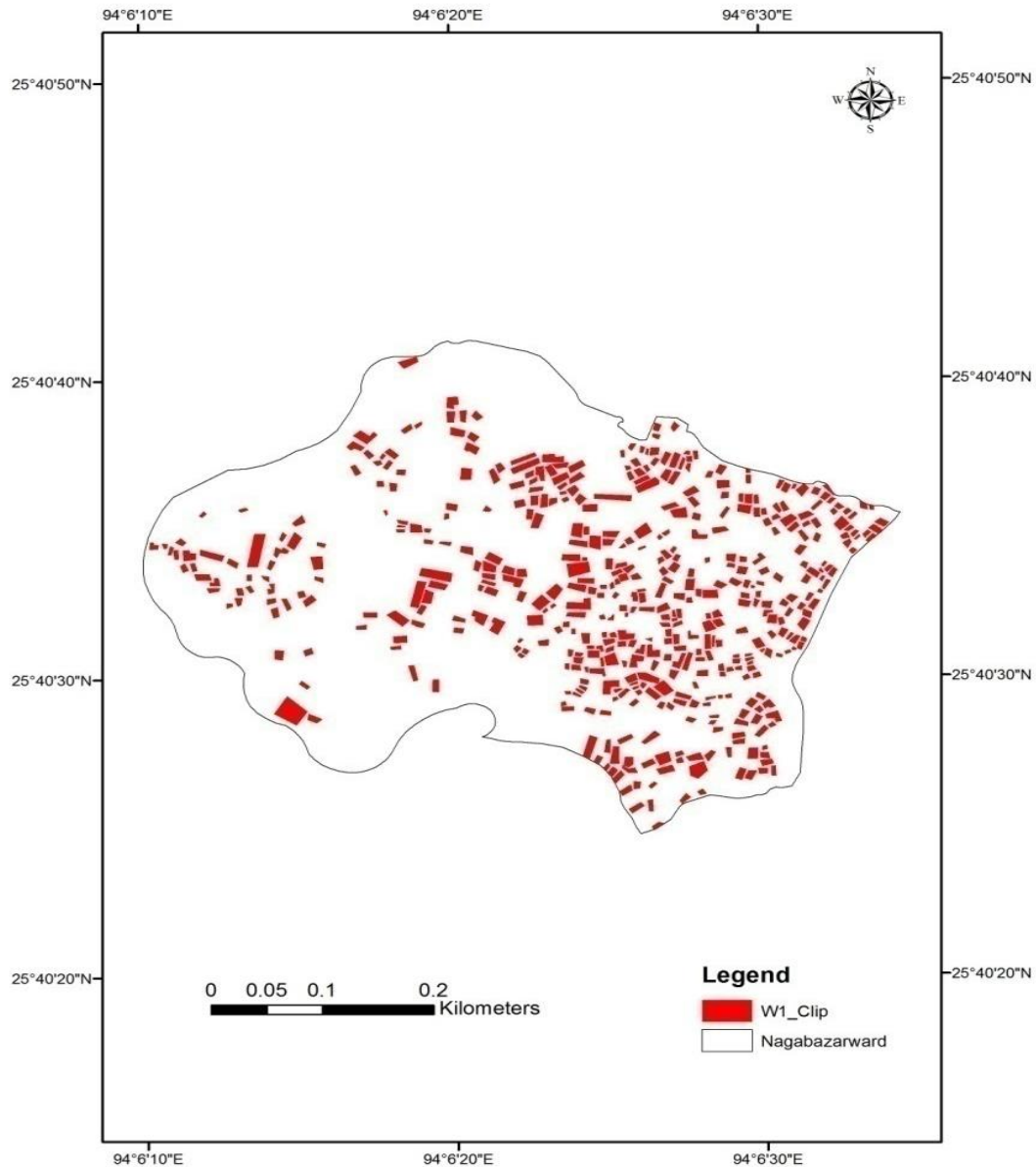


Figure 3.2. W1 building type distribution in Ward no. 4.

The utilisation of building in the study area are as follows; religious purpose buildings are three, commercial building (refers to purely commercial building without residential facilities) are 7, educational institution buildings are 2. Numbers of residential buildings are 437, and residential and commercial purpose buildings are 34. Presence of cracks, unmaintained and maintained walls, peeling of plasters and paints etc., are some of the criteria for categorising the building conditions. Condition of building has been classed into three; good, moderate and poor. There are 112 buildings poorly maintained, 323 are

moderately maintained, and 47 are maintained under good condition. Building design or plan has been classed into two class- regular plan and irregular plan. The regular buildings are 373, and irregular buildings are 109 in Ward no. 4. Buildings with flat roof are 6 and 477 building has sloping roofs (**Table 3.1**).

3.7.2 C3L building type

C3L describe the building type with concrete frame and unreinforced masonry infill walls. It represents low rise storeys from 1-3 storey building (Photo plate 13). The total numbers of C3L buildings are 184 located in present study area (**Figure 3.3**). The number of building with 1 storey is 9, 2 storeys are 82, 3 storeys are 93.

The utilisation of buildings in the study area is as follows; religious buildings are 4, commercial buildings are 4, educational building with C3L type of building is 1. Numbers of residential buildings are 156 and residential and commercial buildings are 4. Maintenance wise buildings are classified like poor conditions are 6, moderate condition 104 and good condition are 68. Building design or plan has been classed into two class- regular plan and irregular plan depending on their frame/structural design. The regular buildings are found to be 144 and irregular buildings are 40 located in Ward no.4. Buildings with flat roof are 105 and 77 building has sloping roofs. A sample of C3L building type is shown in Photo plate 13.

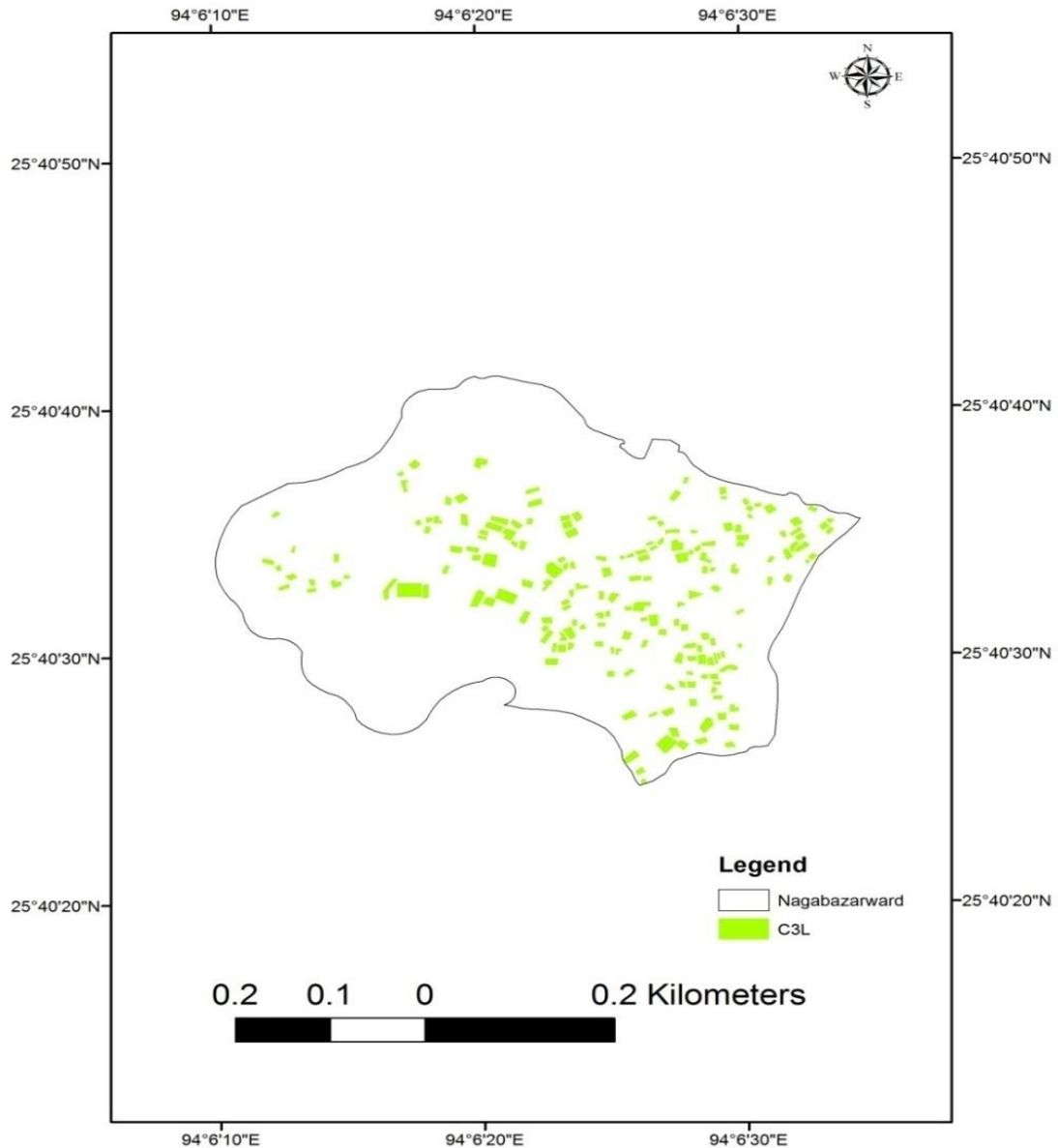


Figure 3.3: C3L building type distribution in Ward 4.

3.7.3 C3M building type

The building type of C3M described are concrete framed, unreinforced and are mid-rise from 4-7 storeys in nature. Total number of C3M building (Photo plate 14) was 52. Buildings according to storey wise in C3M are four storeys are 36, five storeys are 12, and six storeys are 4. The C3M building utilisation for religious building is 1, commercial are 7, educational institution are 2. Residential buildings are 30 and residential and commercial buildings are 12. Maintenance wise 5 buildings are poorly maintained, 14 buildings are

moderately maintained and good condition buildings are 30. The regular buildings in C3M are 45 and irregular buildings are 7. Buildings with flat roof are 33 and 18 building have sloping roofs (**Figure 3.4**).

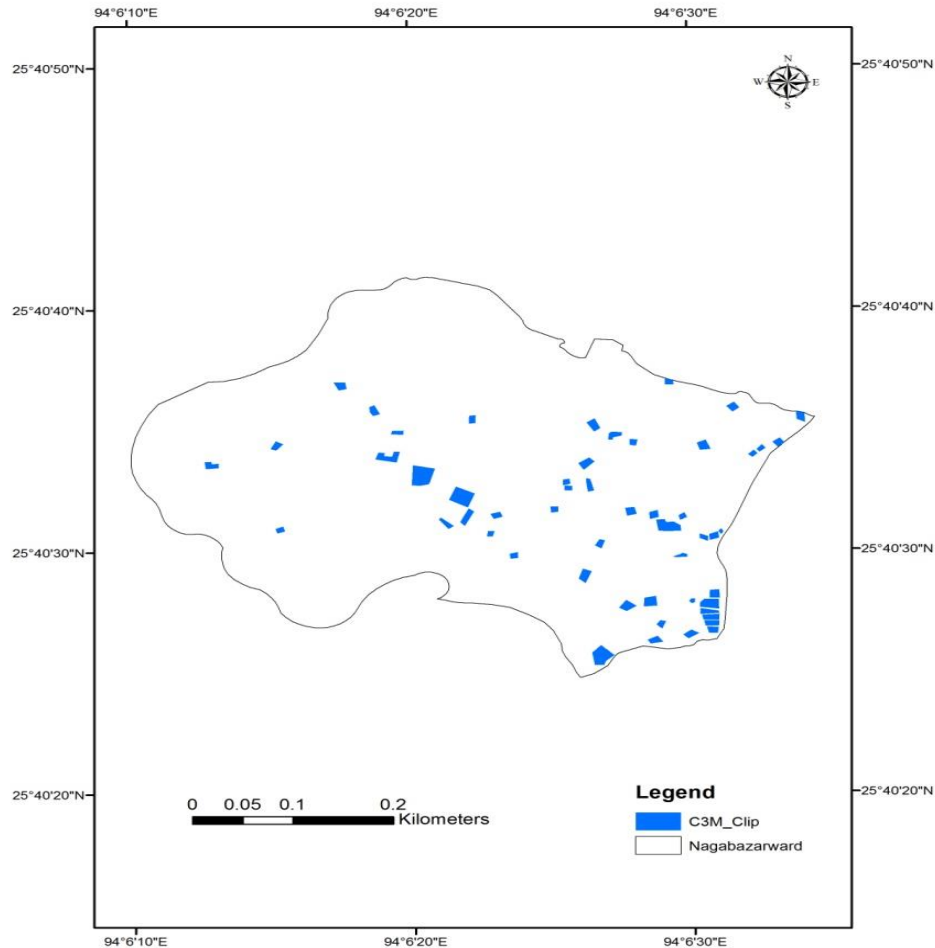


Figure 3.4: C3M building type distribution in Ward 4.

3.7.4 C3H building type

C3H buildings are classed under concrete frame and are unreinforced with masonry infill walls and are 8+ storeys. Only one building was found and demarcated (**Figure 3.5**). The building is in good condition and runs as a hospital. The design is irregular in plan and has a slope not flat roof. The distribution of C3H building type is shown in figure and its sample photograph is seen in [photo plate](#).

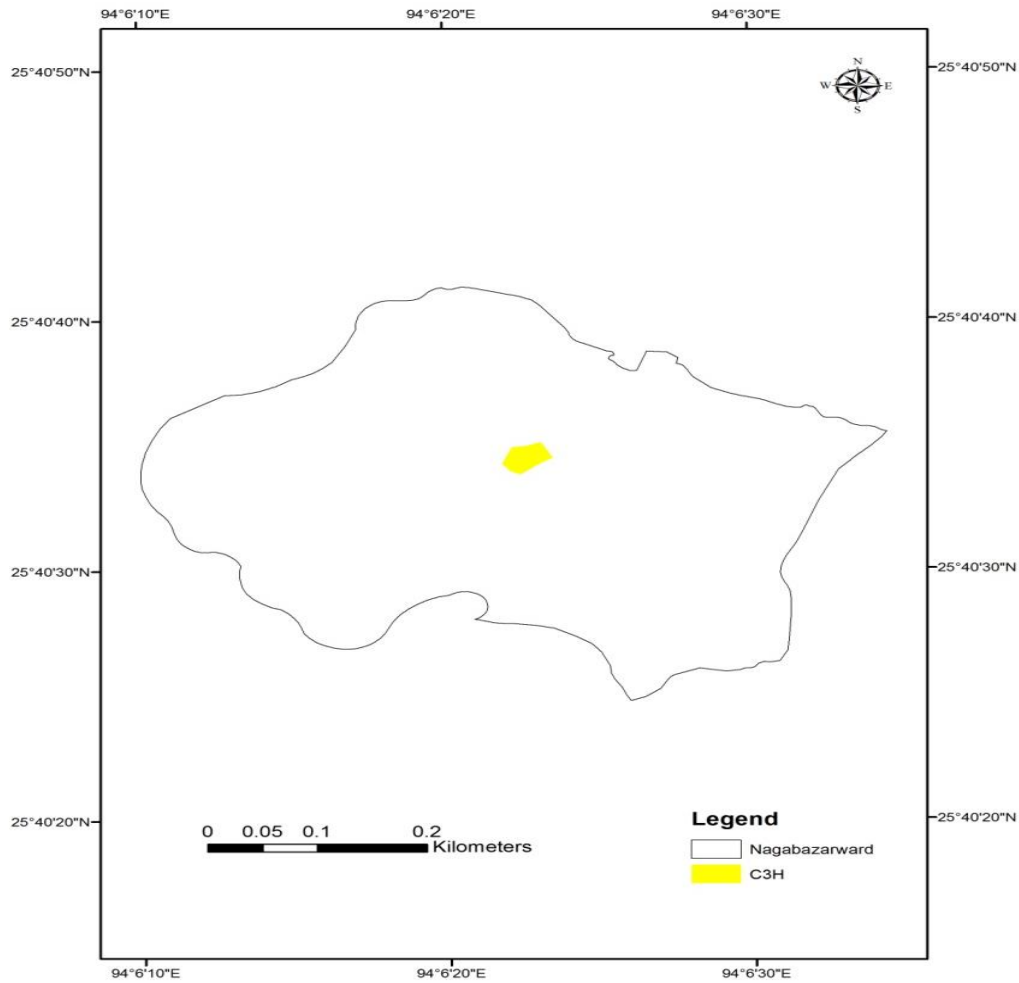


Figure 3.5: C3H building type distribution in Ward 4

3.7.5 Distribution of building in Ward no. 4

The composition of all building types in Ward no. 4 (**Figure 3.6**). Red coloured polygon indicates W1 building type, C3L is represented by green polygon, C3M was represented by blue polygon and C3H was marked by yellow polygon. The total buildings composed in Ward no.4 are 721.

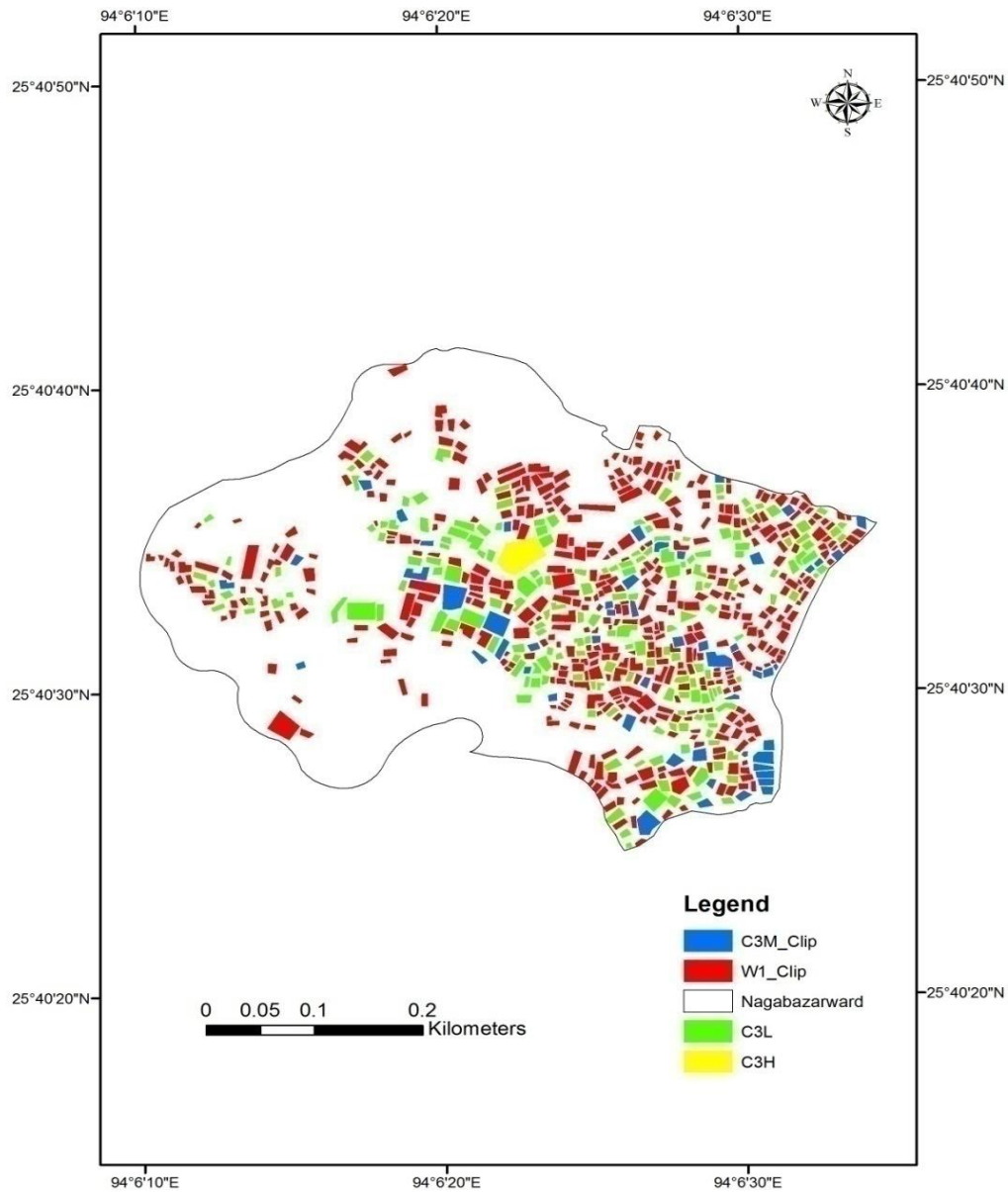


Figure 3.6: Composition of buildings according to their building types in ward 4.

The criterion of condition was based on the maintenance, presence of cracks on the walls (Photo plate 16), beams and columns (Photo plate 17), tilting of roof and walls. The conditions of the buildings in ward no. 4 are shown in **Figure 3.7**. According to building condition marked like poor condition is indicated by pink polygon, moderate condition highlighted by red polygon and blue polygon represents good condition.

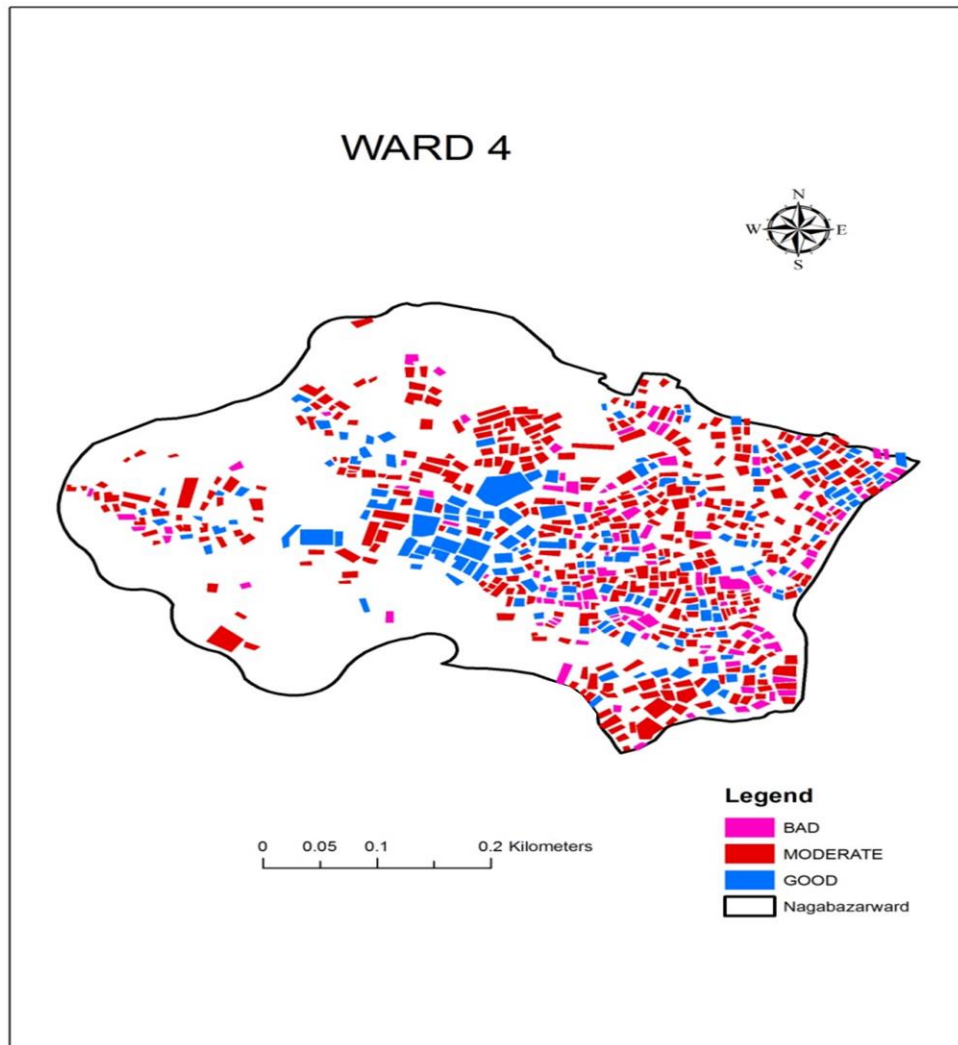


Figure 3.7: Condition of buildings in Ward 4.

3.8 HAZUS building footprint sample selection

For a detail study of the entire study area, delineation of each building would be cumbersome and time consuming. The Ward no. 4 was therefore selected for detail survey where buildings were delineated and evaluated. A sample of 50 buildings in each ward was selected for analysis of building types under simple random technique (**Figure 3.8 & Table 3.2**).

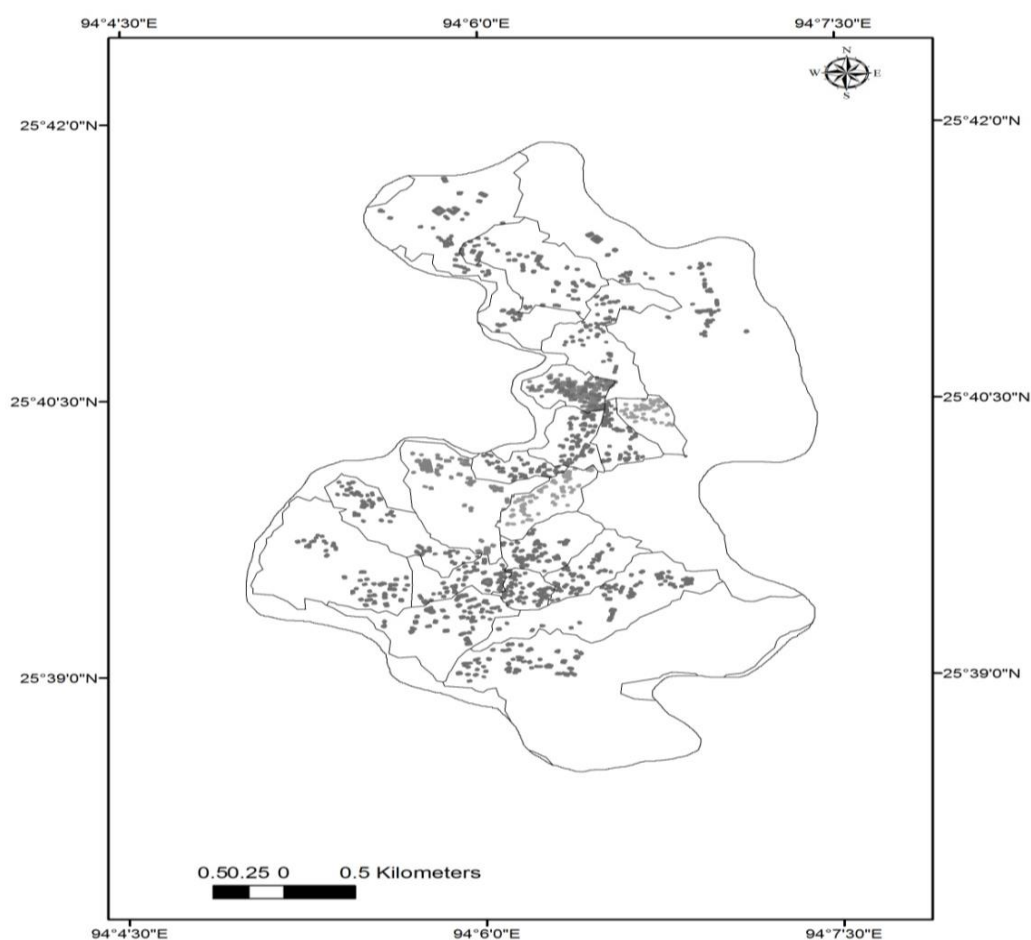


Figure 3.8: Building sample distribution in each ward from study area.

Table. 3.2. Distribution of building in ward 4

Ward	Building	W1		C3L		C3M		C3H	
		Number	%	Number	%	Number	%	Number	%
4	721	484	67.13	184	22.52	52	7.21	1	.14

Source: Computed by Scholar.

3.8.1 Sample building floor characteristics

The sample selected in the ward has been shown in the tables along with its characters- floor, material, purpose, plan etc. The different building floor characters are shown in **table 3.3**. The maximum building number in Ward no. 1 was observed in one, two and three storey buildings. Highest storey was observed to fall under six storeys and lowest number of building was under six storey (1 building) followed by five storey with 2

number of buildings. The maximum building in Ward no. 2 storeys was observed in one storey building. Highest storey was observed to fall under greater than seven storey and lowest number of building was under seven and greater than seven storey (1 building each) followed by four and five storey with 2 number of buildings.

The maximum building in Ward no. 3 storeys was observed in four storey building. Highest storey was observed to fall under greater than seven storey with 1 building and it was also the lowest number of building. The maximum building in Ward no. 5 storeys was observed in two storey building with 20 numbers of buildings. Lowest number of building was six and greater than seven storey (one building each). The maximum building in Ward no. 6 storeys was observed in two storey building with 20 buildings and lowest number of building was in greater than seven storey building with 1 building. The maximum building in Ward no. 7 storeys was observed in four storey building with 14 numbers of buildings. Minimum number of building was observed in greater than seven storey with 1 building. The maximum building in Ward no. 8 storey was observed in three storey building having 10 buildings. Highest storey was observed to fall under greater than seven storey with 1 building. The maximum building in Ward no. 9 storey was observed in two storey building with 10 buildings. Lowest number of building was observed in six storey building with 2 buildings. The maximum building in Ward no. 10 storeys was observed in one storey building with 16 buildings. Lowest number of building was under six storey with 3 building.

Table 3.3. Sample building floor characteristics.

Ward no.	Storeys							
	1	2	3	4	5	6	7	>7
Ward 1	12	12	12	11	2	1	0	0
Ward 2	15	9	8	5	5	6	1	1
Ward 3	10	11	11	12	3	2	0	1
Ward 5	12	20	5	8	3	1	0	1
Ward 6	8	20	8	5	3	5	0	1
Ward 7	2	13	5	14	10	3	2	1
Ward 8	6	19	10	6	5	2	1	1
Ward 9	6	15	10	11	3	2	0	3
Ward 10	16	4	11	10	6	3	0	0
Ward 11	3	9	7	18	8	3	1	1
Ward 12	6	11	11	8	9	2	0	3
Ward 13	9	18	13	5	4	1	0	1
Ward 14	10	9	8	11	4	4	4	0
Ward 15	10	15	10	7	4	2	0	2
Ward 16	16	6	4	9	7	5	2	1
Ward 17	19	3	8	8	8	4	0	0
Ward 18	8	14	10	10	6	2	0	0
Ward 19	9	12	6	12	5	5	0	1
Outer ward	7	19	13	8	2	1	0	0

Source: Computed by Scholar

The maximum building in Ward no. 11 storeys was observed in four storey building with 18 buildings. Lowest number of building was under seven and greater than seven storeys with one building each followed by one storey and six storey with 3 buildings each. The maximum building in Ward no. 12 storeys was observed in two and three storey building with 11 buildings. Lowest number of building was under six followed by greater than seven storeys with 2 and 3 buildings respectively. The maximum building in Ward no. 13 storeys was observed in two storey building with 18 buildings. Lowest number of building was under six and greater than seven storeys with one building each followed by five storey with 4 buildings.

The maximum building in Ward no. 14 storeys was observed in four storey building with 11 buildings. Lowest number of building was under five, six and seven

storeys with 4 building each. The maximum building in Ward no. 15 storeys was observed in two storey building with 15 buildings. Lowest number of building was under six and greater than seven storeys with 2 building each. The maximum building in Ward no. 16 storeys was observed in one storey building with 16 buildings. Lowest number of building was greater than seven storeys with one building. The maximum building in Ward no. 17 storeys was observed in one storey building with 19 buildings. The maximum building in Ward no. 18 storeys was observed in two storey building with 14 buildings followed by three and four storey with 10 buildings each. Lowest number of building was six storeys with 2 building. The maximum building in Ward no. 19 storeys was observed in two and four storey building with 12 buildings followed by one storey with 9 buildings. Lowest number of building was greater than seven storeys with one building. The maximum building in Outer ward was observed in two storey building with 19 buildings followed by three storeys with 13 buildings. Lowest number of building was six storeys with one building (**Table 3.3**).

3.8.2 Building under purpose and material characteristics

Analysis of building use for 50 houses as sample collected from each ward (19) except Ward no. 4 (**Table 3.4**). The buildings are divided into two types; purposely and combination of material used for construction. The purposely used buildings are offices (government and private enterprises) and educational institution (high school, secondary school and colleges) (Photo plate 20, 21). In field survey it was observed that W1 type of buildings are identified, they are brick and wood, bamboo and cement, asbestos sheet, brick houses etc. The above mention type of buildings are all categories under HAZUS W1 category.

The maximum number of building under purpose in Ward no. 1 was observed in residential with 37 buildings followed by education institution with 6 buildings. Under material parameter, a maximum building was seen in RCC with 31 numbers of buildings (**Table 3.4**). The maximum number of building under purpose in Ward no. 2 was observed in residential with 29 buildings followed by office with 9 buildings. Under material parameter, a maximum building was seen in RCC with 30 numbers of buildings. The maximum number of building under purpose in Ward no. 3 was observed in residential with 29 buildings followed by residential and commercial with 12 buildings. Under material parameter, a maximum building was seen in RCC with 30 numbers of buildings. The maximum number of building under purpose in Ward no. 5 was observed in residential with 45 buildings. Under material parameter, a maximum building was seen in RCC with 19 numbers of buildings followed by asbestos with 16 buildings.

The maximum number of building under purpose in Ward no. 6 was observed in residential with 32 buildings. Under material parameter, a maximum building was seen in RCC with 27 numbers of buildings. The maximum number of building under purpose in Ward no. 7 was observed in residential with 20 buildings. Under material parameter, a maximum building was seen in RCC with 33 numbers of buildings. The maximum number of building under purpose in Ward no. 8 was observed in residential with 41 buildings followed by residential and commercial with 8 buildings. Under material parameter, a maximum building was seen in RCC with 20 numbers of buildings. The maximum number of building under purpose in Ward no. 9 was observed in residential with 25 buildings and under material parameter, a maximum building was seen in RCC with 32 numbers of buildings. The maximum number of building under purpose in Ward no. 10 was observed in residential with 35 buildings and material parameter, a maximum building was seen in RCC with 30 numbers of buildings. The maximum number of building under purpose in

Ward no. 11 was observed in residential with 32 buildings and under material parameter, a maximum building was seen in RCC with 35 numbers of buildings.

Table 3.4. Sample building purpose and material characteristics.

Parameter	Purpose						Material					
	Religious	Educational	Residential	Residential & commercial	Office	Hospital	Bamboo	Bamboo & cement	Brick	RCC	Asbestos	Wood
Ward 1	1	6	37	4	2	0	1	5	5	31	7	1
Ward 2	1	1	29	6	9	0	0	3	16	30	1	0
Ward 3	0	2	29	12	1	0	0	1	5	30	13	1
Ward 5	1	0	45	4	0	0	1	0	10	19	16	4
Ward 6	2	2	32	3	3	1	5	4	5	27	5	4
Ward 7	1	1	20	12	4	1	0	0	7	33	7	3
Ward 8	0	0	41	8	0	1	1	0	8	20	15	6
Ward 9	2	1	25	11	0	4	0	2	8	32	7	1
Ward 10	0	3	35	6	0	0	2	9	9	30	0	0
Ward 11	4	0	32	9	5	1	1	1	11	35	2	0
Ward 12	1	0	39	8	1	0	1	0	7	33	7	2
Ward 13	0	1	43	6	0	0	1	2	9	29	6	3
Ward 14	2	3	23	9	5	0	0	1	13	34	2	0
Ward 15	1	3	40	2	4	0	0	1	13	31	5	0
Ward 16	1	3	38	7	1	0	0	5	12	32	1	0
Ward 17	2	0	46	1	0	0	0	7	13	30	0	0
Ward 18	0	0	47	2	1	0	3	0	10	27	9	1
Ward 19	1	0	28	11	10	0	1	3	9	36	1	0
Outer ward	0	3	34	12	1	0	0	0	14	35	0	1

Source: Computed by scholar

The maximum number of building under purpose in Ward no. 12 was observed in residential with 39 buildings followed. Under material parameter, a maximum building was seen in RCC with 33 numbers of buildings followed by asbestos and brick with 7 building each. The maximum number of building under purpose in Ward no. 13 was observed in residential with 43 buildings. Under material parameter, a maximum building was seen in RCC with 29 numbers of buildings followed by brick (9 buildings). The maximum number of building under purpose in Ward no. 14 was observed in residential

with 23 buildings. Under material parameter, a maximum building was seen in RCC with 34 numbers of buildings.

The maximum number of building under purpose in Ward no. 15 was observed in residential with 40 buildings. Under material parameter, a maximum building was seen in RCC with 31 numbers of buildings followed by brick with 13 buildings. The maximum number of building under purpose in Ward no. 16 was observed in residential with 38 buildings and material parameter, a maximum building was seen in RCC with 32 numbers of buildings. The maximum number of building under purpose in Ward no. 17 was observed in residential with 46 buildings and in material parameter, a maximum building was seen in RCC with 30 numbers of buildings. The maximum number of building under purpose in Ward no. 18 was observed in residential with 47 buildings and under material parameter, a maximum building was seen in RCC with 27 buildings and followed by bricks with 10 numbers of buildings.

The maximum number of building under purpose in Ward no. 19 was observed in residential with 28 buildings and in material parameters; a maximum building was seen in RCC with 36 numbers of buildings. The maximum number of building under purpose in outer ward was observed in residential with 34 buildings and material parameter, a maximum building was seen in RCC with 35 numbers of buildings (**Table 3.4**).

3.8.3 Building plan, condition and roof

Condition includes the visible cracks on beams and columns (structural features) and on windows, doors, walls (non-structural features) (Photo plate 33 & 36) presence of soft storey (Photo plate 34) in buildings. Photo plate 27 shows a crack seen on a W1 building type. Photo plate 31 shows peeling off of concrete in the floor plan of a building causing safety issues. Regular and irregular plan (Photo plate 30, 31, 35) are considered in

earthquake design resistant structure, multi-storeyed structures are a concern in seismic study as it can cause imbalance during a shake, pounding of buildings (Photo plate 28, 29) and building damage and collapse are issues faced by multi-storey structure especially on hilly terrain. The building structural plan, its condition and the roof pattern of the buildings in the study area are shown (**Table 3.5**).

Table 3.5. Sample building Plan, condition and roof.

Parameter	Building Plan		Condition			Roof	
	Regular	Irregular	Bad	Good	Moderate	Flat	Slope
Ward 1	10	40	7	26	17	8	42
Ward 2	24	26	5	19	26	18	32
Ward 3	9	41	8	14	28	18	32
Ward 5	13	37	11	14	25	7	43
Ward 6	19	31	13	21	16	13	37
Ward 7	8	42	7	21	22	19	31
Ward 8	16	34	12	18	20	10	40
Ward 9	13	37	10	20	20	18	32
Ward 10	10	40	10	18	22	12	38
Ward 11	15	35	5	30	15	13	37
Ward 12	15	35	5	21	24	18	32
Ward 13	5	45	7	22	21	17	33
Ward 14	10	40	2	23	25	11	39
Ward 15	15	35	3	27	20	19	31
Ward 16	14	36	5	24	21	18	32
Ward 17	17	33	1	24	25	14	36
Ward 18	14	36	10	15	25	17	33
Ward 19	9	41	5	19	26	23	27
Outer ward	12	38	10	19	21	21	29

Source: Computed by Scholar

The building plan observed (**Table3.5**) for Kohima in Ward no. 1 displayed a dominant irregular plan with 40 buildings, maximum number of buildings (26) was under good condition and majority of the building roofs was slope in nature. Ward no. 2 showed 26 buildings under irregular plan, maximum number of buildings (26) was under moderate condition and number of buildings with sloping roof was 32 buildings. Ward no. 3 showed 41 buildings under irregular plan, maximum number of buildings (28) was under moderate

condition and number of buildings with sloping roof was 32 buildings. Ward no. 5 showed 37 buildings under irregular plan, maximum number of buildings (25) was under moderate condition and number of buildings with sloping roof was 43 buildings.

Ward no. 6 showed 31 buildings under irregular plan, maximum number of buildings (21) was under good condition and number of buildings with sloping roof was 37 buildings. Ward no. 7 displayed 42 buildings under irregular plan, maximum number of buildings with 22 buildings was under moderate condition and number of buildings with sloping roof was 31 buildings. Ward no. 8 showed 34 buildings under irregular plan, maximum number of buildings (20) was under moderate condition and number of buildings with sloping roof was 40 buildings. Ward no. 9 showed 37 buildings under irregular plan, 20 number of buildings was under good and moderate conditions and number of buildings with sloping roof was 32 buildings.

The number of buildings in Ward no. 10 had more irregular building plan with 40 buildings, maximum number of buildings was under moderate condition (22 buildings) and number of buildings with sloping roof was 38 buildings. Ward no. 11 showed 40 buildings under irregular plan, maximum number of buildings (22) was under moderate condition and number of buildings with sloping roof was 38 buildings. Ward no. 12 showed 35 buildings under irregular plan, maximum number of buildings (24) was under moderate condition and number of buildings with sloping roof was 32 buildings. The number of buildings in Ward no. 13 had more irregular building plan with 45 buildings, maximum number of buildings was under good condition (22 buildings) and number of buildings with sloping roof was 33 buildings. The number of buildings in Ward no. 14 had more irregular building plan with 40 buildings, maximum number of buildings was under moderate condition (25 buildings) and number of buildings with sloping roof was 39 buildings.

Numbers of buildings in Ward no. 15 had more irregular building plan with 35 buildings, maximum number of buildings was under good condition (27 buildings) and number of buildings with sloping roof was 31 buildings. Ward no. 16 showed 36 buildings under irregular plan, maximum number of buildings (24) was under good condition and number of buildings with sloping roof was 32 buildings. Ward no. 17 showed 33 buildings under irregular plan, maximum number of buildings (25) was under moderate condition and number of buildings with sloping roof was 36 buildings. Ward no. 18 showed 36 buildings under irregular plan, maximum number of buildings (25) was under moderate condition and number of buildings with sloping roof was 33 buildings. Ward no. 19 showed 41 buildings under irregular plan, maximum number of buildings (26) was under moderate condition and number of buildings with sloping roof was 27 buildings. Outer ward displayed 38 buildings under irregular plan, maximum number of buildings (21) was under moderate condition and number of buildings with sloping roof was 29 buildings.

For calculating the distribution of building in the study area, the ratio value was calculated followed by the number of building. The following equations were used;

$$\text{Ratio value} = \frac{\text{Number of household}}{\text{Building}}$$

$$\text{Number of building} = \frac{\text{Number of household}}{\text{Ratio value}}$$

3.8.4 Building type distribution

The number of building (**Table 3.6**) in each ward has been calculated basing on the sampling process. The contribution of buildings in Ward no.1 was highest in W1 building type with 38%. Ward no. 2 W1 building type with percentage of 40% had the highest building type. The highest distribution of building type in Ward no.3 was W1 building type with 40%. The distribution of building type in Ward no.5 was highest in W1 building type

with 62%. The highest distribution of building type in Ward no.6 was W1 building type with 46%.

The highest distribution of building type in Ward no.7 was W1 building type with 34%. The highest distribution of building type in Ward no.8 was W1 building type with 60%. The highest distribution of building type in Ward no.9 was W1 building type with 36%. The distribution of building type in Ward no.10 was highest in W1 building type with 40%. The highest distribution of building type in Ward no.11 was C3M building type with 58%. The distribution of building type in Ward no.12 was highest in C3M building type with 36%. The highest distribution of building type in Ward no.13 was W1 building type with 42%.

The highest distribution of building type in Ward no.14 was C3M building type with 46%. The highest distribution of building type in Ward no.15 was W1 building type with 38%. The distribution of building type in Ward no.16 was highest in C3M building type with 46%. The highest distribution of building type in Ward no.17 was W1 and C3M building types with 40%. The distribution of building type in Ward no.18 was highest in W1 building type with 46%. The highest distribution of building type in Ward no.19 was C3M building type with 44%. The highest distribution of building type in Outer ward was C3L building type with 48%.

Table 3.6. Sample with building type distribution

Ward	Building	W1		C3L		C3M		C3H	
		Number	%	Number	%	Number	%	Number	%
Ward 1	50	19	38	17	34	14	28	0	0
Ward 2	50	20	40	12	24	17	34	1	2
Ward 3	50	20	40	11	22	18	36	1	2
Ward 5	50	31	62	6	12	12	24	1	2
Ward 6	50	23	46	13	26	13	26	1	2
Ward 7	50	17	34	4	8	28	56	1	2
Ward 8	50	30	60	7	14	12	24	1	2
Ward 9	50	18	36	13	26	16	32	3	6
Ward 10	50	20	40	11	22	19	38	0	0
Ward 11	50	15	30	05	10	29	58	1	2
Ward 12	50	17	34	12	24	18	36	3	6
Ward 13	50	21	42	20	40	9	18	0	0
Ward 14	50	16	32	11	22	23	46	0	0
Ward 15	50	19	38	16	32	13	26	2	4
Ward 16	50	18	36	8	16	23	46	1	2
Ward 17	50	20	40	10	20	20	40	0	0
Ward 18	50	23	46	9	18	18	36	0	0
Ward 19	50	14	28	13	26	22	44	1	2
Outer ward	50	15	30	24	48	11	22	0	0

Source: Computed by Scholar.

3.8.5 Building types estimated on the basis of ratio value (Ward no.4)

The building distribution according to its building types in Kohima Town has been estimated based on the ratio value of the Ward no. 4 (1.2 ratio value) after determining the number of building in each type (**Table 3.7**). Maximum number of building type in Ward no. 1 was observed in W1 building type (481) followed by C3M building type (355). The highest number of building type in Ward no. 2 was observed in W1 building type (376) followed by C3M building type (320). Maximum number of building type in Ward no. 3 was observed in W1 building type (421) followed by C3M building type (378). Maximum number of building type in Ward no. 4 was observed in W1 building type (484) followed by C3L building type (184). Maximum number of building type in Ward no. 5 was observed in W1 building type (390) followed by C3M building type (151). Maximum

number of building type in Ward no. 6 was observed in W1 building type (452) followed by C3M building type (256).

Table 3.7. Distribution of building type on the basis of ratio type

Area	W1	C3L	C3M	C3H
Ward 1	481	347	355	0
Ward 2	376	179	320	19
Ward 3	421	186	378	21
Ward 4	484	184	52	1
Ward 5	390	61	151	13
Ward 6	452	206	256	21
Ward 7	196	36	324	13
Ward 8	278	52	110	9
Ward 9	366	211	326	61
Ward 10	378	166	359	0
Ward 11	304	81	587	21
Ward 12	260	147	275	46
Ward 13	234	178	100	0
Ward 14	364	199	522	0
Ward 15	545	367	371	58
Ward 16	730	260	934	41
Ward 17	573	229	572	0
Ward 18	432	135	339	0
Ward 19	196	146	310	13
Outer ward	848	1080	617	0

Source: Computed by Scholar

Maximum number of building type in Ward no. 7 was observed in C3M building type (481) followed by W1 building type (196). Maximum number of building type in Ward no. 8 was observed in W1 building type (278) followed by C3M building type (110). Maximum number of building type in Ward no. 9 was observed in W1 building type (366) followed by C3M building type (326). Maximum number of building type in Ward no. 10 was observed in W1 building type (378) followed by C3M building type (359). Maximum number of building type in Ward no. 11 was observed in C3M building type (587) followed by W1 building type (304). Maximum number of building type in Ward no. 12 was observed in C3M building type (275) followed by W1 building type (260). Maximum

number of building type in Ward no. 13 was observed in W1 building type (234) followed by C3L building type (178).

Maximum number of building type in Ward no. 14 was observed in C3M building type (522) followed by W1 building type (364). Maximum number of building type in Ward no. 15 was observed in W1 building type (545) followed by C3M building type (371). Maximum number of building type in Ward no. 16 was observed in C3M building type (934) followed by W1 building type (730). Maximum number of building type in Ward no. 17 was observed in W1 building type (573) followed by C3M building type (572). Maximum number of building type in Ward no. 18 was observed in W1 building type (432) followed by C3M building type (339). Maximum number of building type in Ward no. 19 was observed in C3M building type (310) followed by W1 building type (196). Maximum number of building type in Outer ward was observed in C3L building type (1080) followed by W1 building type (848).

The highest total number of building types fall under outer ward with 2545 buildings, followed by Ward no. 16 and the lowest total number of buildings is contributed by Ward no. 8 with 449 followed by Ward no. 7 with 569 buildings (**Figure 3.9**). The total distribution of building types in Kohima Town is 20,348 buildings with W1 building type as the largest building composition (8303 buildings), next is C3M building type with 7258 buildings, C3L building type has 4450 buildings and C3H building type has the least number of buildings with 337 buildings (**Figure 3.10**).

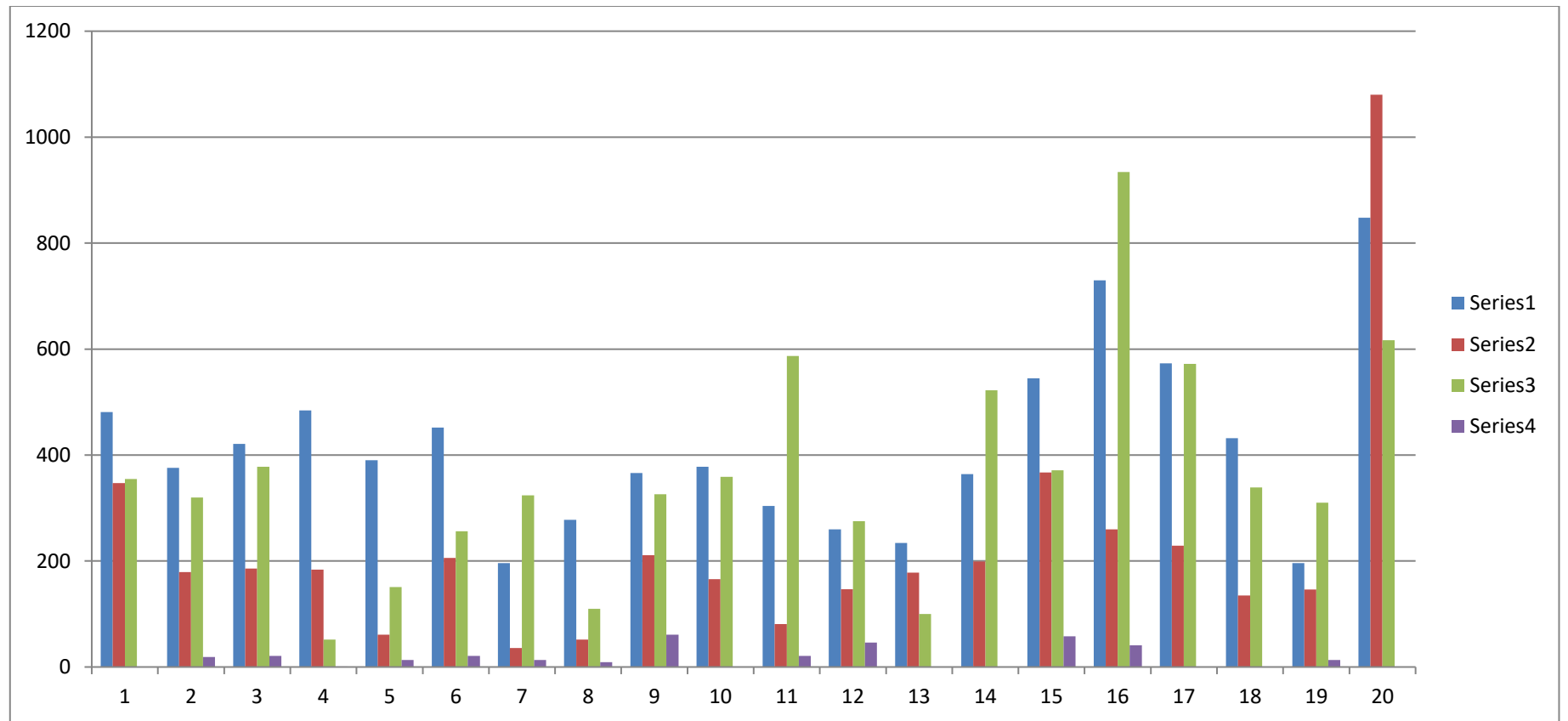


Figure 3.9. Number of distribution of building type in Kohima Town.

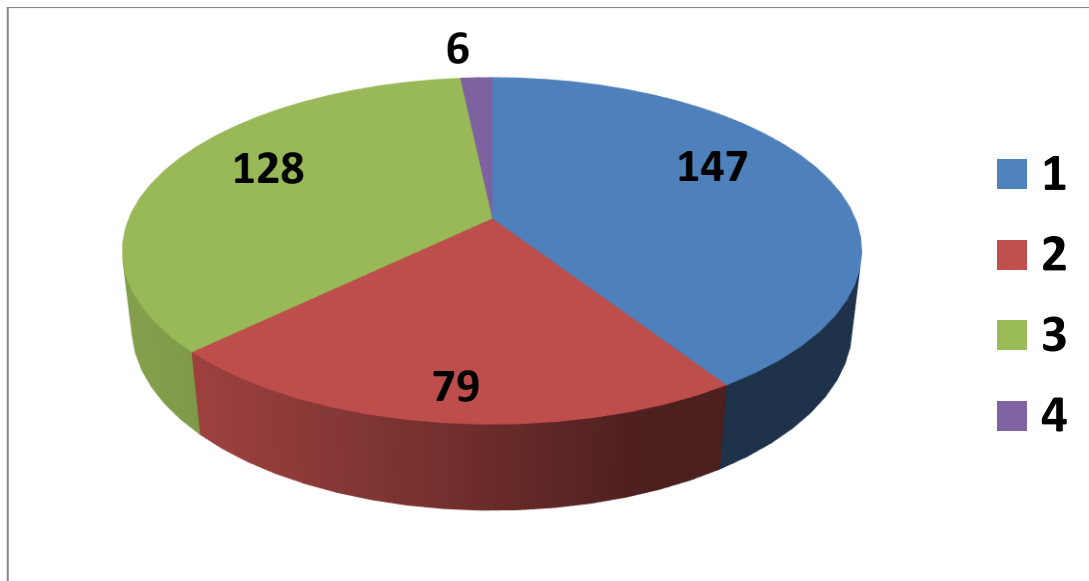


Figure 3.10: Distribution of total number of building types in Kohima Town

4

4.1 Introduction

Vulnerability function in HAZUS method is based on two functions- capacity curve and demand curve. Capacity curve- also known as push-over curve is a plot of building lateral load resistance as a function of a characteristic lateral displacement. It is derived from a plot of static equivalent base shear versus building (e.g. roof) displacement. Capacity curve is defined by three control points- design, yield and ultimate capacity respectively. Design capacity represents nominal building strength required by current model seismic code provision or in other word it is an estimate of nominal strength of buildings not designed for earthquake loads. Wind design is not considered in design capacity and certain buildings may have lateral design strength greater than based on seismic code provision. Yield capacity represents lateral strength of building considering redundancies in design, conservatism in requirement of code and true strength of material

(FEMA). Ultimate capacity represents maximum strength of the building when the structural systems reach a full plastic state. Besides capacity curve the other component of HAZUS is Fragility curve. Fragility curve describe the probability of building damage such as; structural system, non-structural component sensitive to drift and non-structural component sensitive to acceleration. The building response in fragility curve distribute damage between four physical damage states- slight, moderate, extensive and complete (FEMA, 2001). The four physical damage states of FEMA/NIBS methodology are similar to the damage states defined in Expected Seismic Performance of Buildings (EERI, 1994) except that damage descriptions vary for each model building type based on the type of structural system and material.

Buildings are assumed to be deformed beyond its ultimate point without loss in stability. Upto the yield capacity the building capacity curve are assumed to be linear with stiffness based on an estimate of the expected period of the building. From yield to ultimate point, the capacity curve changes from an elastic state to a fully plastic. The capacity curve is assumed to be plastic past the ultimate point. The equations of building capacity curve are

Yield point is denoted by D_y and A_y where,

$$A_y = C_s \gamma / \alpha_1$$

$$D_y = 9.8 A_y T_e^2$$

Ultimate point is denoted by D_u and A_u where,

$$A_u = \lambda A_y$$

$$D_u = \lambda \mu D_y$$

C_s stands for design value

T_e stands for building period

γ, λ stands for over strength and

M stands for ductility

Seismic vulnerability assessment is a method used for quantification of risk involved due to expected earthquake in a region. The vulnerability is usually represented in

terms of either Damage Probability Matrices (DPM) or Vulnerability (Fragility) curves. The seismic vulnerability of structures is commonly expressed through probabilistic fragility functions representing the conditional probability of reaching or exceeding a predefined damage state given the measure of earthquake shaking (Vazurkar and Chaudhari, 2016). Seismic vulnerability functions are an essential component for managing earthquake risk. Seismic risk management involves tradeoffs between the potential loss due to an earthquake, and the costs of reducing this potential loss (Porter *et al.*, 2002).

4.2 Estimation of building damage

The estimate of site shaking as input to a seismic vulnerability function is used which estimates the degree of damage to a building located at a site, given the shaking severity the earthquake causes. The damage as a fraction of the replacement cost of the building is convenient to express the degree of damage as the cost. The ratio of the repair cost to replacement cost is known as damage factor. The damage factor in a seismic vulnerability function can be deterministic giving single value for a given value of severity in shaking or probabilistic i.e., giving an uncertain damage factor as output, with a mean value and a measure of uncertainty. Using the seismic vulnerability function output, one multiplies the damage factor by the replacement cost of the building in question, to estimate the cost of repair to the building, if earthquake occurs (Porter *et al.*, 2002). The design of building structure besides the proximity of buildings (Photo plate 19) plays a major role in seismic hazard.

4.3 Estimation of earthquake hazard

Seismologists, geologists, and geotechnical engineers study on seismic faults in order to understand active earthquake sources, their potential size, frequency, and location.

With earthquake location and magnitude, one can estimate the severity of ground shaking at a particular building site. Severity can be measured in a variety of ways: in qualitative terms such as using the Modified Mercalli Intensity (MMI) scale; or quantitative measures recorded by instruments, such as Peak Ground Acceleration (PGA) or Spectral acceleration (Sa).

HAZUS calculates the building damage using a database that includes seismic hazard information, inventory of building stocks, and a set of fragility functions for various types and qualities of building components and buildings. The probability of structural and non-structural components reaching or exceeding each of the four damage states: slight, moderate, extensive and complete are given by the HAZUS fragility functions.

Earthquake intensity qualitatively describes the effects of ground shaking rather than the energy released. While an earthquake is described by a single magnitude, it produces a range of shaking intensities across an area. The intensity survey in any region after an earthquake provides important information about the directivity, fault strike and attenuation characteristics. The event has presented an opportunity to validate our current knowledge of earthquake risk in the region. The earthquake effects are crucial in understanding the nature of the natural hazard, its impact and extent of the risk exposure to the society (Prajapati *et al.*, 2011).

Seismic intensity and ground motion are two parameters that describe the severity of ground shaking during earthquakes. A more objective representation of the degree of shaking is given by the accelerations that are measured by accelerographs. A relationship between PGA/PGV and MMI provides a tool to rapidly assess damage for any earthquake. Such relationships are useful in generating shake graphs for seismically active regions where more frequent, small to moderate, events occur and are felt widely but cause little or

no damage. Seismic intensity is based on the human perception of the damage, earthquake effects and is commonly measured using an MMI scale (Prajapati *et al.*, 2011).

A new intensity attenuation relation for the Indian subcontinent and the Himalaya region and compared it with the intensity attenuation of the central and eastern North America (Szeliga *et al.*, 2010). Several studies on the relationship between PGA and MMI suggest that such empirical relationships are region specific, and therefore, they should be carefully chosen for use in a particular region (Murphy and O'Brien, 1977 and Kaka and Atkinson, 2004).

One of the first attempts to correlate the above parameters was done by Cancani (1904). Since, there are numerous correlations that have been published for various regions (Gupta 1980; Wu *et al.*, 2003; Tselentis and Danciu, 2008). The low levels of the shaking intensity correlate fairly well with the PGA and PGV, while high intensities correlate best with PGV. PGV correlates better with the intensity than the PGA, based on the correlation of intensity with PGA and PGV for the 1994 Northridge earthquake (Wald *et al.*, 1999 and Boatwright *et al.*, 2001).

The peak ground acceleration is an important strong motion parameter for safe engineering design of the structures. Therefore the zoning based on peak ground acceleration is more useful to predict seismic hazard than the other parameters. The unavailability of strong motion data for different seismically active regions always put hurdle in seismic hazard studies (Mohan *et al.*, 2008). The alternate approach is the simulation of strong ground motion.

4.4 Estimation of Building response

The demand spectrum and building curve intersection determine the building response. Consider three demand spectra- weak, medium and strong ground shaking. The stronger and stiffer construction will displace lesser than weak and more flexible construction for same level of spectral demand, and less damage will be incurred to the structural system. Stronger and stiffer construction will also shake at higher acceleration levels and more damage will be incurred to non-structural components such as door, windows etc.

4.5 Building fragility curve

HAZUS technical manual provides the procedure for deriving the fragility curves for different types of structures. Building fragility curves are log normal functions that describe the probability of reaching, or exceeding, structural and non-structural damage states, given median estimates of spectral response, for example spectral displacement (Vazurkar and Chaudhari, 2016). The Fragility analysis of mid-rise RC buildings was performed using incremental dynamic analysis on 3, 5, 7 storey RC buildings with 12 artificial earthquake records. Yielding and collapse capacity of the buildings was determined from the analysis. They used PGA, elastic spectral displacement as ground motion parameters, inter-storey drift and spectral displacement values as a damage measurement parameter (Murat, 2006).

Raipure (2015) explained a study on development of fragility curves for open ground storey buildings. She had used probabilistic seismic demand model (PSDM) as per power law for the generation of fragility curves. A typical ten storied OGS framed building was considered and the building considered is located in Seismic Zone-V. The design forces for the ground storey columns were evaluated based on various codes such as

Indian, Euro, Israel, and Bulgarian suggested approach. She designed various OGS frames considering MF as 1.0, 2.1 (Israel), 2.5 (Indian), 3.0 (Bulgarian), and 4.68 (Euro). The performance of each building was studied using the fragility analysis method (Cornell *et al.*, 2002).

Fragility curve is a useful tool for predicting earthquake risk of buildings with similar characteristics such as material, height and design code level. The curves can be formed empirical, heuristic or analytical based methods (Singhal and Kiremidjian 1996; Porter *et al.*, 2001; Rossetto and Elnashai 2003; Zhang and Hu, 2005; Wu *et al.*, 2012 and Abo-El-Ezz *et al.*, 2013).

Fragility curves are cumulative distribution functions that probability of reaching or exceeding damage state as demand parameters such as Storey Drift Ratio (SDR), Peak Ground Acceleration (PGA), Spectral acceleration (Sa) or Spectral displacement (Sd). It has been widely accepted that spectral displacement can be closely correlated with seismic damage of structures (Serdar and Polat 2006; Lignos and Karamanci 2013; Su and Lee 2013; Hsieh *et al.*, 2013 and Suppasri *et al.*, 2013)

4.6 Estimating the seismic vulnerability

The vulnerability assessment of the study area was estimated based on HAZUS methodology. The first step involves the mapping of the building i.e., the digital footprint from the high resolution satellite imageries. The various building model type based on HAZUS building type was identified and classified through field survey. The next step involves the formulation of spectral displacement based on PSA and time period. Capacity curve was generated from the yield and ultimate capacity curve provided in the HAZUS technical manual (**Table 4.1 & Figure 4.1**).

From the capacity curve, the peak building response point was determined which helps in formulation of the fragility curve. The fragility curve derived from the capacity curve. Discrete damage probability curve was calculated after fragility curve, it is divided into no damage, slight damage, moderate damage, extensive damage and complete damage are the codes for seismic safety. Finally, the vulnerability of building for Kohima was determined from the damage probability.

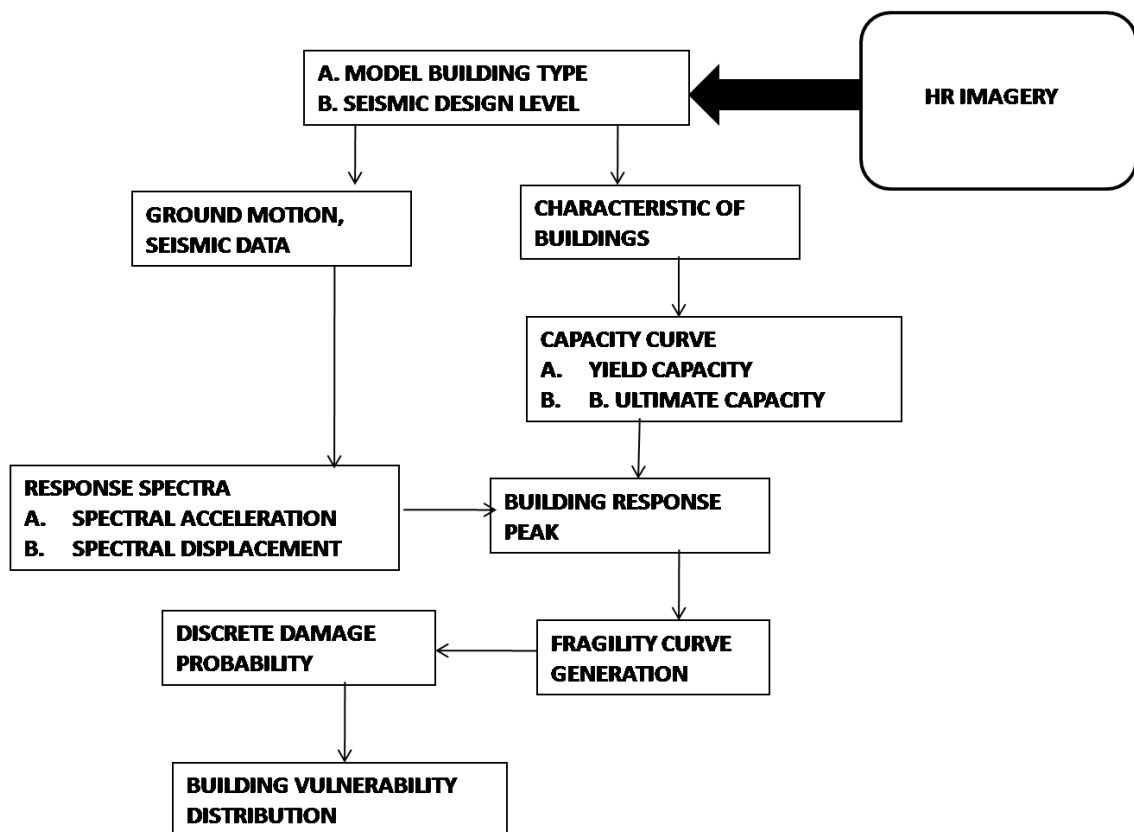


Figure 4.1. Flowchart of the seismic methodology

Table 4.1 Building capacity curve for pre-code seismic design

Building type	Yield Capacity Point		Ultimate Capacity Point	
	D_y	A_y	D_u	A_u
W1	0.24	0.200	4.32	0.600
C3L	0.12	0.100	1.35	0.225
C3M	0.26	0.083	1.95	0.188
C3H	0.74	0.063	4.13	0.143

Source: FEMA, 2003.

4.7 Seismic Hazard map of North East India

Few researches have been done on seismic hazard map particularly NE India. For implementing the seismic hazard map for the study, the attenuation model of Das *et al.*, 2006 has been adopted. Das *et al.*, (2006) determine the seismic hazard map using probabilistic seismic hazard analysis through Pseudo-Spectral Velocity (PSV) or Pseudo-Spectral Acceleration (PSA) developed using 261 accelerograms from 6 different earthquake events.

Table 4.2. Spectral displacement and acceleration of the study area.

Time period	Spectral acceleration	Spectral displacement
0.04	0.26	0.004
0.17	0.79	0.223
0.34	0.49	0.555
.7	0.26	1.248
1	0.23	2.254

Source: Das *et al.*, (2006).

The various time periods along with their specified PSA considered for seismic input in HAZUS model. The seismic hazard maps provide direct and detailed information of the activities particularly the seismic parameters PSA contours on 5% damping. From display the seismic map for PSA 0.26 and 0.79 and time period 0.04 and 0.17s respectively. PSA 0.49 seismic data has a time period of 0.34s. Seismic data for PSA.26 has a time period of 0.7s and lastly, PSA 0.23 has time period 1.0s. The relationship and distribution between spectral displacement and spectral acceleration shows that as time period increase so does spectral displacement however, spectral acceleration does not follow any such trend. The respective seismic parameters were considered for generating the spectrum response curve for estimating the seismic vulnerability assessment of Kohima (Table 4.2 & Figure 4.2).

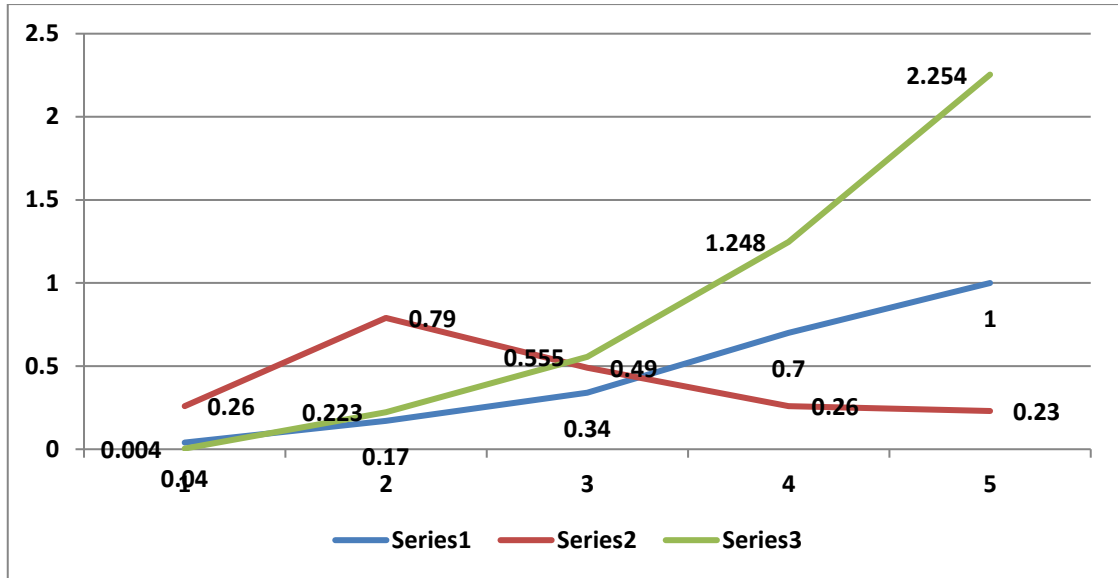


Figure 4.2. Graph showing the distribution of spectral displacement and spectral acceleration

4.8 HAZUS mechanism

The analytical characterization and assessment of earthquake hazard was evaluated by defining the discrete damage probability in the study area. The demand spectra was generated by considering the time period and spectral acceleration available from previous works. The time period considered for 5% damping are-

The formula for calculation of spectral displacement is as follows;

$$S_D = 9.8 \times S_A \times T^2$$

Where,

S_A is spectral acceleration &
 T is time period in seconds

The generation of capacity curve for pre-code seismic design with its respective values are

4.9 Demand spectrum curve

The demand spectrum curve has been generated from the seismic values, time period considered for the curve are 0.04s, 0.17s, 0.34s, 0.7s, and 1.0s. From the figure it is seen that as spectral acceleration increase the lower shear velocity resulting in higher spectral displacement in a given time period (**Figure 4.3**).

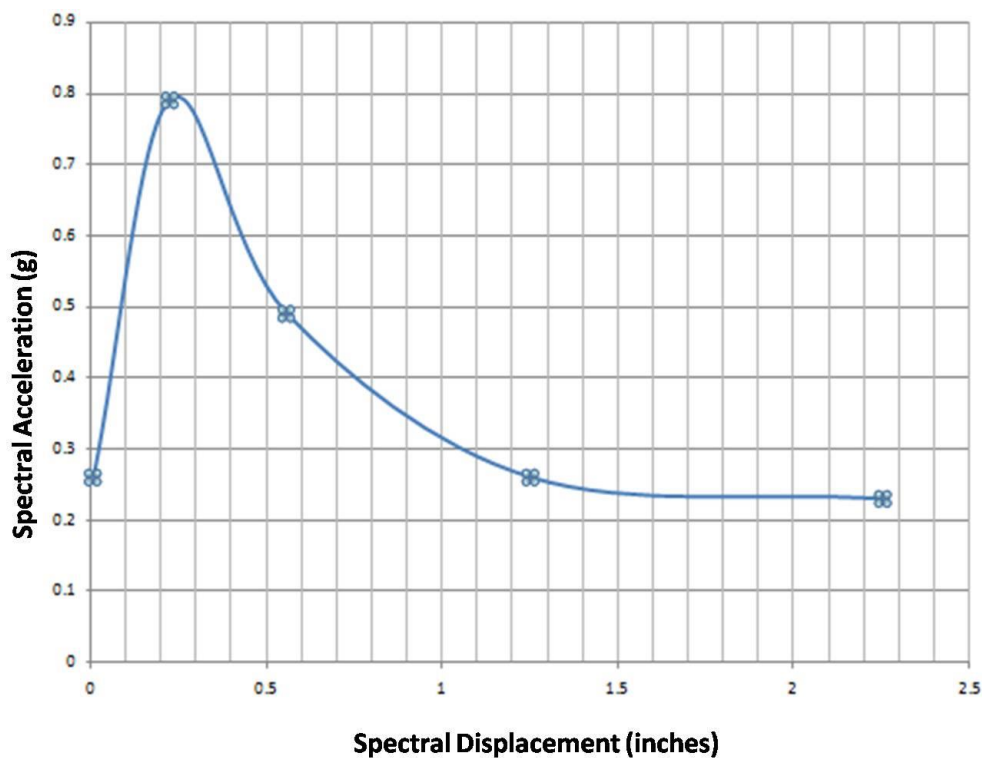


Figure 4.3. Demand spectrum curve for Kohima

4.10 Capacity Curve

Capacity curves are generated from the yield and ultimate capacity points of the building. These values change as per building types based on their seismic design level. Weight of the building and material of the building are important factors in development of these curves (Malladi, 2012). Capacity curves define the strength of the building to resist earthquakes. W1 stands for light weight wooden building type, C3L indicates low rise concrete frame structure with un-reinforced masonry infill walls, C3M indicates mid-rise

concrete frame structure with un-reinforced masonry infill walls and C3H indicates high-rise concrete frame structure with un-reinforced masonry infill walls. .

Capacity curve generated from **Table 4.2** for W1, C3L, C3M and C3H building types. Values are increasing in spectral acceleration as the spectral displacement increases. The lateral strength of the building decreases as the acceleration increases along with the displacement (**Figure 4.4**).

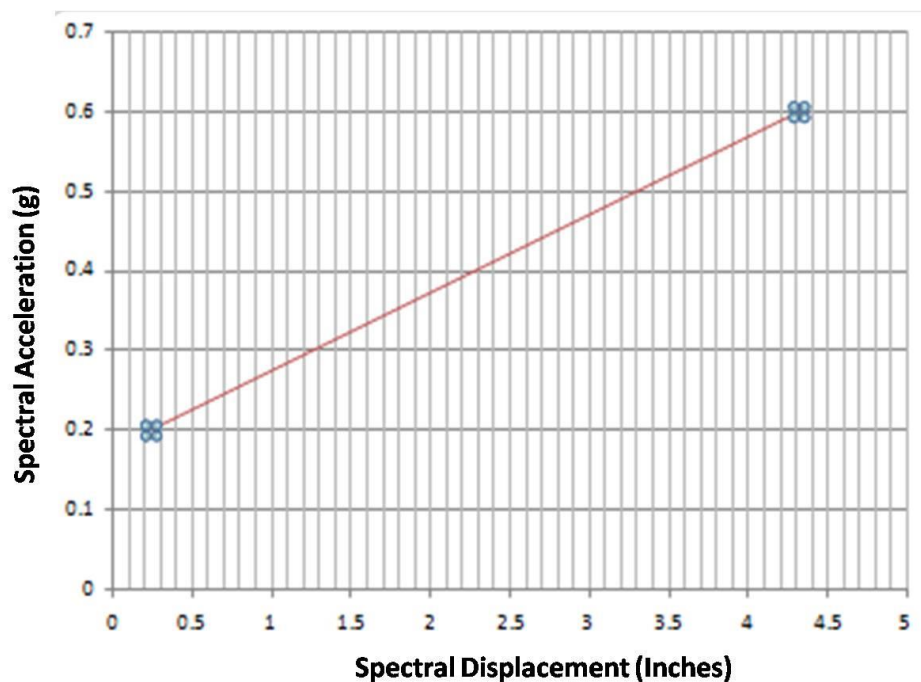


Figure 4.4. Capacity curve for W1 building type.

The capacity curve for C3L building type shows increasing value in spectral acceleration as the spectral displacement increasing resulting in reduction lateral strength of building (**Figure 4.5**).

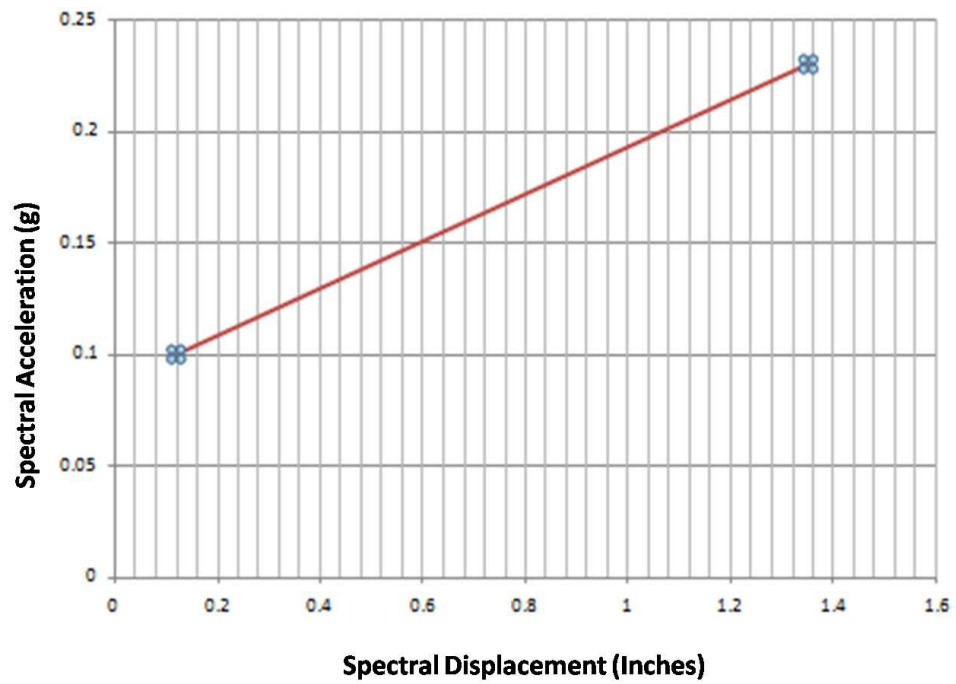


Figure 4.5. Capacity curve for C3L building type.

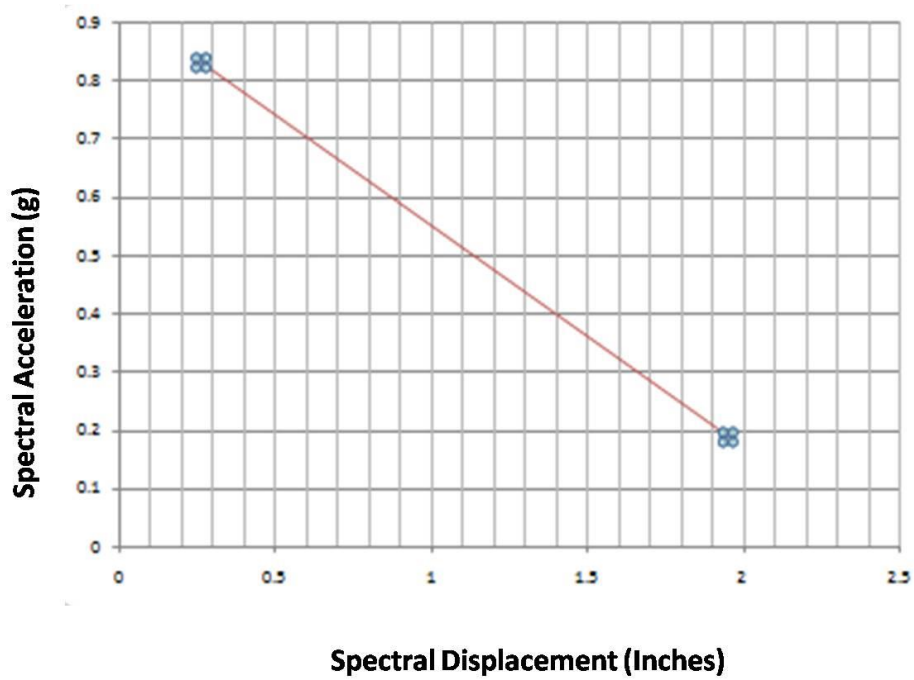


Figure 4.6. Capacity curve for C3M building type.

C3M shows a reverse trend where with increasing acceleration the displacement decreases. The graph depicts the lateral strength of C3M building types in Kohima is relatively strong and lesser damage will be experienced compared to remaining building types (**Figure 4.6**).

C3H building types show increase spectral acceleration for increase in spectral displacement, the lateral building strength decrease as the spectral acceleration increase causing more displacement to the building structure (**Figure 4.7**)

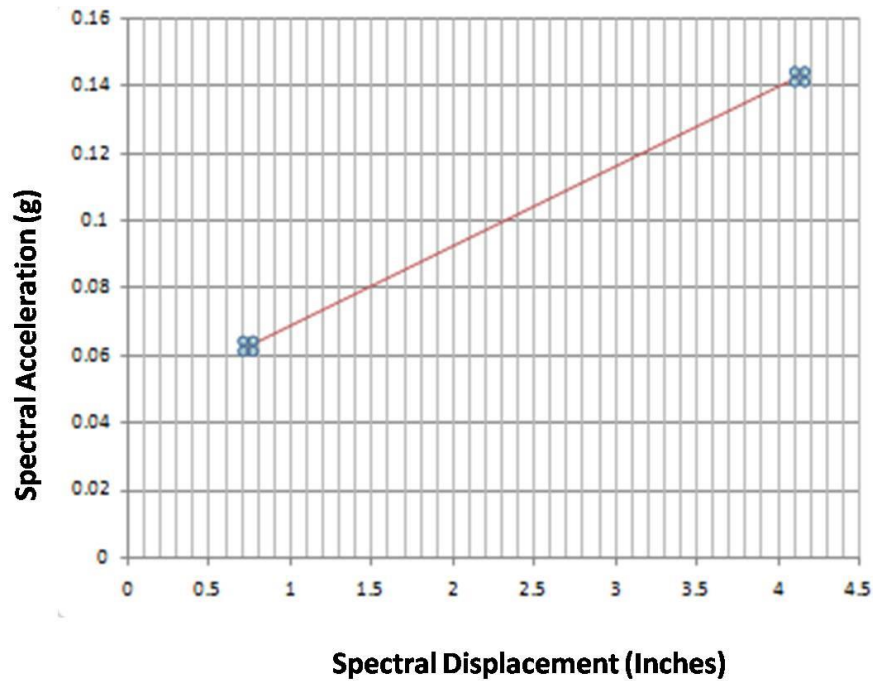


Figure 4.7. Capacity curve for C3H building type.

4.11 Peak building response

The peak building response was generated when the yield and ultimate capacity curve intersect for the building types for pre-code seismic codes. The intersection points of the ultimate and yield capacity curve of two buildings W1 and C3M for representation are shown (**Figure 4.8 & 4.9**).

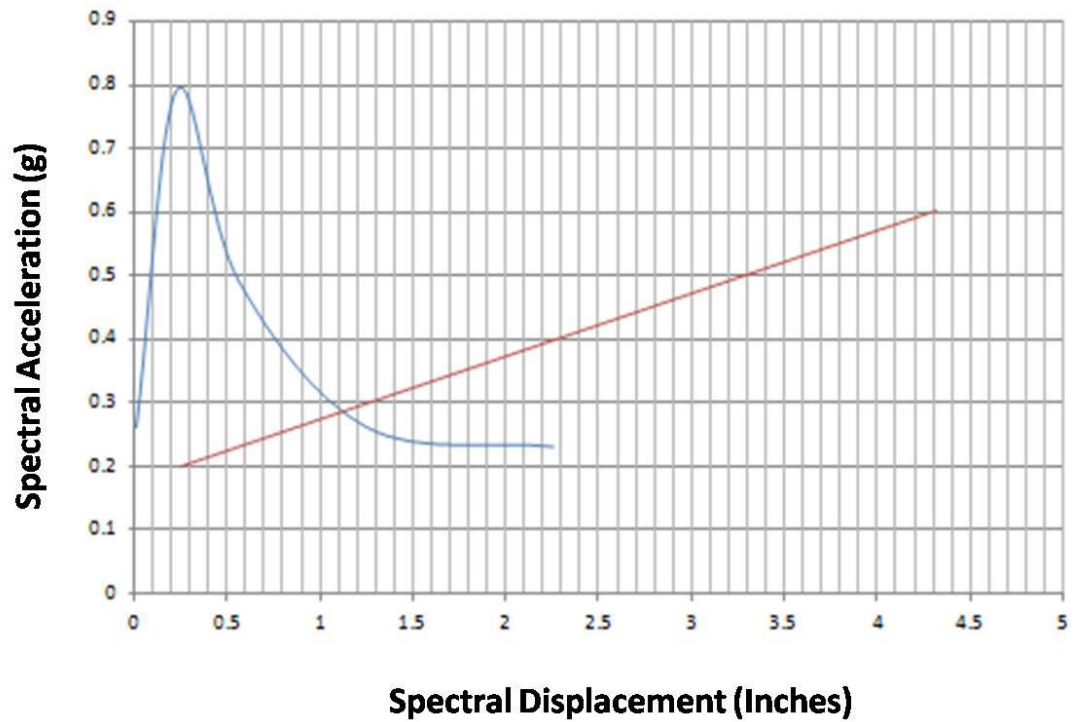


Figure 4.8. Building Peak response for W1 is at 1.1.

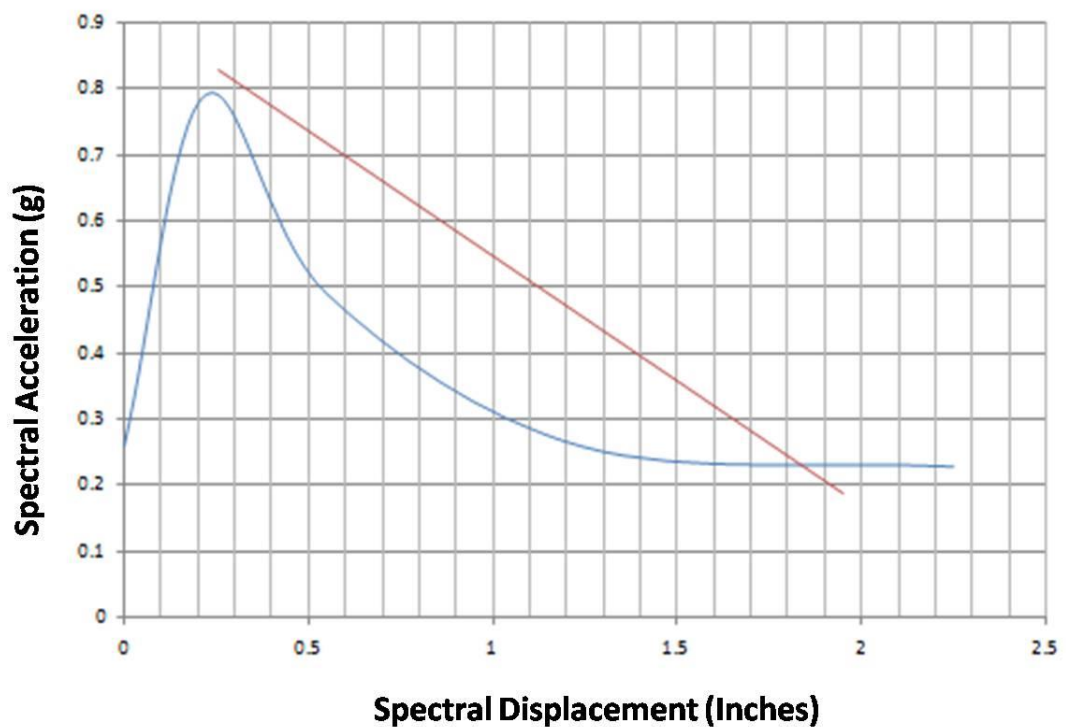


Figure 4.9 Building Peak response for C3M is at 1.85.

The intersection points where the capacity curve and demand spectrum curve intersect in the different building type of Kohima (**Table 4.3**). C3H building has the highest peak response value 3.2 which describe that C3H buildings will experience shaking

till 3.2 m/s and beyond the point it will experience maximum damage. C3M has peak response of 1.85 m/s, C3L has a peak response of 1.35 m/s and W1 building type has 1.1 m/s peak response. W1 building type has the least peak response value, the buildings under W1 building will experience shaking till 1.1 m/s and maximum damage will incur when the peak response is reached. The graph shows the building peak response increase from W1 to C3H building type (**Figure 4.10**).

Table 4.3. Building Peak response of the Building types in the study area

Building Type	Building peak response (m/s)
W1	1.1
C3L	1.35
C3M	1.85
C3H	3.2

Source: Computed by Scholar.

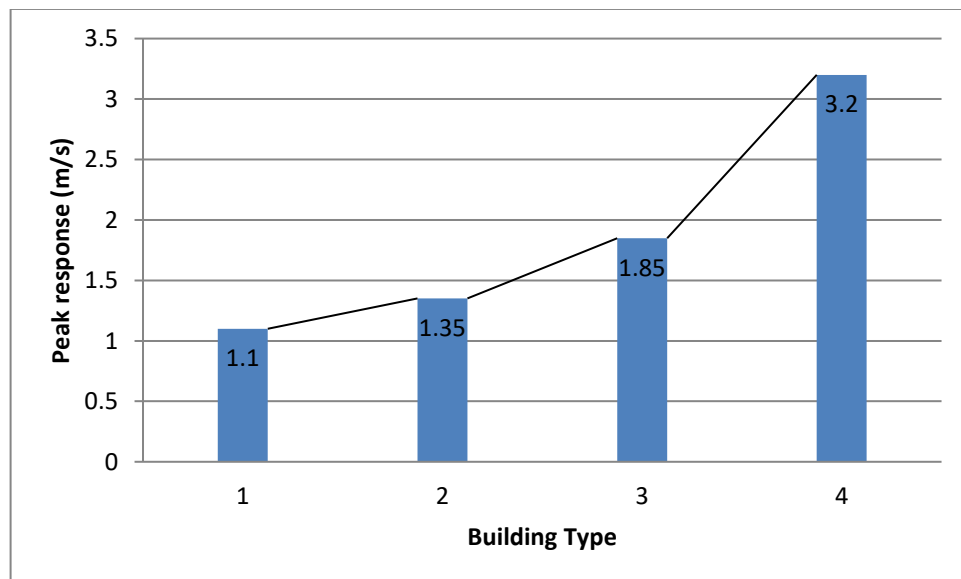


Figure 4.10. Graph showing the peak response in the HAZUS building types

4.12 Fragility Curve

Fragility curve of the various building types are generated based on the value present in HAZUS technical manual (**Table 4.4**). Using the fragility curve based on the spectral displacement, the discrete damage probabilities are estimated.

Table 4.4. Fragility curve parameter for Pre-code seismic design level.

Building Type	Spectral Displacement (Inches)							
	Slight		Moderate		Extensive		Complete	
	Median	Beta	Median	Beta	Median	Beta	Median	Beta
W1	0.50	1.07	1.01	1.11	3.15	1.11	6.30	1.14
C3L	0.72	1.19	1.44	1.11	4.50	0.99	9.00	1.02
C3M	1.80	0.92	3.60	0.95	11.25	1.03	22.50	1.09
C3H	3.46	0.86	6.91	0.90	21.60	1.04	43.20	1.09

Source: FEMA, 2003.

4.12 Damage probabilities

4.12.1 Cumulative damage probability curve

Cumulative damage probabilities are calculated using the following equation;

$$P[ds/S_d] = \Phi \left[\frac{1}{\beta_{ds}} \ln \left(\frac{S-d}{\hat{S}_{d.ds}} \right) \right]$$

Where,

$P[ds/S_d]$ = probability of being in or exceeding a damage state, ds

S_d = given spectral displacement (inches)

\hat{S}_{ds} = median value of S_d at which the building reaches the threshold of damage state, ds .

β_{ds} = Lognormal standard deviation of spectral displacement of damage state, ds

Φ = Standard normal cumulative distribution function

Using the cumulative equation, the values of cumulative probabilities are summarized as,

Table 4.5. Cumulative damage probabilities for the study area

Cumulative probability	P (S/S _d)	P (M/S _d)	P (E/S _d)	P (C/S _d)
W1	.8413	.5000	.1841	.0359
C3L	.8159	.6179	.3446	.0808
C3M	.8413	.5793	.2420	.0668
C3H	.9332	.6915	.3085	.0808

Source: Computed by Scholar

Where,

$P(S/S_d)$ = probability of being in or exceeding a slight damage state, S.

$P(M/S_d)$ = probability of being in or exceeding a moderate damage state, M.

$P(E/S_d)$ = probability of being in or exceeding an extensive damage state, E.

$P(C/S_d)$ = probability of being in or exceeding a complete damage state, C.

The discrete damage probabilities for HAZUS methodology are calculated using,

Probability of complete damage, $P(C) = P(C/S_d)$

Probability of extensive damage, $P(E) = P(E/S_d) - P(C/S_d)$

Probability of moderate damage, $P(M) = P(M/S_d) - P(E/S_d)$

Probability of slight damage, $P(S) = P(S/S_d) - P(M/S_d)$

Probability of no damage, $P(\text{None}) = 1 - P(S/S_d)$

Table 4.6. Discrete damage probabilities of building in study area

TYPE	NO DAMAGE	SLIGHT	MODERATE	EXTENSIVE	COMPLETE
W1	0.1587	0.3413	0.3159	0.1482	0.0359
C3L	0.1841	0.198	0.2733	0.2638	0.0808
C3M	0.1587	0.262	0.3373	0.1752	0.0668
C3H	0.0668	0.2417	0.383	0.2277	0.0808

Source: Computed by Scholar

The discrete damage probability was calculated, where the different building types with discrete probabilities is shown (**Table 4.6 & Figure 4.11**). The discrete damage probabilities generated are converted into percentage to generate database for the entire Kohima Town.

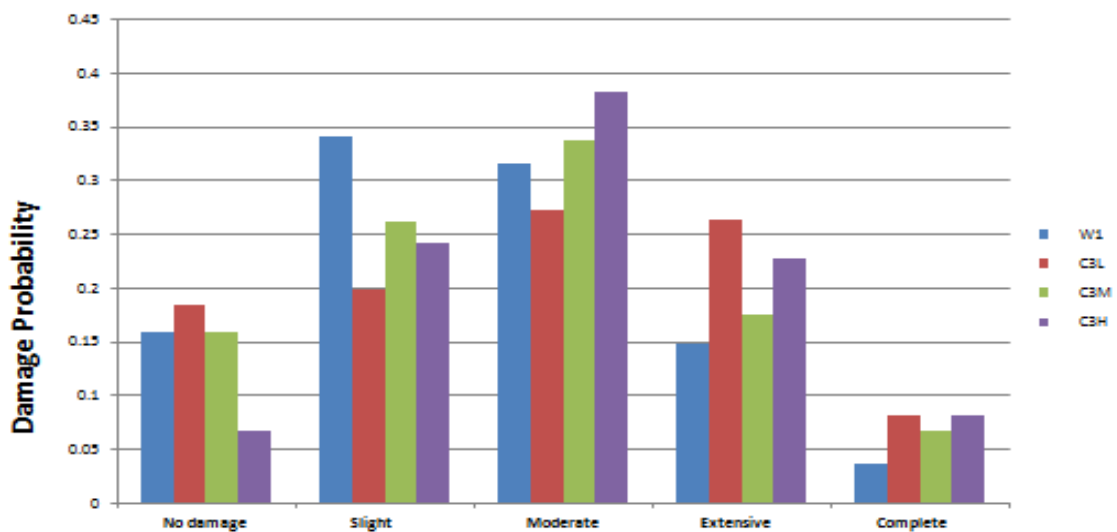


Figure 4.11. Damage probability of the building type in Kohima

The discrete damage probabilities in percentage for the building types show in W building type, highest damage probability is seen in slight damage probability (34.13%) and least damage is seen in complete damage (3.59%). C3L building types show maximum damage probability in moderate damage (27.33%) and lowest damage probability was seen in complete damage (8.08%). C3M building type showed lowest damage probability in complete damage (6.68%) and highest damage probability was in moderate damage probability (33.73%). In C3H building type, highest damage probability was observed in slight damage probability and lowest damage probability was in moderate damage probability (3.83%) (Table 4.7 & Figure 4.12).

Table 4.7. Discrete damage probabilities of building in percentage.

TYPE	NO DAMAGE (in %)	SLIGHT (in %)	MODERATE (in %)	EXTENSIVE (in %)	COMPLETE (in %)
W1	15.87	34.13	31.59	14.82	3.59
C3L	18.41	19.8	27.33	26.38	8.08
C3M	15.87	26.2	33.73	17.52	6.68
C3H	6.68	24.17	3.83	22.77	8.08

Source: Computed by Scholar

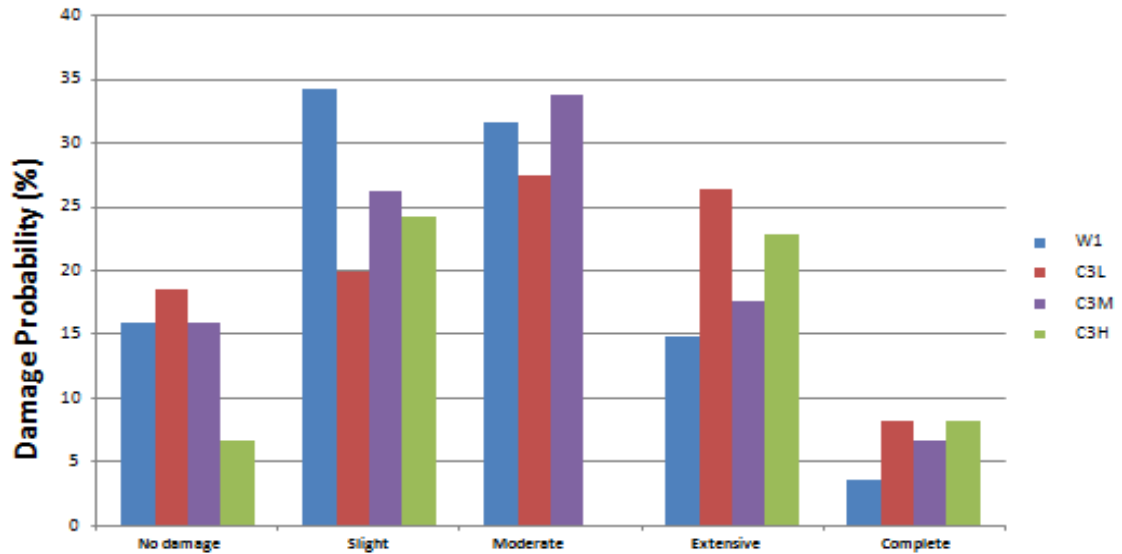


Figure 4.12. Damage probability in percentage of the building type in Kohima

For estimating the damage probability of the entire study area the generated damage probability (**Table 4.7**) from Ward no.4 was considered and applied to each Ward in the study area. The number of buildings with no damage probable in building was generated after the damage probable for the entire ward in the study area was calculated based on the damage probability of Ward no. 4 (Table 4.7).

The number of buildings affected in **no damage** probable was 3511 buildings where maximum was observed in Outer ward (482 buildings) followed by Ward no. 16 (327 building). The least number of buildings in no damage probable was observed in Ward no.8 (75 building) followed by Ward no. 7 (91 buildings). The building type under maximum number of no damage probable was observed in C3L building type and least number was seen in C3H. From this study it is observed C3L and W1 building types are safer as compared to C3M and C3H (**Table 4.8 & Figure 4.13, 4.14**).

Table 4.8. Number of buildings with no damage

Ward	W1	C3L	C3M	C3H	Total building	Ward Population
1	76	80	56	0	212	7082
2	60	41	51	1	153	5207
3	67	43	60	1	171	5692
4	77	34	8	0	119	3568
5	62	14	24	1	101	3197
6	72	47	41	1	161	5381
7	31	8	51	1	91	2721
8	44	12	18	1	75	2348
9	58	49	52	4	163	4808
10	60	38	57	0	155	4820
11	48	19	93	1	161	5267
12	41	34	44	3	122	3848
13	37	41	16	0	94	3228
14	58	46	83	0	187	6101
15	86	84	59	4	233	7970
16	116	60	148	3	327	11603
17	91	53	91	0	235	7775
18	69	31	54	0	154	4809
19	31	34	49	1	115	3614
Outer ward	135	249	98	0	482	15734

Source: Computed by Scholar

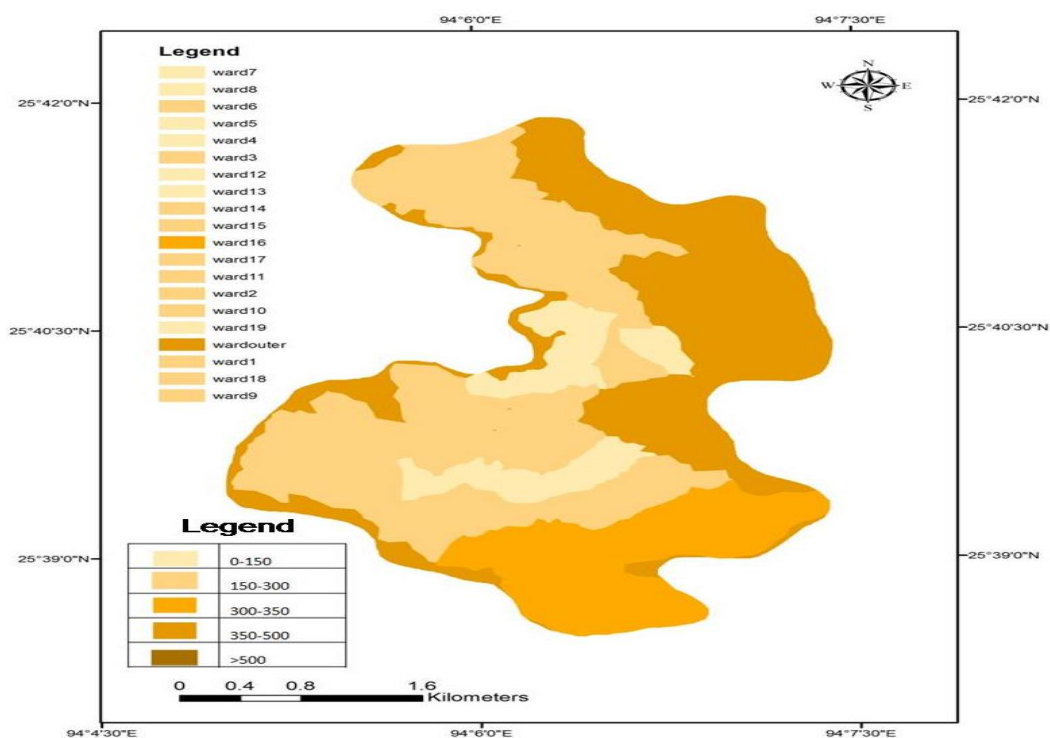


Figure 4.13 Total number of buildings with no damage

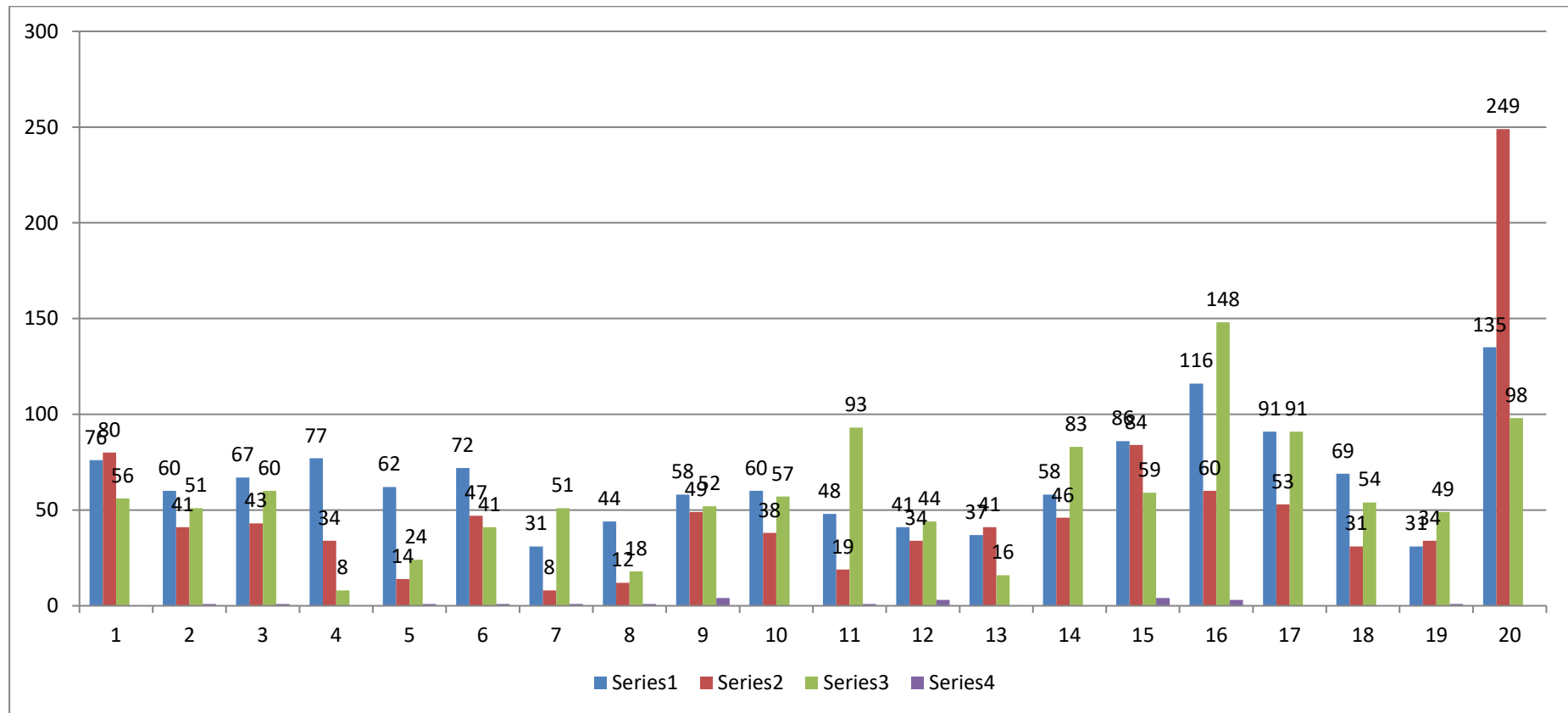


Figure 4.14. Number of building type under no damage in each ward

The number of buildings affected in **slight damage** probable was 5910 buildings where maximum was observed in Outer ward (718 buildings) followed by Ward no. 16 (568 building). The least number of buildings in slight damage probable was observed in Ward no.8 (139 building) followed by Ward no. 13 (150 buildings). The building type under maximum number of slight damage probable was observed in W1 building type and least number was seen in C3H building type. From this study it is observed W1 building types are safer as compared to C3L, C3M and C3H building types (**Table 4.9 & Figure 4.15, 4.16**).

Table 4.9. Number of buildings with slight damage

Ward	W1	C3L	C3M	C3H	Total building	Ward Population
1	165	86	93	0	344	7082
2	128	45	84	5	262	5207
3	144	46	99	5	294	5692
4	165	36	14	0	215	3568
5	133	15	40	3	191	3197
6	154	51	67	5	277	5381
7	67	9	85	3	164	2721
8	95	13	29	2	139	2348
9	125	52	85	15	277	4808
10	129	41	94	0	264	4820
11	104	20	154	5	283	5267
12	89	36	72	11	208	3848
13	80	44	26	0	150	3228
14	124	49	137	0	310	6101
15	186	91	97	14	388	7970
16	249	64	245	10	568	11603
17	195	57	150	0	402	7775
18	147	33	89	0	269	4809
19	67	36	81	3	187	3614
Outer ward	289	267	162	0	718	15734

Source: Computed by Scholar

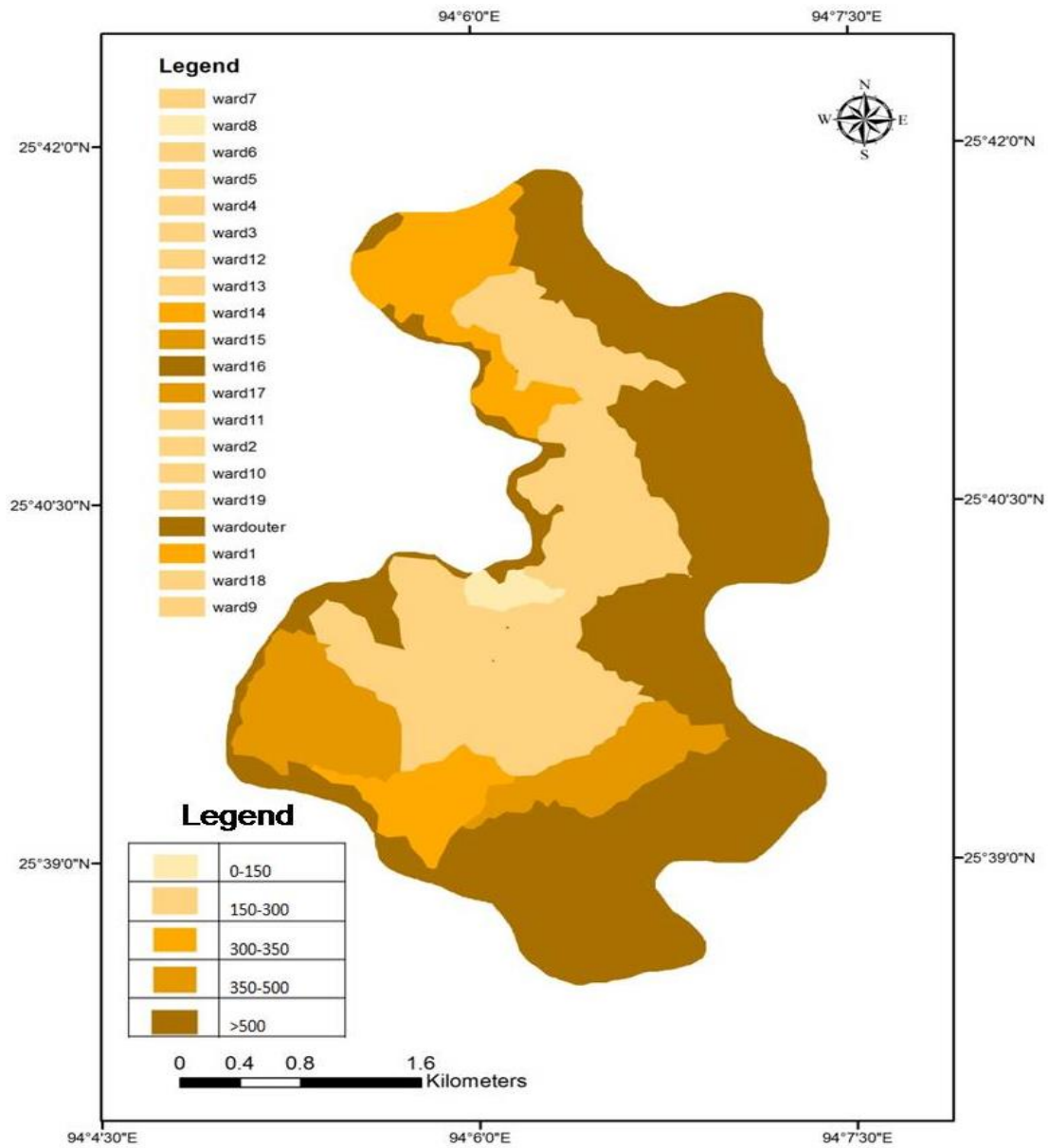


Figure 4.15. Number of buildings with slight damage

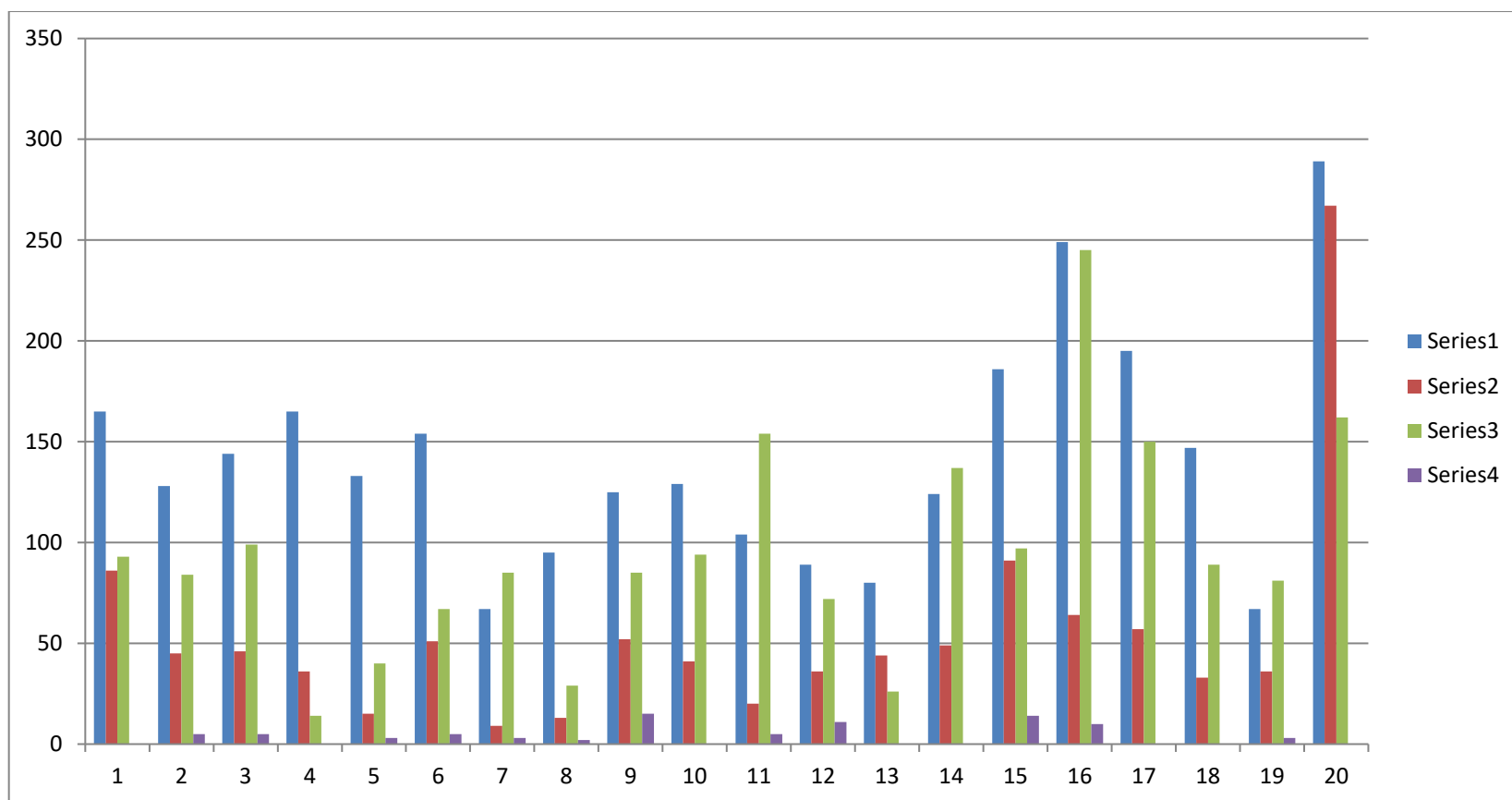


Figure 4.16 Number of building type under slight damage in each ward

The number of buildings affected in **moderate damage** probable was 5641 buildings where maximum was observed in Ward no.16 (586 buildings) followed by Outer Ward (575 buildings). The least numbers of buildings in moderate damage probable was observed in Ward no.13 (123 building) followed by Ward no. 8 (133 buildings). The building type under maximum number of moderate damage probable was observed in W1 building type and least number was seen in C3H building type. From this study it is observed C3L and W1 building types are safer as compared to C3M and C3H (Table 4.10 & Figure 4.17, 4.18).

Table 4.10. Number of buildings with moderate damage

Ward	W1	C3L	C3M	C3H	Total building	Ward Population
1	152	32	120	0	304	7082
2	119	16	108	7	250	5207
3	133	17	128	8	286	5692
4	153	50	18	1	222	3568
5	123	6	51	5	185	3197
6	143	19	86	8	256	5381
7	62	3	109	5	179	2721
8	88	5	37	3	133	2348
9	116	19	110	23	268	4808
10	119	15	121	0	255	4820
11	96	7	198	8	309	5267
12	82	13	93	18	206	3848
13	74	16	33	0	123	3228
14	115	18	176	0	309	6101
15	172	34	125	22	353	7970
16	231	24	315	16	586	11603
17	181	21	193	0	395	7775
18	136	12	114	0	262	4809
19	62	13	105	5	185	3614
Outer ward	268	99	208	0	575	15734

Source: Computed by Scholar

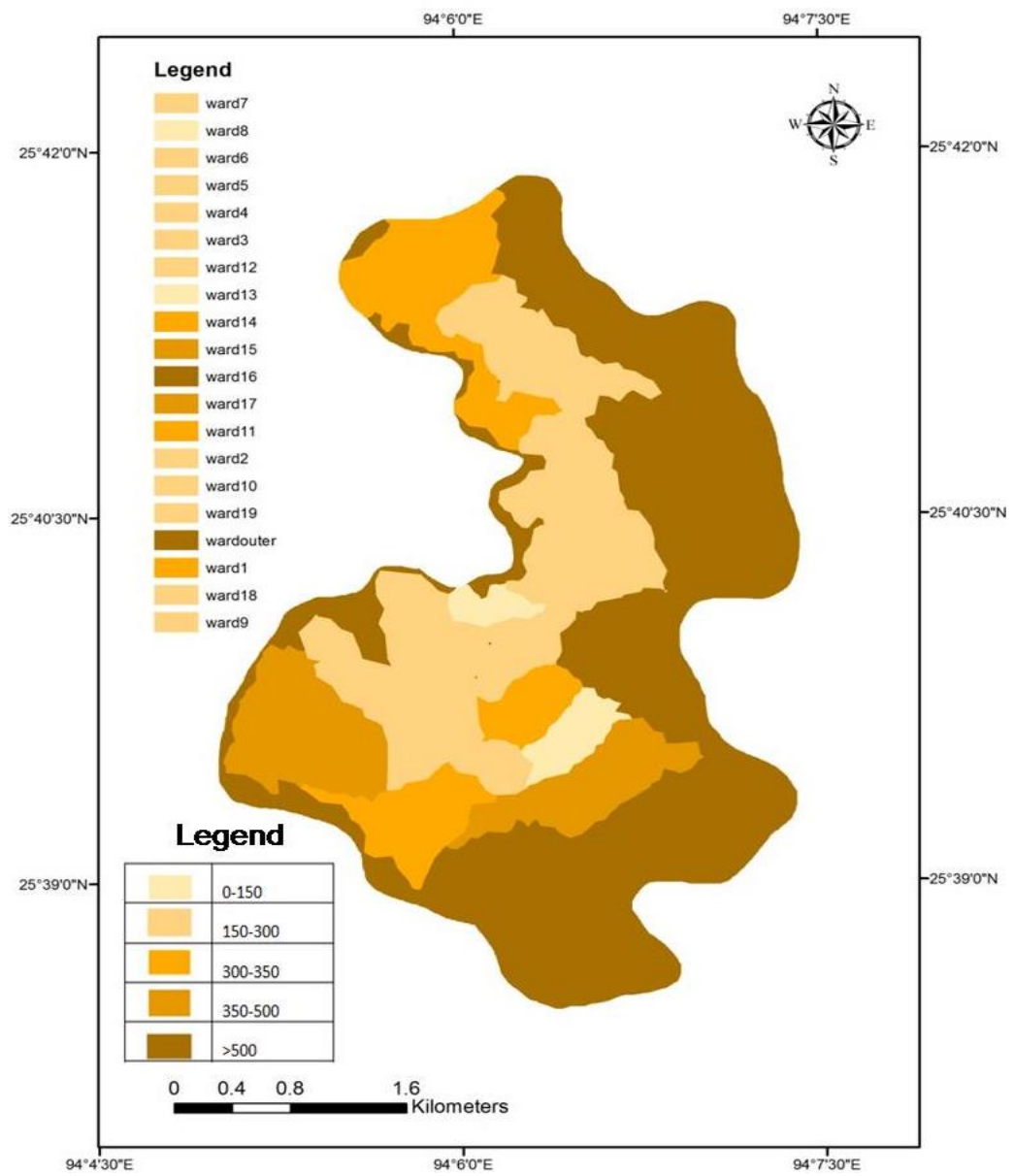


Figure 4.17. Number of buildings with moderate damage

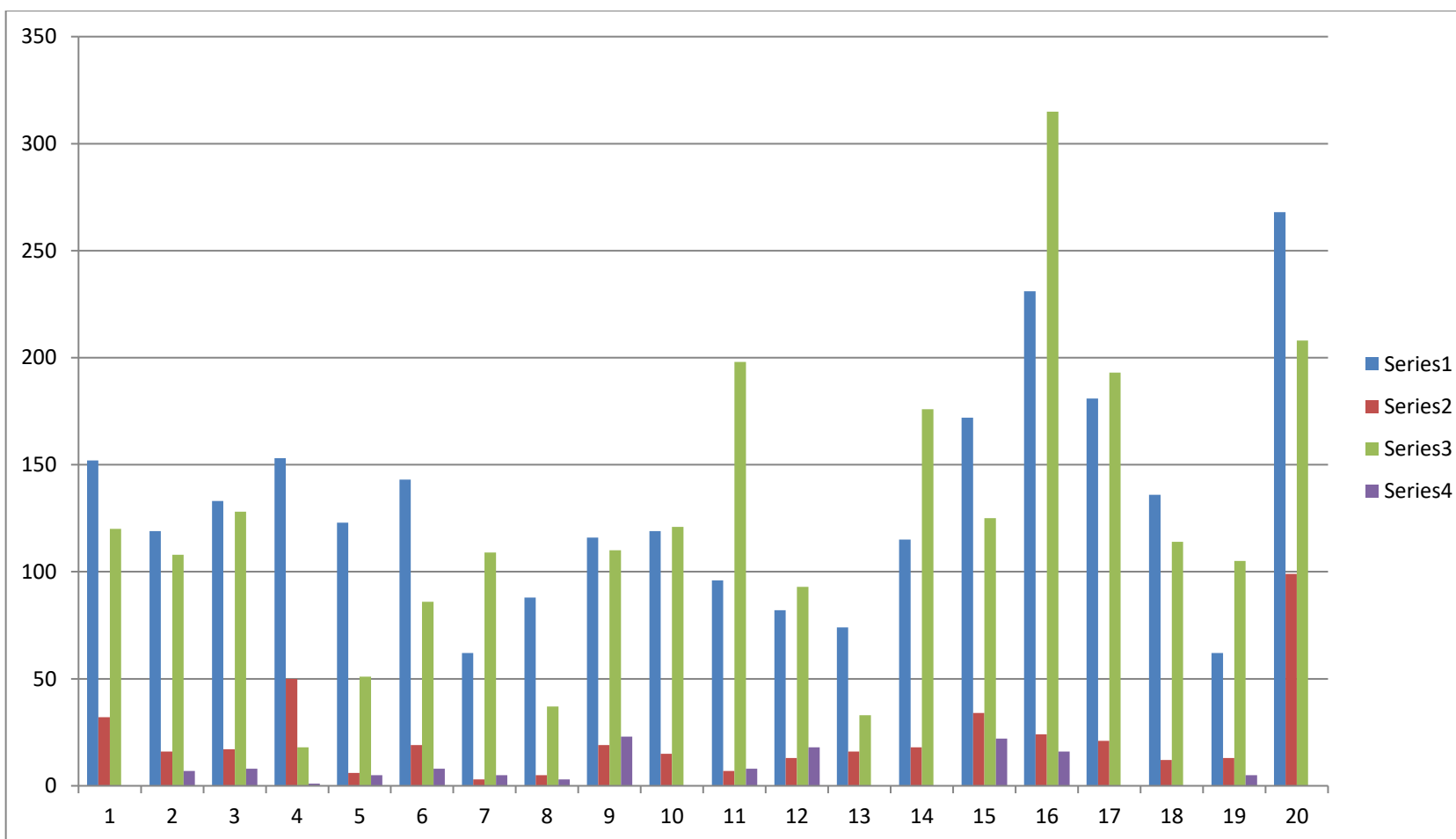


Figure 4.18 Number of building type under moderate damage in each ward

The number of buildings affected in **extensive damage** probable was 4035 buildings where maximum was observed in Outer ward (590 buildings) followed by Ward no. 16 (367 building). The lowest number of buildings in extensive damage probable was observed in Ward no.8 (79 building) followed by Ward no. 7 (101 buildings). The building type under maximum number of extensive damage probable was observed in C3L building type and least number was seen in C3H. From this study it is observed C3L and W1 building types are comparatively safer as compared to C3M and C3H (**Table 4.11 & Figure 4.19, 4.20**).

Table 4.11. Number of buildings with extensive damage

Ward	W1	C3L	C3M	C3H	Total building	Ward Population
1	71	114	62	0	247	7082
2	56	59	56	4	175	5207
3	62	61	66	5	194	5692
4	72	49	9	0	130	3568
5	58	20	26	3	107	3197
6	67	68	45	5	185	5381
7	29	12	57	3	101	2721
8	41	17	19	2	79	2348
9	54	70	57	14	195	4808
10	56	55	63	0	174	4820
11	45	27	103	5	180	5267
12	39	49	48	10	146	3848
13	35	59	18	0	112	3228
14	54	66	91	0	211	6101
15	81	121	65	13	280	7970
16	108	86	164	9	367	11603
17	85	75	100	0	260	7775
18	64	45	59	0	168	4809
19	29	48	54	3	134	3614
Outer ward	126	356	108	0	590	15734

Source: Computed by Scholar

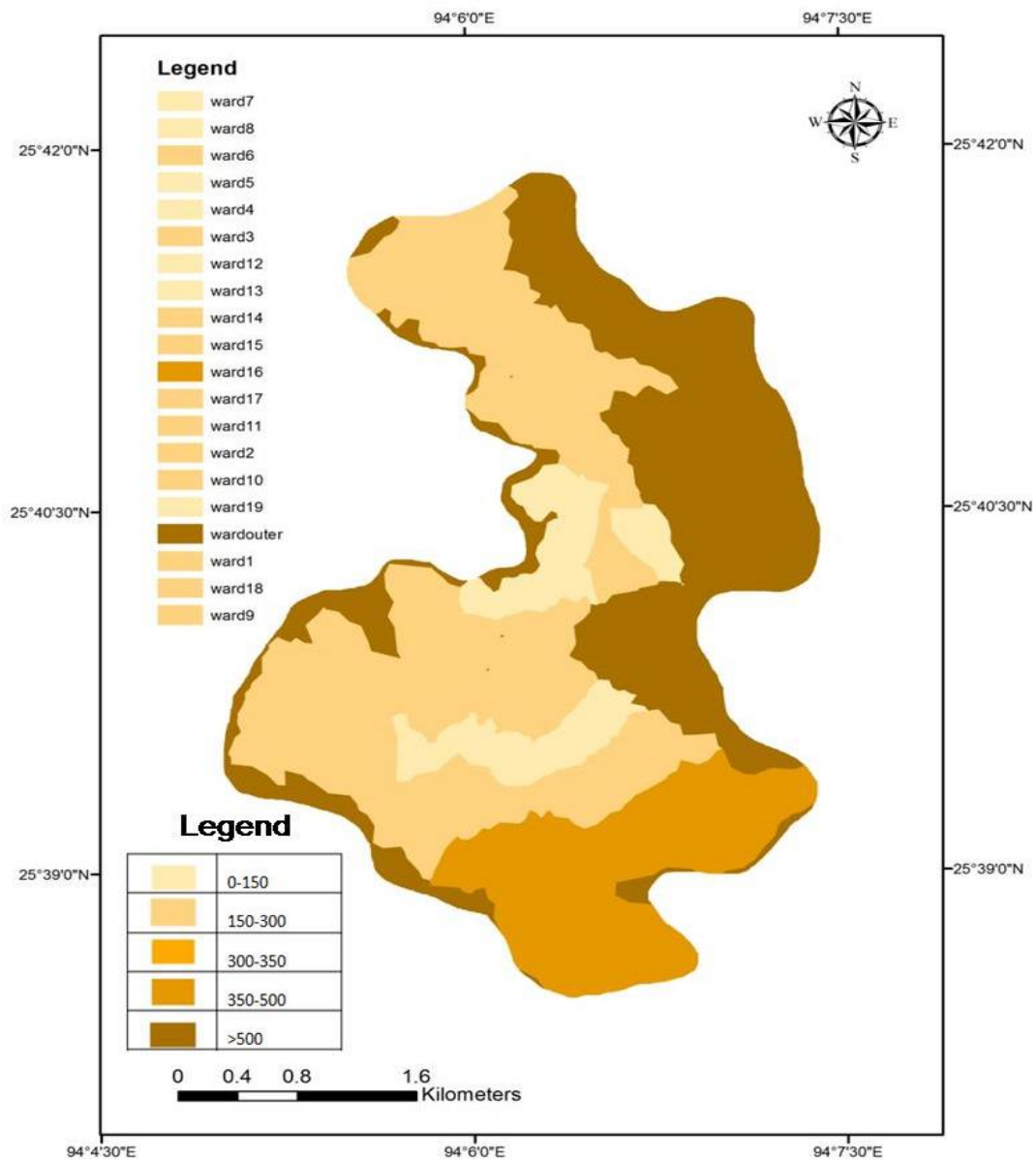


Figure 4.19. Number of building with extensive damage

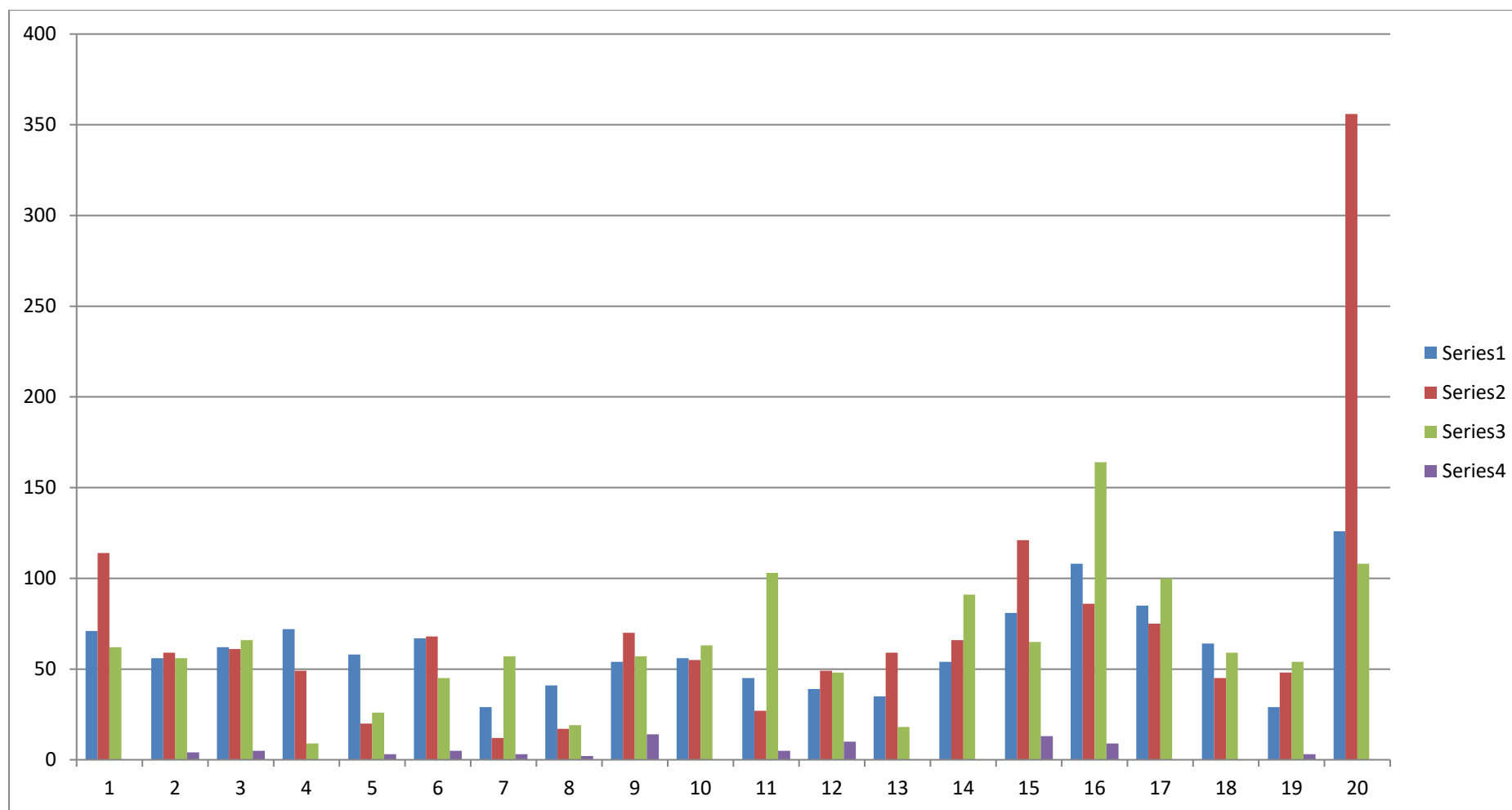


Figure 4.20 Number of building type under extensive damage in each ward

The number of buildings affected in **complete damage** probable was 1256 buildings where maximum was observed in Outer ward (180 buildings) followed by Ward no. 16 (117 building). The least numbers of buildings in complete damage probable was observed in Ward no.8 (23 building) followed by Ward no. 5 (31 buildings). The building type under maximum number of complete damage probable was observed in C3L building type and least number was seen in C3H. From this study it is observed C3L and W1 building types are safer as compared to C3M and C3H (Table 4.12 & Figure 4.21, 4.22).

Table 4.12. Number of building with complete damage

Ward	W1	C3L	C3M	C3H	Total building	Ward Population
1	17	35	24	0	76	7082
2	13	18	21	2	54	5207
3	15	19	25	2	61	5692
4	17	15	3	0	35	3568
5	14	6	10	1	31	3197
6	16	21	17	2	56	5381
7	7	4	22	1	34	2721
8	10	5	7	1	23	2348
9	13	21	22	5	61	4808
10	14	17	24	0	55	4820
11	11	8	39	2	60	5267
12	9	15	18	4	46	3848
13	8	18	7	0	33	3228
14	13	20	35	0	68	6101
15	20	37	25	5	87	7970
16	26	26	62	3	117	11603
17	21	23	38	0	82	7775
18	16	14	23	0	53	4809
19	7	15	21	1	44	3614
Outer ward	30	109	41	0	180	15734

Source: Computed by Scholar

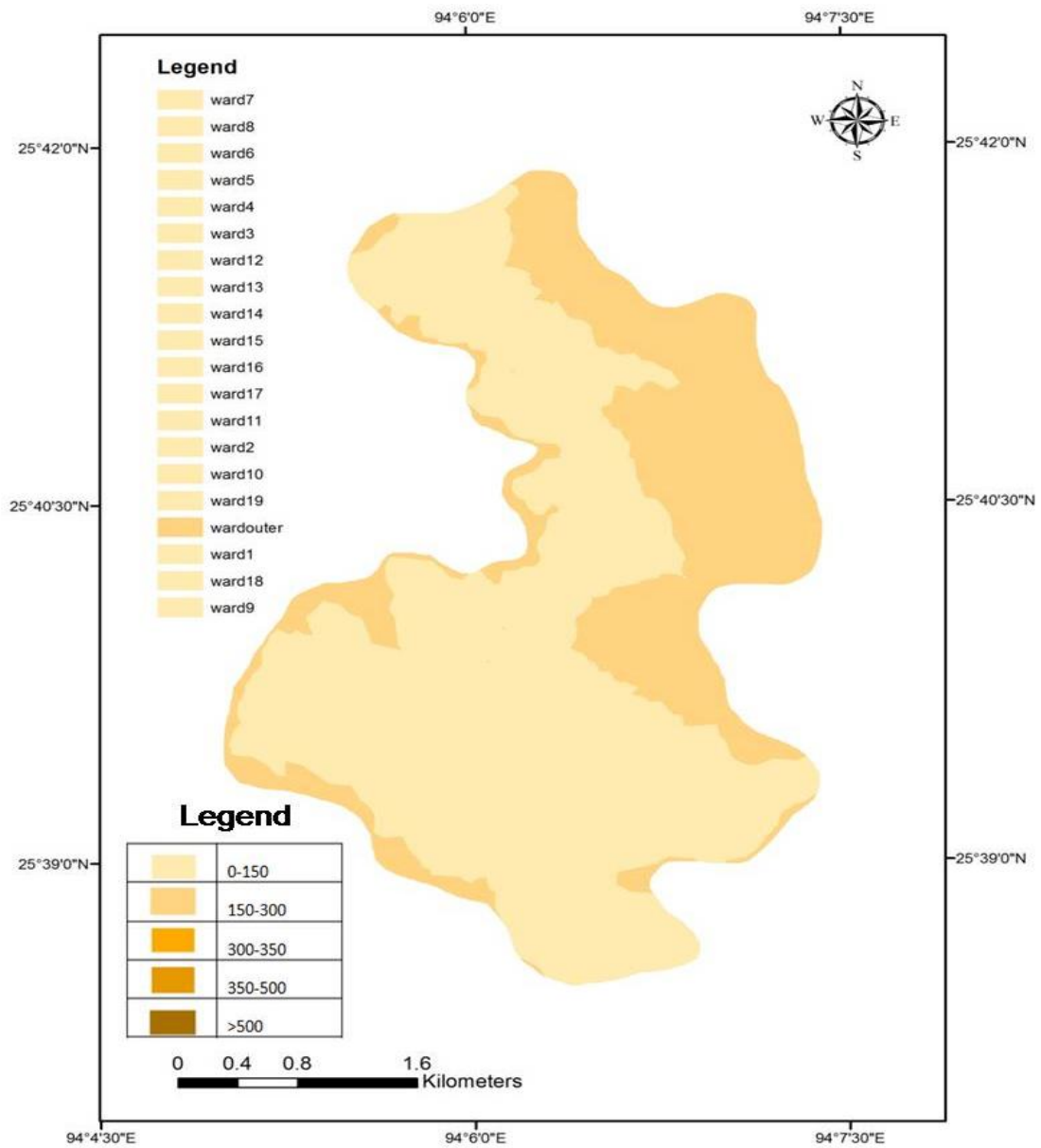


Figure 4.21. Number of building with complete damage

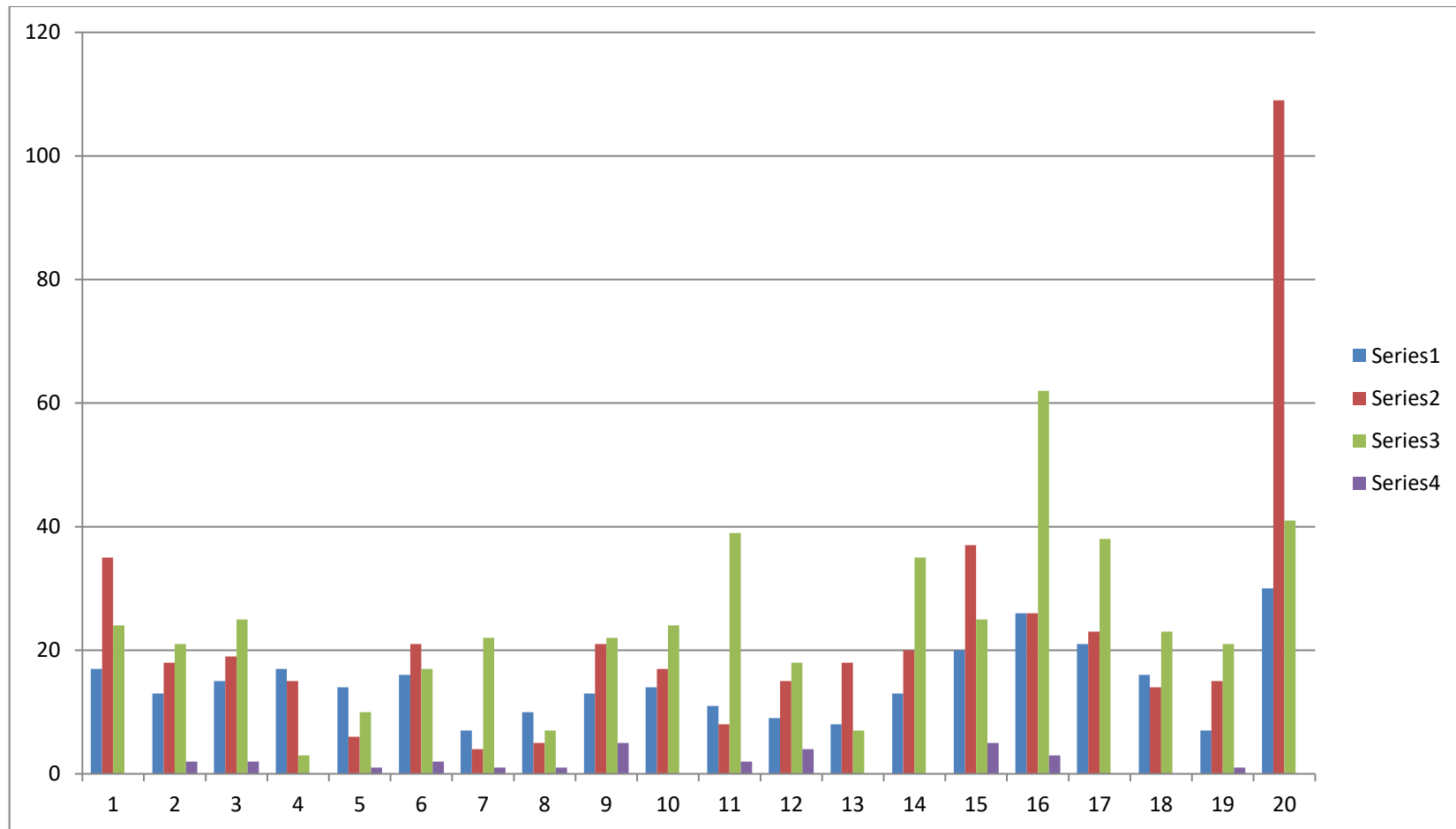


Figure 4.22. Number of building type under complete damage in each ward

The number of buildings having the maximum number of buildings in damage probable was observed in slight damage probable with 5910 buildings followed by moderate damage probable with 5641 number of buildings and least number of buildings was observed in complete damage probable with 1256 buildings. Among the wards, Ward no.10, Ward no.11 and Ward no. 12 have highest complete damage in C3M building type. Ward no. 13 has highest complete damage in C3L building type. Ward no. 14 has highest complete damage in C3M building type. Ward no. 15 has highest complete damage in C3L building type and Ward no. 16 has highest complete damage in C3M building type. Ward no. 17, Ward no. 18 and Ward no. 19 have highest complete damage probable in C3M building type and Outer ward in C3L building type respectively.

5

5.1 Introduction

Landslides are a natural process that plays a key role in landscape evolution of mountainous and hilly environments (Tseng *et al.*, 2015). The geo-environmental features of an area affect the occurrence of landslides in different ways, and can be applied as affecting factors in the prediction of future landslides (Van Westen *et al.*, 2008). The selection of affecting factors depends on the scale of the analysis, the characteristics of the study area, the landslide type etc (Glade *et al.*, 2005). Nevertheless, there are no general guidelines for selecting these factors (Ayalew *et al.*, 2005 and Yalcin, 2008).

Landslide velocity, as well as total or differential displacements, can be measured through monitoring techniques. Generally, the conventional monitoring techniques such as geotechnical (extensometers, inclinometers, distometers,

piezometers etc) and topographic (manual triangulation, total station, and GPS measurements) provide information affected by slope instability phenomena on a selected number of points on slopes. Single point data behaviour cannot be considered as representative for a whole landslide mass. Extensive conventional monitoring networks are installed on landslides to get rid of such spatial limiting characteristics, however, it cannot be employed on sectors which are high landslide risk zone or are not accessible. Remote sensing monitoring system based on radar techniques such as Persistent Scatterers Interferometry (PSI and Ground-Based Interferometric Synthetic Aperture Radar (GBInSAR) can overcome most of these limitations. The advantage of radar sensor is that it can operate continuously over a long time period in almost any weather condition over wide areas, providing real-time widespread information with millimetre accuracy of the study area without the need of accessing the area (Veronic *et al.*, 2014). The implementation of geo-processing technique in GIS environment allow the computation of some significant topographic terrain attributes such as slope angle, slope aspect, elevation and curvature profile on the basis of DTM processing (Nichol *et al.*, 2006; Ardizzone *et al.*, 2007; Miyagi and Hamasaki, 2014). Slope gradient is the most influencing factor for landslide hazard assessment and susceptibility mapping (Guzzetti *et al.*, 1999 and Dai *et al.*, 2002) at local scales, it affects the concentration of moisture and the pore water pressure, at larger scales, and it controls the regional hydraulic conditions (Ayalew and Yamagishi, 2005).

Anthropogenic factors are predisposing and triggering factors. For example, road-cuts are one of the most important anthropogenic causative factors of slope instability. The traditional methods in most GIS-based studies consider the effect of landslides on roads through the definition of a buffer around them (Van Westen *et al.*, 2008 and Bai, 2011).


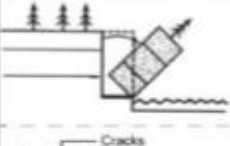

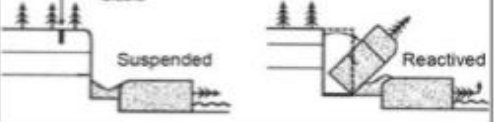

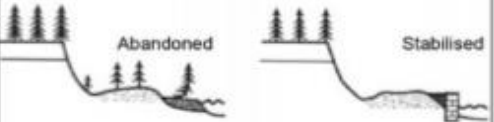



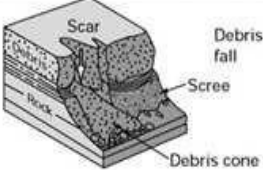
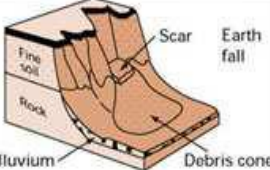
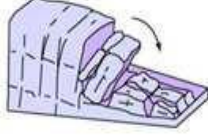
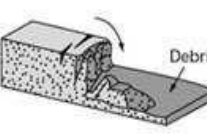
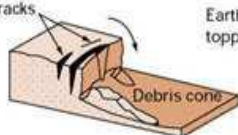
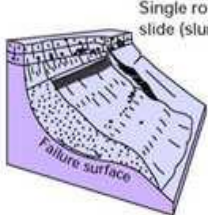
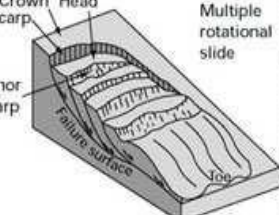
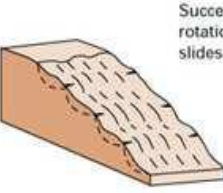
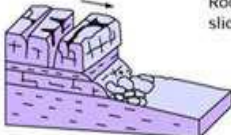
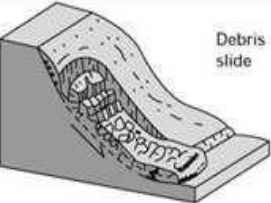
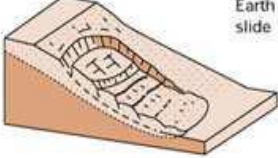
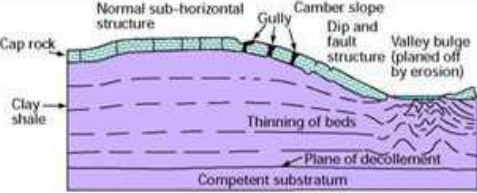
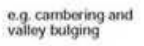
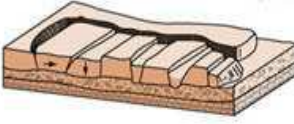
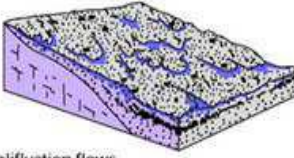


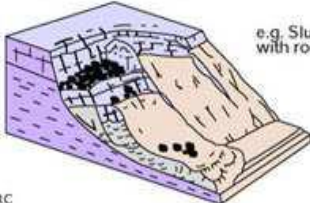
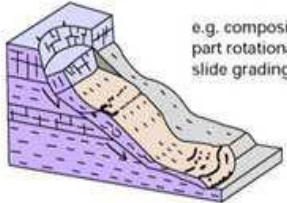
AGE	RETURN PERIOD	MORPHOLOGIC CHANGES	ACTIVITY		
Present	1 day	 Fresh morphology, distinct from the surroundings. Cracks are clearly visible.		Continuous	ACTIVE
Historical 150 BP	1 year	 The morphology remains different from the surroundings. However, the forms are softer than before.		Intermittent	
Holocene	10 years	 The surface is modified by water erosion. The landslide becomes covered with vegetation.		Dormant	INACTIVE
10,000 BP	> 1000 yr	 The morphology is slightly noticeable, there are only morphological traces of the phenomenon.		Relict	
Pleistocene 20,000 BP					

Figure 5.1. Classification of landslide activity level in function of geomorphical features (Schlogel, 2015).

Present is the key to the past where the morphological changes of landslide gradually along the course of time is depicted. The presence of old scars of landslide (Photo plate 37), hence, becomes crucial for the possibility of landslide occurrences in the future, as old landslide can be triggered easily (**Figure 5.1**).

Different types of landslide are influenced by rock type, debris and earth composition besides that composition of materials plays a critical role in the landslide events (**Table 5.1 & Figure 5.2**).

The different type of landslide along with its morphological characteristics, from the beginning on landslide morphology i.e., crown to the toe, a detail and comparative assessment of each landslide (**Table 5.2**).

Material		ROCK	DEBRIS	EARTH
Movement type				
FALLS				
TOPPLES				
SLIDES	Rotational			
	Translational (Planar)			
SPREADS				
FLOWS				
COMPLEX				

BGS © NERC

Figure 5.2. Landslide classification (Varnes, 1978 and Cruden and Varnes, 1996).

Table 5.1. Landslide damage type related to element at risk and its location

Type	Likely damage to elements at risk		Factors determining risk	
Impact by large rockmass	Buildings: Total collapse likely Infrastructure: Coverage and obstruction/ destruction of traffic	Persons in building: Loss of life/ major injury likely Persons in traffic: Loss of life / major injury possible	-Volume of rockfall mass -Location of source zone -Distance to elements at risk -Triggering factors	-Location topography along track -Intermediate obstacle -Precursory events
Impact by single blocks	Buildings: Total collapse not likely, localized damage Infrastructure: Coverage and obstruction of traffic	Persons in building: Minor to major injury likely Persons in traffic: Loss of life / major injury possible	-Volume of rockfall blocks -Number of rockfall blocks -Location of source zone -Distance to elements at risk	-Triggering factors -Location topography along track -Intermediate obstacle
Impact by landslide mass	Buildings: Collapse/ major damage depending on volume Infrastructure: Coverage and obstruction of traffic	Persons in building: None, persons are normally able to escape Persons in traffic: None, persons are normally able to escape	-Volume of landslide mass -Water content -Landslide material type -Triggering factors -Distance to elements at risk	-Location topography along track -Speed of landslide movement
Loss of support due to undercutting	Buildings: Collapse/ major damage likely Infrastructure: Complete destruction of road surface	Persons in building: None, persons are normally able to escape Persons in traffic: None, persons are normally able to escape	-Volume of landslide mass -Water content -Landslide material type -Triggering factors	-Retrogressive landslide -Cliff erosion -Speed of landslide movement
Differential settlement/ tilting due to slow movement	Buildings: Tilted buildings with cracks. Normally no collapse Infrastructure: Tilting and cracks, traffic slowed down	Persons in building: None, slow movement, people not in danger Persons in traffic: None, slow movement	-Volume of landslide mass -Water content -Landslide material type -Triggering factors	-Speed of landslide movement -Amount of displacement
Impact by debris flow on alluvial fan	Buildings: Filled by mud, damage to contents Infrastructure: Coverage of road surface, obstruction of traffic	Persons in building: Major-minor injuries, depends on speed Persons in traffic: Minor-major injuries, depends on speed	-Volume of landslide mass -Water content -Slope steepness -Local topography -Landslide material type	-Triggering factors -Speed of movement -Size of blocks transported
Impact by Sturzstrom	Buildings: Total collapse Infrastructure: Total destruction	Persons in building: Loss of life Persons in traffic: Loss of life	-Volume of rockfall mass -Location of source zone -Distance to elements at risk -Triggering factors	-Local topography along track -Distance from source zone -Precursory events
Liquefaction	Buildings: Differential settlement, cracks Infrastructure: Differential settlement, cracks	Persons in building: Minor injuries or no injuries Persons in traffic: No injuries	-Soil types -Soil strength -Grainsize distribution	-Foundation types -Earthquake intensity -Water table
Deep seated creep movement	Buildings: Differential settlement, tilting, cracks Infrastructure: Differential settlement, cracks, broken pipes	Persons in building: Minor injuries or no injuries Persons in traffic: No injuries	-Speed of movement -Local geological situation -Age of landslide -Seasonality of movement	

Source: Van Westen *et al.*, (2006).

Table 5.2. Landslide types along with the landslide morphology characteristic

Landslide type	Crown	Main scarp	Flanks	Head	Body	Foot	Toe
Fall, topple	Consists of loose rock, debris or soil; probably has crack behind scarp; in rock has irregular shape controlled by local joint system	Usually almost vertical, irregular bare and fresh, consisting of joint or fault shears in rock and spalling on the surface if debris or soil	Mostly bare edge of rock often nearly vertical	Usually not well defined, consist of fallen material that form a heap of rock, debris or soil next to the scarp	Fall; irregular surface of jumbled rock that slopes away from the scar and that, if large, tree may show direction of movement radial from the scarp; may contain depression. Topple: consist of unit or units tilted away from the crowd	Commonly buried; if visible, generally shows evidence of reason for failure, such as prominent joint or bedding surface, underlying weak rock, or banks undercut by water	Irregular piles of debris or talus if slide is small; may have rounded outline and consist of broad, curved transverse ridge if slide is large
Rotational slid (single, multiple or successive)	Consists of cracks that tend to follow fracture patterns in the original rock; in debris or soil crack are mostly curved concave toward the slide	Steep, bare, concave toward the slide and commonly high; may show striae and furrow on the surface running from crown to head; may be vertical in the upper part	Have striae with strong vertical components near head and strong horizontal component near foot; have scarp height that decreases towards foot; maybe higher than original ground surface between foot and toe, have “an echeleon” cracks that outline slide in earlier stages	Remnants of land surface flatter than original slope or even tilted into hill, creating at base of main scarp depressions in which perimeter ponds for, has transverse cracks, minor scarps, grabens, fault blocks; bedding attitude different from surrounding; trees lean uphill	Consists of original slump blocks generally broken into smaller masses; has longitudinal cracks, pressure ridges and occasional over thrusting; commonly develops small pond just above the foot	Commonly transverse cracks developing over the foot line and transverse pressure ridges developing below the foot line, have zone of uplift, no large individual blocks and trees that lean downhill	Often a zone of earth flow of lobate form in which material is rolled over and buried; has trees that lie flat or at various angles and are mixed into the toe material; in rock there is little or no flow, often nearly straight and close to the foot may have steep front
Translational slide; rock slide, debris slide, mudslide	Consists of loose material and has cracks between blocks	Usually stepped according to spacing of joints or bedding planes in rock; has irregular surface in upper part and is planar or gently sloping in lower part	Irregular	Many blocks of rock, debris or soil	Rough surface of many blocks some of which maybe in approximately their original altitude but lower if movement was slow, shows flow structure		Consists of an accumulation zone of rock, debris or soil; spreading and lobate often consists of material rolled over and buried
Debris flow	Few cracks	Typically has V-shaped upper part, is long and narrow, bare and commonly striated	Commonly diverges in direction movement		Consists of large blocks pushed along in a matrix of finer material; has flowlines; follows drainage patterns; is very long compared to its breadth	Buried in debris	Spreads laterally in lobes; if dry, may have a steep front about a meter high
Soil flow	Few cracks	Steep and concave toward slide; may have a variety of shapes in outline; nearly straight, arcuate, circular or bottled-shaped			Conical heap of soil, equal in volume to the head region		Spreading and lobate

5.2 Landslide zonation

Landslide zonation will consists of two aspects- slope failure under terrain condition or other aspect- the triggering event which leads to the slide. The division of land into homogenous area and their ranking according to degrees of actual or potential landslide susceptibility, hazard or risk can be defined as landslide zoning (Fell *et al.*, 2008). The most important is selecting appropriate zoning method which depends on quality and accuracy of data, the resolution of zoning, scale of zoning, the type of analysis, complexity of the landslide features and outcome (Cascini, 2008). Also conditions which triggered slide in the past is most likely to create landslide in the future in accordance with present is the key to past (**Table 5.3**).

Table 5.3. Landslide zoning scale and its application

Scale description	Indicative range of scales	Example of zoning application	Typical area of zoning
Small	<1:100,000	Landslide inventory and susceptibility to inform policy makers and the general public	>10,000 km ²
Medium	1:100,000 to 1:25,000	Landslide inventory and susceptibility zoning for regional development; or very large scale engineering projects. Preliminary level hazard mapping for local areas	1,000-10,000 km ²
Large	1:25,000 to 1:5,000	Landslide inventory, susceptibility and hazard zoning for local areas. Intermediate to advance level hazard zoning for regional development. Preliminary to intermediate level risk zoning for local areas and the advance stage of planning for large engineering structures, roads and railways.	10-1,000 km ²
Detailed	>5,000	Intermediate and advance level hazard and risk zoning for local and site-specific areas and for the design phase of large engineering structures, roads and railways	Several hectare to 10 km ²

Source: Fell *et al.*, 2008.

5.3 Estimating landslide hazard

The method chosen for estimation of landslide vulnerability in Kohima was based on bivariate statistical technique viz- Information Value Method. The statistical method was chosen because it was robust and the input thematic layers were easier in generating the landslide susceptibility map.

The flowchart for estimation of landslide hazard zonation is as follows; seven thematic geospatial layers were generated from satellite imageries, geological and topographical maps (**Figure 5.3**). The thematic layers were divided into- geological, hydrological, topographical and anthropological based parameters respectively. Geological parameter based on fault and lithology was used to generate thematic layers using existing maps and satellite imageries. Hydrological map was generated using topographic sheets and satellite imagery. Topographic map- slope and aspect layers were generated by rasterizing the contour map from Survey of India topographical maps. Anthropogenic based thematic layers such as road, landuse maps were generated using Survey of India topographical maps and satellite imagery. Landuse and land cover map was interpreted and manually classified followed validation through field survey. Landslide inventory map was generated by interpreting satellite imageries, consulting literatures and field survey. For the tabulation process, the seven thematic geospatial maps was crossed with the landslide map, the crossed layers was ranked as “0” and “1”, where “0” means no landslide and “1” indicates presence of landslide.

The generated landslide crossed maps was converted to grid (grid size was 10m) and Information Value Method (IVM) was implemented on the grids. After IVM was implemented, weights were assigned to the layers; weights are normally based on bivariate statistical analysis in order to distinguish the contribution of each landslide on the layers.

The landslide susceptible map was generated based on various classification methods (Natural Break, Geometrical Interval, Equal Interval and Quantile). The susceptible map after classification was validated using R index method. The validated landslide susceptible map was finally divided into low, moderate, high and very high landslide susceptibility zones respectively.

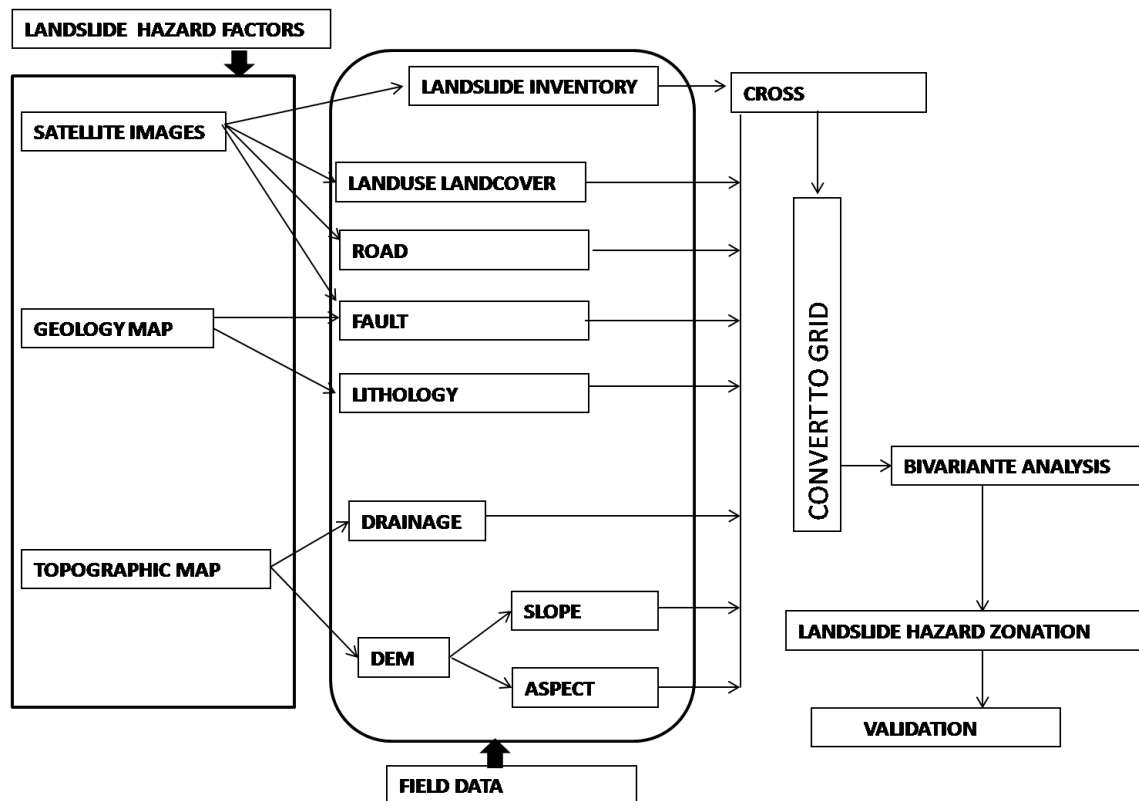


Figure 5.3. Flowchart for estimating landslide vulnerability

5.4 Morphology of landslide

5.4.1 Falls

There are abrupt movements of masses of geologic materials like rocks and boulders that become detached from steep slopes or cliffs. In fall, separation occurs along discontinuities such as fractures, joints, and bedding planes. Movement occurs by free-fall, bouncing, and rolling. Falls are strongly influenced by gravity, mechanical weathering, and

the presence of interstitial water. In the study area fall was observed on paramedical area. Fall movement is observed in Ward no. 10 along the AH1 (Photo plate 41).

5.4.2 Creep

Creep is the slow, steady, downward movement of slope forming soil or rock. Movement is caused by shear stress sufficient to produce permanent deformation, but too small to produce shear failure. Creeping movement in the study area is observed in Ward no. 1 (High School area) (Photo plate 42), paramedic and in Ward no. 4 (Nagabazar area). The movement of creep is slow and gradual, Ward no. 1 has been affected by creep movement of landslide and within one year the entire landscape has changed (Photo plate 47 & 48).

5.4.3 Slide

Slides are usually classed into rotational and translational slide. Rotational slide is a slide in which the surface of rupture is curved concavely upward and the slide movement is roughly rotational about an axis that is parallel to the ground surface and transverse across the slide. In translational slide, mass moves along a roughly planar surface with little rotation or backward tilting. A block slide is a translational slide in which the moving mass consists of a single unit or a few closely related units that move down slope as a relatively coherent mass. Translational slide was observed in ward no.5 (Photo plate 46). The damming of drainage have influenced landslide in the study area, recently it occurred in the road leading to New Secretariat Office (Photo plate 39 & 45). Heavy structures like multiple building storeys are common sight without proper approval of concern authority in Kohima, it would be affected in particular area (Photo plate 43).

5.4.4 Debris flow

Debris flows are commonly caused by intense surface water flow, due to heavy precipitation that erodes and mobilizes loose soil or rock on steep slopes. Debris flow is a form of rapid mass movement in which a combination of loose soil, rock, organic matter, air and water mobilize as slurry that flows down slope. Debris-flow source areas are often associated with steep gullies, and debris-flow deposits are usually indicated by the presence of debris fans at the mouths of gullies (Photo plate 44).

5.5 Information Value Method (IVM)

Information value method was used for estimation of weight for each class in a factor map and obtained by rationing the density of landslide in each class to the landslide present in the entire area. The method was originated by Yin and Yan in 1988 (Yin *et al.*, 1988).

$$IVM = \ln \frac{Npix (si)/Npix (Ni)}{\sum Npix (s)/\sum Npix (N)}$$

Where,

- si represents number of pixels with landslide in the class,
- Ni represents number of pixel in each class,
- S represents number of landslide pixels,
- N represents total number of pixels.

Combining all the crossed weighted parameters with landslide distribution, and after passing various classification methods, the final landslide susceptibility map was prepared. The different parameter after crossing with landslide distribution has been displayed along with its weight (**Table 5.4**). The slope parameter shows the slope angle between 10°-20° having the highest weight (0.05) with maximum geographical area under landslide (56.78%) and between 20°-30° slope angle shows a weight of 0.01 indicating

landslide presences. The value having slope angle greater than 30° did not show any value which may be due to its less landslide distribution.

In the aspect map North area shows the highest value (0.62), followed by Southwest (0.47) for landslide susceptibility. Under the fault category greater than 10 m showed more extensively landslide distribution. The lithology category showed weathered shale area weight is high (0.68), it means the highest susceptibility for landslide occurrence which also has the most geographical area covering 39.22%. The road and landslide show positive correlation where landslide is most susceptible along the road and it decreases as one moves away from the road corridor. The built-up category has the highest value (14.52) for landslide susceptibility zone; it covered a geographical area about 63.57% of the total geographical area. The positive correlation occurred between drainage and landslide susceptibility, the susceptible value was 0.96 in the study area.

5.6 Validation using R Index

R index an indication for goodness of fit and is derived from the ratio of percentage of total landslide area in each class to total area in the class.

$$R = \left[\frac{ni/Ni}{\sum (ni/Ni)} \right] \times 100$$

Where,

ni is the number of landslides occurring in the sensitivity class *i*

Ni is the number of pixels in the same sensitivity class *i*.

The relative landslide density (R) index represents the ratio of percentage of total landslide area in each class to total area. The R index value increases as the susceptibility zone progresses from low to very high susceptible zone. In R index value, the landslide factors are only considered, very high susceptible zone (82.61%) and high susceptible zone

(10.72%) which together constitute a R index value of 93.33% which is high and shows a good landslide density index.

Table 5.4. Information value obtained from the various parameters

Parameter	Category	Number of Pixel	Percentage (%)	Weight
Slope	0-10	1363	24.81	-0.16
	10-20	3119	56.78	0.05
	20-30	944	17.19	0.01
	30-40	66	1.20	-
	40-50	1	0.02	-
Aspect	North	651	11.85	0.62
	Northeast	656	11.94	-0.32
	East	712	12.96	-0.10
	Southeast	738	13.44	-0.64
	South	699	12.73	-0.48
	Southwest	670	12.20	0.47
	West	653	11.89	0.22
	Northwest	714	13.00	-0.73
Fault	0-10m	29321	20.89	0.57
	>10m	111017	79.12	-0.23
Lithology	Shale	47813	34.08	-0.64
	Crumpled	5809	4.14	-1.50
	weathered	55033	39.22	0.68
	shale	753	0.54	-
	Weathered	30906	22.03	-1.79
	shale			
	Shale with S.stone			
Road	0-20	47516	33.86	0.21
	>20	92822	66.14	-0.62
Land use land cover	Water body	22	0.02	-
	Open space	1049	0.75	-
	Built-up	89070	63.57	14.42
	Barren land	27629	19.72	1.25
	Agricultural land	3548	2.53	-0.31
	Vegetation	18800	13.42	0.04
Drainage	0-50	37927	53.84	0.96
	50-100	32515	46.16	-0.18

Source: Compiled by scholar.

The generated landslide susceptibility map was validated using Relative landslide density (R) index which represents the ratio of percentage of total landslide area in each class to total area in the class. The R index value increases as the susceptibility zone progresses from low to very high susceptible zone (**Table 5.5**). In R index value, the landslide factors are only considered, very high susceptible zone had R value 82.61 % and high susceptible zone showed 10.72% which together constitute R index value of 93.33% which is high and shows a good landslide density index.

Table 5.5. Landslide relative index (R) value from landslide susceptible zones.

Susceptible Zone	Area (Pixel)	Landslide area (pixel)	R index (%)
Low	36581	150	2.67
Moderate	43637	269	4.01
High	41630	686	10.72
Very high	16887	2145	82.61

Source: Compiled by scholar.

5.7 Landslide susceptibility model

The landslide susceptibility model highlights the areas where there is a possibility of slope instability. The output of the model is a landslide susceptibility map which is intended to be used as a general guide for the local authority to check against disaster. However, one should remember that susceptibility map does not provide information on the time frame of failure, type of failure, or volume of material. Moreover, the susceptible map generated at a medium scale to local scale should not be used as a substitute for site-specific work as it defers region to region and place to place.

The susceptible map basing on the classification method generated based on different methods, they are i). Natural Break Method, ii). Quantile Method, iii). Equal Interval Method and iv). Geometrical Interval Method.

Table 5.6. Distribution of values from different methods & R Index

Methods'	Class	Area (pixel)	Landslide area (Pixel)	R Index (%)
Equal Interval Method	Low	12368	15	0.65
	Moderate	74741	459	3.31
	High	39352	852	11.66
	Very High	12274	1924	84.39
Quantile Method	Low	33230	146	4.62
	Moderate	36184	188	5.47
	High	35357	338	10.06
	Very High	33964	2578	79.85
Geometrical Interval Method	Low	44083	178	2.79
	Moderate	43026	296	4.76
	High	32473	530	11.29
	Very High	19153	2246	81.15
Natural Break Method	Low	36581	150	2.67
	Moderate	43637	269	4.01
	High	41630	686	10.72
	Very High	16887	2145	82.61

Source: Compiled by scholar.

5.7.1 Equal Interval Method

Equal interval classification method defines the range of possible values which are divided into equal-sized intervals. This option is useful to highlight changes in the extremes. Under this classification, the study area equal area values are shown where, low landslide susceptibility pixel value was 15 pixels for landslide area and R Index value was 0.65%. Very high landslide susceptibility pixel for landslide area was 1924 out of 12274 pixels respectively from total area with R Index value of 84.39% (**Table 5.6 & Figure 5.4**).

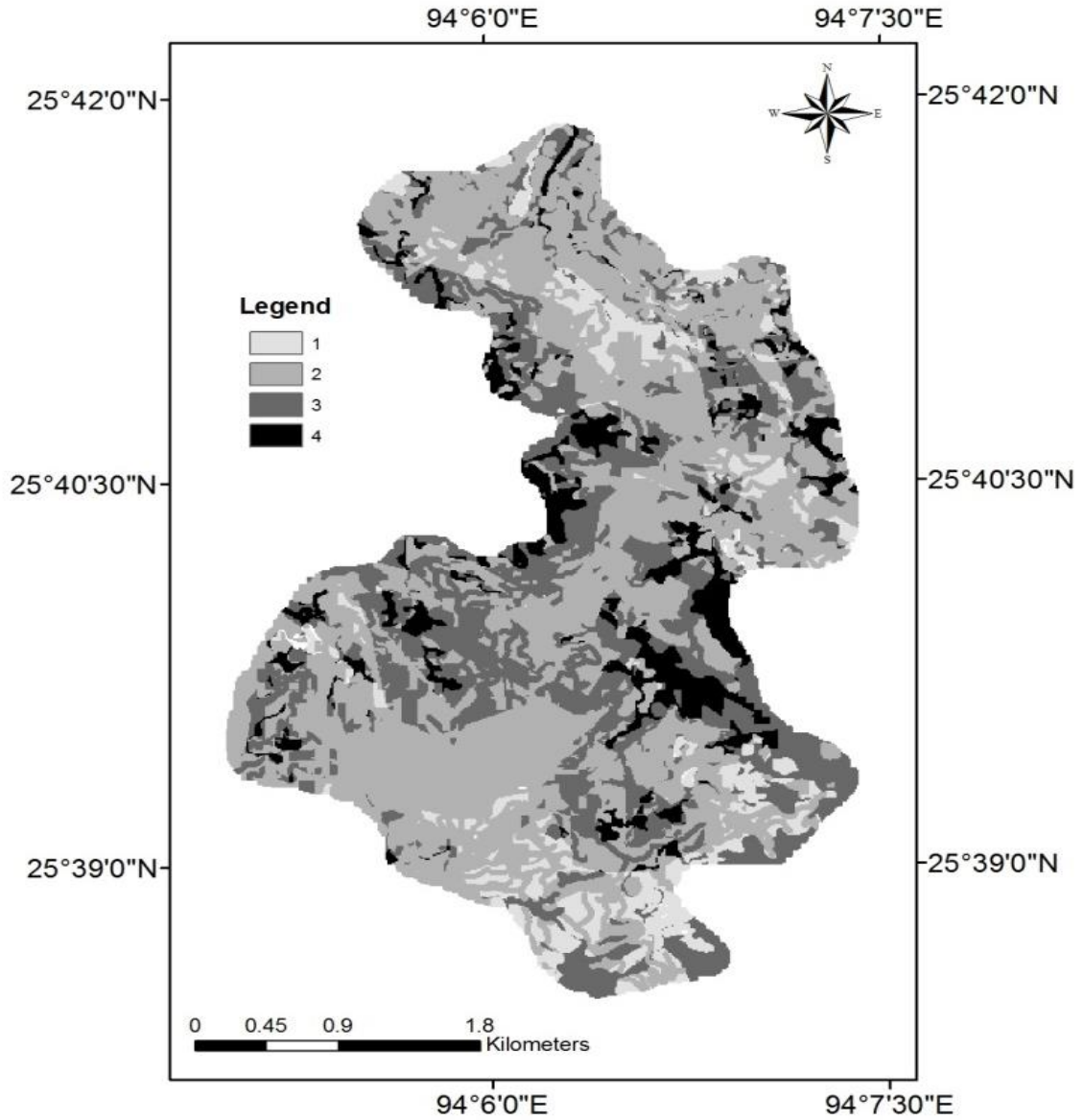


Figure 5.4. Landslide zonation (Equal Interval Method)

5.7.2 Quantile Method

The range of possible values is divided into unequal-sized intervals so that the number of values is the same in each class. Hence, classes at the extremes and middle have the same number of values. Class intervals are generally wider at the extremes; this is useful to highlight changes in the middle values of the distribution. The number of pixels in landslide area in very high susceptible class was 2578 and total pixel was 33964 with 79.85% of R index value. Low susceptible class pixel was 33230 with 146 pixel under

landslide area and R index was 4.62%. High susceptible class occupied 35357 pixel with 338 pixels under landslide area with R index value 10.06% (**Table 5.6 & Figure 5.5**).

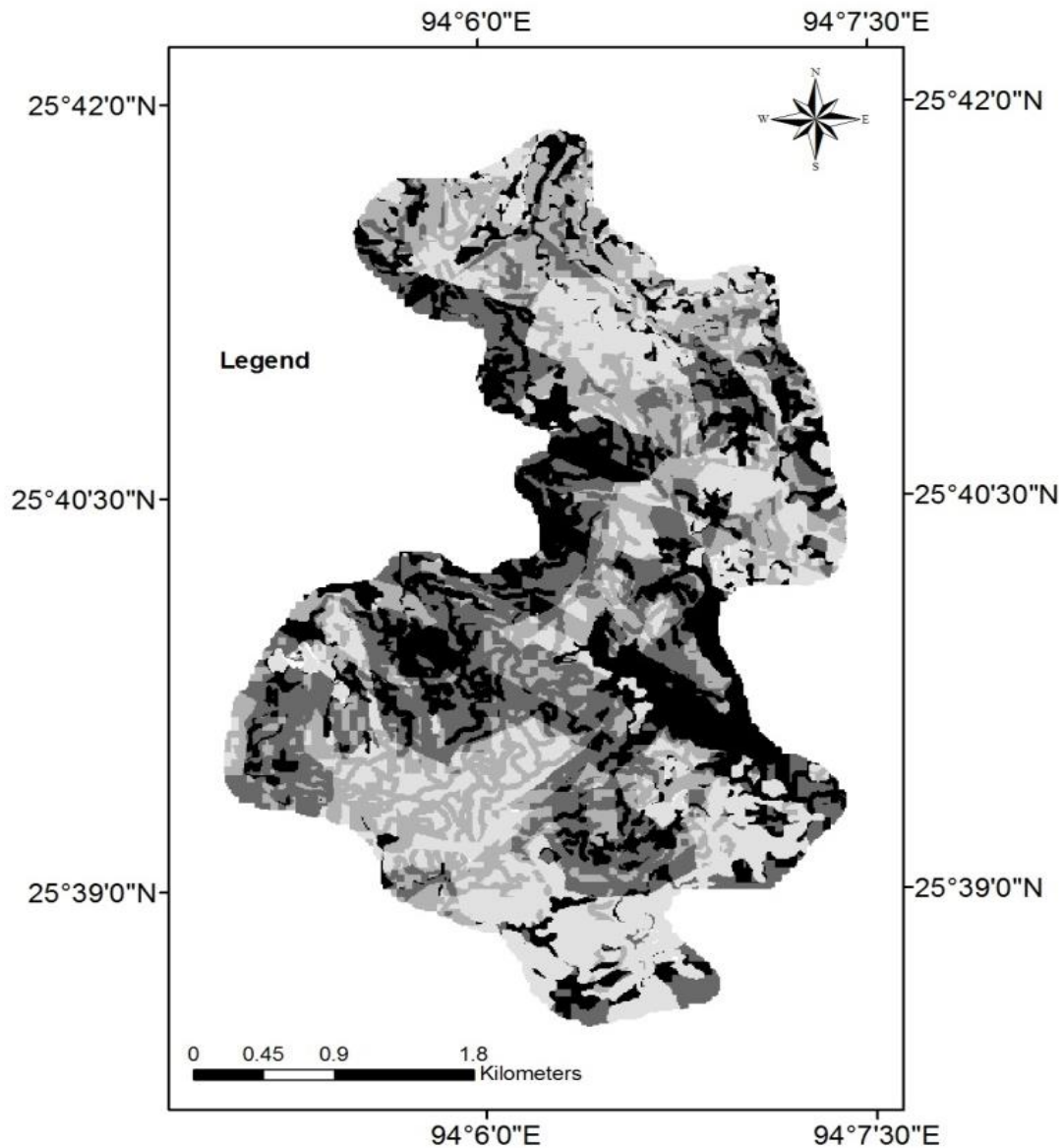


Figure 5.5. Landslide zonation (Quantile Method)

5.7.3 Geometrical Interval Method

Geometric interval classification is designed to give a visually appealing representation of continuous data, but it can also work quite well on non-normally distributed data. Using geometric intervals the class breaks are determined geometrically in such a way that the variance within classes is minimised so that each class has

approximately the same number of values. The study area values under geometrical classification where number of pixels in landslide area in very high susceptible class was 2246 and total pixel was 19153 with 81.15% of R index value (**Table 5.6 & Figure 5.6**). Low susceptible class pixel was 44083 with 178 pixel under landslide area and R index was 2.79%. High susceptible class occupied 32473 pixel with 530 pixels under landslide area with R index value 11.29%.

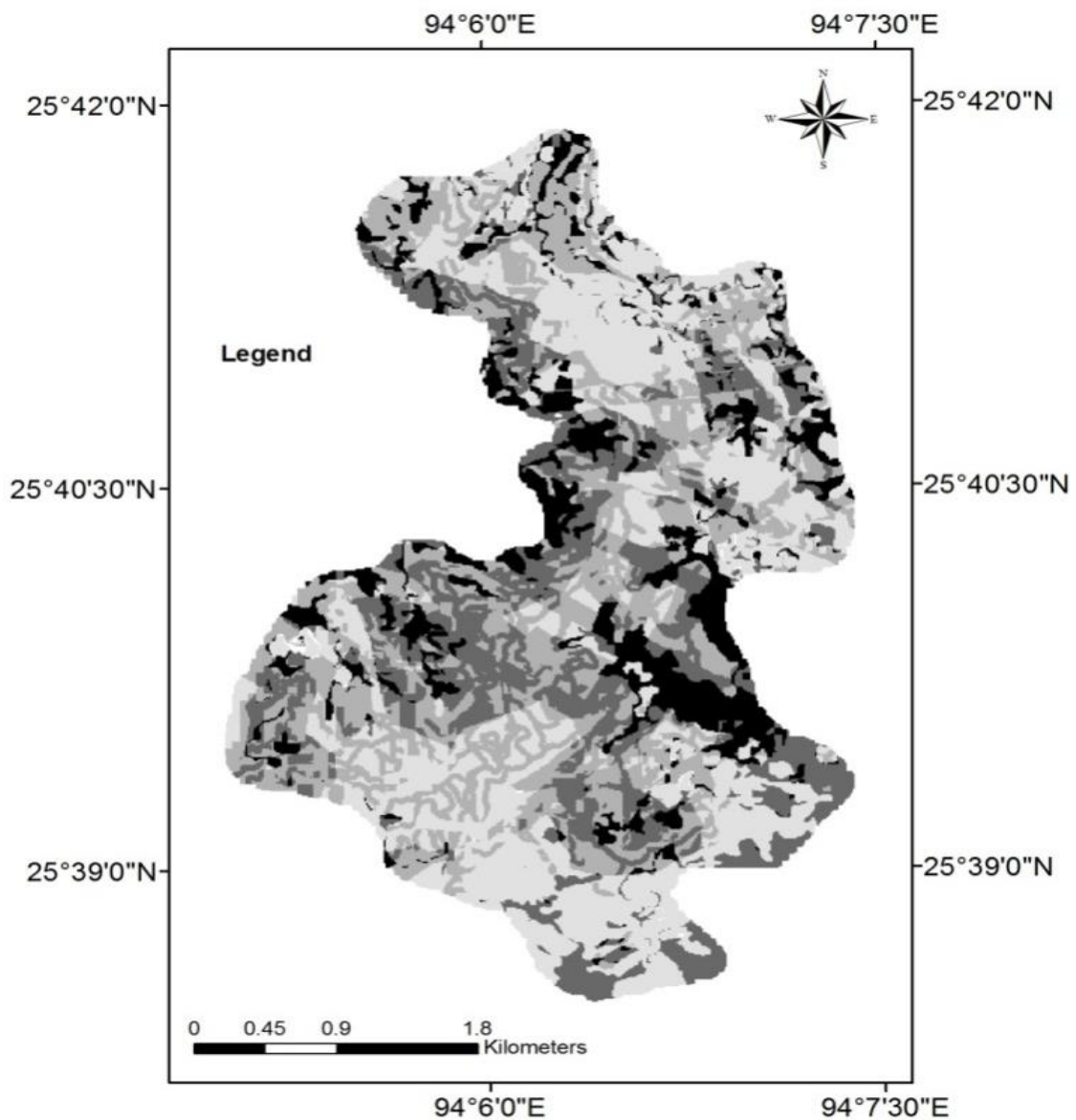


Figure 5.6. Landslide zonation (Geometrical Interval Method)

5.7.4 Natural Break Method

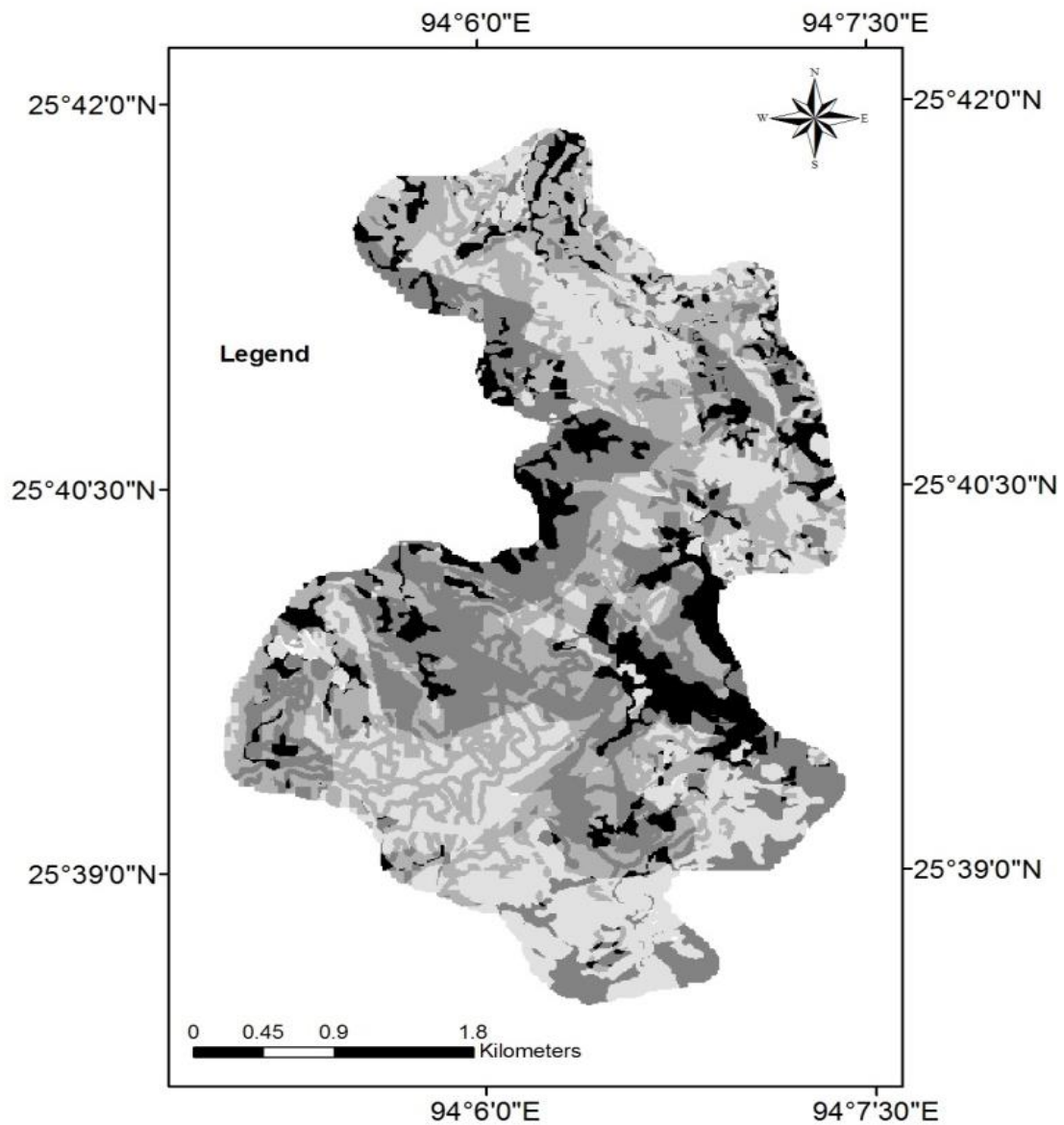


Figure 5.7. Landslide zonation (Natural Break method)

Natural Break Method is based on natural grouping of the data values. Normally, the break points are identified by looking for groups and patterns inherent in the data. The features are divided into classes whose boundaries are set and there are relatively big jumps in the data values. The number of pixels in landslide area in very high susceptible class was 2145 and total pixel was 16887 with 82.61% of R index value. Low susceptible

class pixel was 36581 with 150 pixel under landslide area and R index was 2.67% (**Table 5.6 & Figure 5.7**).

5.7.5 Analysis of R-index

R index was used for validation of the landslide susceptible map generated from each method. The index shows an increase in the number of landslides with each landslide classes as it progresses in all the methods. Equal interval has the highest index with 84.39% in very high class and the lowest index with 0.65% in low class. Quantile has the highest index in very high class with 79.85% and low class with 4.62%. Geometrical Interval has very high class with an index of 81.15% and in low class with an index of 2.79%. Natural Break has an index of 82.61% in very high class and in low class an index of 2.67% was obtained (**Table 5.6**).

5.8. Analysis of Landslide susceptible area

5.8.1 Total area in the study area

The percentage **statistics** of total area in each class was derived from the different methods (Natural Break, Equal Interval, Quantile and Geometrical Interval methods). Equal Interval method showed vast differences in its distribution range therefore it cannot be considered for landslide hazard zonation, for very high susceptibility class in total area was 8.85% while the moderate class showed the highest percentage with 53.87% followed by high class with 28.37%. For Quantile method, the class classification under total area was equally distributed with low range difference for moderate class it was 26.08% having the highest percentage and low susceptible class with lowest percentage at 23.95%. Quantile method showed poor distribution for landslide hazard zonation consideration. Geometrical Interval method under low susceptible class showed 31.78% followed by

moderate class with 31.01% and very high class with 13.81% having the lowest percentage. Natural break method displayed percentages for susceptible class as follows- moderate class have the highest percentage with 31.45%, followed by high class with 30.01% and very high class had the lowest percentage with 12.17% (Table 5.7 & Figure 5.8).

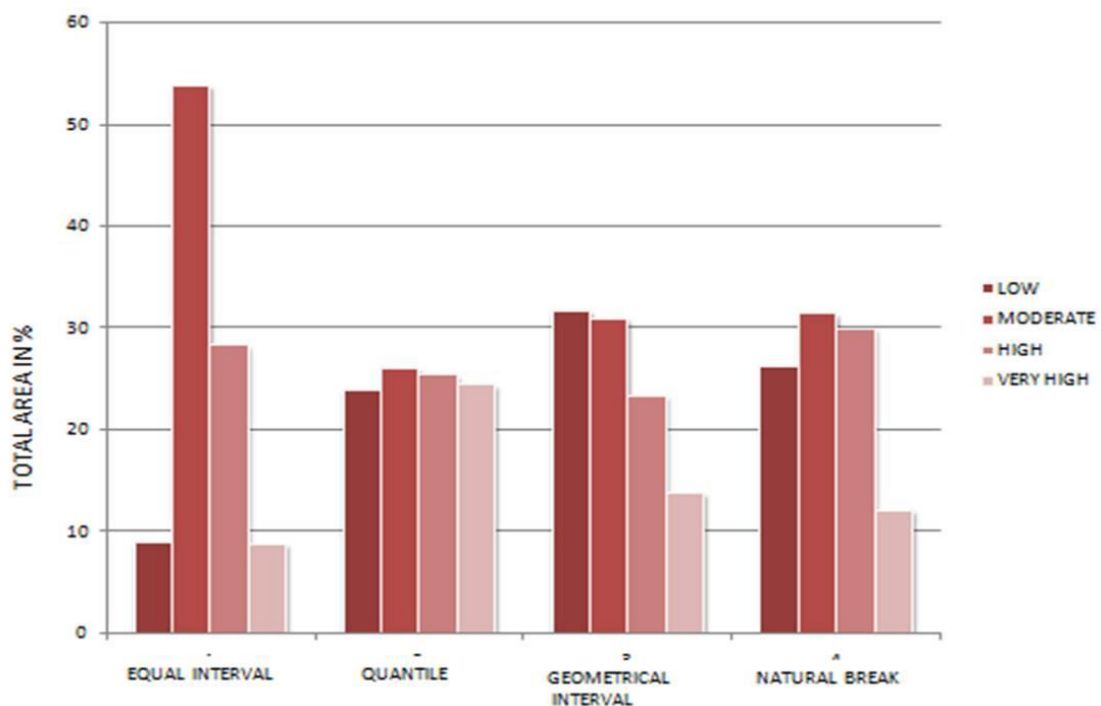


Figure 5.8. Percentage of total area for each class derived by classification method

Table 5.7. Percentage of total area for each class derived by classification method

Class	Equal Interval Method (%)	Quantile Method (%)	Geometrical Interval Method (%)	Natural break Method (%)
Low susceptible	8.92	23.95	31.78	26.37
Moderate	53.87	26.08	31.01	31.45
High	28.37	25.49	23.41	30.01
Very high	8.85	24.48	13.81	12.17

Source: Compiled by scholar.

5.8.2 Total landslide area

The landslide maps derived from IVM crossed with landslide distribution using different methods to generate their respective R index (Table 5.6). The results of the four methods (Natural Break, Equal Interval, Quantile and Geometrical Interval methods) used for deciphering landslide information are shown in Figure 5.4, 5.5, 5.6 and 5.7 respectively. The percentage **statistics** of area in each class was derived from the different methods. Equal Interval method for very high susceptibility landslide class was 59.2% but had very low value for low susceptible landslide class (0.46%) in landslide area which was not proportional.

Quantile has high value in very high landslide susceptible class (79.32%) but the values under moderate class was 5.79% and low susceptible class under landslide area was 4.49%. Geometrical interval method showed in very high susceptible class (69.11%) and low value (5.48) in low susceptible class. The landslide area in high and very in the geometrical interval was 85.42%. The value of R index value (Table 5.6) in Geometrical interval increases as the landslide susceptibility class also increases. Natural break method showed very high landslide susceptible class (66%) and 4.62% under low susceptible class. The landslide area in high and very high classes in Natural break is 87.11% (**Table 5.8 & Figure 5.9**).

Table 5.8. Percentage of landslide area for each class derived by classification method

Class	Equal Interval Method (%)	Quantile Method (%)	Geometrical Interval Method (%)	Natural Break Method (%)
Low susceptible	0.46	4.49	5.48	4.62
Moderate	14.12	5.79	9.11	8.28
High	26.22	10.4	16.31	21.11
Very high	59.2	79.32	69.11	66

Source: Compiled by scholar.

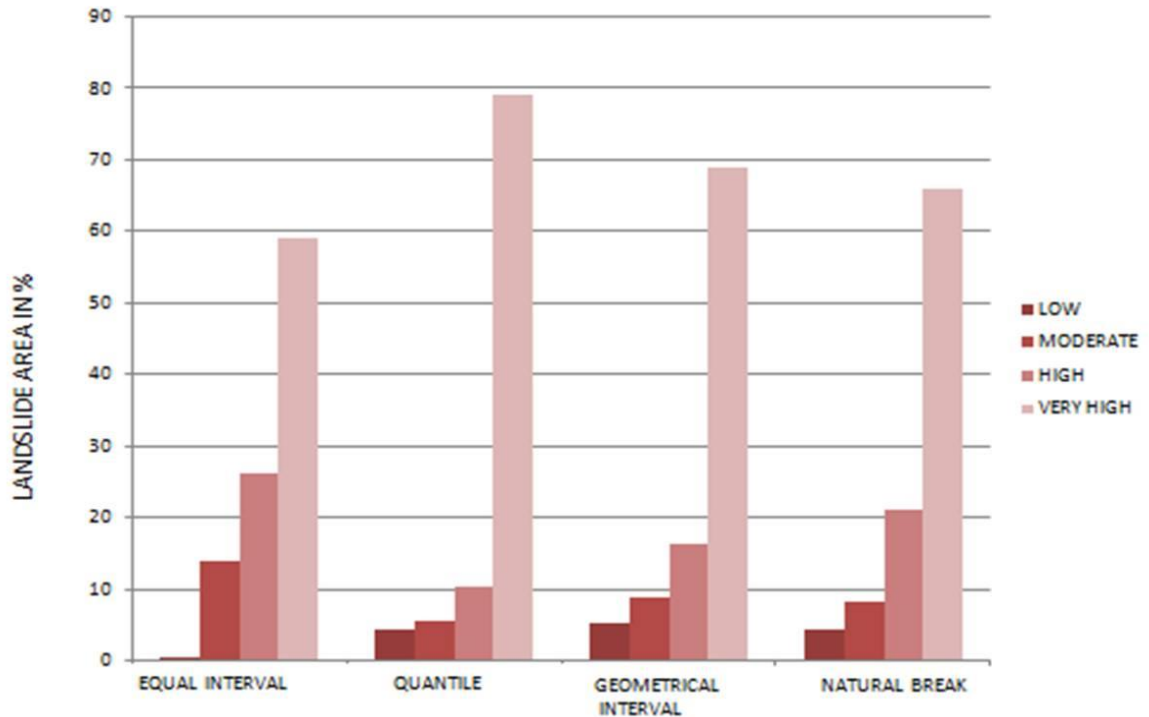


Figure 5.9. Percentage of landslide area for each class derived by classification method

5.8.3 Total area without landslide

The total percentage of area without landslide in Equal Interval method for moderate susceptible class had the highest percentage with 54.83%, high susceptible class was 28.42% and the lowest percentage was 7.64% in very high susceptible class. Quantile method showed an equal distribution for the susceptible class with low susceptible class at 24.42%, moderate class was 26.57%, high susceptible class was 25.85% and very high susceptible class are 23.17%. Geometrical Interval method under very high susceptible class showed the lowest percentage with 12.48%, high susceptible class was 23.58%, moderate susceptible class was 31.54% and low susceptible class was 32.41% (**Table 5.9 & Figure 5.10**).

Table 5.9. Percentage of area without landslide for each class derived by different methods

Class	Equal Interval Method (%)	Quantile Method (%)	Geometrical Interval Method (%)	Natural break Method (%)
Low susceptible	9.12	24.42	32.41	26.89
Moderate	54.83	26.57	31.54	32.01
High	28.42	25.85	23.58	30.22
Very high	7.64	23.17	12.48	10.88

Source: Compiled by Scholar.

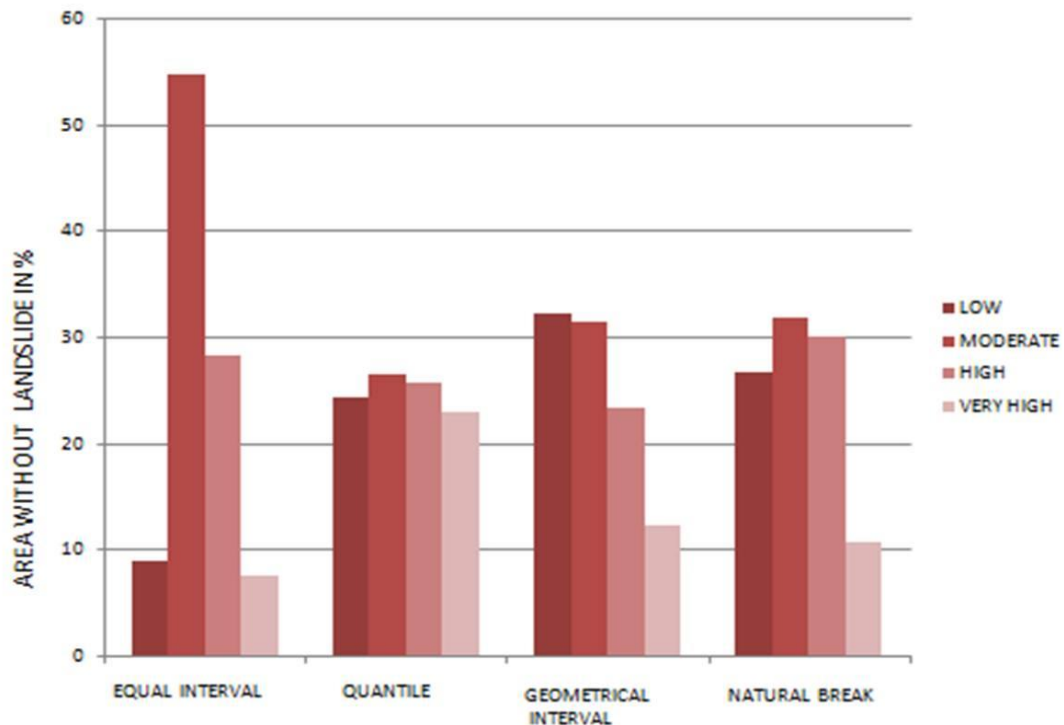


Figure 5.10. Percentage of area without landslide for each class derived by different methods

5.9 Analysis of land distribution from landslide susceptibility map

The landslide susceptibility map of the study area was generated after undergoing different method for better landslide susceptibility class representation (**Table 5.10 & Figure 5.11, 5.12**). After classification, the study area has been divided into four susceptible zones- very high susceptible zone covered about an area of 1.68 km, it occupied 12% of the study area. High hazard zone is observed around the periphery of very high hazard zone. These zones are characterised by steep slopes which disturbed can

be susceptible to landslide. This zone occupies an area of 30% constituting 4.21 km² of the study area. Precaution if not taken to check construction of building, retention walls on slopes can trigger landslide after heavy rainfall in high hazard zone. Landslide in the study area is caused by unplanned construction, unplanned drainage system, geologic factors such as steep slope, plate movement etc (Photo plate 38, 39, 40 and 41). Moderate landslide susceptible hazard zone is far away from drainage and also covered by vegetation. The zone constitutes 32% with an area of 4.49 km² in the study area. Low hazard zone is observed in areas where the slope is gentle observed in northern part of the study area or in well vegetated area observed towards the southern part of the study area which is located near the Reserve forest in Kohima. The low hazard zone is 26% which is about 3.65 km² of the study area.

Table 5.10. Land distribution determined from the Landslide susceptibility map.

Zone	Land distribution in Percentage (%)	Area (km²)
Very high	12	1.68
High	30	4.21
Moderate	32	4.49
Low	26	3.65

Source: Compiled by scholar

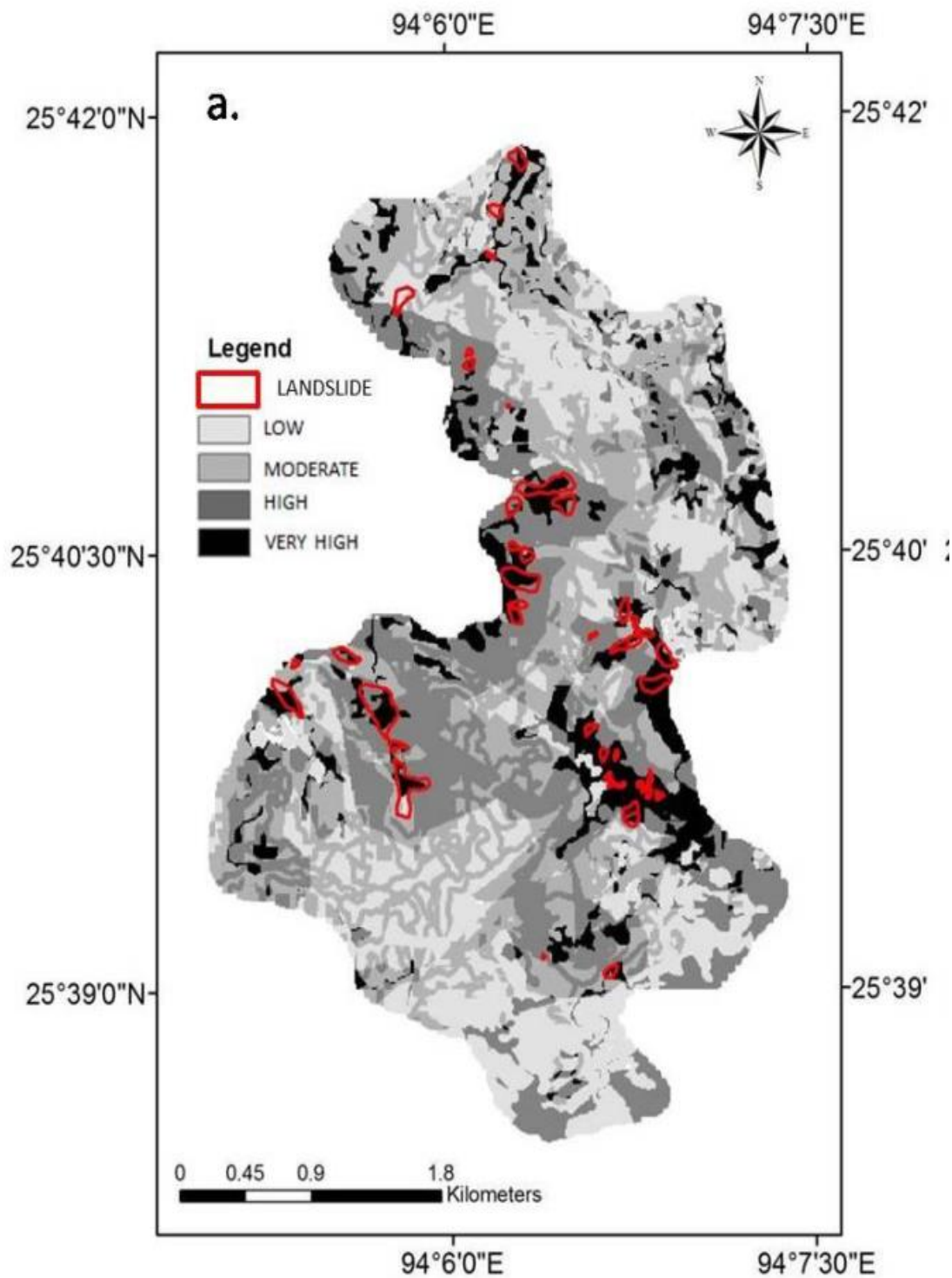


Figure 5.11. Landslide susceptibility map (landslide shown in red line)

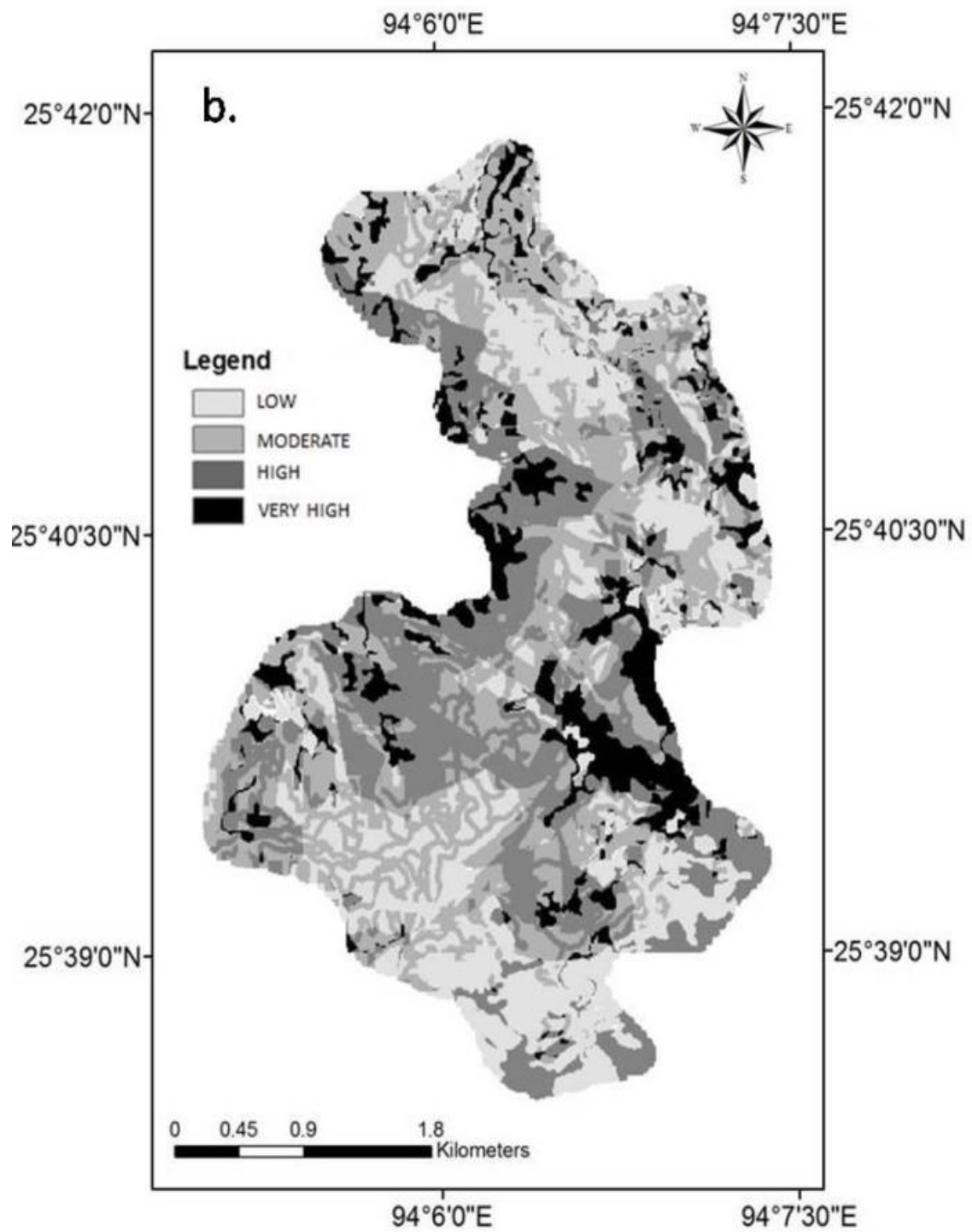


Figure 5.12. Landslide susceptibility map of Kohima

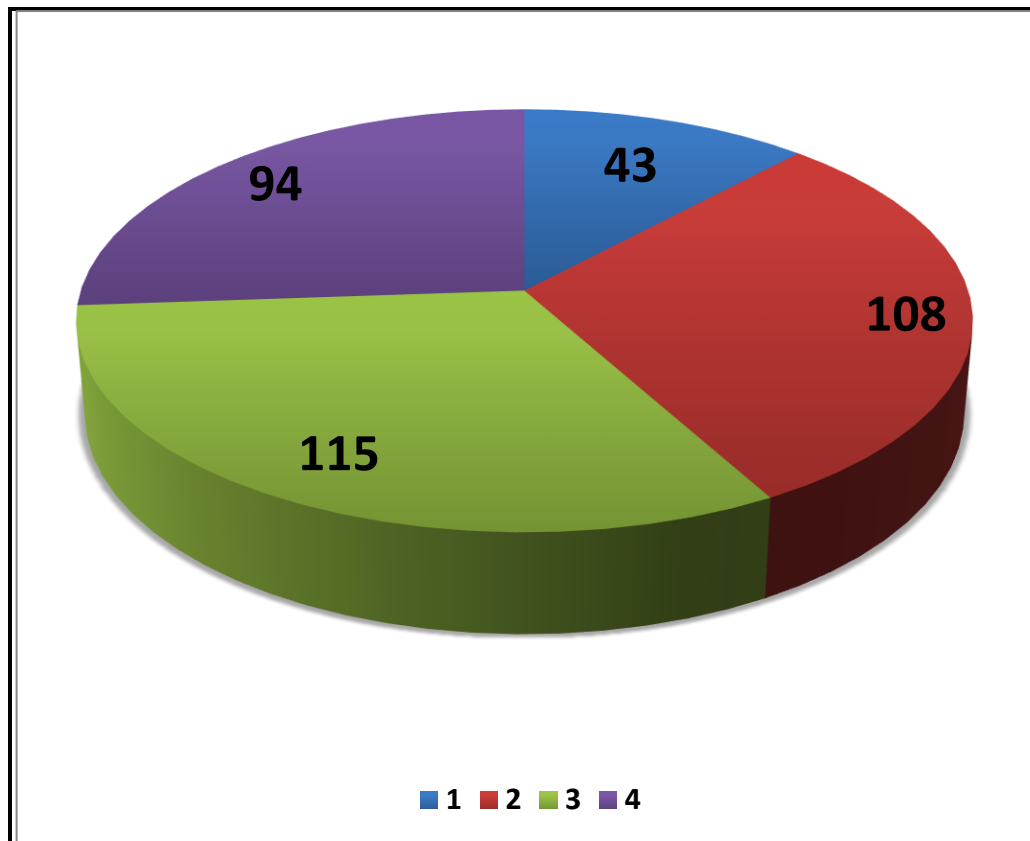


Figure 5.13. Distribution of landslide susceptibility in Kohima

The distribution of landslide in the study area is shown in **Figure 5.13** where moderate landslide susceptibility followed by high landslide susceptibility zones has maximum spatial distribution. From the landslide susceptible map, very high susceptible zone was seen in Ward no.1 where slow creeping movement was observed. This particular area falls under Disang shales which are geologically poor. The soil gets easily absorbed by rainfall causing more subsidence and creeping movement. The poor geological settings, heavy rainfall along with vehicular movement has caused landslide in Ward no. 18 (Photo plate 38). This particular stretch of road is constantly paralysed owing to landslide almost every year. The area falls under very high hazard zone where the landslide is caused mainly due to geological structural failure as fault line passes through this area (Aier *et al.*, 2011).

Torrential prevalence of precipitation along with unfavourable geological settings caused debris flow. One such landslide located at Ward no. 6 is shown in Photo plate 44. The steep slope along with less vegetation cover influenced the landslides and erosion. From this study it is observed that the areas with vegetation cover and stable geologic structure observed towards the South (near Reserve Forest) and towards the North where topography is gentle denotes that the presence of trees and a gentler sloping terrain is stable as compared to a barren and steep sloping terrain.

Areas indicated under very high and high landslide susceptible zone in the landslide susceptibility map should be avoided for any construction purposes or if at all developmental activity has to be taken up in these zones, it must be properly review and carefully supervised. The susceptible map generated can be used by the planners to demarcate the areas susceptible to landslide hazard. In conclusion, owing to high population pressure, the study area is expanding vertically as well as horizontally in spatial dimension.

The geologic formation in the study area is very poor and made up of crumpled and weathered shale's. Barail sandstone formation passes through a thin stretch of the study area towards the southwestern part which falls under low hazard zone. The occurrence of landslide is further triggered with anthropogenic activities particularly building constructions which are built without any regulations (without concerned authority approval). The scarcity of land has pressured the citizens to vertically expand their construction, further aggravating the danger of a catastrophic event in case of a seismic activity.

Anthropogenic activities should therefore be discouraged in high and very high hazard zone. Various remedial measures like afforestation and construction of retaining

wall should be undertaken to minimise the slope failures. The landslide hazard zonation map will help the planners to utilise and manage the area in the best suitable manner. The areas susceptible to landslide should be avoided and care must be taken to avoid this areas. If at all the land has to be utilised it should be properly supervised and care should be taken to prevent slides.

6

The study area experienced an average maximum temperature of 23.49°C in 2014 and average minimum temperature was 11.43 °C in 2013. Highest dew point was recorded in the year 2015 and lowest was in 2011. In 2013, the annual rainfall recorded was 1749mm with 151 rainy days and an average rainfall was 1552 mm from 2011 to 2015. The decadal population of Kohima town from 1901 to 1961 was less than 10,000. However, from 1961 onwards the population has increase rapidly, in 2011 census the population was 1,14,773 where 99,039 was contributed by the nineteen wards and remain 15,734 population was contributed from Outer ward of Kohima town. During 1961 to 2011the population growth gradually increased from 7,246 to 99, 039, but percentage of decadal variation drastically fell down from 200% (1971) to 57.9% (1981). The density of population in Kohima Town increased from 220 person/ sq.km (1901) to 7059 person/ sq. km (2011).

The ward wise distribution of population showed that minimum of 2,348 (6.2%) was occupied in Ward no.8 and maximum population of 15,734 (13.7%) was found in outer ward according to 2011 census report. Decadal ward wise house hold population distribution in Kohima Town was increased about 12,242(1991), 18,311(2001) and 25,686(2011). The highest recorded number of household population was observed in Outer ward (3374) followed by Ward no. 16 (2437) and Ward no. 15 (1718).

The topography recorded from the Digital Elevation Model (DEM) of Kohima show the highest elevation at the range of 1747 m above msl and lowest elevation is 1220.61 m above msl. Landslides in Kohima are about 66 small, medium and large sized, and the geographical area under landslide covered 0.33 km² out of the total geographic area of 14.03 km² of the study area. There are five lithology namely shale, crumpled weathered shale, weathered shale, shale with sand stone, and sandstone with shale. The total length of the road linkages in the study area was 8.236 km. Landuse and landcover parameter for the study area has been divided into six classes; water body covering an area of 22 pixels, open space includes the parks and play grounds which covers an area of 1049 pixels, the built up area has the highest geographical extent with 89070 pixels, followed by barren land constitute 27629 pixels, agricultural land with 3548 pixels. Total length of drainage was 42.80 km, the drainage lines were buffered into two (less than 50 m and more than 50m) the areal extent was 0-50 m buffer zone had 37,927 pixels and greater than 50 m buffer zone had 32,515 pixels.

For studying the buildup setting of Kohima, the building was divided into four types; W1 consisting of wood frame and light material like bamboo, cement, brick, C3L was concrete with unreinforced masonry infill walls with one to three storeys. C3M was concrete with unreinforced masonry wall and was 4 to 7 storeys and C3H was greater than

eight storeys with concrete unreinforced masonry infill walls. W1 building type number of building with one storey was 189, two storeys was 251, three storeys was 37, four storeys was 3 and five storey building was 3. C3L buildings type under 1 storey was 9, 2 storeys were 82, 3 storeys were 93. C3M building type was for four storeys, buildings present were 36, five storeys were 12, and six storeys were 4. C3H building type was one having more than 8 storey. The total number of buildings in Ward no. 4 was 721. The distribution of buildings in ward no.4 was 67.13% for W1, 22.52 % for C3L building, 7.21 % for C3M building and C3H building was 0.14%.

The building purpose was divided into religion, educational institution, residential, residential and commercial, office and hospital. Out of these, residential purpose had the maximum number of buildings. The building material was divided into bamboo, bamboo and cement, brick, RCC, asbestos and wood, where RCC building material had the highest number of buildings. In the study area, the highest number of buildings under W1 building type was observed in outer ward with 848 number of buildings and lowest was Ward no.7 and Ward no.19 with 196 buildings each. Outer ward had 1080 buildings under C3L building type and lowest by Ward no. 7 with 36 buildings. C3M had highest number of buildings in Ward no. 16 with 934 buildings and the lowest was observed in Ward no. 4 with 52 buildings. C3H had the highest number of building distribution in Ward no. 9 with 61 buildings and lowest was observed in Ward no. 1, 10,13,14,17,18 and outer ward with 0 buildings.

The building peak response for W1 building type was 1.1 m/s, C3L building type was 1.35 m/s, C3M was 1.85 m/s and C3H was 3.2 m/s. In case of damage probabilities in W1 type of building, slight damage had the maximum damage probable with 34.13% and lowest was in complete damage probable with 3.59%. C3L had highest damage probable in moderate damage with 27.33% and lowest was observed in complete damage with 8.08%.

C3M maximum damage was incurred in moderate damage probable with 33.73% and lowest was in complete damage probable with 6.68%. C3H had highest damage probable in slight damage with 24.7% and lowest was observed in moderate damage probable with 3.83%.

The total buildings in Kohima Town classed under no damage probable was 3511 and highest was observed in outer ward with 482 buildings. The total buildings under slight damage probable was 5910 and highest was observed in outer ward with 718 buildings and lowest is in ward no. 8 with 139 buildings. The total buildings under moderate damage probable was 5641 and highest was observed in outer ward with 575 buildings and lowest is in Ward no. 13 with 123 buildings. The total buildings under extensive damage probable was 4035 and highest was observed in outer ward with 590 buildings and lowest is in Ward no. 8 with 79 buildings. The total buildings under complete damage probable was 1256 and highest was observed in outer ward with 180 buildings and lowest is in Ward no. 8 with 23 buildings.

The information value obtained from the crossed weighted thematic layers under slope parameter showing highest landslide susceptibility was observed in 10-20° slope class with 0.05. Percentage of area under the 10-20° category was 56.78%. Aspect parameter showing highest landslide susceptibility was observed in North facing slope with 0.62. Fault parameter showing highest landslide susceptibility was observed in 0-10 m buffer with 0.57. Lithology parameter showing highest landslide susceptibility was observed in weathered shales with 0.68. Road parameter showing highest landslide susceptibility was observed in 0-20 m with 0.21. Landuse and landcover parameter showing highest landslide susceptibility was observed in builtup area with 14.42 and geographical area affected was 63.57%. Drainage parameter showing highest landslide susceptibility was observed in 0-50 m buffer with 0.96. The percentage of area under

landslide distribution was for very high landslide susceptibility zone it was 12% with area of 1.68 km², high landslide susceptibility zone it was 30 % with area of 4.21 km², moderate landslide susceptibility zone it was 32% with area of 4.49 km² and low landslide susceptibility zone it was 26% with area of 3.65 km². R index value of Kohima showed for very high susceptible zone the value of R index was 82.61 % and high susceptible zone showed 10.72% which together constitute R index value of 93.33% which is high and shows a good landslide density index.

PHOTO PLATE

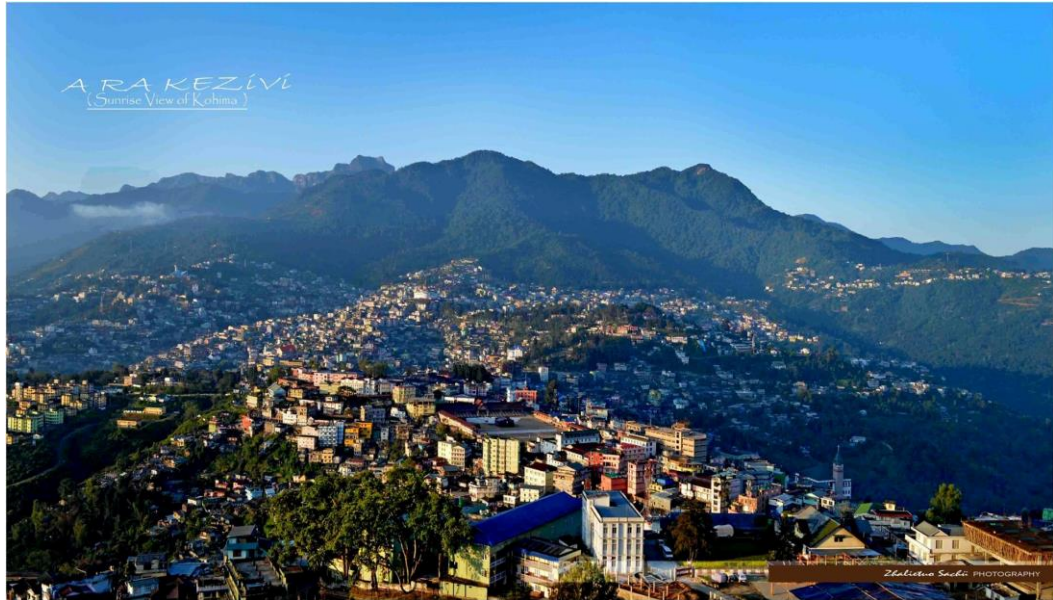


Photo plate 1. Panaromic view of Kohima (source. Kezha Sanchü)



Photo plate 2. A section of the study area, located at the foot hills of Japfü range.



Photo plate 3. Expose rock outcrop, highly jointed and bend indicating high tensional stress.



Photo plate 4. Sandstone interbedded with crumbled shales



Photo plate 5. Vertical bedding plane- signs of a geologically active zone.



Photo plate 6. Outcrop of Barail sandstone towards southwest of Kohima.



Photo plate 7. Agricultural land and barren land in the study area



Photo plate 8. Horticulture and agriculture amidst settlement.



Photo plate 9. Vegetation tract in the study area



Photo plate 10. Agricultural land in the study area.



Photo plate 11. An aerial view of Ward 4 (notice the fight for space)



Photo plate 12. Asbestos sheet House (class under W1 HAZUS building type).



Photo plate 13. Two storey house made of RCC (class under C3L HAZUS building type)



Photo plate 14. RCC house class under C3M building type for HAZUS



Photo plate 15. Multi-storeyed house made of asbestos sheet

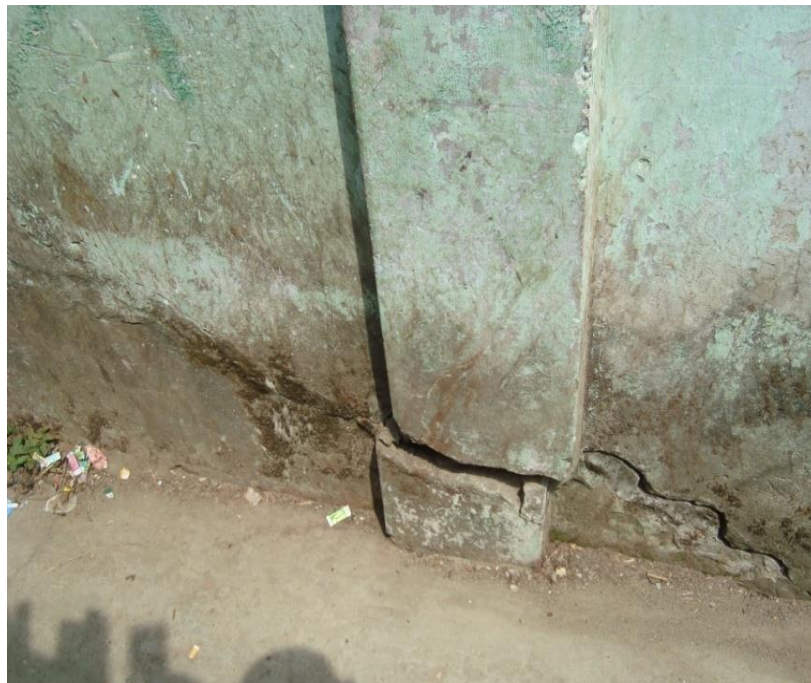


Photo plate 16. Cracks along the Column.



Photo plate 17. Visible cracks on the wall and columns.



Photo plate 18. Old and unsafe construction with no engineering safety.



Photo plate 19. Close proximity of buildings with no space in between them.



Photo plate 20. Government Office for building purpose.



Photo plate 21. Building purpose showing education institute.



Photo plate 22. W1 building type made of bricks and wood.



Photo plate 23. W1 HAZUS building type made of bamboo.



Photo plate 24. W1 HAZUS building type



Photo plate 25. W1 HAZUS building type made of asbestos tin sheet.



Photo plate 26. W1 HAZUS building type showing Brick house



Photo plate 27. Development of cracks on the wall.



Photo plate 28. Multi-storied C3H HAZUS building type, pounding and danger of damage to nearby buildings in case of collapse.

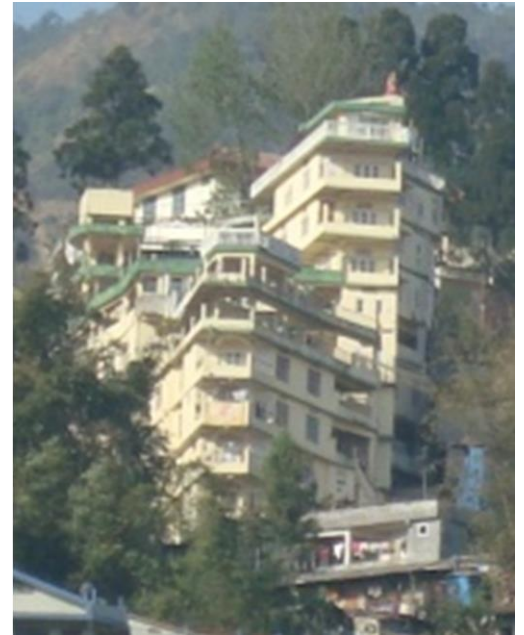
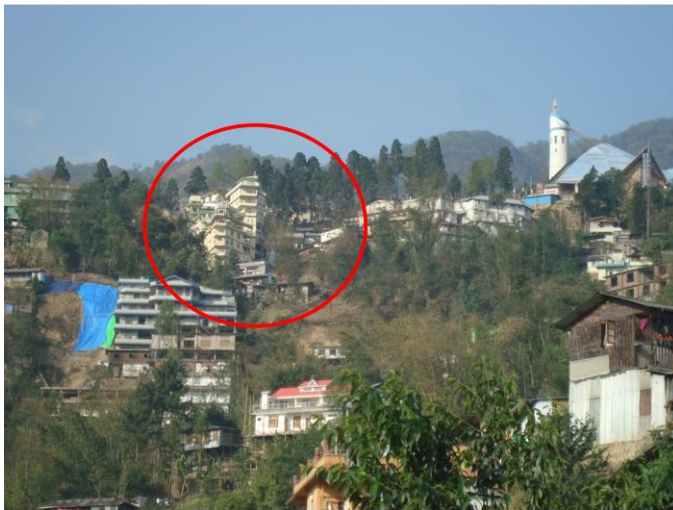


Photo plate 29. Unsafe structure, a multi-storeyed structure on hillslope highlighted with red circle and enlarged



Photo plate 30. Vertical expansion of building creates unsafe structural design.



Photo plate 31. Peeling of concrete floor exposing the iron rods of the floor.



Photo plate 32. Vertical expansion of buildings causing safety issues in building design.



Photo plate 33. W1 building type showing a dilapidated house of asbestos, bamboo and cement construction material.



Photo plate 34. Soft storied house of W1 building type.



Photo plate 35. Unsafe RCC house- irregular plan.



Photo plate 36. Dilapidated condition of house made of bamboo and cement building materials.



Photo plate 37. Old landslide- old slides can be reactivated.



Photo plate 38. Portion of the study area- note the closely constructed concrete houses on unstable slope. b). Affected buildings in Ward no.1 of the study area. c). Landslide with an approximate length of 150 m in Ward no. 6. d). Landslide at Asian Highway (AH) 1 in Ward no. 18.



2007

Source- Aier, I. *et al.*,

2016



Photo plate 39. A section of a road affected by landslide near Merhulietsa, past is the key to present (2007 and 2016).

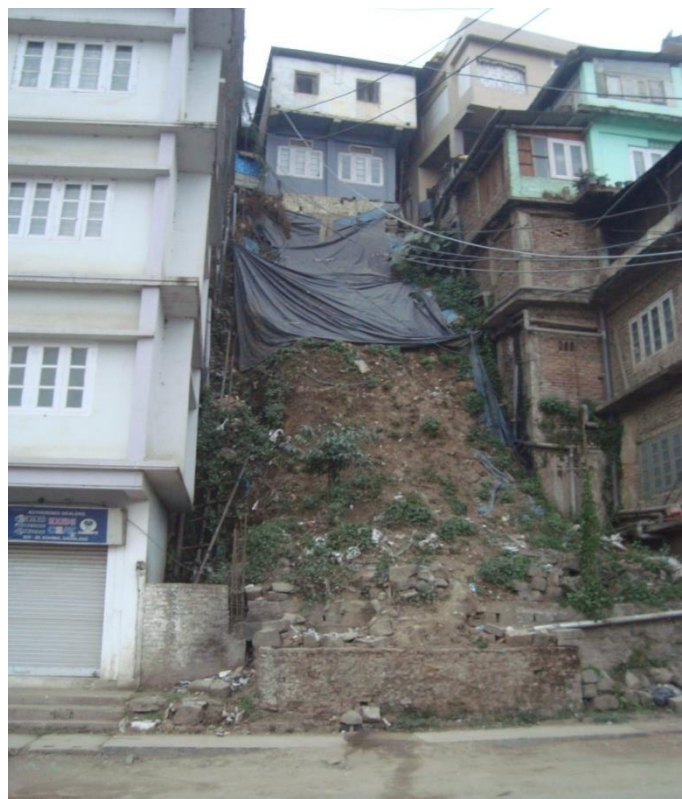


Photo plate 40. Landslide and seismic safety design issues in a picture.



Photo plate 41. Landslide occurrence along AH1 at ward 10 and right image shows landslide at Kitsubozou (ward 5).



Photo plate 42. Devastation cause on landslide path (Ward 1)



Photo plate 43. Houses affected by slide- ward 18 and ward 1. Red arrows indicate direction of slide and building weight exerted.



Photo plate 44. Debris flow at Ward 6, the entire length is more than 150 m.



Photo plate 45. Landslide caused by breakage of culvert (New Sect. road)



Photo plate 46. Translational slide at Ward 5.



Photo plate 47. Ward 1 taken on 10:04:2016, prevalence of creeping slide.



Photo plate 48. Ward 1 taken on 24:07:2017, houses damaged by the earth movement.

REFERENCES

- Ahmed, M.M., Jahan, I. and Alam, M.J. (2014). Earthquake vulnerability assessment of existing buildings in Cox-Bazar using field survey and GIS. *International journal of engineering research and technology*. Vol.3 (8), pp. 1147-1156.
- Anbazzhagan, P, Manish, S, Thomas JV, Arunachalam, A, Dinesh, SV (2014), 'Seismic vulnerability assessment using satellite data', in ST Smith (ed.), 23rd Australasian Conference on the Mechanics of Structures and Materials (ACMSM23), vol. II, Byron Bay, NSW, 9-12 December, Southern Cross University, Lismore, NSW, pp. 985-990.
- Amod Mani Dixit, Ryuichi Yatabe, Ramesh Guragain, Ranjan Kumar Dahal & Netra Prakash Bhandary (2014). Non-structural earthquake vulnerability assessment of major hospital buildings in Nepal, *Georisk: Assessment and Management of Risk for Engineered Systems and Geohazards*, Vol. 8:1, pp. 1-13.
- Abo-El-Ezz, A., M.-J. Nolle and M. Nastev (2013). "Seismic fragility assessment of low-rise stone masonry buildings. *Earthquake Engineering and Engineering Vibration*, Vol. 12(1), pp. 87-97.
- Aste, J.P., (1991). Landslide hazard analysis- Landslide risk mapping. In Almeida-Teixeira, M.E., Fantechi, R., Oliveira, R., and Gomes Coelho, A. (Eds), *Prevention and control of landslides and other mass movements*, Commis. European communities, Brussels, pp.165-170.
- Aleotti, P. and Chowdury, R. (1999). Landslide hazard assessment: summary review and new perspectives, *Bulletin of Engineering Geology and Environment*. Vol. 58(1), pp. 21–44.
- Ardizzone, F., Cardinali, M., Galli, M., Guzzetti, F. and Reichenbach, P. (2007). Identification and mapping of recent rainfall-induced landslides using elevation

- data collected by airborne LiDAR. *Natural Hazard Earth System*, Vol. 7, pp.637–650.
- Ayalew, L. and Yamagishi, H. (2005). The application of GIS-based logistic regression for landslide susceptibility mapping in the Kakuda-Yahiko Mountains, Central Japan. *Geomorphology*. Vol. 65, pp.15–31.
- Boatwright, J., Thywissen, K. and Seekins, L. (2001). Correlation of ground motion and intensity for the 17 January 1994 Northridge California earthquake. *Bulletin Seismological Society of America*, Vol.91, pp.739–752.
- Bonham-Carter, G.F. (1994). Geographic Information Systems for Geoscientists; modelling with GIS, *Computational Method in Geoscience*, Vol. 13, pp. 1-398.
- Bai, S., Lv, G., Wang, J., Zhou, P. and Ding, L. (2011). GIS-based rare events logistic regression for landslide-susceptibility mapping of Lianyungang, China. *Environment Earth Science*, Vol. 62, pp. 139–149.
- Baruah, S., Baruah, S., Kalita, A. and Kayal, J.R. (2011). Ground motion parameters in Shillong and Mikir Plateau supplemented by mapping of amplification factors in Guwahati city, Northeastern India. *Journal of Asian Earth Sciences*. Vol 42, pp. 1424-1436.
- Baruah, S., Baruah S. and Kayal, J.R. (2013). State of tectonic stress in Northeast India and adjoining South Asia region: An appraisal. *Bulletin of the seismological Society of America*, Vol. 103 (2A), pp. 894-910.
- Barani, S., Spallarossa, D., Eva, C., (2007). On the use of fault sources for probabilistic seismic hazard analysis in Italy. *GNGTS 2007, Session 2.1*, pp. 258-259.
- BHRC (Building and Housing Research Center) (1988). Iranian Code of Practice for Seismic Resistant Design of Buildings, 1st Edn., Iran, pp. 1-71.

- BHRC (Building and Housing Research Center), (1999). Iranian Code of Practice for Seismic Resistant Design of Buildings, 2nd Edn., Iran, pp. 1-127.
- Bhattacharya, P.M., Pujol, J., Majumdar, R.K. and Kayal, J.R. (2005). Relocation of earthquakes in the Northeast Indian region using joint hypocentre determination method. *Current Science*, Vol. 89 (8), pp. 1404- 1413.
- Bonham-Carter GF, Agterberg FP, Wright DF (1988). Integration of geological datasets for gold exploration in Nova Scotia. *Photogrammetry of Engineering and Remote Sensing* Vol.54: pp.1585–1592.
- Barreca, G., Bonforte, A., and Neri, M. (2013). A pilot GIS database of active faults of Mt. Etna (Sicily): A tool for integrated hazard evaluation, *Journal of Volcano Geothermal Research*, Vol. 251, pp.170–186.
- Bhandari, R.K. (2013). Indian national agenda for landslide disaster mitigation: challenges and recommendations. *Current Science*, Vol. 105 (5), pp. 845- 846.
- Bhandari, R.K. (2013). Challenges of the Devastating Indian Landslides. *Current Science*, Vol. 105 (5), pp. 563-564.
- BHRC (Building and Housing Research Center) (2005). Iranian Code of Practice for Seismic Resistant Design of Buildings, publication PNS-253, 3rd Edn., Iran, pp.1-135.
- Brabb, E. (1984) Innovative Approaches to Landslide Hazard Mapping. *4th International Symposium on Landslides. Toronto*, pp. 307-324.
- Catani, F., Segoni, S. and Falorni, G. (2010) An Empirical Geomorphology-Based Approach to the Spatial Prediction of Soil Thickness at Catchment Scale. *Water Resources Research*, 46, W05508.

- Calvi, G.M. Pinho, R., Magenes, G., Bommer, J.J., Restrepo-Vélez, L.F. and Crowley, H. (2006). Development of seismic vulnerability assessment methodologies over the past 30 years. *ISET journal of earthquake technology*. Vol. 43 (3), pp. 75-104.
- Chen, W., Li, W. P., Hou, E.K., Zhao, Z., Deng, N. D., Bai, H.Y., Wang, D. Z. (2014). Landslide susceptibility mapping based on GIS and information value model for the Chencang District of Baoji, China. *Journal of Arab Geoscience*. Vol. 7, pp. 4499–4511.
- Carrara, A, Pugliese-Carratelli, E. and Merenda, L. (1977). Computer-based data bank and statistical analysis of slope instability phenomena. *Zeitschrift fur Geomorphologic* N.F Vol. 21, pp. 187-222.
- Chung, C. J., Fabbri, A., and Van Westen, C. J. (1995). Multivariate regression analysis for landslide hazard zonation, In: A. Carrara and F. Guzzetti (eds), *Geographical Information Systems in Assessing Natural Hazards*, Kluwer, pp. 107–133.
- Ciurean, R.L., Schröter, D. and Glade, T. (2013). Conceptual Frameworks of Vulnerability Assessments for Natural Disasters Reduction. In Tiefenbacher, J. (ed) *Approaches to Disaster Management- Examining the Implications of Hazards, Emergencies and Disasters*. Intech, Croatia- European Union. pp. 1-228.
- CSIR-NEIST (2013). M 8.7 Shillong 1897 Earthquake scenario: NE Multi state preparedness campaign, *NDMA & CSIR NEIST report*, pp 1-384.
- Che, V.B., Kervyn, M., Suh, C.E., Fontijn, K., Ernst, G.G.J., Marnol, M.A.del., Trefois, P., and Jacobs, P. (2012). Landslide susceptibility assessment in Limbe (SW Cameroon): A field calibrated seed cell and information value method. *Catena*. Vol. 92, pp 83-98.

- Chiroiu, L., Eeri, M., Andre, G., Guillande, R. and Bahoken, F., (2002). Earthquake damage assessment using high resolution satellite imagery. Presented in *7th US National Conference on Earthquake Engineering*. Boston Massachusetts
- Cascini, L. (2008). Applicability of landslide susceptibility and hazard zoning at different scales. *Engineering Geology*, Vol. 102, pp. 164-177.
- Cancani A (1904) Sur L' Emploid'une Double Echelle Seismic Des Intensities Empirical Et Absolute. *J Beritrigae Zur Geophysik*. Vol.2, pp.281–283.
- Cruden DM. (1991). A simple definition of a landslide. *Bulletin of International Association Engineering Geology*. Vol.43, pp.27–29.
- Das, S., Gupta, I.D., and Gupta, V.K. (2006). A probabilistic seismic hazard analysis of Northeast india. *Earthquake Spectra*, Vol. 22 (1), pp. 1-27.
- Das, S., Gupta, I.D. and Gupta, V.K. (2006). A probabilistic seismic hazard aanalysis of Northeast India. *Earthquake Spectra*, Vol. 22 (1), pp. 1-27.
- Dai, F.C., Lee, C.F. and Nhai, Y.Y. (2002). Landslide risk assessment and management. *An overview of Engineering Geology*. Vol. 64, pp.65–87.
- Dai, F., and Lee, C.H. (2002). Landslide on natural terrain. *Mountain research and development*. Vol.22, No.1, pp 40-47.
- DeGraff, J. V. and Romesburg, H.C. (1980) Regional landslide-susceptibility assessment for wildland management: a matrix approach. In: Coates DR, Vitek JD (eds) *Thresholds in geomorphology*, Vol 19. Alien & Unwin, Boston, pp 401–414.
- Devi, A. and Kalita. S. (2014). Seismic hazard analysis of Northeast India and its adjoining region. *International journal of environmental sciences*. Vol.4(4), pp. 589-604.
- Dai, F., and Lee, C.H. (2002). Landslide on natural terrain. *Mountain research and development*. Vol.22, No.1, pp 40-47.

- Dong L, Shan J. (2013). A comprehensive review of earthquake-induced building damage detection with remote sensing techniques. *ISPRS Journal of Photogrammetry*. Vol. 84, pp.85–99.
- Dhakal *et al* (2000). Landslide Hazard Mapping and its Evaluation Using GIS: An Investigation of Sampling Schemes for a Grid-Cell Based Quantitative Method. *Photogrammetric Engineering & Remote Sensing*, Vol. 66(8), pp. 981-989.
- Dewey, J.F. and Bird, J.M. (1970). Mountain belts and new global tectonics. *Journal of Geophysical research*. Vol 75. Pp. 2625-2647.
- Disaster Management in India 2011, Ministry of Home Affairs, India. *GOI-UNDP Disaster Risk Reduction Programme (2009-2012)*. pp.1-255.
- Erdik M. (1994) .Developing a comprehensive earthquake disaster masterplan for Istanbul. In Tucker et al (eds) *Issues in Urban Earthquake Risk*. Kluwer Academic Publ. NL. pp. 125-166.
- Erdik, M., Sesetyan, K., Demirciog, M.B.,  lu, C., Zuo U., Hancilar, C. T., and Harmandar, E. ().Rapid Earthquake Loss Assessment After Damaging Earthquakes. A. Ansal (ed.), *Perspectives on European Earthquake Engineering and Seismology, Geotechnical, Geological and Earthquake Engineering* Vol. 34, pp. 53-95.
- Erdik M. 1994 .- Developing a comprehensive earthquake disaster masterplan for Istanbul. In Tucker et al (eds) *Issues in Urban Earthquake Risk*. Kluwer Academic Publ. NL. pp. 125-166.
- Ebert, A. and Kerle, N. (2008). Urban social vulnerability assessment using object oriented analysis of remote sensing and GIS data. A case study for Tegucigalpa, Honduras.

- The International archives of the Photogrammetry, *Remote sensing and spatial information sciences*. Vol. 36 (B7), pp. 1307-1312.
- Farsi, M. et. al., (2015). Seismic Vulnerability of Reinforced Concrete Structures in Tizi-Ouzou City (Algeria), *1st International Conference on Structural Integrity, Science direct*, pp. 838 – 845.
- Feng, T., Hong, Z., Fu, Q., Ma, S., Jie, X., Wu, H., Jiang, C. And Tong, X., (2014). Application and prospect of a high resolution remote sensing and geo-information system in estimating earthquake casualties. *Natural Hazards Earth System Science*. Vol. 14, pp. 2165-2178.
- FEMA. Multihazard loss estimation methodology, earthquake model, Technical model, pp. 1-718.
- FEMA (2001). Hazus-MH MR5; Earthquake loss estimation methodology, advanced building engineering building module (AEBM). Department of Homeland security, Washington, pp. 1-119.
- FEMA, 2001. Earthquake loss estimation methodology, Hazus-MH MR5. Advanced engineering building module (AEBM). Technical and User manual. Pp. 1-119.
- Fell, R., Corominas, J., Bonnard, C., Cascini, L., Leroi, E., Savage, W.Z. (2008). Guidelines for landslide susceptibility, hazard and risk zoning for landuse planning. *Engineering geology*. Vol. 102, pp.85-98.
- Farrokhnia A, Pirasteh S, Pradhan B, Pourkermani M, Arian M. (2011). A recent scenario of mass wasting and its impact on the transportation in Alborz Mountains, Iran: contribution from geo information technology. *Journal of Arab Geoscience*. Vol.4, pp.1337–1349.
- FEMA, (2003). Multi-hazard Loss estimation methodology, Earthquake Model, *HAZUS MR4 Technical Manual*. pp. 1-712.

- Guzzetti, F., Carrara, A., Cardinali, M. And Reichenbach, P., (1999). Landslide hazard evaluation: a review of current techniques and their application in a multi-scale study, Central Italy. *Geomorphology*, Vol. 31, pp. 181-216.
- Guzzetti, F., Carrara, A., Cardinali, M. and Reichenbach, P. (1999). Landslide hazard evaluation: A review of current techniques and their application in a multi-scale study, Central Italy. *Geomorphology*, Vol.31, pp. 181–216.
- Gulati, B. (2006). Earthquake risk assessment of buildings: Applicability of HAZUS in Dehradun, India. M.Sc Thesis. ITC Enschede, pp. 1-121.
- Gahalaut, V.K., Martin, S.S., Srinagesh, D., Kapil, S.L., Suresh, G., Saikia, S., Kumar, V., Dadhich, H., Patel, A., Prajapati, S.K., Shukla, H.P., Gautum, J.L., Baidya, P.R., Mandal, S. And Jain, A. (2016). Seismological, geodetic, macroseismic and historical context of the 2016 Mw 6.7 Tamenglong (Manipur) India earthquake. *Tectonophysics*, Vol. 688, pp. 36-48.
- Ghose, N.C., Agrawal, O.P. and Chatterjee, N. (2010). A geological and mineralogical study of eclogite and glaucophane schists in the Naga Hills Ophiolite, Northeast India. *Island Arc*, Vol. 19, pp. 336-356.
- Gupta, I. (1980). A note on the correlation of modified Mercalli intensity with peaks of far-field ground motion. *Bulletin Seismological Society of America*. Vol.70, pp.925–932.
- Guzzetti, F. (2005). Landslide Hazard and risk assessment. Ph.D dissertation, pp. 1-389.
- GHI, 2004 GeoHazards International (GHI) (2004). RADIUS Introduction. Available from: <http://www.geohaz.org>
- Guragain, J. (2000). GIS for seismic building loss estimation: A case study from Lalitpur sub-metropolitan city area, Kathmandu, Nepal. ITC thesis pp. 1-95.

- Guzzetti, F., Carrara, A., Cardinali, M. And Reichenbach, P., (1999). Landslide hazard evaluation: a review of current techniques and their application in a multi-scale study, Central Italy. *Geomorphology*, Vol.31, pp. 181-216.
- Harvas, J. and Bobrowsky, P., (2009). Mapping: Inventories, susceptibility, hazard and Risk. In: Sassa, K. and Canuti, P. (Eds), *Landslides- Disaster Risk Reduction*. Springer, Berlin, pp. 321-349.
- Hataminejad, H., Fathi, H., and Eshghabadi, F. (2009). Criterion vulnerability assessment earthquake about city, case study region 10 Tehran, *Journal of Human Geography Research*, Vol.68, pp.1-2.
- Hao, W., Cheng, Z., Shi, W., Miao, Z. and Xu, C. (2014). An object-based image analysis for building seismic vulnerability assessment using high-resolution remote sensing imagery. *Natural Hazards*, Vol.71, pp. 151-174.
- Huber, M., Marconi, F. and Moscatelli, M. (2015). Risk based characterisation of an urban building site, *Georisk* Vol.9(1), pp 49-56.
- Hao, W., Cheng Z., Shi, W., Miao, Z. And Xu, c. (2014). An object-based image analysis for building seismic vulnerability assessment using high-resolution remote sensing imager. *Natural Hazards*, Vol.71, pp.151–174.
- Hamid Reza Ranjbar, Hamid Dehghani, Ali Reza Azmoude Ardalan & Mohammad Reza Saradjian (2016): A GIS-based approach for earthquake loss estimation based on the immediate extraction of damaged buildings, *Geomatics, Natural Hazards and Risk*, vol., pp.1-21.
- Hong, Y., Adler, R., and Huffman, G., (2007). Use of satellite remote sensing data in the mapping of global landslide susceptibility. *Natural Hazards*. Vol. 43(2). pp 245-256.

- Hancilar, U., Tunzun, C., Yenidogan, C. and Erdik, M. (2010). ELER software- a new tool for urban earthquake loss assessment. *Natural Hazard Earth system science*, Vol. 10, pp. 2677-2696.
- Harvas, J. and Bobrowsky, P., (2009). Mapping: Inventories, susceptibility, hazard and Risk. In: Sassa, K. and Canutti, p. (Eds), *Landslides- Disaster Risk Reduction*. Springer, Berlin, pp. 321-349.
- Hsieh, M. H., Lee, B.J., Lei, T.C. and Lin, J.Y. (2013). Development of medium- and low-rise reinforced concrete building fragility curves based on Chi-Chi Earthquake data. *Natural Hazards*, Vol.69 (1), pp. 695-728.
- IDNDR (1993) International agreed Glossary of Basic Terms related to Disaster Management. Department of Humanitarian Affairs, DHA-Geneva.
- Jebur, M. N., Pradhan, B., and Tehrany, M. S. (2013). Detection of vertical slope movement in highly vegetated tropical area of Gunung pass landslide, Malaysia, using L-band InSAR technique, *Journal of Geoscience*, Vol.18, pp.61–68.
- Jebur MN, Pradhan B, Shafapour TM. (2014). Optimization of landslide conditioning factors using very high-resolution airborne laser scanning (LiDAR) data at catchment scale. *Remote Sensing of Environment*. Vol.152, pp.150–165.
- Jebur, M. N., Pradhan, B., and Tehrany, M. S. (2013). Using ALOS PALSAR derived high-resolution DInSAR to detect slow-moving landslides in tropical forest: Cameron Highlands, Malaysia, *Geomatic Natural Hazards Risk*, pp.1–19,
- Jagadish, K.S., Raghunath, S. and Nanjunda Rao, K.S. (2003). Behaviour of masonry structures during the Bhuj earthquake of January 2001. *Proceeding of Indian Academy Science (Earth Planet Science)*, Vol. 112(3), pp. 431-440.

- Kienholz, H., Bichsel, M., Grunder, M. and Mool, P. (1983). Kathmandu-Kakani area, Nepal: mountain hazards and slope stability map. Mountain hazards mapping project map 4 (scale 1:10.000). United Nations University, Tokyo.
- Khatsu, P. And Van Westen, C.J., (2005). Urban multi-hazard risk analysis using GIS and remote sensing: A case study from Kohima town, Nagaland, India. In: *Proceeding of ACRS*, Hanoi, Vietnam, pp. 1-9.
- Khatsü, P. (2004). Urban multi-hazard risk analysis using GIS and Remote Sensing: A case study of landslide, earthquake and fire hazard in a part of Kohima Town, India. ITC, The Netherlands and Indian Institute of Remote Sensing, Dehradun. Pp.1-83.
- Kumar, T.N. (2012). Managing disasters in India. *Yojana*. Vol. 56, pp. 5-10.
- Khodadad, S. And Jang, D. (2015). Landslide susceptibility mapping in the Penang Island, Malaysia- Using the AHP and OLS methods. *Journal of the Korean Geomorphical association*, Vol. 22(1), pp. 109-121.
- Kohle, M. P., Neuhauser, B., Ratzinger, K., Wenzel, H. and Howes, D. (2007). Element at risk as a framework for assessing the vulnerability of communities to landslides. *Natural hazard Earth System Sciences*, Vol.7, pp. 765-779.
- Kenny, C. (2012). Disaster risk reduction in developing countries: costs, benefits and institutions. *Disasters*, Vol. 36, pp.559–588.
- Kayal, J.R. (2014). Seismo-tectonics of the great and large earthquakes in Himalaya, *Current Science*, Vol. 106(2). Pp. 188-197.
- Kaka, S. and Atkinson, G. (2004). Relationship between instrumental ground motion parameters and modified Mercalli intensity in eastern North America. *Bulletin Seismological Society of America*. Vol.94, pp.1728–1736.

- Kayal, J.R., Arefiev, S.S., Barua, S., Hazarika, D., Gogoi, N., Kumar, A., Chowdhury, S.N., and Kalita, S. (2006). Shillong Plateau earthquakes in Northeast India region: complex tectonic model. *Current Science*. Vol. 91(1), pp. 109-114.
- Kimand, Z.W. and R.Nevatia. (2004). Automaticdescriptionofcomplexbuildingsfrommultiple images. *Computer Vision and Image Understanding*, Vol. 96(1), pp.60-95.
- Kayal, J.R., Arefiev, S.S., Barua, S., Hazarika, D., Gogoi, N. Kumar, A., Chowdhury, S.N. and Kalita, S. (2006). Shillong Plateau earthquakes in Northeast India region: complex tectonic model. Vol. 91(1),pp.109-114.
- Karaca E. and Luco, N. (2008). Development of hazard compatible building fragility and vulnerability models. *Proceedings of 14th World Conference on Earthquake Engineering* . pp 1-8.
- Kircher, C.A. (2003). Near-Real-Time Loss Estimation Using HAZUS and SHAKEMAP Data, *SMIP03 Seminar on Utilization of Strong-Motion Data*, pp. 59 – 66.
- Ladas, I., Fountoulis, I., and Mariolakos, I., (2007). Using GIS and multicriteria decision analysis in landslide susceptibility mapping- A case study in Messinia prefecture area (SW Peoloponnesus, Greece).Bulletin of the Geological Society of Greece.v.40, *Proceedings of the 11th international Congress, Athens*, pp. 1-13.
- Lefevre, S. and Weber. J. (2007). Automatic building extraction in vhr images using advanced morphological operators. *Urban Remote Sensing Joint Event*, pp. 1 -5.
- Lan H X, Zhou CH, Wang LJ, Zhang HY, Lier H (2004). Landslide hazard spatial analysis and prediction using GIS in the Xiaojiang watershed, Yunnan, China, *Engineering geology*, Vol. 76, pp.109-128.

- Ladas, I., Fountoulis, I., and Mariolakos, I., (2007). Using GIS and multicriteria decision analysis in landslide susceptibility mapping- A case study in Messinia prefecture area (SW Peoloponnesus, Greece). *Bulletin of the Geological Society of Greece*. Vol.40, pp. 1-13.
- Lignos, D. G. and E. Karamanci (2013). Drift-based and dual-parameter fragility curves for concentrically braced frames in seismic regions. *Journal of Constructional Steel Research*, Vol.90, pp. 209-220.
- Lateltin, O., Haemmig, C., Raetzo, H., and Bonnard, C. (2005). Landslide risk management in Switzerland. *Landslides*, Vol. 2, pp. 313-320.
- Lumantarna, E., Lam, N., Tsang, H.H., Wilson, J., Gad E., and Goldsworthy H. (2014). Review of Methodologies for Seismic Vulnerability Assessment of Buildings. *Proceeding of Australian Earthquake Engineering Society*, pp. 1-12.
- Miyagi, T. and Hamasaki, E. (2014). Risk evaluation of landslide topographic area by aerial photointerpretation. *Landslide Science for a Safer Geoenvironment*. Sassa, K., Canuti, P., Yin, Y., Eds.; Springer: Berlin, Germany, Vol.2, pp. 491–497.
- Murphy JR, O'Brien LJ (1977) The correlation of peak ground acceleration amplitude with seismic intensity and other physical parameters. *Bulletin Seismological Society America*. Vol. 67, pp.877–915.
- Murty, C.V.R. (2005). Earthquake tips; Learning earthquake design and construction. NICEE, IIT Kanpur, pp. 1-55.
- Murty, C.V.R., Gowami, R., Vijayanarayanan, A.R., and Mehta, V.V. (2012). Some concepts in Earthquake behaviour of buildings. *GSDMA*. Pp. 1-268.
- Meten, M., Bhandary, N.P. and Yatabe, R. (2015). Effect of Landslide factor combinations on the prediction accuracy of landslide susceptibility maps in the blue Nile gorge of Central Ethiopia. *Geoenvironmental disasters*, Vol. 2 (9), pp. 1-17.

- Malladi, V.P.T. (2012). Earthquake building vulnerability and damage assessment with reference to Sikkim earthquake, 2011. M.Sc Dissertation, ITC Eschede. Pp. 1-111.
- Murat S. K.(2006). Fragility analysis of mid-rise R/C frame buildings. *Engineering Structures*, Vol.28, pp. 1335-1345.
- Mohamed YA, Mohamed AK, Biswajeet P, Turki E. (2016). Debris flow impact assessment along the Al-Raith Road, Kingdom of Saudi Arabia, using remote sensing data and field investigations. *Geomatics of Natural Hazards Risk*. Vol.7, pp.620– 638.
- Montoya. A.L., (2002). Urban Disaster Management. A case study of Earthquake Risk Assessment in Cartago, Corta Rica. ITC Publication series 96.
- Mayer. H. (1990). Automatic object extraction from aerial imagery. a survey focusing on buildings. *Computer vision and image understanding*, Vol.74(2):pp.138-149.
- Mohan, K., Joshi, A. and Patel, R.C., (2008). The assessment of seismic hazard in two seismically active regions in Himalyas using deterministic approach. *Journal of Indian Geophysical Union*, Vol. 12(3), pp. 97-107.
- Mohan, K., Joshi., A. and Patel, R.C. (2008). The assessment of seismic hazard in two seismically active regions in Himalayas using deterministic approach. *Journal of Indian Geophysics Union*. Vol. 12(3), pp. 97-107.
- Mehdi, R. and Armin, G. (2011). Automatic 3D building extraction from aerial and space images for earthquake risk management, *Georisk: Assessment and Management of Risk for Engineered Systems and Geohazards*, Vol.5(1), pp. 77-96.
- Mueller, M., Segl, K., Heiden, U. and Kaufmann, H. (2006). Potential of high-resolution satellite data in the context of vulnerability of buildings. *Natural Hazards*. Vol. 38, pp.247–258.

- Mathur, L. P., and P. Evans, 1964, Oil in India: 22nd Session International Geological Congress Proceedings, pp. 7–52.
- Mohan, K., Joshi, A. and Patel, R.C. (2008). The assessment of seismic hazard in two seismically active regions in Himalayas using deterministic approach. *Journal of India Geophysical Union*. Vol. 12(3). pp. 97-107.
- Midorikawa, S. (1993). Semi-empirical estimation of peak ground acceleration from large earthquakes, *Tectonophysics*, Vol. 218, pp.287-295.
- Marrapu, B.M. and Jakka, R.S., (2014). Landslide hazard zonation methods: A critical review. *International journal of civil Engineering research*, Vol. 5(2), pp.215-220.
- Nagarajan, R., Mukherjee, A., Roy, A. and Khire, M. V. (1998). Technical note Temporal remote sensing data and GIS application in landslide hazard zonation of part of Western ghat, India, *International Journal of Remote Sensing*, Vol.19(4),pp. 573-585.
- Nagarajan, R., Roy, A., Vinodkumar, R., Khire, M. (2000). Landslide hazard susceptibility mapping based on terrain and climatic factors for tropical monsoon region. *Engineering Geology*, Vol. 58, pp.275–287.
- Neighbors, C. J., Cochran, E. S., Caras, Y. and Noriega, G. R. (2013). Sensitivity Analysis of FEMA HAZUS Earthquake Model: Case Study from King County, Washington. *Natural Hazards Review*. Vol. 14, pp. 134-146.
- Nichol, E.J., Shaker, A. and Wong, M. S. (2006). Application of high-resolution stereo satellite images to detailed landslide hazard assessment. *Geomorphology*, Vol.76, pp.68–75.
- Naveen Pareek, Pal, S., Kaynia, A.M. and Sharma, M.L. (2014) Empirical-based seismically induced slope displacements in a geographic information system

- environment: a case study, *Georisk: Assessment and Management of Risk for Engineered Systems and Geohazards*, Vol.8(4), pp.258-268.
- NIBS, 2002. HAZUS'99; Earthquake loss estimation methodology: technical manual in FEMA (ed) *Technical manual federal emergency management agency (FEMA)*, National institute of Building Sciences (NIBS), pp. 1- 325.
- Nouri, H., Beecham, S., Anderson, S., and Nagler, P. (2014). High spatial resolution WorldView 2 Imagery for mapping NDVI and its relationship to temporal urban landscape evapotranspiration factors. *Remote Sensing*. Vol.6, pp. 580-602.
- Nath, S.K., Adhikari, M.D., Devaraj, N. and Maiti, S.K. (2015). Seismic vulnerability and risk assessment of kolkata city, India. *Natural Hazards Earth System Science*. Vol. 15, pp. 1103-1121.
- Oldham, T. (1882) In Oldham RD (ed) The Cachar earthquake of 10th January, 1869. *Mem Geol Surv India*, Vol. 19(1), pp.1–88.
- Oldham, R.D. (1899) Report of the great earthquake of 12th June, 1897. *Mem Geological Survey of India*, Vol.29, pp.1–379.
- Osna, T., Sezer, E. A., and Akgun, A. (2014). GeoFIS: An Integrated Tool for the Assessment of Landslide Susceptibility, *Computational Geoscience*, Vol.66, pp. 20–30.
- Okimura, T. and Kawatani, T. (1986). Mapping of the potential surface-failure sites on Granite Mountain slopes. In: Gardiner J (ed) *International geomorphology*, part 1. Wiley, New York, pp 121–138.
- Pack, R.T., Tarboton, D.G. and Goodwin, C.N. (1998). The SINMAP approach to terrain stability mapping. *Proceedings of 8th congress of the international association of engineering geology*, Vancouver, British Columbia, Canada, pp. 1157–1165.

- Pardeshi, S.D., Autade, S.E. and Pardeshi, S.S. (2013). Landslide hazard assessment: recent trends and techniques. *SpringerPlus*, Vol.2 (523), pp. 1-11.
- Porter, K. A., A. S. Kiremidjian and J. S. LeGrue (2001). "<TR139_Porter.pdf>." *Earthquake Spectra* 17(2), pp. 291-312.
- Panahi, M., Rezaie, F. and Meshkani, S.A. (2014) Seismic vulnerability assessment of school buildings in Tehran city based on AHP and GIS. *Natural hazard earth system science*. Vol. 14, pp. 969-979.
- Prajapati, S.K., Kumar, A., Chopra, S. and Bansal, B.K. (2013). Intensity map of Mw 6.9 2011 Sikkim–Nepal border earthquake and its relationships with PGA: distance and magnitude. *Natural Hazard*, Vol. 69, pp. 1781-1801.
- Ploeger, S.K., Atkinson, G.M. and Samson, C. (2010). Applying the HAZUS-MH software tool to assess seismic risk in downtown Ottawa, Canada. *Natural hazard* Vol. 53, pp.1-20.
- Pradhan, B., Hagemann, U., Shafapour Tehrany, M., and Prechtel, N. (2014). An easy to use ArcMap based texture analysis program for extraction of flooded areas from TerraSAR-X satellite image, *Computational Geoscience*, Vol. 63, pp.34–43.
- Panikkar S, Subramaniyan V. (1997) Landslide hazard analysis of the area around Dehra Dun and Mussoorie, Uttar Pradesh. *Current Science*, Vol.73, pp.1117–1123.
- Prajapati, S.K., Kumar, A., Chopra, S. And Bansal, B.K. (2013). Intensity map of Mw 6.9 2011 Sikkim–Nepal border earthquake and its relationships with PGA: distance and magnitude. *Natural Hazard*, Vol. 69, pp. 1781-1801.
- Porter, K.A., Beck, J.L., Seligson, H.A., Scawthorn, C.R., Tobin, L.T., Young, R. and Boyd T. (2002). Improving Loss Estimation for Woodframe Buildings Volume 1: Report, Final Report of Tasks 4.1 and 4.5 of the CUREE-Caltech Woodframe

- Project , *Consortium of Universities for Research in Earthquake Engineering*,
Richmond, C, pp. 1-154.
- Prajapati, S.K., Kumar, A., and Chopra, S. (2013). Intensity map of Mw 6.9 2011 Sikkim-Nepal border earthquake and its relationships with PGA: distance and magnitude. *Natural hazards*, Vol. 63, pp. 1781-1801.
- Panagiota, M., Jocelyn, C., Erwan, P., Philippe, G. (2012). A support vector regression approach for building seismic vulnerability assessment and evaluation from remote sensing and in situ data. In: 2012 IEEE International geoscience and remote sensing symposium. *IEEE international symposium on geoscience and remote sensing IGARSS*. pp. 7533–7536,
- Rautela, P. and Thakur, V.C. (1999). Landslide hazard zonation in Kaliganga and Madhyamaheshwar valleys of Garhwal Himalaya: A GIS based approach. *Himalayan Geology*, Vol.20(2), pp. 31-44.
- Rashed, T. and Weeks, J. (2003). Assessing vulnerability to earthquake hazards through spatial multicriteria analysis of urban areas. *International journal of Geographical information Science*, Vol. 17(6), pp. 547-576.
- Rawat, M.S., Uniyal, D.P., Dobhal, R., Joshi, V., Rawat, B.S., Bartwal, A., Singh, D. And Aswal, A., (2015). Study of landslide hazard zonation in Mandakini valley, Rudrapur district, Uttarakhand using remote sensing and GIS. *Current Science*, Vol. 109 (1), pp. 158-170.
- Raman, R. and Punia, M. (2012). The application of GIS-based bivariate statistical methods for landslide hazards assessment in the upper Tons river valley, Western Himalaya, India, *Georisk: Assessment and Management of Risk for Engineered Systems and Geohazards*, Vol 6(3), pp. 145-161.

- Roxana, L., Schröter, C.D. and Glade, T. (2013). Approaches to Disaster Management - Examining the Implications of Hazards, Emergencies and Disaster . *Intech*, pp.1-30.
- Risk-UE (2004). An advanced approach to earthquake risk scenarios with applications to different European towns. Final Report, www.risk-ue.net).
- Roberds, W. (2005). Estimating temporal and spatial variability and vulnerability. *Landslide risk management*. Edit by Hunger, Fell, Couture and Eberhardt. Taylor and Francis group, London. pp. 129-157.
- Rashed, T. and Weeks, J. (2003). Assessing vulnerability to earthquake hazards through spatial multicriteria anysis of urban areas. *International journal of Geographical Information Science*. Vol. 17(6), pp 547-576.
- Rossetto, T. and A. Elnashai (2003). "Derivation of vulnerability functions for European-type RC structures based on observational data." *Engineering Structures* 25(10): 1241-1263.
- Raipure P., seismic vulnerability assessment of open ground storey RC buildings by using fragility curves, Government College of Engineering, Amravati, M-Tech thesis, 2013-14.
- Rahman, S.A.A.A. and Salik, A., (2016). Seismic analysis of vertically irregular buildings. *Current Science*. Vol. 111 (10), pp. 1658- 1663.
- Sharifikia, M. (2010). Vulnerability assessment and earthquake risk mapping in part of North Iran using geospatial techniques. *Journal of Indian Society of Remote Sensing*, Vol. 38(4), pp. 708-716.
- Shahabi, H. and Hashim, M. (2015). Landslide susceptibility mapping using GIS-based statistical models and Remote sensing data in tropical environment. *Scientific reports*, Vol. 5, pp.1-15.

- Sharifzadegan, M. H. and Fathi, H.: Application of seismic risk assessment models in urban planning and design, *Journal of Architecture and Urban Planning Faculty of Shahid Beheshti University*, Vol. 46, pp.109–124.
- Shayannejad, A. and Bahram, A.A. (2014). Earthquake Vulnerability Assessment in urban areas using MCDM Case study: The central part of 6th district of Tehran Municipality. *International review for spatial planning and sustainable development*, Vol.2 (2), pp.39-51.
- Shit, P.K., Bhunia, G.S. and Maiti, R. (2016). Potential landslide susceptibility mapping using weighted overlay model (WOM). *Model of Earth System Environ.* Vol 2 (21), pp. 1-10.
- Singh, P. (2005). Population vulnerability for earthquake loss estimation using community based approach with GIS. M.Sc Thesis, ITC Enschede, pp. 1-120.
- Singleton, A., Li, Zi., Hoey, T. And Muller, J.P. (2014). Evaluating sub-pixel offset techniques as an alternative to D-InSAR for monitoring episodic landslide movements in vegetated terrain. *Remote Sensing of environment*. Vol. 147, pp. 133-144.
- Singh, M., Singh, R.B. and Hassan, M.I. (Eds) (2014). Landscape ecology and water management: Proceedings of IGU Rohtak Conference. *Advances in Geographical and Environmental Sciences*. Vol. 2, pp 15-32.
- Sarkar, S., Roy, A.K. and Martha, T.R. (2013). Landslide susceptibility assessment using information value method in parts of Darjeeling Himalayas. *Journal of Geological society of India*. Vol. 82, pp.351-362.
- Su, R. K. L. and C.-L. Lee (2013). Development of seismic fragility curves for low-rise masonry infilled reinforced concrete buildings by a coefficient-based method. *Earthquake Engineering and Engineering Vibration*, Vol. 12(2), pp. 319-332.

- Singhal, A. and A. S. Kiremidjian (1996). Method for Probabilistic Evaluation of Seismic Structural Damage. *Journal of Structural Engineering*, Vol. 122(12), pp. 1459-1467.
- Su, R. K. L. and C.-L. Lee (2013). "Development of seismic fragility curves for low-rise masonry infilled reinforced concrete buildings by a coefficient-based method. *Earthquake Engineering and Engineering Vibration*, Vol.12(2), pp. 319-332.
- Serdar Kirçil, M. and Z. Polat (2006). Fragility analysis of mid-rise R/C frame buildings. *Engineering Structures*, Vol.28(9), pp. 1335-1345.
- Suppasri, A., I. Charvet, K. Imai and F. Imamura (2013). Fragility curves based on data from the 2011 Great East Japan tsunami in Ishinomaki city with discussion of parameters influencing building damage. *Earthquake Spectra*: 131218125838008.
- Serdar Kirçil, M. and Z. Polat (2006). Fragility analysis of mid-rise R/C frame buildings. *Engineering Structures* 28(9), pp. 1335-1345.
- Szeliga, W., Hough, S., Martin, S. and Bilham, R. (2010). Intensity, Magnitude, Location, and attenuation in India for felt earthquakes since 1762. *Bulletin Seismological Society of America*, Vol. 100(2), pp.570–584.
- Sreekesh S. (2012). Geospatial Techniques and methods. *Yojana*. Vol 56, pp 37-38.
- Saied, P. and Li, J. (2016). Landslides investigations from geoinformatics perspective: quality, challenges, and recommendations, *Geomatics, Natural Hazards and Risk*, pp.1-18.
- Schultz, M., Gouldby, M.B., Simm, J. and Wibowo, J. (2010). Beyond the factor of safety: Developing fragility curves to characterize system reliability. *Technical report, DTIC document*. pp. 1-70.
- Sharma, L.P., Patel, N., Ghose, M.K., Debnath, P. (2015). Development and application of Shannon's entropy integrated information value model for landslide susceptibility

- assessment and zonation in Sikkim Himalayas in India. *Natural Hazards*, Vol. 75, pp. 1555–1576.
- Sitharam, T.G., Anbazhagan, P., and Ganesha Raj, K. (2006). Use of remote sensing and seismotectonic parameters for seismic hazard analysis of Bangalore. *Natural hazards earth system science* Vol.6, pp. 927-939.
- Stevenson, P.C. (1997). An empirical method for the evaluation of relative landslide risk. *Bulletin of International Association of Engineering Geology*. Vol. 16, pp.69–72.
- Sreekesh, S. (2012). Geospatial Techniques and methods. *Yojana*. Vol 56, pp 37-38.
- Steiniger, S. and Hunter, A. J. (2013). The 2012 free and open source GIS software map—A guide to facilitate research, development, and adoption, *Computer Environment Urban*, Vol.39, pp. 136–150.
- Tselentis, G.A. and Danciu, L. (2008). Empirical relationships between modified Mercalli intensity and engineering ground-motion parameters in Greece. *Bulletin Seismological Society of America*. Vol.98(4), pp.1863–1875.
- Thiery, Y., Malet, J. P., Sterlacchini, S., Puissant, A., and Maquaire, O. (2007). Landslide susceptibility assessment by bivariate methods at large scales: Application to a complex mountainous environment. *Geomorphology*, Vol.92, pp. 38-59.
- Tsafirir, L., Barak T., Oded, K., Rivka A., David S., Yariv H., Bar-Lavi, Y., Romach, S. Amos Salamon (). Earthquake loss estimation in Israel using the new HAZUS-MH software: preliminary implementation, *Ministry of national infrastructures geological survey of Isreal report*, pp 1-45.
- Tarolli, P. and Tarboton, D.G. (2006). A New Method for Determination of Most Likely Landslide Initiation Points and the Evaluation of Digital Terrain Model Scale in Terrain Stability Mapping. *Hydrology and Earth System Sciences*, Vol.10, pp.663-677.

- Tseng, C.M., Lin, C.W., and Hsieh, W.D. (2015). Landslide susceptibility analysis by means of event-based multi-temporal landslide inventories. *Natural Hazards and Earth System sciences*. Vol. 3, pp. 1137-1173.
- The Nagaland Gazette (2013). The Nagaland building Bye-laws 2012. Government of Nagaland, Vol. 13, pp. 338-418.
- Taubenbock, H., Roth, A. and Dech, S. (2007). Vulnerability assessment using remote sensing: The earthquake prone megacity Istanbul, Turkey. *Proceedings of ISRSE 2007*, pp. 1-5.
- Tareq, H., Mezughi, J. M. A., Rafek, A.G. and Abdullah, I (). Landslide Susceptibility Assessment using Frequency Ratio Model Applied to an Area along the E-W Highway (Gerik-Jeli). *American Journal of Environmental Sciences*, Vol.7(1), pp. 43-50.
- Tandon, A.N. and Srivastava, H.N. (1975). Focal mechanism of some recent Himalayan earthquakes and regional plate tectonics. *Bulletin of seismology society of America*. Vol. 65. pp. 963-969.
- Talib, J.A. and Napiah, A., (2000). Landslide hazard zonation mapping using remote sensing and GIS techniques. *Geological society of Malaysia Bulletin*, Vol. 44, pp. 101-107.
- UN International Strategy for Disaster Reduction (UNISDR) (2009). Terminology on Disaster Risk Reduction. Geneva, Switzerland (2009). http://www.unisdr.org/files/7817_UNISDRTerminologyEnglish.pdf accessed 21 August 2012)).)
- USGS 2016 <https://earthquake.usgs.gov/earthquakes/eventpage/us10004b2n#shakemap>
- Unsalan, C. and Boyer, K.L. (2011). Land classification to Building and Road Detection. *Springer*. Pp. 1-186.

- UNISDR. Living with Risk. A global review of disaster reduction initiatives: United Nations; (2004). http://www.unisdr.org/files/657_lwr21.pdf accessed 20 August 2012)
- Van Westen, C. J., Van Asch, T. W. J and Soeter, R., (2006). Landslide hazard and risk zonation why is still so difficult? *Bulletin Engineering geology Environment*, Vol. 65, pp. 167-184.
- Van Westen, C.J., (2000). The modelling of landslide hazards using GIS. *Survey in Geophysics*, Vol. 21, pp. 241-255.
- Van Westen, C.J., Castellanos, E. and Kuriakose, S.K. (2008). Spatial data for landslide susceptibility, hazard, and vulnerability assessment. *An overview of Engineering Geology*. Vol. 102, pp.112–131.
- Veronica, T., Del Ventisette, C., Moretti, S. and Casagli. N. (2014). Integration of Remote Sensing Techniques for Intensity Zonation within a Landslide Area: A Case Study in the Northern Apennines, Italy, *Remote sensing*, Vol. 6, pp. 907-924.
- Vazurkar, U.Y. and Chaudhari, D.J. (2016). Development of fragility curves for RC buildings. *International journal of engineering research*. Vol.5 (3), pp. 591-594.
- Vahdani, R., Khodakarami, M. I., and Rahimi, V. (2015). Seismic risk assessment of bildings with HAZUS methodology and determination of damage probalistic matrices. *10th International Congress on Civil Engineers*. Pp. 1-9.
- Varnes D. J. and the International Association of Engineering Geology Commission of Landslides and the Mass Movements on Slopes (1984). Landslide hazard zonation: a review of principles and practice . *UNESCO*, Paris, pp. 1-63.
- Vijith, H., Krishnakumar, K.N., Pradeep, G.S., Ninu Krishnan, M.V. and Madhu, G., (2013). Shallow landslide initiation susceptibility mapping by GIS-based weights-of-evidence analysis of multi-class spatial data-sets: a case study from the natural

- sloping terrain of Western Ghats, India. *Georisk: Assessment and management of risk for engineered systems and geohazards*. Taylor and Francis, Vol.8(1), pp. 48-62.
- Varnes, D.J. (1984). Landslide Hazard Zonation: A review of principles and practice, Commission on landslides of the IAEG, *UNESCO. Darantiere, Quetigny*, pp1-63.
- Vicente, R., Parodi, S., Lagomarsino, S., Varum, H. and Mendes da Silva, J.A.R. (2008). Seismic vulnerability assessment, damage scenarios and loss estimation; Case study of the old city centre of Coimbra, Portugal. *The 14th World Conference on Earthquake Engineering*, Beijing, China pp. 1-8.
- Van Westen, C. J., Castellanos, E, Kuriakose. S. L., (2008). Spatial data for landslide susceptibility, hazard and vulnerability assessment: An overview. *Engineering geology*, Vol.102, pp. 112:131.
- Van Westen C.J., Rengers, N., Terlien, M.T.J. and Soeters, R. (1997). Prediction of the occurrence of slope instability phenomena through GIS-based hazard zonation. *Geol Rundsch*, Vol.86, pp. 404–410.
- Van Westen, C.J. (2000). The modelling of landslide hazards using GIS. *Survey Geophysics*, Vol. 21, pp.241–255.
- Valero, S., Chanussot, J. and Gueguen, P. (2008). Classification of basic roof types based on VHR optical data and digital elevation model. *International geoscience and remote sensing symposium (IGARSS)*. Institute of electrical and electronics engineers Inc., pp. 149-152.
- Van Westen, C.J., Van Asch, T.W.J. and Soeters, R., (2006). Landslide hazard and risk zonation-why is it so difficult. *Bulletin of engineering geology and environment*. Vol. 65. pp. 167-184.

- Van Westen CJ (1993). Application of geographic information systems to landslide hazard zonation. PhD Dissertation, Technical University Delft, ITC-Publication Number 15, ITC, Enschede, The Netherlands))
- Van Westen, C.J. (1997). Statistical landslide hazard analysis. In: van Westen, C.J. (Ed.), ILWIS 2.1 for Windows Application Guide. ITC Publication, Enschede, pp. 73–84).
- Vervaeck, A. and Daniell, J. (2012). Earthquake near the India/Myanmar border (Manipur and Nagaland Provinces)- No reports of damage or injuries. *Earthquake report*. pp. 1-3.
- Vazurkar, U.Y. and Chaudhari, D.J. (2016). Development of fragility curves for RC buildings. *International journal of engineering research*. Vol.5 (3), pp. 591-594.
- VanWesten, C. J. (2000). The Modelling of landslide hazards using GIS. *Surveys in Geophysics*, Vol. 21, pp. 241-255.
- Wu, D., Tesfamariam, S., Stiemer, S. F. and Qin, D. (2012). Seismic fragility assessment of RC frame structure designed according to modern Chinese code for seismic design of buildings. *Earthquake Engineering and Engineering Vibration*. Vol. 11(3), pp.331-342.
- Walling, T., (2005). Geological investigation of land instability in Kohima town, Nagaland.PhD Thesis.Department of Geology, Nagaland University.
- Wu, Y., Teng, T., Shin, T. and Hsiao, N. (2003). Relationship between peak ground acceleration, peak ground velocity and intensity in Taiwan. *Bulletin Seismological Society of America*, Vol.93, pp.386–396.
- Wald, D.J., Quintoriano, V., Heaton, T.H. and Kanamori, H. (1999). Relationship between peak ground acceleration, peak ground velocity and modified Mercalli intensity in California. *Earthquake Spectra*. Vol. 15, pp.557–564.

- Wang, Q., Wang, D., Huang, Y., Wang, Z., Zhang, L., Guo, Q., Chen, W., Chen, W. And Sang, M. (2015). Landslide susceptibility mapping based on selected optimal combination of landslide predisposing factors in a large catchment. *Sustainability*. Vol. 7, pp. 16653-16669.
- Wang, H., Liu, G., Xu, W. and Wang, G. (2005). GIS- based landslide hazard assessment: an overview, *Progress in Physical Geography*. Vol.29(4), pp.548-567.
- Wu, Y., Chen, L., Cheng, C., Yin, K. and Torok, A. (2014). GIS-based landslide hazard predictive system and its real-time test during a typhoon, Zhejiang Province, Southeast China. *Engineering Geology*. Vol. 175, pp 9-21.
- Xu, W.B., Yu, W.J., Jing, S.C., Zhang, G.P., and Huang, J.X. (2013). Debris flow susceptibility assessment by GIS and information value model in a large-scale region, Sichuan Province (China). *Natural Hazards*, Vol. 65, pp. 1379–1392.
- Xiao, P., (2008). Multispectral quickbird-2 image segmentation based on Vector field model. *International archives of the Photogrammetry, remote Sensing and Spatial Information Sciences*. Vol. 37 (B4), pp. 1171- 1176.
- Yamazaki, F., Mitomi, H., Matsuoka, M. and Honda, K. (2000). Inventory Development for Natural and Built Environments-Remote Sensing Technologies for Inventory Development and Risk Assessment-Characteristics of Satellite Images in Bangkok, Thailand. Report on ‘*The Development of Earthquake and Tsunami Disaster Mitigation Technologies and Their Integration For the Asia-Pacific Region*’, *Earthquake Disaster Mitigation Research Center, Japan*.
- Yazdadi, E.A. and Ghanavati, E (2016). Landslide Hazard Zonation by using AHP (Analytical Hierarchy Process) model in GIS (Geographic Information System) Environment (Case study: Kordan Watershed) *International journal of progressive sciences and technologies*. Vol. 2 (1), pp. 24-39.

- Yahya, Y., Bayraktarli and Faber, M.H. (2011). Bayesian probabilistic network approach for managing earthquake risks of cities, *Georisk: Assessment and Management of Risk for Engineered Systems and Geohazards*, Vol. 5(1), pp. 2-24.
- Zhang, J. and S. Hu (2005). State of the Art of Bridge Vulnerability Analysis Research. *Structural Engineers*, Vol. 21(5), pp. 76–80.
- Zezere, J.L. (2002). Landslide susceptibility assessment considering landslide typology. A case study in the area north of Lisbon (Portugal). *Natural Hazards and earth System Science*. Vol. 2, pp. 73-82.